NPY effect on synapses via autophagy:

Dynamic reorganization of GluA1

Thesis

for the degree of

doctor rerum naturalium (Dr. rer. nat.)

approved by the Faculty of Natural Sciences of Otto von Guericke
University Magdeburg

by **MSc. Elisa Redavide**

born on 12.10.1991 in Cosenza

Examiners:

Prof. Dr. Dr. Anne Albrecht

Prof. Dr. Erin M. Schuman

submitted on: 22.02.2021

defended on: 15.09.2021

Abstract

Stress can be defined as an influence that creates bodily or mental pressure on a system. Excessive psychological stress may eventually lead in the generation of pathological states such as anxiety disorders and depression. One of the candidates that has been shown to have a beneficial effect during such stressful conditions is the neuropeptide Y (NPY): NPY can be found as co-transmitter of GABAergic interneurons in the hippocampus and in particular in the DG where it acts as an anxyiolitic and antidepressant, promoting resilience. Recently, it was as well demonstrated that NPY increases autophagy, a cellular mechanism that is routinely used to recycle old or damaged components. In neurons, autophagy is a strong modulator of pre- and postsynaptic neuronal plasticity and it seems to have a role as well in memory formation. Taken all these evidences together, the molecular mechanisms of the NPY action in synapses via autophagy were studied: at first, it was found the long-lasting increase of autophagy induced by NPY (up to 24 after the NPY application and medium change). Then, it was discovered the subunit of the excitatory AMPA receptor, GluA1, as synaptic protein modulated by the NPY-induced autophagy. The modulation of GluA1 induced by NPY relies on the concomitant activation of both protein degradation and synthesis and it shows the same long-lasting effect as autophagy. Moreover, the GluA1 modulation exhibits a specific time-course and dynamic reorganization in the hippocampal cultures: during the NPY stimulation there is an initial removal of GluA1 from the synapses and its shuffling towards the soma, that is then followed by a relocation of this subunit on the membranes 24h after the NPY application, that is not accompanied by an increase in the pre-synaptic to post-synaptic colocalization. When looking at the NPY effect *in vivo*, it was possible to observe similar phenomena: the application of NPY in the dDG of mice produces an increase in the GluA1 intensities across the dendritic portions of the granule cells. Such a characterisation of the NPY effect on autophagy and GluA1, both *in vitro* and *in vivo*, is further unveiling the complex role of NPY during stressful conditions and displaying its target, GluA1, thus adding a piece of knowledge in the intricate stress modulation puzzle. Understanding the molecular effect of NPY via autophagy during stressful conditions could give insight into new molecular players of this complex biological mechanisms and eventually novel targets for therapies against neuropsychopathologies.

Zusammenfassung

Stress kann als ein Einfluss definiert werden, der körperlichen oder psychischen Druck auf ein System erzeugt. Übermäßiger psychischer Stress kann schließlich zur Entstehung von pathologischen Zuständen wie Angststörungen und Depressionen führen. Einer der Kandidaten dem eine positive Wirkung bei solchen Stresszuständen nachgewiesen wurde, ist das Neuropeptid Y (NPY): NPY findet sich als Co-Transmitter von GABAergen Interneuronen im Hippocampus und insbesondere im DG, wo es als Anxiolytikum und Antidepressivum wirkt und die Resilienz fördert. Kürzlich wurde auch gezeigt, dass NPY die Autophagie steigert- ein zellulärer Mechanismus- der routinemäßig dazu dient, alte oder beschädigte Komponenten zu recyceln. In Neuronen ist die Autophagie ein starker Modulator der prä- und postsynaptischen neuronalen Plastizität und sie scheint auch eine Rolle bei der Gedächtnisbildung zu spielen. Schließich, wurden die molekularen Mechanismen der NPY-Wirkung in Synapsen über die Autophagie untersucht: zunächst wurde die langanhaltende Steigerung der durch NPY induzierten Autophagie gefunden (bis zu 24 Stunden nach der NPY-Applikation und dem Mediumwechsel). Dann wurde die Untereinheit des exzitatorischen AMPA-Rezeptors, GluA1, als synaptisches Protein entdeckt, das durch die NPY-induzierte Autophagie moduliert wird. Die durch NPY induzierte Modulation von GluA1 beruht auf der gleichzeitigen Aktivierung sowohl des Proteinabbaus als auch der Proteinsynthese und zeigt den gleichen langanhaltenden Effekt wie die Autophagie. Darüber hinaus zeigt die GluA1-Modulation einen spezifischen zeitlichen Verlauf und eine dynamische Reorganisation in den Hippocampus-Kulturen: während der NPY-Stimulation kommt es zu einer anfänglichen Entfernung von GluA1 aus den Synapsen und seiner Verlagerung in Richtung Soma. 24 Stunden nach der NPY-Applikation von einer Verlagerung dieser Untereinheit auf den Membranen gefolgt wird, die nicht von einer Zunahme der präsynaptischen zu postsynaptischen Kolokalisation begleitet wird. Bei der Betrachtung des NPY-Effekts in vivo konnten ähnliche Phänomene beobachtet werden: die Applikation von NPY im dDG von Mäusen führt zu einem Anstieg der GluA1-Intensitäten in den dendritischen Bereichen der Körnerzellen. Eine solche Charakterisierung der NPY-Wirkung auf Autophagie und GluA1- sowohl in vitro als auch in vivo- deckt die komplexe Rolle von NPY unter Stressbedingungen weiter auf

Zusammenfassung

und zeigt sein Ziel, GluA1, und fügt so ein weiteres Stück Wissen im komplizierten Puzzle der Stressmodulation hinzu. Das Verständnis der molekularen Wirkung von NPY über die Autophagie unter Stressbedingungen könnte Einblicke in neue molekulare Akteure dieses komplexen biologischen Mechanismus und schließlich neue Ziele für Therapien gegen Neuropsychopathologien geben.

Table of Content

Table of Content

List of Figures

List of Figures

List of Tables

Abbreviations

AMPA	α-amino-3-hydroxy-5-methyl-4-isoxazolepropionic acid
ASDs	autism spectrum disorders
ATGs	autophagy-related proteins
BDNF	brain-derived neurotrophic factor
CHX	cycloheximide
CMA	chaperone-mediated autophagy
CNO	clozapine-N-oxide
CNS	central nervous system
CORT	corticosterone
CQ	chloroquine
CR	conditioned response
CS	conditioned stimulus
dDG	dorsal dentate gyrus
DG	dentate gyrus
e.g.	exempli gratia
FC	fear conditioning
GABA	γ-aminobutyric acid
GCL	granule cell layer
GPCR	G protein-coupled receptor
HPA	hypothalamic-pituitary-adrenal
HSC70	heat shock cognate 70 kDa Protein
ICD	International Classification of Diseases
i.e.	id est – that is
IML	inner molecular layer
i.p.	intraperitoneally
KD	knock-down
KO	knock-out
LAMP-2	lysosomal-associated membrane protein 2A
LC3	light chain 3
LTP	long term potentiation
ML	molecular layer
MML	medial molecular layer
mTOR	mammalian target of rapamycin
NMDA	N-methyl-D-aspartate

Abbreviations

NPY	neuropeptide Y
OML	outer molecular layer
PAS	pre-autophagosomal Structure
PE	phosphatidylethanolamine
PFC	pre froextal cortx
PI3P	phosphatidylinositol-3-phosphate
PTSD	post-traumatic stress disorder
SSRIs	serotonin selective reuptake inhibitors
SST	somatostatin
ULK1	UNC51-like kinase1
UPS	ubiquitin proteasome system
US	unconditioned stimulus
VGlut	vesicular glutamate transporter
WHO	World Health Organization's

1. Introduction

1.1.   Stress induced psychopathologies

Stress can be defined as a state of disharmony, in which homeostasis is actually threatened or perceived to be so, that is therefore counterbalanced by a complex range of physiological and behavioural responses aimed to restore the homeostasis (Chrousos 2009). The stress-response involves changes in the central nervous system (CNS) and in several peripheral tissues, allowing for a facilitation of processes that perform adaptive tasks, such as arousal, vigilance and analgesia, while inhibiting vegetating functions, for instance feeding, growth and reproduction (Chrousos 2009). Each individual reacts to stress with an adaptive response determined by a variety of genetic, environmental and developmental factors. However, changes in the capacity to successfully respond to stress, as it might be, for example, an excessive or prolonged reaction, may lead to diseases (Tsigos et al. 2000). For instance, stress during embryonic development or early life may determine brain vulnerability, while exposure to acute stressors later on in life, like during adolescence, may trigger the onset of the first psychotic episode (Corcoran et al. 2003). Around 10% to 20% of the general population suffers from neuropsychopathologies that include depressive disorders, several forms of clinical anxiety including generalized anxiety, trauma and stressor-related disorders such as obsessive-compulsive and related disorders, schizophrenia, eating disorders, addiction and post-traumatic stress syndrome (PTSD) (American Psychiatric Association 2013). PTSD in particular is a chronic impairment anxiety disorder that often occurs as a result of exposure to severe stressors, as it might be a traumatic event such as a conflict or a natural disaster, in high-risk population groups (for example, Vietnam war veterans, victims of rape or natural disasters) (Miao et al. 2018). Even if most people experience traumatic episodes at some point during their life, individual differences in stress susceptibility limit the development of PTSD symptoms to a minor faction (7–30% of the population) (Brunello et al. 2001; Kessler et al. 1995, 2005). The World Health Organization's (WHO) International Classification of Diseases (ICD) simplified PTSD symptoms in the most recent ICD-11 version (Version 04/2019) under three clusters, including constant re-experiencing of the traumatic event, a sense of threat and avoidance of traumatic reminders. Moreover, major depressive disorder and substance abuse and/or

dependence are commonly reported in PTSD patients (Chilcoat and Breslau 1998; Kessler et al. 1995). Current treatments for this disorder are mostly forms of cognitive therapy, but non responders for such therapies might be as high as 50% (Mello et al. 2013; Kar 2011) and psychopharmacological treatments (mostly serotonin selective reuptake inhibitors -SSRIs-) are non-specific for PTSD and in fact equivalent to placebo treatments, as some meta-analysis studies suggest (Kozarić-Kovačić 2008; Ragen et al. 2015). In order to obtain etiological and molecular insights into PTSD and other stress-induced psychopathologies, it has been fundamental to establish animal models to investigate the underlying neural mechanisms of this disorder and consequently fulfil the need for novel and more specific drugs and treatments for PTSD patients.

1.1.1. Fear conditioning as stressor-related disorder model

Stressful experiences can cause long-lasting sensitization of fear and anxiety that extends beyond the circumstances of the initial trauma and could eventually develop into psychiatric disorders such as depressive disorders or forms of clinical anxiety (American Psychiatric Association 2013). Particularly, PTSD patients show, among other symptoms, lasting increase in anxiety, hyperexcitability, intrusive traumatic memory retrieval in response to traumatic events, an abnormal regulation of fear and display an increased baseline startle response. For example, usually neutral stimuli, such as loud sounds or objects, are associated with the aversive experience (e.g., assault, kidnap) and this causes physiological and behavioural reactions (Grillon et al. 1998; Grillon 2002; Kumari et al. 2001; C. A. Morgan et al. 1995). An animal model that can recapitulate trigger-induced persistent and exaggerated learned fear is the Pavlovian fear conditioning (FC). FC has been used to explore the neurobiological basis of fear learning and it is one of the most used laboratory protocols to study the pathogenesis of stress-induced psychopathologies. This behavioural paradigm is a form of associative learning in which an initially neutral conditioned stimulus (CS; e.g., a tone) is paired with a noxious unconditioned stimulus (US; e.g., a footshock), determining the formation of a fear memory that changes the salience of the CS: when, for example, the tone is presented without the footshock, the tone alone elicits the conditioned fear response (CR; e.g., freezing) (Rescorla and Wagner 1972). In this case, the context in which the CS-US pairing happened is processed as "background context", that when presented without the neutral stimulus

might evokes a partial CR. On the other hand, when the CS is not associated with the US, i.e. the CS loses the predictive value for the US, the context in which the noxious stimulus is delivered becomes the "foreground context" and it is able to cause full memory retrieval when the animal is re-exposed to it. (Calandreau, Jaffard, and Desmedt 2007; Phelps 2004; Rescorla and Wagner 1972). FC is an adaptive phenomenon that helps detect warning and safety signals: when detecting a warning signal, it is normal that an organism exhibits fear. However, when a subject has pathological anxiety or another stress-related disease, it will show an out-of-measure behaviour, such as excessive avoidance or exceedingly high levels of subjective fear when confronted with the same stimulus, as both clinical and non-clinical studies show and suggest that abnormalities in FC play a major role in the ethiology of stress-induced psychopathologies (Barlow 2002). Moreover, in the past years, the neurobiological mechanisms of fear conditioning were extensively studied, and some key brain structures associated with mood, anxiety and emotional memory formation were identified. Interestingly, human studies on PTSD patients revealed that the symptomatology of PTSD involves these same brain areas. The neural structures involved in the PTSD belong to the limbic system and the main ones are the amygdala, the hippocampus, and the prefrontal cortex (PFC). The PFC and hippocampus have dense connections with the amygdala, the area that regulates learned fear (van Marle et al. 2009). In PTSD patients, both the PFC, that is thought to be responsible for reactivating past emotional associations, and the hippocampus, that is thought to play a role in explicit memories of the traumatic events and in mediating learned responses to contextual cues, show reduced activation and this may possibly result in a hyper-responsive amygdala signal to fearful stimuli (de Carvalho, Rozenthal, and Nardi 2009; Etkin and Wager 2007; Francati, Vermetten, and Bremner 2007; Gilbertson et al. 2002).

More and more researches are pointing towards a fundamental role of the hippocampus in PTSD, as it is one of the brain areas that has an important function in the regulation of the neuroendocrine stress response, it is crucial for the formation of long-term declarative (explicit) memory in humans and spatial (relational) memory in rodents and over the years it has been seen to be highly susceptible to stress (Maren 2001; McEwen, Gould, and Sakai 1992; Morris et al. 1982). The hippocampus is a medial temporal lobe that contains two distinguishable substructures, the cornu ammonis (CA) and the dentate gyrus (DG), with a well-studied circuit connectivity:

Introduction

while in the classical trisynaptic loop the DG receives projections from the entorhinal cortex on the excitatory granule cells, that will then transmit the information on to the CA3 and CA1 areas and to the subiculum, there are also backprojections from CA3 on to the DG, as well as direct inputs from the entorhinal cortex on all different substructures of the hippocampus (Anand and Dhikav 2012; Schultz and Engelhardt 2014). The DG itself has a laminar organization and it is divided into molecular layer (ML), granule cell layer (GCL) and hilus. The ML is a relatively cell-free layer occupied by, amidst other things, the dendrites of the granule cells, the major cell type of the DG, and it can be divided into three zones that are approximately the same width: outer molecular layer (OML), middle molecular layer (MML) and inner molecular layer (IML). The GCL is composed of several layers of densely packed granule cells, while the hilus is a polymorphic layer that includes the subgranular zone and a larger area that ends in the CA3 area (Amaral, Scharfman, and Lavenex 2007; Scharfman and Myers 2013). The hippocampal structure presents not only a complex connectivity inside and outside the hippocampus itself, but also from the dorso-ventral axis, where the dorsal component is involved in cognitive functions, such as spatial navigation, learning and memory, and the ventral region is associated with emotional responses and motivated behaviour (Bannerman et al. 2003, 2004; Fanselow and Dong 2010; E. Moser, Moser, and Andersen 1993; M. B. Moser and Moser 1998). A firmly established role of the hippocampus is the integration of multimodal information into higher-order representations of context (e.g. during FC) (Phillips and LeDoux 1994; Rudy 2009) and in particular, the DG has a pivotal role in the context memory formation (Lee and Kesner 2004; McHugh et al. 2007) by local γ-aminobutyric acid (GABA)ergic circuits: neurons located in the hilus and expressing both somatostatin (SST) and neuropeptide Y (NPY) as co-transmitters receive cholinergic inputs from the septum, therefore prompting the release of NPY on the granule cells, that in turns attenuates the granule cells activity and regulates the context salience in a background context fear conditioning paradigm (Raza et al. 2017). Since exposure to traumatic experiences determines PTSD only in some of the exposed individuals, it indicates that there are somehow resilient mechanisms that prevents the damages of the trauma in some individuals. A better understanding of the neurobiology of PTSD can help in predict which individuals might be more susceptible to developing it after trauma, but also it will point towards novel molecular targets for drug development and potential new approaches to treat PTSD symptoms.

1.2. Synaptic consequences of stress in the hippocampus

As previously mentioned, stress takes a high toll on the hippocampus, but it affects the hippocampal structure differently, depending on the length of the stressors: on one hand, chronic stress promotes an adaptive plasticity in the dorsal part of the hippocampus, possibly to facilitate avoidance of the stressor, while the ventral region is involved with more affective responses (Hawley et al. 2012); on the other hand, when the stress is acute, there is a decrease in the long term potentiation (LTP) in the dorsal hippocampus, while in the ventral region facilitation mechanisms take place (Maggio and Segal 2007). These same patterns of stressors and their different regional effects can be very well mimicked by the application of corticosterone (CORT), demonstrating the pivotal role of the hypothalamic-pituitary-adrenal (HPA) stress axis in these hippocampal processes and the dual relationship between the level of CORT and LTP (Diamond et al. 1992). Stress affects hippocampal neurons and their synapses as well, via a modulation of their excitatory and inhibitory ionotropic receptors. The word synapse was coined over 100 years ago by Sir Charles Sherrington to indicate the physical connection between neurons (Foster and Sherrington 1897). Synapses are generally composed of a pre-synaptic compartment from the signal-sending neuron, that contains neurotransmitter-filled synaptic vesicles, and a post-synaptic terminal from the signal-receiving neuron, that contains membrane receptors to whom neurotransmitters can bind to (Pickel and Segal 2013). The two main types of central synapses are glutamatergic and GABAergic synapses and they play opposite roles in excitation and inhibition of neurons. Excitatory neurotransmission is mediated primarily through glutamate and the most abundant ionotropic neurotransmitter receptors present at these synapses are α-amino-3-hydroxy-5-methyl-4-isoxazolepropionic acid (AMPA) and N-methyl-D-aspartate (NMDA), which control local flux of sodium (Na+), potassium (K+) and the second messenger calcium (Ca++) at the synapse. On the other hand, inhibitory synaptic transmission is mediated via GABA or glycine, that binds to GABAA and glycine receptors and it control neuronal excitability through regulated chloride (Cl-) influx (Eccles 1959; Gray 1959; Kennedy 2000). Synapses are highly dynamic sub-cellular structures that can be promptly formed or eliminated during plasticity processes, from early developmental stages throughout the entire lifespan of an organism (Engert and Bonhoeffer 1999; Matsuzaki et al. 2001). Stress can shape this neuronal structure, in

particularly in the hippocampus, and its effects depends once more on the length of the stressor and on the hippocampal area considered.

As far as it concerns inhibitory ionotropic receptors, using a chronic mild stress protocol, Czeh and colleagues were able to demonstrate that chronic stress reduces the number of GABAergic interneurons, affecting the structural integrity of GABAergic networks, but with dorso-ventral and region-specific differences (Czéh et al. 2015). A history of juvenile stress later associated with an acute adult stressor is affecting the GABAergic signalling in the dorsal hippocampus, where the shift of excitatory/inhibitory balance is due to a reduction in the GABA uptake by astrocytes (Albrecht et al. 2016; Hadad-Ophir et al. 2014). On the other hand, the subunits alpha 1 and 2 of the GABA A receptor are upregulated in the ventral CA1 and DG regions of resilient animals after underwater trauma, suggesting that an increase in the inhibitory neurotransmission in the ventral hippocampus can be associated with a resilient behaviour (Ardi et al. 2016, 2019). Also excitatory ionotropic receptors can be modulated by stress: while acute stress in the form of a single immobilization stressor is able to increase the mRNA levels of the NMDA NR1 and NR2B subunits in the hippocampus (Bartanusz et al. 1995), chronic stress can increase both the transcriptional and translational levels of the NMDA receptor subunits N1, N2A and N2B, particularly in the ventral hippocampus, allowing for speculation on the role of depression in enhancing glutamate activity via increasing the number of available post-synaptic receptors (Calabrese et al. 2012). Since increasing evidences are pointing towards glutamatergic mechanisms as crucial mediators during stress, the specifics of these phenomena will be further discussed in the following subchapter.

1.2.1. Stress effect on GluA1 receptor

AMPA receptors are tetramers assembled by different combinations of four subunits, GluA1–4, encoded by the genes Gria1-4. They can be homo- or heterotetramers and each subunit has different characteristics in relation to its contribution to channel kinetics, ion selectivity, and receptor trafficking properties (Collingridge et al. 2009; Hollmann and Heinemann 1994; Mayer and Armstrong 2004). Specifically, mature hippocampal pyramidal neurons express two predominant combinations of AMPAR subunits, GluA1/GluA2 or GluA2/GluA3 heterotetrameric receptors (Wenthold et al. 1996). AMPA receptors are localised at excitatory synapses and are in close proximity with NMDA receptors: they are the gatekeepers of NMDAR-

dependent synaptic plasticity by removing their voltage-dependent channel block by Mg2+ and allowing the postsynaptic calcium entry that promotes the changes in synaptic strength (Bliss and Collingridge 1993; Huganir and Nicoll 2013; Mayer, Westbrook, and Guthrie 1984; Nowak et al. 1984). Studies show that AMPA receptors can be either directly at the synapse or to extrasynaptic areas and the movement from extrasynaptic sites to the synapse follows LTP induction (Hirling 2009; Kropf et al. 2008; Passafaro, Piãch, and Sheng 2001; Shi et al. 2001). This exocytotic/endocytotic recycling cycle between intracellular and membrane receptor pools of receptors takes place via endosomes, specialised vesicles that usually form directly from the plasma membrane (Beattie et al. 2000; Carroll et al. 2001; Kobayashi et al. 1998): these endosomes are called early endosomes and from these, AMPA receptors can be sorted to late endosomes for degradation or to recycling endosomes for reinsertion into the plasma membrane (Ehlers 2000; Rubino et al. 2000), a mechanism that is induced with LTP and depends in part on the activation of NMDA receptors, that eventually determines changes in spine morphology (Ehlers 2003; Park et al. 2004; Sossa, Court, and Carroll 2006).

Many evidences show how stress can modulate this cycling of AMPA receptors: in cultured hippocampal neurons, CORT increases the membrane mobility of GluA2-containing AMPA receptors during bi-directional synaptic plasticity (Groc, Choquet, and Chaouloff 2008; Martin et al. 2009). This result was further confirmed by an *in vivo* study, where mice trained under stressful conditions showed an increase in the synaptic expression of the GluA2 subunit of the AMPA receptor in the hippocampus, compared to mice trained under non-stressful conditions, thus allowing for speculations that this increase might underlie a possible facilitation of spatial learning and memory by stress (Conboy and Sandi 2010). Also the trafficking of GluA1 containing AMPARs is essential for the formation of fearful memories in a tone-cued conditioning (Rumpel et al. 2005) and studies in mutant mice confirm that the GluA1 subunit is essential for spatial working memory (Reisel et al. 2002). On the other hand, chronic unpredictable stress also leads to a loss of the AMPAR subunit GluA1 and synaptic proteins PSD-95 and synapsin, as it would be expected with a loss of spines (Li et al. 2010). Another example can be how acute stress can change the phosphorylation profile of AMPA subunits, once more depending on the hippocampal region considered: while in the dorsal hippocampus the GluA1 subunit shows a decrease in phosphorylation in the Serine sites that can mediate generation of LTP,

in the ventral compartment we have an increase in phosphorylation in the same site, thus determining a decrease in the LTP induction in the dorsal hippocampus and an increase in the ventral (Malinow and Malenka 2002; Vouimba et al. 2004); on the other hand, acute stress produces, only in the ventral hippocampus, a decrease in phosphorylation of the GluA2 subunit in the Serine site involved in the internalization of the receptor, which can in turn impede the generation of LTD (Caudal et al. 2010; Hayashi and Huganir 2004). Conversely, in contextual learning paradigms, the phosphorylation of GluA1 is enhanced and GluA1 and GluA2 subunits protein levels are rapidly and transiently enhanced in synapses, indicating that such a cognitive task is accompanied by changes in AMPAR trafficking in hippocampal neurons (Whitlock et al. 2006). Learning increases the protein synthesis of AMPA receptors: 24h after fear conditioning, newly synthesised AMPA receptor are selectively recruited to mushroom-type spines in adult hippocampal CA1 neurons (Matsuo, Reijmers, and Mayford 2008). All together, these evidences on the role of stress and fear memories on AMPA receptors modulation (via both phosphorylation and protein synthesis), cycling and dysregulation of glutamate transmission at the synapse can link stress exposure to psychopathologies and can guide in the discovery of new targets for future therapies.

1.3.   NPY as a resilience factor

One of the players and modulators of the complex stress-response regulation system in the hippocampus is NPY, that might adapt the whole organism to stressful, potentially life-threatening conditions, by orchestrating resilience to traumatic events, both in rodents and humans (Cohen et al. 2012; G. Wu et al. 2013). NPY is a 36-amino acid peptide which belongs to the so-called NPY family, together with two other members, peptide YY and pancreatic polypeptide (PP) (Holzer, Reichmann, and Farzi 2012). NPY is one of the most abundant neuropeptides in the brain and periphery and it co-localizes with a variety of neurotransmitters (Rasmusson and Pineles 2018). It has an important role in many physiological functions, that range over energy homeostasis, food intake, circadian rhythm, stress response and cognition (Catalani et al. 2017; Malva et al. 2012; Reichmann and Holzer 2016). These many functions of NPY are related to its expression in different brain areas, such as the hypothalamic arcuate nucleus or the locus coeruleus (Kask et al. 2002; Holzer, Reichmann, and Farzi 2012). NPY is expressed preferentially in interneurons but it is also present in

long projection neurons (Chronwall et al., 1985). In particular, it is also a marker peptide for a specific class of GABAergic interneurons in the cortex and hippocampus, where NPY-positive interneurons build local circuits that control the activity of principal cells and thereby affect emotional memory formation (Flood et al. 1989; Raza et al. 2017). The NPY receptors belong to the G protein-coupled receptor (GPCR) family and, in the hippocampus, this family includes the Y1, Y2, Y4 and Y5 subtypes (Michel et al., 1998): the CA3, CA2 and CA1 pyramidal cell layers of the hippocampus, as well as the DG, show high to moderate levels of Y1 receptor mRNA (Dumont et al. 1998; Kishi et al. 2005; Larsen et al. 1993). Y2 receptor mRNA is discretely localized in the hippocampus as well, with a general lower expression level compared to the Y1 receptor (Dumont et al., 1998; Gustafson et al., 1997; Parker et al., 1999), and the co-localization of Y2 receptor mRNA with NPY mRNA in some neuronal cell strengthens pharmacological studies indicating a presynaptic localization where it acts as an autoreceptor, inhibiting the release of NPY and other neurotransmitters. Due to the Y2 receptor presynaptic localization, the release of NPY from interneurons upon increased neuronal activation can in turn act as a positive feedback for the neurons (Caberlotto et al., 2000; King et al., 1999, 2000; Martire et al., 1995). Y4 mRNA expression is displayed by certain areas of the hippocampus, but it was not possible to report any Y4 protein (Caberlotto et al., 2000; Whitcomb et al., 1997). Modest levels of Y5 mRNA can be found in neurons of the regions CA3, CA2, CA4 and DG with even lower levels in CA1 and usually its expression coincides with Y1 receptor (Nichol et al., 1999).

NPY has a well-established role in stress modulation: it can reduce the stress-induced increased anxiety via an NPY-mediated anxiolysis, as several studies show (Heilig et al. 1989; Śmiałowska et al. 2007). However, the Y2 receptor has an anxiogenic effect and this is possibly due to its presynaptic location and its function as autoreceptor, as researches using an agonist or a blocker of the Y2 receptor show behaviours that are associated with anxiety in animal models, as it is the preference for the closed arms of the elevated plus maze (Bacchi et al. 2006; Nakajima et al. 1998; Sajdyk et al. 2002). Conversely, the anxiolytic effect is mediated by the Y1 receptor as the administration of the Y1 receptor antagonist BIBP 3226 in the amygdala is anxiogenic, while the use of the selective Y1 receptor agonist [Leu^{31},Pro^{34}]-NPY produces an anxiolytic effect (Primeaux et al. 2005; Molosh et al. 2013; Sørensen et al. 2004). Indeed, more and more studies are pointing in the direction of NPY as a resilience

factor during stress exposure: the serum and plasma levels of soldiers that were subjected to stressful and traumatic events but are resilient to PTSD present higher levels of NPY (Charles A. Morgan et al. 2000; Reijnen et al. 2018). NPY has a pivotal role during fear conditioning: NPY knock-out (KO) mice have an increase acquisition of conditioned fear and this strong phenotype can be reproduced in KO mice for both Y1 and Y2 receptors (Verma et al. 2012). Also in a social fear conditioning paradigm, the intracerebroventricular administration of NPY before the extinction reduced the expression of social fear via simultaneous activation of Y1 and Y2 receptors, allowing for speculations on the possible use of NPY to improve recovery from a traumatic social experience by reducing the expression of social fear (Kornhuber and Zoicas 2019). In particular, the role of NPY in fear memory formation seems to be carried out in the DG: not only NPY balances contextual salience in a FC paradigm through control of the dorsal DG (dDG) granule cells via the Y1 receptor (Raza et al. 2017), but it was recently demonstrated in rats that the NPY positive interneurons in the dDG show a significantly enhanced activation only in trauma exposed but unaffected animals (Regev-Tsur et al. 2020). Taken together, all these studies point towards the DG as the main character in memory formation under emotional and stressful conditions and, more specifically, NPY manipulation in the dDG as a possible strategy to change the behavioural outcome of exposure to trauma.

1.4.   Cellular effects of NPY

The GPCR NPY receptors are coupled either/or with a Gi/PKA pathway or a Gq/PLC pathway (Goldberg et al., 1998; Persaud and Bewick, 2014) and this can in turn lead to a modulation in neuronal excitability via pre- or postsynaptic mechanisms. For example, in the ventral tegmental area, NPY affects the dopamine neuron activity: it can activate an outward current that exhibited characteristics of a G protein-coupled inwardly rectifying potassium channel current, while also decreasing the amplitude and increasing paired-pulse ratios of evoked excitatory postsynaptic currents, therefore modulating neuronal transmission with presynaptic mechanisms (West and Roseberry 2017). In the amygdala, NPY inhibits principal neurons via suppression of a tonically active, somatodendritic, hyperpolarization-activated, depolarizing current (Giesbrecht et al. 2010), while it also decreases the activity of the basolateral amygdala by enhancing GABAA-mediated currents and reducing the NMDA-mediated ones (Molosh et al. 2013). In the hippocampus, NPY is able to inhibit the evoked

release of glutamate through presynaptic inhibition of glutamate release in CA1 via the activation of Y2 receptors (Bleakman et al., 1992), but it also inhibits postsynaptic transmission in DG, CA1 and CA3 via Y1 and Y5 receptors (Silva et al., 2001, 2003), showing that the effect is dependent on the different hippocampal subregions and the receptor involved. Besides its role in modulating neuronal excitability, NPY carries out many different physiological functions in neurons, depending on the area and receptor activated: for example, it affects cell migration, cytokine release and antibody production through its Y1 receptors (Wheway, Herzog, and Mackay 2007; Farzi, Reichmann, and Holzer 2015); it is neuroprotective via the Y2 receptors by reducing the neurotoxic effect of kainic acid on CA1 and CA3 pyramidal cells (Gonçalves et al. 2012; Xapelli et al. 2008); it can reduce the apoptosis of pyramidal neurons induced by kainic acid in CA1 and CA3 through the Y2 and Y5 receptors (Y. F. Wu and Li 2005; Farzi, Reichmann, and Holzer 2015). In addition, Aveleira (2014) and Ferreira-Marques (2016) recently showed that NPY is able to increase autophagy both in hypothalamic and cortical neuronal rat primary culture via the Y1, Y2 or Y5 receptors through the coordinated activation of PI3K, MEK/ERK and PKA signalling (Aveleira et al. 2014; Ferreira-Marques et al. 2016), leaving space for speculations on a possible NPY-induced modulation of autophagy that could be used as an experimental system to investigate into synaptic markers and their autophagy-mediated regulation during fear memories formation.

1.5.   Intracellular protein degradation pathways

Autophagy and the ubiquitin–proteasome system (UPS) are the two major evolutionary conserved intracellular protein degradation and recycling pathways of eukaryotic cells. The UPS is in charge of degrading short-lived and misfolded soluble proteins one by one through the covalent attachment of a ubiquitin tag through an enzymatic cascade, in which the precursor ubiquitin is processed by a protease that cleaves it at a C-terminal glycine residue. The cleaved ubiquitin is activated by binding to E1 (ubiquitin activating enzymes) and from E1 it is transferred to E2 (ubiquitin conjugation enzymes). Depending on the type of ubiquitin ligase, either E2 directly or E3 (ubiquitin ligase) catalyses the final conjugation of ubiquitin to the lysine on the target protein (Callis 2014). This process is called ubiquitination and it then directs the tagged proteins to the proteasome, the catalytic machinery that will subsequently recycle their components (Cohen-Kaplan et al. 2016). Ubiquitylation-dependent

degradation is involved in the regulation of several cellular processes, including protein quality control, transcription, cell cycle progression, DNA repair, cell stress response and apoptosis (Brinkmann et al. 2015). On the other hand autophagy ("self-eating" from Greek) is a degradative route of eukaryotic cells, highly conserved from yeast to mammals, for the bulk degradation of cytosolic material and organelles through delivery to lysosomes/vacuole, resulting in the recycling of macromolecular constituents (D. J. Klionsky et al. 2011; Lippai and Szatmári 2017). The main difference between these two degradative systems is that while the UPS mainly degrades single, unfolded polypeptides or proteins able to enter into the narrow channel of the proteasome, autophagy recycles larger, cytosolic structures, such as protein complexes, insoluble cellular aggregates, dysfunctional organelles and pathogens (Groll and Huber 2004; D. J. Klionsky 2007).

1.5.1. Autophagy

The fundamental physiological importance of autophagy was uncovered in the early 1990s, when a genetic screen in yeast allowed to dissect the autophagic process, identifying 15 autophagy-related proteins (ATGs), essential for the autophagic delivery of cargo to the vacuole (the counterpart of the lysosome in yeast) (Tsukada and Ohsumi 1993). Routinely, autophagy has a role in cellular quality control where it degrades protein aggregates and damaged or dysfunctional organelles, in order to adapt to changing environmental conditions and maintain cellular homeostasis (Todde, Veenhuis, and van der Klei 2009). However, the adaptive process of autophagy occurs in particular in response to different forms of stress, like nutrient deprivation, growth factor depletion and hypoxia (Murrow and Debnath 2013). Since the main role of autophagy is to provide nutrients for vital cellular functions during stressful situations like fasting, it has long been considered a nonselective process. Nonetheless, it has been recently shown that autophagy might selectively eliminate unwanted, potentially harmful cytosolic material, such as damaged mitochondria or protein aggregates, via a process known as selective autophagy, thereby acting as a major cytoprotective system (Dikic and Elazar 2018). More and more studies are addressing the role of autophagy in disease mechanisms: for example, in Danon disease, a genetic condition that shows cardiomyopathy, myopathy and variable mental retardation, the mutation in the lysosomal lysosomal-associated membrane protein 2A (LAMP-2) protein produces and accumulation of

autophagosomes in the muscles (Tanaka et al. 2000). Also, cancer studies show many links between defective autophagy and tumours, as the regulation pathway of autophagy interplays closely with the cancerogenic one. An example worth citing, and also the first identified link between autophagy and cancer, might be beclin 1, a protein involved in the nucleation step of autophagosomes formation (Furuya et al. 2005): studies showed indeed that the monoallelic deletion of the beclin 1 gene, as well as a decrease in its expression, is present in a high number of human breast, ovarian, prostate and brain cancers, while its gene transfer with the consequent activation of autophagy inhibits cell proliferation, in vitro clonogenicity and tumorigenesis (Liang et al. 1999; Miracco et al. 2007). Autophagy has a cytoprotective function in several neuropathologies like neurodegeneration, where it prevents the accumulation of toxic proteins, as well as it seems to have a link with complex diseases like depression, where findings show that the use of several classes of antidepressants increase autophagy (Gassen et al. 2015; Gassen and Rein 2019; Nikoletopoulou, Papandreou, and Tavernarakis 2015).

1.5.2. Types of autophagy

The term "autophagy" defines a series of highly regulated catabolic processes that deliver cytoplasmic components to the lysosome for degradation, and that are broadly classified into three types, on the basis of different modes of cargo delivery to the lysosomes: microautophagy, chaperone-mediated autophagy and macroautophagy. Microautophagy refers to the invagination of the lysosomal or endosomal membrane, resulting in the direct engulfment of substrates that are subsequently degraded by lysosomal proteases, therefore bypassing vesicular intermediates (Fig.1 A) (Bingol 2018; Farré and Subramani 2004; Kaur and Debnath 2015). The substrate can be sequestered in bulk (non-selectively) or selectively with the help of cytoplasmic chaperones that recognize the substrates. Likewise, in the chaperone-mediated autophagy (CMA) cargo is not sequestered within a membrane delimited vesicle. Proteins containing an accessible KFERQ-like pentapetide motif are recognized by the cytosolic chaperone heat shock cognate 70 kDa protein (HSC70) (Olson, Terlecky, and Dice 1991); HSC70 then promotes the translocation of these targets across lysosomal membranes into the lysosomal lumen via the LAMP-2 receptor (Fig.1 B) (Chiang et al. 1989). Macroautophagy involves the compartmentalisation of cytoplasmic proteins and/or organelles in double membrane-bound vesicles called

Introduction

autophagosomes (Galluzzi, Baehrecke, et al. 2017); these autophagosomes are trafficked to lysosomes, at which point the sequestered cargo is degraded (Fig.1 C) (Mizushima and Komatsu 2011).
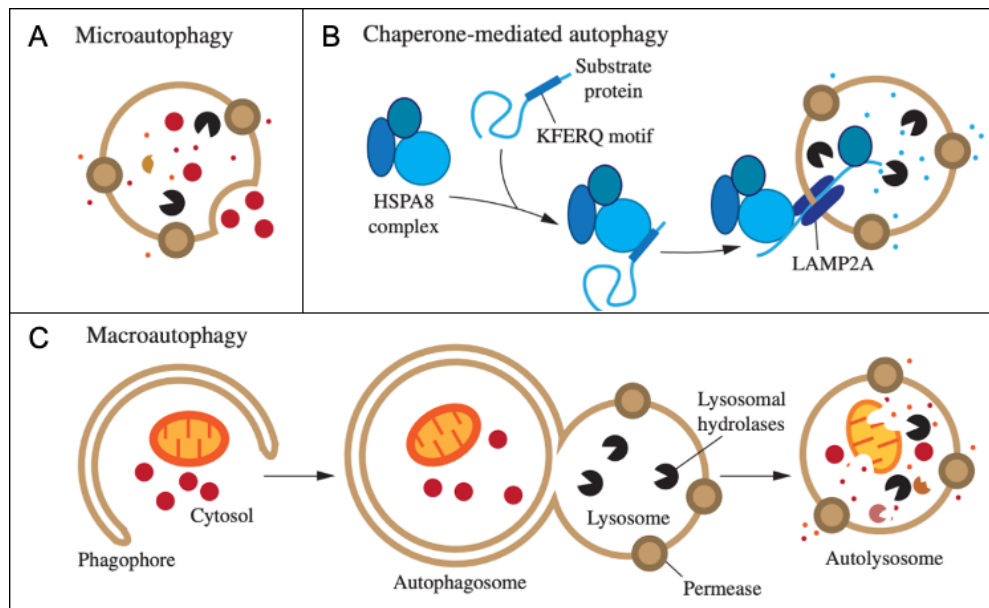
<u>**Figure 1.**</u> **Mammalian autophagy pathways.**
(A) The direct engulfment and subsequent degradation by lysosomal proteases of substrates through the lysosomal or endosomal membrane invagination. (B) Proteins containing a pentapeptide motif are recognized by a chaperone that then promotes the translocation of these targets across lysosomal membranes via a lysosomal transmembrane protein. (C) The de novo formation of a double membrane vesicle that sequesters and transports its cargo to the lysosome for degradation. Modified from Parzych and Klionsky, 2014.

1.5.3. Molecular mechanisms of autophagy

The core machinery for the formation of autophagosomes is composed by a conserved group of 15 autophagy-related proteins (ATGs). These genes were initially discovered and characterized in yeast (Thumm et al. 1994; Tsukada and Ohsumi 1993; Harding 1995), but homologs are now known in all eukaryotes (Kraft and Martens 2012; Lamb, Yoshimori, and Tooze 2013; Mizushima, Yoshimori, and Ohsumi 2011). The landmark event in macroautophagy is the generation of autophagosomes, double-membrane structures that sequester a portion of the cytoplasm, including proteins and organelle, that is then trafficked to the lysosomes. The morphological characteristic that makes macroautophagy unique compared to other intracellular vesicle-mediated trafficking processes is that the autophagosomes form *de novo* rather than by membrane budding, that means, autophagosomes form by expansion and do not bud from a pre-existing organelle, already containing cargo (Z. Yang and Klionsky 2010). After nucleation, the phagophore begins to expand and elongate at

both ends to form a cup-shaped structure while sequestering a portion of the cytoplasm (He and Klionsky 2009). Once the two ends of the phagophore meet, the membranes seal to close autophagosomes and sequester the cytoplasmic cargo. One of the most used autophagy markers is the light chain 3 (LC3), a molecule belonging to the Atg8 family, that comprises the three subfamilies LC3, GABARAP and GATE-16. LC3 is incorporated in the membrane of the budding autophagosomes, after the addition of a phosphatidylethanolamine (PE) group that transforms it in its LC3-II form, and it remains associated with the autophagosomes membrane through degradation. Therefore, measuring the ratio of the LC3-II over LC3-I form of this protein can give an idea of the amount of autophagosomes formation at a given point (Evans et al. 2018). Autophagosomes can sequester cargo non-selectively in a bulk fashion and degrade it, for example, to increase the availability of amino acids upon nutrient deprivation (Mortimore and Schworer 1977). Alternatively, proteins and organelles can be selectively degraded through a mechanism that engages specific cargo with the autophagic membranes binding, identifying the target with autophagy cargo adapters such as p62 (Mijaljica, Prescott, and Devenish 2012; Pankiv et al. 2007). With this tagging process, p62 is engulfed in the autophagosome and taken for lysosomal degradation in the process along with the cargo (Bjørkøy et al. 2005). Consequently, since p62 is an autophagy substrate, its levels can inversely correlate with the autophagy activity: a decrease in p62 would suggest an increased rate of degradation and thus elevated autophagy (Mizushima, Yoshimorim, and Levine 2010).

After membrane closure, autophagosomes move along the microtubules and eventually fuse with lysosomes, generating structures termed autolysosomes (Z. Yang and Klionsky 2009). Once exposed to the acidic lumen and to the hydrolases provided by the lysosomes, the cargoes and the inner membrane of the autophagosomes are degraded and the component parts are transported back into the cytoplasm through lysosomal permeases for use by the cell in biosynthetic processes or to generate energy (Yorimitsu and Klionsky 2005b). In mammals, macroautophagy (which by convention will be called autophagy in this thesis) usually converges with the endocytic pathway. Consequently, before fusing with lysosomes, autophagosomes might also fuse with early or late endosomes to form amphisomes, which will later fuse with lysosomes to become autolysosomes (Parzych and Klionsky 2014). For ease of discussion, the autophagic process can be divided into three steps that will be further discussed into details.

1.5.3.1. Autophagy initiation and vesicles nucleation

During metabolic stress or starvation condition, vesicle nucleation takes place at pre-autophagosomal structure (PAS), that is believed to be an organizational site for the assembly of the autophagy initiation machinery. A pivotal role in autophagy initiation is played by the mammalian target of rapamycin (mTOR), a serine/threonine kinase master regulator of cellular metabolism that is able to promote anabolic cellular metabolism, by integrating various stimuli, and promoting synthesis of protein, lipid and nucleotides while blocking catabolic processes such as autophagy (Laplante and Sabatini 2013; Shimobayashi and Hall 2014). mTOR critically regulates autophagy initiation by activating or deactivating UNC51-like kinase1 (ULK1) via phosphorylation, thereby inhibiting ULK1 kinase activity (Ashford and Porter 1962; Weidberg, Shvets, and Elazar 2011; Mercer, Kaliappan, and Dennis 2009). Upon nutrient depletion, mTOR is deactivated and it dissociates from the ULK1 complex, leading to the activation of ULK1 kinase activity (Lippai and Szatmári 2017). Activated ULK1/2 also enhances the activity of the autophagy nucleation complex by phosphorylation (Kim et al. 2013). PI3K is recruited to the PAS and is required for the synthesis of phosphatidylinositol-3-phosphate (PI3P) (Fig.2) (Chan 2009; Russell et al. 2013).

1.5.3.2. Autophagosomes elongation and closure

The elongation of membranes that evolve into autophagosomes is regulated by two ubiquitination-like reactions (Callis 2014). In the first ubiquitination-like reaction, Atg12, an ubiquitin-like protein, is conjugated to Atg5 by Atg7, which acts like an E1 ubiquitin-activating enzyme, and by Atg10, which is similar to an E2 ubiquitin-conjugating enzyme (Tanida et al. 1999; Shintani et al. 1999; Ohsumi 2001). The complex resides on the outer side of the autophagosomes and facilitates the second ubiquitination-like reaction. In the second of the ubiquitination-like reactions, LC3 is conjugated to the PE (Shpilka et al. 2011). Nascent LC3 is first processed to a glycine-exposed form by the protease Atg4, then the conjugation with the PE is mediated by E1 and E2-like enzymes named Atg7 and Atg3 respectively (Nakatogawa 2013). The result of this elaborate process is a lipidated LC3 (defined as LC3-II), that is subsequently attached to both the inner and outer membrane of the expanding phagophore.

Before autophagosome completion, all Atg proteins except for LC3 dissociate from the isolation membrane and are recycled to the PAS. While the LC3-II on the cytoplasmic

surface is separated from the autophagosome membrane by LC3-PE de-conjugation mediated by Atg4, the LC3-II bound on the inner autophagosome membrane is trapped inside and will be degraded by lysosomal enzymes (Fig.2) (Satoo et al. 2009). Although the exact function of LC3 in the process of autophagy remains unclear, it is a widely used autophagy marker, since it localizes to autophagic structures from the early steps till degradation (Klionsky et al. 2016). All proteins involved in autophagosome elongation steps are summarized in Table 1.

Table 1. **Summary of proteins complexes involved in autophagosomes elongation steps of autophagy.**

Protein complexes	Specific protein components
ATG12-conjugation system	Atg12, Atg5, Atg7, Atg10
LC3-conjugation system	LC3-I, Atg4, Atg7, Atg3

1.5.3.3.   Autophagosomes maturation

The last step of this process involves the maturation of the autophagosomes into autolysosomes, by the fusion of this newly formed and fully closed vesicles with lysosomes, where the degradation of the enclosed cargo happens (Mizushima 2007). The acidic lumen and resident hydrolases of the lysosome degrade the autophagic cargo and the inner membrane of the newly formed autolysosome and the components are recycled for biosynthetic processes or energy production via lysosomal permeases, that allows the transport back into the cytoplasm (Yorimitsu and Klionsky 2005a). A crucial point of this process is the full closure of the autophagosome membranes, in order to prevent massive disintegration of cytoplasmic components by the wide variety of hydrolases contained within the lysosome and the point of no return for the whole process.

Therefore, completed autophagosomes move to the cellular site where lysosomes are clustered in microtubule and dynein-dynactin motor complex dependent manner, allowing fusion of the vesicles and subsequent degradation of autophagic contents by lysosomal proteases (Fig.2) (Kimura, Noda, and Yoshimori 2008).

Introduction
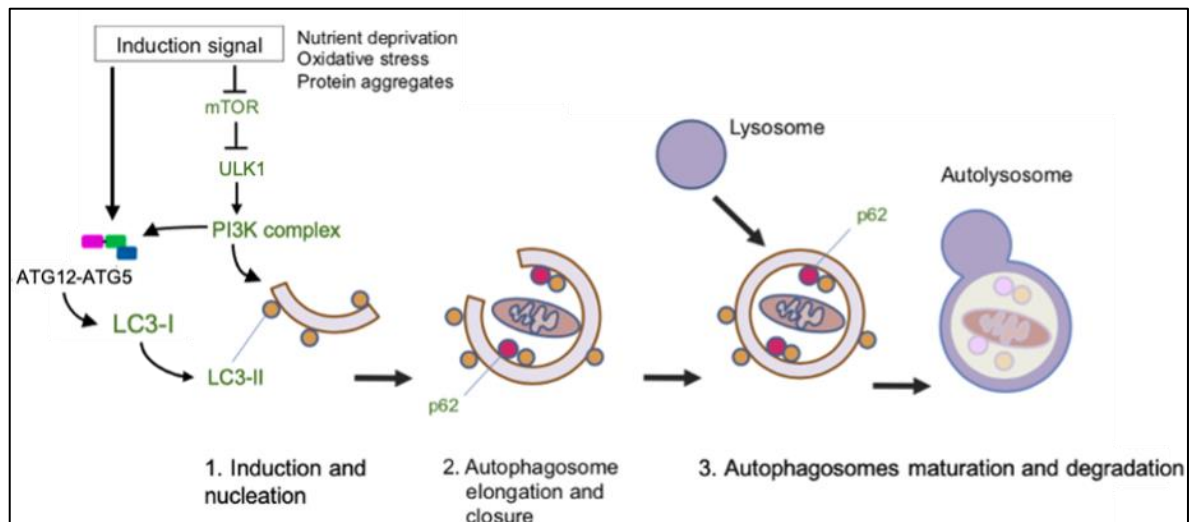
Figure 2. Simplified overview of the different steps of autophagy.
An induction signal, such as metabolic stress, starvation or other autophagy inductor signals inhibits mTOR, therefore activating ULK1 complex. ULK1 complex activates PI3K complex that initiates the phagophore formation. The phagophore is then elongated via the ATG12-conjugation system and LC3-conjugation system. Eventually, maturation of the autophagosome takes place with the fusion of lysosome and degradation of the cargo. Modified from Tomoda et al., 2019.

1.5.3.4. Amphisomes

Endosomes form from the invagination of the plasma membrane and their cargo includes a wide range of nutrients, receptor-ligand complexes, membrane proteins, fluids, as well as extracellular components, bacteria, viruses and so on (Maxfield and McGraw 2004; Piper and Katzmann 2007). These organelles are dynamic membrane-enclosed structures that undergo morphological and biological changes accompanied by vesicle trafficking: in the peripheral cytoplasm, endocytic vesicles deliver their contents and their membrane to early endosomes, that act as a sorting station for recycling (Helenius et al. 1983). On the other hand, late endosomes no longer receive endocytic vesicles and eventually fuse unidirectionally with lysosomes to degrade their cargo (Maxfield and McGraw 2004). For example, in the receptor mediated endocytosis, that internalizes both the receptor and its ligand, the ligands are subsequently degraded in late endosomes or lysosomes, while the receptors are usually recycled many times (Piper and Katzmann 2007). In mammals, studies suggest that autophagy might cross paths with early and late endosomes before fusing with lysosomes: autophagosomes can interact with components of the endocytic pathway (early or late endosomes) to form hybrid organelles called

amphisomes, which then fuse with lysosomes to become autolysosomes and recycle their cargoes (Berg et al. 1998; Eskelinen 2005; Tooze et al. 1990).

1.6. Autophagy in the brain

Neurons are perennial cells that are generated during a time window that closes before birth, after which only few neurons can replace the ones lost by age or injury in the majority of brain regions (Purves et al. 2001). Moreover, neurons have an elaborate morphology characterized by a uniquely polarized cellular architecture that allow them to transmit electric signals along their structure sometimes up to meters away from their generation point. Such features represent a striking challenge for managing proteins and organelles turnover in order to ensure the removal of the dysfunctional ones (Ariosa and Klionsky 2016; Kulkarni et al. 2018; Yamamoto and Yue 2014). Therefore, autophagy has a pivotal role for neuronal homeostasis that was confirmed initially by the neural-specific depletion of genes required for autophagy: the CNS specific deletion of ATG5 or ATG7, two proteins belonging to the ATG12-conjugation system and involved in the elongation step of the autophagosomes formation during embryonic development (Tanida et al. 1999; Shintani et al. 1999; Ohsumi 2001), resulted in viable pups that at 3 weeks of age start to develop progressive motor and behavioural deficits, with their cortex and cerebellum that show, among other pathological signs, ubiquitin containing inclusions, an accumulation that can be found as well in many neurodegenerative diseases such as Alzheimer's disease and Parkinson's disease (Hara et al. 2006; Komatsu et al. 2006). Likewise, defects in the autophagic pathway, or its natural diminished activity that occurs with age, might lead to accumulation of misfolded proteins, as it is the case of neurodegenerative diseases like Alzheimer's disease and Parkinson's disease (Menzies et al. 2017). All these studies show how the continuous quality control of proteins via basal constitutive autophagy is critical to neuronal survival and, accordingly, many other researches demonstrate the beneficial role of the upregulation of autophagy in animal models of neurodegenerative diseases (Ghavami et al. 2014; Menzies et al. 2017). Researches have been focusing on ways to induce an increase in autophagy in neurons, but even under strong autophagy induction conditions such as inhibitors of the mTOR kinase pathway like rapamycin (E. F.C. Blommaart et al. 1995; Sabers et al. 1995) and nutrient deprivation (Barber et al. 2001; Vander Haar et al. 2007), the efficiency of neuronal autophagy is not perturbed, as the

fusion of autophagosomes with lysosomes is highly active in these cells (Boland et al. 2008). Moreover, in rodent brains, ATG proteins, that are essential for autophagic delivery of cargo to the vacuole, are highly expressed, but autophagic activity markers are low compared with other tissues and detecting autophagy has been particularly challenging in neurons compared to other cell types, since autophagic vesicles are difficult to visualise by electron microscopy or even when fluorescent reporters are used (Mizushima et al. 2004; Nixon et al. 2005). Another evidence of the fine tuning of neuronal autophagy is its adaptation to the microenvironment of synapses, that requires temporal and spatial regulation in order to accomplish functions that might be related also to synaptic transmission (Ariosa and Klionsky 2016; Vassiliki Nikoletopoulou and Tavernarakis 2018). An example of this tight regulation of autophagy in synapses could be the different motility of autophagosomes along the neuronal compartments: on the presynaptic bouton, autophagosomes form in the distal end of the axon and undergo a primarily unidirectional motility toward the soma (Hollenbeck 1993; Maday and Holzbaur 2014; Maday, Wallace, and Holzbaur 2012): after formation, autophagosomes migrate from the distal axon to the soma while they mature into degradative autolysosomes (M.-M. Fu, Nirschl, and Holzbaur 2014; Cheng et al. 2015) and, upon entry into the soma, autophagosomes are confined to the somatodendritic compartment (Maday and Holzbaur 2016). On the other hand, the motility of autophagosomes in dendrites is bidirectional or oscillatory within a confined region along the dendritic shaft (Maday and Holzbaur 2014) (Fig. 3).
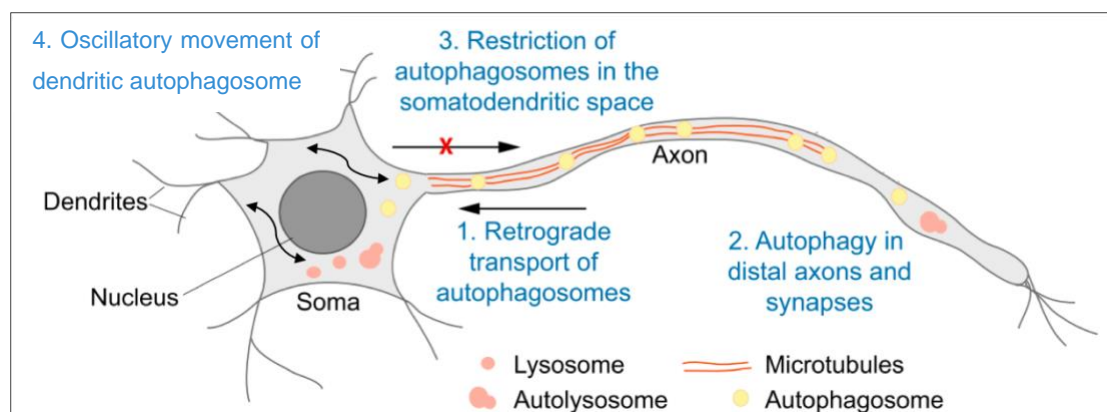
Figure 3. **Neuronal autophagosomes different motilities.**
Autophagosomes that form in the presynaptic compartment in the distal end of the axon are subjected to a primarily unidirectional motility toward the soma: upon entry into the soma, autophagosomes are confined to the somatodendritic compartment and their movement is restricted. Conversely, autophagosomes that form in dendrites can have a bidirectional or oscillatory motility within a confined region along the dendritic shaft. Modified from Ariosa and Klionsky, 2016.

1.6.1. Presynaptic autophagy

More and more researches are showing how presynaptic autophagy is distinct from basal autophagy and activated only under certain conditions, allowing for speculations on how autophagy can shape synapses: for example, the normal aging-induced decrease in synaptic vesicle density can be counteracted by dietary supplementation of spermidine, a substance usually declining with age, that can restore levels of core autophagic proteins and rescue the age-dependent reduction in synaptic vesicles density in hippocampal mossy fiber-CA3 synapses, possibly including autophagic turnover of presynaptic components (Maglione et al. 2019). The age-induced memory impairment in the mushroom bodies of *Drosophila* can be reproduced by impairing the transcript expression level of an NPY family member (sNPF), that are controlled by autophagy in this area. This manipulation disrupts the mushroom bodies integration of the metabolic state of the flies, through the cross-talk between autophagy and sNPF signalling, initiating the age-induced memory impairment in *Drosophila* (Bhukel et al. 2019). On the other hand, autophagy controls developmental spine pruning, that requires mTOR-regulated autophagy, as it corrects synaptic pathologies and social behaviour deficits in autism spectrum disorders (ASDs) with hyperactivated mTOR (Tang et al. 2014). Moreover, autophagy seems to mediate degradation of synaptic vesicles and therefore it seems to regulate neurotransmitter release under some conditions: the induction of autophagy in dopaminergic neurons can stimulate synaptic vesicles degradation, while loss of this pathway leads to an increase in synaptic vesicles release and/or number (Hernandez et al. 2012). Similarly, in *Drosophila*, the loss of Skywalker, a GTPase activating protein that in humans causes severe neurodegeneration, epilepsy, and DOOR (deafness, onychdystrophy, osteodystrophy, and mental retardation) syndrome, determines a larger readily releasable pool of synaptic vesicles and show a dramatic increase in basal neurotransmitter release, that can be rescued by the homotypic fusion and vacuole protein sorting complex, rescued the neurotransmission and neurodegeneration defects in sky mutants (Fernandes et al. 2014; Uytterhoeven et al. 2011). In rat cortical neurons, interfering with the endosomal sorting complex required for transport system and Rab GTPases affects the activity-dependent degradation of synaptic vesicles, as they are as essential components of this use-dependent degradative pathway (Sheehan et al. 2016). Also the brain-derived neurotrophic factor (BDNF) can suppress autophagy in neurons and its conditional deletion shows an

overabundance of autophagosomes in the presynaptic compartment (Vassiliki Nikoletopoulou et al. 2017). It was recently demonstrated that the BDNF/TrkB signalling can restrain the amphisomes in axon terminals and use them as signaling and sorting platforms while trafficking in a retrograde direction, therefore mediating activity-dependent synaptic change (Andres-Alonso et al. 2019). Instead, an opposite effect can be seen in the absence of Bassoon, a presynaptic active zone protein that interact with ATG5, and this loss triggers an increase in presynaptic autophagy, accompanied by a decrease in the number of synaptic vesicles and the elimination of synaptic junctions (Okerlund et al. 2017; Waites et al. 2013).

1.6.2. Postsynaptic autophagy

In the postsynaptic end, Nikoletopoulou et al. (2017) demonstrated that autophagy might modulate synapses by degrading postsynaptic scaffolding proteins (such as PSD-95, SHANK3 and PICK1), providing a possible mechanism through which autophagy could control synapse morphology and synaptic transmission. Few studies show as well how autophagy contributes to the direct degradation of neurotransmitter receptors, thus modulating synaptic organization and plasticity: Rowland *et al.* (2006) demonstrated that without presynaptic innervation, autophagy is upregulated in the postsynaptic cells and $GABA_A$ receptors accumulate in autophagosomes that are targeted for degradation (Rowland et al. 2006). Likewise, Shehata *et al.* (2012) showed how chemical long-term depression (LTD) promotes an increase in autophagy that internalizes and eventually degrades AMPA receptors, an effect that was mitigated by autophagy inhibitors. As a matter of fact, lysosomes degrade AMPA in an activity-dependent manner and their trafficking into dendritic spines is regulated by synaptic activity (Ehlers 2000; Schwarz, Hall, and Patrick 2010). The trafficking of lysosomes at spine bases and shaft synapses is regulated via actin patches, that frequently co-localizes with excitatory synapse markers in dendrites of mature neurons: these actin patches act as passive, physical barriers by slowing down the transport of vesicles and they potentially could be rapidly altered by synaptic activation (Bommel et al. 2019). Therefore, the regulation of AMPA receptor seems to be possible via the lysosomes locally positioned at dendritic spines in an activity-dependent manner, in order to facilitate the remodelling of synapses through local degradation (Goo et al. 2017).

1.6.3. Autophagy & psychopathologies

More and more evidences are showing how autophagy deficits are linked to neuropsychiatric conditions, synaptic plasticity deficits and cognitive impairments at the cellular and organismal level: the Fmr1-KO mice, a model of human FXS, have an excessive mTOR activity that provokes a decrease in autophagy, with subsequent spine defects, exaggerated synaptic plasticity, and impaired cognition (Yan et al. 2018). Autophagy is downregulated as well in patients with schizophrenia and bipolar disorder, as neuronal cells sampled from living human subjects via nasal biopsy show, compared with healthy control subjects: it seems that this decrease in the autophagic activity is misbalancing the excitatory-inhibitory neurotransmission, by selectively downmodulating surface GABAA receptor levels without affecting surface NMDA receptor levels (Sumitomo et al. 2018). Conversely, an increase in autophagy seems to be beneficial, as it is the case for the role that autophagy plays in depression: Gassen *et* al. (2014) showed that autophagy markers were increased after an antidepressant treatment with the FKBP51 (a regulator of the glucocorticoid receptor) in both mice brains and human blood cells, and Kara *et al.* (2013) showed that the use of trehalose, an mTOR-independent autophagy enhancer (Sarkar *et al.*, 2007), has antidepressant effects in mice. Indeed, the interplay between antidepressants and autophagy has been proven as well in a more recent study by Gulbins et al. (2018): this research shows how several classes of antidepressants (e.g., amitriptyline, fluoxetine and so on) commonly activate autophagy and reverse depressive behaviour in a stress-induced depression model. Upregulation of autophagy is also able to alleviate deficits in synaptic plasticity and improve cognition in drug- or stress-induced rodent models of cognitive impairment: rapamycin, an inhibitor of mTOR, efficiently alleviated the melamine-induced impairments of LTP and depotentiation, while at the same time increasing the expression level of autophagy markers (J. Fu et al. 2017); also rapamycin relieves the anxious emotion, and partly alleviate the hippocampal synaptic plasticity deficits, in a hindlimb unloaded animal model of synaptic plasticity impairment (Zhai et al. 2018). The induction of autophagy in hippocampal neurons is as well required for shaping activity-dependent synaptic plasticity: in this work, Glatigny and colleagues show how the stimulation of neurons promotes an autophagic response that in turn determines memory formation by promoting the production of dendritic spines and increasing synaptic molecular strength, in order to modulate the

adaptive responses of hippocampal neurons to novel stimuli (Glatigny et al. 2019a). Conversely, autophagy could be employed to augment the erasure of memories: Shehata and colleagues showed that in an auditory fear reconsolidation mice model, autophagy contributes to fear memory destabilization and its induction could enhance the erasure of this a reconsolidation-resistant fear memory, thus providing a potential therapeutic opportunity for the treatment of anxiety disorders (Shehata et al. 2018). Taken all this evidences together, it appears likely that autophagy may have an important role in certain forms of synaptic plasticity and memory formation, in particular during fear memory formation, where the regulation of the stress response might as well take part.

2. Hypothesis

Evidences show how NPY has an anxiolytic effect during stressful conditions (Heilig *et al.,* 1989; Śmiałowska *et al.*, 2007, Raza *et al.*, 2017) and it also increases neuronal autophagy *in vitro* and *in vivo* (Aveleira et al. 2014; Ferreira-Marques et al. 2016), a cellular process that is a strong modulator of pre- and postsynaptic neuronal plasticity. Since an increase in autophagy seems to be important during presentation of novel stimuli in hippocampus (Glatigny et al. 2019a), as well as in fear memory destabilization of a reconsolidation-resistant fear memory (Shehata et al. 2018), it can be speculated that NPY could be a possible synaptic factor linking experience driven synaptic plasticity and autophagy in the framework of stress and anxiety: the NPY-induced autophagy may modulate synaptic plasticity, thereby ultimately contributing to behavioural stress resilience *in vivo*.

By using the NPY-induced autophagy increase in primary hippocampal and primary cortical neuronal co-cultures and a FC stress paradigm that is able to activate the same neural structures of PTSD patients and can recapitulate some of its symptoms, such as trigger-induced persistent and exaggerated learned fear, in this thesis the molecular mechanisms and behavioural aspects of the NPY action in synapses via autophagy will be elucidate by addressing the main following objectives:

- Identify NPY targets affected by autophagy and consequences for neuronal function in primary neuronal cell co-cultures;
- Verify NPY targets in an animal model of stress and evaluate the effects of the NPY action on a behavioural and histological level.

Understanding the molecular effect of NPY via autophagy during stressful conditions could give insight into new molecular players of this complex biological mechanisms and eventually novel targets for therapies against PTSDs.

3. Materials and Methods

3.1. Materials

3.1.1. Chemicals and solutions

All chemicals and solutions were purchased from Invitrogen, Roche, Roth, Sigma Aldrich, Thermo Scientific, Tocris and Merck in *pro analysis* or molecular-biology grade. In the method description, supplier and composition information of special chemicals and solutions are mentioned. Molecular biology-graded H_2O (Roth) was used for protein biochemical experiments and cloning experiments. For all other experiments, such as buffer preparation, bi-distilled water (ddH$_2$O) from the Milli-Q System (Millipore) was used. Special chemicals and solutions are mentioned at the beginning of each corresponding methods section.

3.1.2. Primary antibodies

Table 2. Primary antibodies

Antibody	Specie	Dilution		Supplier
		WB	ICC/IHC	
α-β-actin	ms, monoclonal	1:2500		Sigma
α-ATG5	rb, monoclonal	1:1000		Cell Signalling
α-EAAT3	rb, polyclonal	1:1000		Abcam
α-4EBP2	rb, polyclonal	1:1000		Cell Signalling
α-ERK1/2	ms, monoclonal	1:1000		R&D systems
α-pERK1/2	rb, polyclonal	1:2000		R&D systems
α-GABA-A receptor β1	ms, monoclonal	1:1000		Neuromab
α-GABA transporter 1	rb, polyclonal	1:1000		SYnaptic SYstems
α-GAD65	ms, monoclonal	1:1000		Abcam
α-GluR1 (AMPA)	rb, monoclonal	1:1000	ICC/IHC 1:200	Cell Signalling
α-GluR1 (extracellular)	gp, polyclonal		ICC 1:200	Alomone Labs
α-LC3 A/B	rb, polyclonal	1:2000	ICC/IHC 1:250	Cell Signalling
α-MAP2	ck, polyclonal		ICC 1:1000	SYnaptic SYstems

α-MAP2	ms, monoclonal		ICC 1:1000	Sigma
α-NMDAR1	rb, polyclonal	1:1000		Cell Signalling
α-p62	rb, polyclonal	1:2000		Cell Signalling
α-shank2	gp, polyclonal		ICC 1:1000	SYnaptic SYstems
α-synaptophysin 1	gp, polyclonal	1:20000		SYnaptic SYstems
α-VGlut	ms, monoclonal	1:1000	ICC 1:1000	SYnaptic SYstems
α-VGat	gp, polyclonal	1:1000		SYnaptic SYstems
α-Ubiquitin	rb, polyclonal	1:1000		Cell Signalling

3.1.3. Secondary antibodies

Table 3. Secondary antibodies.

Antibody	Specie	Dilution		Supplier
		WB	ICC/IHC	
α-rb IgG, HRP conjugated	donkey	1:7500		Jackson ImmunoResearch
α-ms IgG, HRP conjugated	goat	1:7500		Jackson ImmunoResearch
α-ms IgG IRDye® 800CW conjugated	goat	1:15000		Li-Cor
α-rb IgG IRDye® 800CW conjugated	goat	1:15000		Li-Cor
α-gp IgG IRDye® 800CW conjugated	donkey	1:15000		Li-Cor
α-ms IgG IRDye® 680CW conjugated	donkey	1:15000		Li-Cor
α-ms IgG Alexa Fluor® 488 conjugated	goat		ICC 1:2000	Abcam
α-rb IgG Cy3 conjugated	donkey		ICC 1:2000	Jackson ImmunoResearch
α-ch IgY Alexa Fluor® 647 conjugated	donkey		ICC 1:1000	Jackson ImmunoResearch
α-rb IgG Alexa Fluor® 555 conjugated	donkey		IHC 1:1000	Invitrogen
α-rb IgG Alexa Fluor® 488 conjugated	donkey		IHC 1:1000	Invitrogen
DAPI (1 mg/ml)	-		ICC/IHC 1:100	Sigma

Materials and Methods

3.2. Cell culture

3.2.1. Animals

In this study, Wistar rats (*Rattus norvegicus*/Wistar) from the animal facility of the Institute of Pharmacology and Toxicology (Magdeburg, Germany) were used. Adult rats were housed in groups of 5-6 animals, under a regular 12 h light-dark schedule (lights on 6 AM-6 PM) with food and water available *ad libitum* at constant temperature (22± 2°C) and relative humidity (50%). Any effort was made to minimize the number of animals used and their suffering during experiments.

3.2.2. Primary cortical and hippocampal cells

- Poly-d-lysine (PDL): 150mM borate buffer pH8.5, poly-d-lysine (100µg/mL);
- Neurobasal™ medium: Neurobasal™ medium, 1xB-27, 0.8mM glutamine (from Invitrogen);

Primary cortical cells were obtained from E18-E19 *Rattus norvegicus* (Wistar) and were prepared as described by Müller et al. 2015. Briefly, adult rats were deeply anaesthetized with Isofluran Baxter (Baxter GmbH) prior decapitation using an animal guillotine. Embryos and pups were decapitated without prior treatment using decapitation scissors. Primary cortical cells were seeded in DMEM into different culture vessels and on glass coverslips coated with PDL. For immunocytochemistry experiments, cells were seeded into 24 well plates containing glass coverslips on the bottom of each well at a density of 20.000 cells per well. For western blot experiments, cells were seeded into 6 well plates at a density of 300.000 cells per well. Cells were cultured at 37°C and 5% CO_2. 24h after seeding, the medium was exchanged by Neurobasal™ medium. Cell viability was maintained by adding 10% fresh Neurobasal™ medium once a week.

3.2.3. Cell treatments and drugs

- NPY (Tocris): 100nM for 6h;
- Chloroquine (CQ, Sigma-Aldrich): 50µM for 4h;
- Cycloheximide (CHX, Sigma-Aldrich): 355Mm for 6h;
- Actinomycin D (Sigma-Aldrich): 30µM, 5min before the 6h NPY treatment.

3.2.4. Harvest of primary cortical and hippocampal cells for SDS-PAGE

- Phosphate buffered saline (PBS)-MC: 1 x PBS pH 7.4, 0.1 mM $CaCl_2$, 1 mM $MgCl_2$;
- 4x protein sample buffer: 250mM Tris-HCL pH 6.8, 4% (v/v) SDS, 40% (v/v) glycerol, 20% (v/v) ß-mercaptoethanol, 0.004% (v/v) bromphenol blue;

Primary cortical cells grown in 6 well plates at a density of 300.000 cells per well were washed once with 1mL of ice-cold PBS-MC and then scraped of in 100µL 1x protein sample buffer and transferred into a reaction tube. The cell lysates were incubated at 95°C for 5min and stored at -20°C until further use.

3.2.5. Amido black protein assay

- Amido black solution: 1,44% (w/v) Amido black dye, 10% (v/v) acetic acid, 90% (v/v) methanol);
- Standard: 0.5 mg/ml BSA solution;
- Wash solution: methanol-acetic acid solution composed of 10% (v/v) acetic acid, 90% (v/v) methanol);

The amido black protein assay (Heda et al. 2014) was executed in a 96-well plate to determine the total protein concentration of a certain lysate. Triplets of each sample and the BSA standard were pipetted. The BSA standard was adiluted from a 0.5mg/mL stock solution to reach a final concentration of 2, 4, 8, 12, 16 and 20µg of total protein in a volume of 100µL with molecular biology graded H_2O. 5µL of each protein lysate sample was diluted in 95µL molecular biology graded H_2O. 200µL of amido black solution was added to each well and the mix was incubated for 10min at RT. Centrifugation was carried at 3220xg (Eppendorf centrifuge 5810R), followed by a 10min incubation at RT. After carefully decanting the supernatant, 300 µL of wash solution was applied and the plate was centrifuged with the same settings. This step was repeated twice and then the pellets were air-dried after decanting. Resuspension of the pellets was conducted with 300µL of 0.1M NaOH with gentle agitation. Extinction at 620nm was measured with a photometer (Infinite® F50, Tecan) and the read out displayed with the Magellan™ software. All the lysates were diluted to reach a final concentration of 0.5 µg/µL.

3.2.6. Sodium dodecyl sulfate polyacrylamide gel electrophoresis (SDS-PAGE)

Table 4. Composition of SDS-PAGE Tris Glycine gradient (5-20%) gels

Components	Volume for separating gel		Components	Volume for stacking gel
	5%	20%		

1.8M Tris-HCL pH8.8 (mL)	6.84	6.84	0.5M Tris-HCL pH6.8 (mL)	9.00
40% (v/v) acrylamide (Applichem) + 0.8% (w/v) bis-acrylamide (Serva) (mL)	4.06	16.20	Rotiphorese® Gel 30 (mL)	5.76
ddH$_2$O (mL)	18.94	1.39	ddH$_2$O (mL)	11.88
10% (v/v) SDS (µL)	316.8	316.8	10% (v/v) SDS (µL)	360
0.2M EDTA pH8.0 (µL)	316.8	316.8	0.2M EDTA pH8.0 (µL)	360
87% (v/v) glycerol (mL)	1.8	7.2	87% (v/v) glycerol (mL)	8.28
0.5% (v/v) bromphenol blue (µL)	-	150	0.5% (w/v) phenol red (µL)	175
10% (w/v) APS (µL)	115.2	72	10% (w/v) APS (µL)	222.30
TEMED (µL)	21.6	21.6	TEMED (µL)	27.30

- Electrophoresis buffer: 0.25M Tris-base, 1.92M glycine, 1% (v/v) SDS;

In order to separate proteins according to their molecular weight, SDS-PAGE that was conducted according to the standards described by Laemmli 1970. SDS-PAGE gradient gels (5-20%) (Table 6) were inserted into the Hoefer™ Mighty Small System SE250 basic unit electrophoresis chamber from Hoefer™ (Amersham Biosciences). Samples were loaded into the pockets of the gel at a concentration of 0.5 μg/μl for a total of 10μg/μl per sample loaded. The protein separation was carried at a voltage of 12mA per gel and the electrophoretic run was terminated when the bromphenol blue front left the separating gel. The PageRuler™ prestained protein ladder (4µL, ThermoFisher Scientific) was used as marker in SDS-PAGE.

3.2.7. Westernblot (WB)

- Blocking solution: 1x Tris buffered saline (TBS), 5% (w/v) dry milk (Spinnrad®)
- Primary antibody solution: 1x TBS supplemented with 0.1% (v/v) Tween® 20 (TBS-T), 0.02% (v/v) Azide, 0.1% (w/v) BSA;
- Ponceau staining solution: 0.5% (w/v) Ponceau, 3% (v/v) acetic acid;
- Western Blot buffer: 0.25M Tris-base, 1.92M glycine, 0.2% (v/v) SDS;

WB was performed to identify the amount of a specific protein in different samples by the use of protein specific antibodies. The proteins in the separating gel were transferred onto a 0.45µm (GE healthcare) in the TE22 mighty small transpher unit from Hoefer™ at 200mA for 1.5h. When the transfer process was over, membranes

were incubated for 10min with Ponceau staining solution for protein visualization and -fixation. The stain was removed by few washings in ddH$_2$O and 1xTBS. To avoid unspecific binding of the primary antibody, the membrane was blocked with 5 % dry milk in TBS for 1h at RT under gentle agitation. After three times washing with 1xTBS, primary ABs were incubated overnight at 4 °C under permanent agitation. On the next day, membranes were washed 10min with 1xTBS, 10min with 1xTBS-T, 5min with 1xTBS-T and 5min with 1xTBS. Afterwards, the membranes were incubated with the specie corresponding secondary HRP-conjugated AB (1:7500 in 5 % milk in TBS-T) for 1h or with the specie corresponding secondary IRDye conjugated AB (1:15000 in 2% BSA in TBS) for 1.5h at RT under gentle agitation, followed by the same washing procedure. Immunoblotting was visualized either directly for fluorescent secondary Abs in an Odyssey Fc (Model: 2800 from LI-COR® Biosciences GmbH), with exposure times set to 2 or 5, or membranes were developed with ECL reagents (ThermoFisher Scientific) according to the manufacturer's instructions for HRP-conjugated secondary antibodies and the chemiluminescence captured with the Odyssey Fc luminescence detector (Model: 2800 from LI-COR® Biosciences GmbH) with exposure times set to 10 min.

3.2.7.1. WB pictures analysis

Tif pictures exported from Image Studio Lite software (version 5.2.5) in print quality mode were analysed in FIJI. Briefly, the densitometry bands were segmented using the "Rectangle selections" tool. The first band was marked by pressing "Ctr" "1. The box was then dragged to the next band and "Ctr" "2" was pressed to select it and this step was repeated for each band. Once all the bands were selected, "Ctr" "3" was pressed to bring up a histogram indicating the intensity of each of the bands. Starting with the histogram for the first band, the "Draw line" button was selected to draw a line across the top of the histogram from where it first begins to drop steeply until where it levels out again. To obtain the intensity of the band as a numerical value, the "Magic wand" button was used inside the area of the histogram that contains the peak. Samples used for SDS-PAGE and WB were from at least three independent experiments and they were used for a minimum of three technical replicates. Technical replicates of the same sample were then averaged during statistical analysis, in order to obtain one value per sample per independent experiment.

3.2.8. Immunostaining

3.2.8.1. Fixation and immunocytochemistry

- Periodate-lysine-paraformaldehyde (PLP) fixative: 4% (v/v) PFA, 2.16% (w/v) glucose, 1.83% (w/v) lysine hydrochloride, 0.2M phosphate buffer pH 7.4, 0.336% (w/v) sodium (meta) periodate;
- B-Block: 10% (w/v) normal horse serum, 5% (w/v) sucrose, 2% (w/v) BSA, 1x PBS pH 7.4, 0.2% (v/v) Triton-X-100;
- Mowiol: 10% (w/w) Mowiol, 25% (v/v) Glycerol, 100mM Tris-HCL pH 8.5, 2.5% (w/v) DABCO;

Cells were washed once in ice-cold PBS-MC before covered with the fixation solution. Cells were incubated in PLP fixative prepared as described by McLean and Nakane 1974 for 30min at RT. After three washing steps with 1x PBS pH 7.4 for 10min, cells were incubated with B-Block for 1h at RT. Fixed and permeabilised cells were incubated with primary antibodies diluted in B-Block overnight at 4 °C. The next day, cells were washed three times with 1x PBS pH 7.4 for 10min and then incubated with the respective secondary antibody diluted in B-Block for 1h at RT. Following this step, cells were incubated with DAPI (Invitrogen) in 1x PBS pH 7.4 for 10min at RT. After three times wash with 1x PBS pH 7.4, the coverslips were briefly rinsed in ddH$_2$O and then mounted in Mowiol (6µL for 24 well coverslips), with cells facing the object slide. When using the external portion recognizing GluA1 antibody, cells were live stained: the antibody was added to the medium 30 minutes before fixation, during which the cells were put back in the incubator. Cells were then fixed and stained as described above. A microscope from Axioplan 2 imaging (Zeiss) was used for imaging the cells and z-stack pictures were captured with the CCD camera Spot RT camera and the ZEN 2012 SP5 FP1 (black) software (version 14.0.9.201, Zeiss). The objective EC Plan Neofluar 63x/1.40 Oil DIC M27 (AA=0.19mm) as well as different filter sets (Zeiss) were used.

3.2.8.2. ICC pictures analysis

All the ICC stainings described in this thesis were performed in three independent experiments with two coverslips per conditions, and a minimum of 10 pictures per experiments per condition were taken (a minimum of 5 pictures per coverslip). Maximum intensity projections confocal pictures (89,97x89,97µm – 1024x1024 pixels) were processed and analysed in FIJI (version 2.0).

To analyse the number of puncta (either LC3 or GluA1), each picture was manually segmented. Briefly, to count the puncta the in the soma of the neurons, the "Oval selections" tool was used to segment the area of the soma. To count the puncta in the main dendrite, the first 50μm of the main dendrite were manually segmented using the "New image" tool with a width of 568 pixels. The area outside the selected soma or dendrite was then filled with black and the image was split into the different channels. The channel displaying the puncta of interest (either LC3 or GluA1) was converted in 8 bit and a threshold was set. The value of the threshold was selected using the pictures of the control condition over the three biological replicates. Puncta were counted using the "Analyze particles" tool. The settings used to define the particles were a size comprised between $3\text{-}75\mu^2$ in pixel units and a circularity of 0.05-1.

The colocalization analysis was performed in "OpenView" (version 1.5), a software written by Noam E. Zlv (Tsuriel et al. 2006). Pictures were first pre-processed in FIJI: the first 50μm of the neuron main dendrite were segmented as previously described, but after splitting the picture into the different channels, the separate channels pictures were all converted into 8 bit/black and white pictures and individually saved as .tif files. A mask for either the pre- (vesicular glutamate transporter - VGlut) or post-synaptic (Shank2) marker was created selecting a threshold value over the control condition pictures in the three independent experiments. The different channels and the mask were then fed into the "OpenView" software for the analysis. The analysis of the colocalization was performed using 6x6 box centred on the mask of either the pre- (VGlut) or post-synaptic (Shank2) marker ("Box_puncta_Ex tool"). The 6x6 boxes were visually checked for each picture, in order to delete overlapping boxes. After the check, the boxes were superimposed on the GluA1 or external-GluA1 puncta using the "Match_Set1", in order to visualise the number and intensity of GluA1 or external-GluA1 puncta inside the boxes. A cut-off value for the intensity was set after careful visualization of the GluA1 or external-GluA1 puncta intensity values obtained from "OpenView" and the actual puncta displayed in the 6x6 boxes in the control condition pictures over the three independent experiments, in order to reduce the possible background noise puncta values.

3.2.9. Molecular biology

Primarily standard molecular procedures were used in this research. Protocols as described in "Molecular Cloning: A Laboratory Manual" (Green and Sambrook,

2012) were followed. Consequently, all protocols are described briefly unless they were significantly altered.

3.2.10. DNA sequences for lentiviral production and vector

The short hairpin (sh) RNA sequences used to KD the genes of interest were inserted into the pFUGW-H1 empty vector (a gift from Sally Temple (Addgene plasmid #25870; http://n2t.net/addgene:25870; RRID: Addgene_25870)). The sequences were found in the literature: the shATG5 sequence against rat ATG5 was generated by Lee and Gao (2009), as well as a scramble sequence used as a control for the viral infections having the pFUGW-H1 as a vector. Oligos were designed as specified in the pFUGW-H1 shRNA cloning protocol described in Addgene. The sequences of each shRNAs and forward and reverse sequences of the oligos ordered to can be seen in table 5.

Table 5. shRNA sequences

shATG5 (rat)	sequence	**ATC TGA GCT ATC CAG ACA A**	Generated by Lee and Gao (2009)
	Top	ATC TGA GCT ATC CAG ACA A**TT CAA GAG A**TT GTC TGG ATA GCT CAG AT**T TTT TTG T**	
	Bottom	**CTA GAC AAA AAA** ATC TGA GCT ATC CAG ACA A**TC TCT TGA A**TT GTC TGG ATA GCT CAG AT	
shScramble	sequence	**GTC CCG GAT ACC TAA TAA**	According to Lee and Gao (2009)
	Top	GTC CCG GAT ACC TAA TAA A**TT CAA GAG A**TT TAT TAG GTA TCC GGG AC**T TTT TTG T**	
	Bottom	**CTA GAC AAA AAA** GTC CCG GAT ACC TAA TAA A**TC TCT TGA A**TT TAT TAG GTA TCC GGG AC	

3.2.11. pFUGW-H1 cloning protocol

The pFUGW-H1 shRNA cloning protocol described in Addgene was followed.

3.2.11.1. Oligos annealing

Briefly, the oligos ordered were dissolved in biology-graded H_2O at a final concentration of 100nM. To perform the primer annealing, 41 μl of H_2O, 5 μl of 10x PCR buffer and 2 μl of each oligos (specifically, 2 μl of top oligos and 2 μl of bottom oligos), with a final volume of 50 μl, were prepared into PCR tubes and the following PCR

program was run: 95°C for 10min followed by a step down to 4°C at a rate of 1°C per minute.

3.2.11.2. Harvest of pFUGW-H1 plasmid fragments

To insert oligos into an empty DNA vector complementary binding sides have to be obtained. To create sticky ends in the vector, two different restriction digest reactions were performed for the pFUGW-H1 vector. While digestion A was performed with both restriction enzymes for 3h at 37°C, digestion B was performed for 1.5h at 25°C and then, after the addition of the second restriction enzyme, the digestion continued at 37°C for another 1.5h. The restriction enzymes used, the buffer concentrations and the final products are listed for each reaction in table 6.

Table 6. **List of restriction digest reactions and final products.**

Digestion A:	1.5μl of XbaI 1.5μl of BshTI (AgeI) 2μl of pFUGW-H1 vector 3μl CutSmart buffer 12μl of H$_2$O	3h, 37°C
Final volume:	20μl	
Final product:	Two bands in gel electrophoresis: one large band (10-12kb) and one small band (1.5kb). **Cut out the large band.**	
Digestion B:	1.5μl of SmaI 2μl of pFUGW-H1 vector 3μl CutSmart buffer 15.5μl of H$_2$O	1.5h, 25°C
Final volume:	20μl	
	Then add 1.5μl of BshTI (AgeI)	1.5h, 37$^{\circ C}$
Final product:	Three bands in gel electrophoresis, the smallest is around 1.5kb. **Cut out the smallest band.**	

3.2.11.3. Agarose gel electrophoresis and gel extraction

- 50x TAE buffer: 24,2% (w/v) Tris, 5,71% (v/v) acetic acid, 0.5M EDTA pH8.0;
- 6x DNA sample loading buffer: 10mM Tris pH7.6, 0.15% (w/v) Orange G, 60% (v/v) glycerol, 60mM EDTA pH7.5;

Materials and Methods

DNA restriction digest products were then cleaned up and separated according to sizes using a 1% agarose gel electrophoresis and subsequent gel extraction. The agarose gel electrophoresis was conducted in the Biometra compactM system from Analytikjena. 1.0% (w/v) LE Agarose (Biozym) was heated up in 1xTAE, until the LE-Agarose was completely dissolved. The solution was then cooled down under mild agitation and, once cooled, and Midori green advanced DNA stain (6µL/100mL LE Agarose-1xTAE, Nippongenetics) was added to the solution before the gel was casted. The gel was placed in the gel chamber with 1x TAE buffer. The DNA fragments contained in the 20µl volume resulting from the restriction digest reactions were diluted in 6x DNA sample loading buffer (to a reach a final concentration of 1x loading buffer) and were loaded in the gel pockets. The gel electrophoretic separation was conducted at 80V. The 1kbp (8µL) GeneRuler DNA ladder (Fermentas) was used as marker. The gel was imaged with a gel documentation system from Vilber and the results printed with the digital graphic printer UP-D897 (Sony). After visualization of the correct run, the gel was placed on a UV table (302nm, Bachhofer Laboratoriumsgeräte) to mark the DNA bands with a scalpel for gel extraction. Depending on the digestion performed, different sizes of fragments were collected for the gel extraction: digestion A results in two bands, one large band (10-12kb), that was cut out and gel extracted, and one small band (1.5kb); digestion B results in three bands,of which the smallest one is around 1.5kb and is the one that was cut out and later gel extracted.The gel extraction was performed using the NucleoSpin® gel and PCR clean-up kit from Macherey-Nagel according to the manufacturer's instructions, including all optional steps. Briefly, the gel fragment was dissolved and the whole sample transferred onto a spin column. After washing the spin column with several buffers, the sample was eluted in 30µL pre-heated elution buffer.

3.2.11.4. Ligation of the annealed oligos and the pFUGW-H1 fragments

The annealed oligos and the pFUGW-H1 fragments deriving from the different restriction digestion reactions were ligated together after their clean up in agarose gel electrophoresis and gel extraction. In order to determine the ratio of the gel extracted fragments, a gel electrophoresis was conducted with a small volume of the pFUGW-H1 fragments. When the intensity of the bands from the pFUGW-H1 fragments visible under UV-light was equal in intensity, a ratio of 7.5:1 was used in the subsequent ligation reaction. In addition, 1µL of the annealed oligos, 1µL 10x T4 DNA ligase buffer

and 0.5µL T4 DNA ligase were added to the reaction, and H_2O was used to bring up the final volume to 20µL. Ligation was performed overnight at 4°C.

3.2.12. Bacterial strain

The bacterial strain used for transformations was XL10-GOLD with the genotype *endA1 glnV44 recA1 thi-1 gyrA96 relA1 lac Hte (mcrA)183 (mcrCB-hsdSMRmrr) 173 tetR FproAB lacIqZM15 Tn10 (TetR Amy CmR)* (Agilent).

3.2.13. Bacterial plasmid DNA transformation

- SOC medium: 2% (w/v) Trypton/Pepton, 0.5% (w/v) yeast extract, 10mM NaCl, 2.5mM KCl, 10mM Mg2SO4, 10mM MgCl2, 20mM glucose;
- LB-plates: 5 g/l yeast-extract, 10 g/l bacto-tryptone, 5 g/l NaCl, 15 g agar
- Antibiotic dilution in LB-Agar: ampicillin 100µg/ml;

pFUGW-H1 empty vector, as well as the ligated pFUGW-H1 vector, psPAX2 packaging vector and pVSVg envelope plasmid (Lois et al. 2002) were amplified in bacteria. For the transformation, the DNA was introduced into heat-shock-competent XI10-Gold bacteria (Stratgene): 0.5 or 1µl of empty vector/20 µl of ligated DNA was added to 100 µl of bacteria and incubated on ice for 10 min. Bacteria were then heat-shocked for 45-second at 42°C and directly put on ice for 2 min. Afterwards, the bacteria suspension was transferred into SOC medium and shook at 37°C for 1h. The mixture containing bacteria with ligated plasmid DNA was centrifuged for 1min at 21000xg. The supernatant was removed until 50µL were left. The bacteria pellet was resuspended in that volume and everything was streaked onto a LB-agar plate with ampicillin resistance encoded by the plasmid DNA. Plates were incubated overnight at 37°C.

3.2.14. Plasmid DNA Mini and Midi preparation

- LB-medium: 5 g/l yeast-extract, 10 g/l bacto-tryptone, 5 g/l NaCl;

To extract the shRNAs ligated in the pFUGW-H1 amplified by bacteria and verify the correctness of the sequences (see section 3.4.6. for details on the sequencing), the NucleoSpin® Plasmid kit from Macherey-Nagel was used. Then, once the sequencing came back positive, the shRNAs inserted in the pFUGW-H1, the psPAX2 packaging vector and the pVSVg envelope plasmid were amplified and subsequently purified with the NucleoBond® Xtra Midi EF/ Maxi EF kit from Macherey-

Nagel in order to produce enough DNA for the lentivirus production. The kits were used according to the manufacturer protocols.

3.2.15. Sequencing and sequence analysis

Sequencing of the shRNA sequences inserted in the pFUGW-H1 plasmid was performed by the company SeqLab using a primer binding with the H1 promoter (ACA GCA GAG ATC CAG TTT G). The program Standard Nucleotide Blast by NCBI was used for sequence analysis.

3.2.16. Lentiviral production

- Vectors: - pVSVg envelope plasmid: $7.14\mu g/75cm^2$ (2 x T75 culture flask);
  - psPAX2 packaging vector: $14.3\mu g/big$ flask/$75cm^2$(2 x T75 culture flasks);
  - shRNAs ligated pFUGW-H1: $28.6\mu g/$ big flask/$75cm^2$ (2 x T75 culture flask);
- 6 x T75 culture flask per batch;
- Solution A: 500mM $CaCl_2$;
- Solution B: 140mM NaCl, 50mM HEPES, 1.5mM Na_2PO_4;
- DMEM$^{3+ or 2+}$: 10%, 4% or 0% (v/v) FCS, 1% (v/v) L-Glutamine; 1% (v/v) Penicillin-Streptomycin (10.000 U/ml) (Gibco);
- Neurobasal ™ (NB$^+$): 2% (v/v) B27; 0.1% (v/v) L-Glutamine; 1% (v/v) Penicillin-Streptomycin (10.000 U/ml) (Gibco)
- Corning® 250 ml vacuum filter/storage bottle system, 0.45 µm pore 19.6cm² CA membrane

Human embryonic kidney (HEK) cells were transfected to produce lentiviruses using the calcium phosphate method and the procedure was performed under S2 safety conditions, all according to Zufferey and Trono, 2000. Briefly, the vectors pVSVg (14.28 µg in total), psPAX2 (28.6 µg) and each cloned pFUGW-H1 vector (57.2 µg) were added to 1ml of solution A. 1ml of solution B was added to the mix and, after thorough mixing, it was incubated for exactly 1min. 1ml of the reaction mixture was added to one T75 culture flask of HEK cells dropwise and the flask was gently mixed. The flasks incubated for 6-8h, after which the medium was changed with DMEM^{3+} with 10% FCS. On the following day, 7 ml of the old medium were removed from each culture bottle and 5 ml of DMEM^{2+} were to the flask, leading to 4% FCS. The first harvest took place after about 24 hours: the medium was removed and centrifuged at 1000 x g for 10 minutes and the supernatant was stored at 4°C. 8ml of 4% DMEM^{3+} medium were added to the T75 culture flask of HEK cells. The second and last harvest took place 24h after the first harvest. The medium was removed once again and centrifuged following the same aforementioned conditions. The supernatant was

combined with the appropriate medium from the first harvest, sterile filtered and then centrifuged at 75,000 x g for 2h at 4°C in a SW28 rotor. The supernatant was discarded and the virus (pellet) was resuspended in 50μl NB⁺ after draining the leftover medium. To better resuspend the virus, the suspension was put on a shaker for 40 minutes at 300 rpm. Afterwards the lentivirus suspension was aliquoted and at stored at 80°C.

3.2.16.1. <u>Virus titration</u>

- DMEM^{3+}: 10%, 4% or 0% (v/v) FCS, 1% (v/v) L-Glutamine; 1% (v/v) Penicillin-Streptomycin (10.000 U/ml) (Gibco);

To determine of the virus titer, 50% confluent HEK cells were plated in a 96-well plate (coated with poly-D-lysine) and infected. The lentivirus was previously serially diluted (from 10^{-1} to 10^{-10}) and infections per each dilution (40μl per well) was done in double. After an overnight incubation, the medium was changed with DMEM^{3+}. 24h after the medium change, the infected HEK cells (GFP positive) were counted. The titer was calculated using the following formula:

$$\frac{\text{Number of GFP positive cells } * \text{ Dilution factor}}{40\mu l} = \text{Virus}/_{\mu l \text{ in stock}}$$

3.2.16.2. <u>Viral infection</u>

Cortical or hippocampal neuronal co-cultures were infected at DIV 14 with the lentiviruses. 24h after the infection, the medium was completely removed and replaced with freshly prepared half conditioned medium and the cells were left in the incubator until DIV21. The success of the infection was visually checked on a fluorescent microscope before treating the cells and using them either for WB or ICC.

3.2.17. Quantitative Real Time Polymerase Chain Reaction (qRTPCR)

3.2.17.1. <u>RNA extraction</u>

The Qiagen RNeasy® Plus Mini Kit was used to extract the RNA from rat primary neuronal coculture (DIV21). The extraction was performed as per manufacturer protocol, including optional steps. However, the total RNA used was half of the quantity described in the protocol.

Materials and Methods

3.2.17.2. Reverse transcription

The "Transcriptor First Strand cDNA Synthesis Kit" by Roche was used to produce the cDNA from the RNA derived from rat primary neuronal coculture (DIV21). 0.5μg of RNA were used. The reverse transcription was performed according to as per manufacturer protocol, including optional steps. Briefly, the reaction components (see Table 6) were added in a nuclease free microcentrifuge tube placed on ice.

Table 7. cDNA synthesis Template-Primer Mix

Reagent	Volume	Final Concentration
total RNA	variable	0.5μg
Anchored-oligo(dT)$_{18}$ Primer, 50 pmol/µl	1 µl	2.5 µM
Random Hexamer Primer, 600 pmol/µl	2 µl	60 µM
Water, PCR Grade (provided in the kit)	variable	
Final volume	13µl	

The Template-Primer Mix was denatured by heating the tube for 10 min at +65°C in a block cycler with a heated lid (to minimize evaporation). The tubes were then put on ice and the remaining components of the reverse transcriptase mix were added (see Table 7), before continuing with the protocol.

Table 8. Remaining components of the Template-Primer Mix

Reagent	Volume	Final Concentration
Transcriptor Reverse Transcriptase Reaction Buffer, 5x conc.	4µl	1x 8mM MgCl2
Protector RNase Inhibitor, 40 U/µl	0.5µl	20U
Deoxynucleotide Mix, 10 mM each	2µl	1mM each
Transcriptor Reverse Transcriptase, 20U/µl (Vial 1)	0.5µl	10U
Final volume	20µl	

The products were then diluted 1:5 in water (PCR Grade, provided in the kit) and stored at -20°C for further uses.

3.2.17.3. qRTPCR

Quantitative PCR was performed in a QuantStudio™ 3 Real-Time PCR System (Applied Biosystems, Germany) using TaqMan reagents with predesigned assays for Gria1 and the housekeeping gene glyceraldehyde 3-phosphate dehydrogenase

(GAPDH), serving as internal control, in triplicate assays. All runs consisted of 50 cycles of 15s at 95°C and 1 min at 60°C and were preceded by a 2min 50°C decontamination step with uracilN-glycosidase.

3.2.17.4. qRTPCR data analysis

The mean cycle threshold (CT) values obtained were used for the relative quantification of the expression levels for Gria1 according to the ddCT method described by Livak and colleagues (Livak and Schmittgen 2001). Briefly, the expression values of the gene of interest (Gria1) were normalized to GAPDH, used as internal control that refers to the starting amount of cDNA, obtaining the dCT.

$$\text{dCT (gene of interest)} = (\text{CT gene of interest}) - (\text{CT GAPDH})$$

The averaged dCT values of the CTR group were then averaged and this mean CTR dCT value was subtracted from each dCT value of the samples, in order to obtain the ddCT of the control and treatment group.

$$\text{ddCT (gene of interest)} = (\text{dCT gene of interest}) - (\text{mean dCT GAPDH})$$

The qRTPCR is based on an exponential function, therefore the ddCT value for each treatment group was transformed in the Relative Quantification value (RQ).

$$\text{RQ (gene of interest)} = 2^{-\text{ddCT(gene of interest)}}$$

3.2.18. Softwares

NCBI blast® (https://blast.ncbi.nlm.nih.gov/Blast.cgi) and ApE (version 2.0) were used for examination of DNA.

Maximum intensity projections of immunofluorescence images are displayed in this thesis. Please note that the brightness and contrast of immunofluorescence signals were not adjusted in FIJI in order to allow a quantitative analysis of puncta. The same brightness and contrast setups were chosen for an experimental set in which the signal intensity was compared between different conditions such as treatment or viral infection. Microsoft PowerPoint (version 2020) were used to rotate, size and annotate images. Colocalization analysis of puncta was done with OpenView software (Tsuriel et al. 2006) (version 1.5) after preprocessing of maximum intensity projections confocal pictures in FIJI.

3.3.   Animal experiments

3.3.1. Animals

All procedures including handling of animals were ethically approved and conducted according to standards of the German federal state of Sachsen-Anhalt (Institutional Animal Care and Use Committee: Landesverwaltungsamt Sachsen-Anhalt; Permission Nrs. 42502-2-1284-UniMD, 42502-2-1563-UniMD, 42502-2-1626-UniMD, in accordance with the European Communities Council Directive; 86/609/EEC). In this study, C57BL/6BomTac (M&B Taconic, Germany) and SST-CreERT2 (B6(Cg)-Ssttm1(cre/ERT2)Zjh/J) mice, that allow to manipulate NPY releasing cells in the hilus without perturbing the NPY gene function and mRNA expression profiles, from the animal facility of the Institute of Biology (Magdeburg, Germany) were used. Adult mice were housed in groups of 4-5 animals, under a regular 12 h light-dark schedule (lights on 7 AM-7 PM) with food and water available *ad libitum* at constant temperature (22± 2°C) and relative humidity (50%). Any effort was made to minimize the number of animals used and their suffering during experiments.

3.3.2. Stereotaxy

Stereotactical injections were performed by Prof. Dr. Dr. Anne Albrecht. Briefly, mice were anesthetized with 5% isoflurane, that was used as well to maintain the mice sedated during the surgery at a concentration of 1.5-3 Vol.%. After craniotomy, 33G injection needles attached to 10 µl NanoFil microsyringes (World Precision Instruments, Berlin, Germany) were lowered into the dorsal hilus anterioposterior (AP): −1.94mm, mediolateral (ML): ±1.3mm from Bregma and dorsoventral (DV): −1.7mm from brain surface. NPY (final concentration 0.15mg/ml) diluted in saline solution was injected bilaterally at flow rate of 0.1 µl per min via a digital microsyringe pump (World Precision Instruments, Berlin, Germany). Each hemisphere received 1 µl of NPY solution or saline as a control. Viral vectors (10^9 particles/µl) were injected as well bilaterally at flow rate of 0.1 µl per min via a digital microsyringe pump. Each hemisphere received 1 µl of virus solution. Each mouse received 5 mg/kg Caprofen (Sigma-Aldrich) in 0.9% saline subcutaneously for post-operative analgesia. Mice were single caged after the surgery and until the sacrifice period.

3.3.3. Viruses

AAV hSyn-DIO-hM4Di-mCherry was obtained from the Vector Core Facility of University of North Carolina (Chapel Hill, NC, USA). The NPY KD virus contained an shRNA to specifically silence NPY, using a previously shown shRNA sequence (5'-CTACTCCGCTCTGCGACACTA-3', shNpy2) (L. Yang et al. 2009) and it was cloned by Regev-Tsur and colleagues (Regev-Tsur et al. 2020). Behavioural experiments were performed 2 weeks after injection to ensure efficient expression or KD of the protein of interest. AAV hSyn-DIO-hM4Di-mCherry virus, that allows for transient silencing upon systemic administration of clozapine-N-oxide (CNO), was activated 1h before the fear memory conditioning training via intraperitoneally injection of 10 mg/kg body weight CNO (Enzo Life Sciences, Germany) in distilled water. Expression of viral constructs was verified histologically after completion of behavioral experiments.

3.3.4. Behavioural experiments

Behavioral experiments were conducted during the dark phase, between 9 am and 5 pm.

3.3.4.1. Fear conditioning (FC)

FC was conducted in a sound-isolated conditioning chamber containing a 16cm × 32cm × 20cm acrylic glass arena fitted with a grid floor for delivery of foot shocks, a loudspeaker and a ventilator (background noise 70dB SLP, light intensity < 10 lux; TSE Systems, Bad Homburg, Germany). Before conditioning, mice were habituated individually to the conditioning chamber for 6min twice a day (morning and afternoon) for 2 days to provide a stable pre-training habituation of the new environment without inducing latent inhibition (Albrecht et al. 2010; Laxmi, Stork, and Pape 2003). On the third day after an initial 2 min pretraining phase in the fear conditioning box, mice were exposed to three CS (10kHz tone for 10s, 80dB), each co-terminating with an US (foot shock: 0.4mA for 1s), with inter-stimulus intervals (ISI) of 20s. Animals were sacrificed exactly 24h after this last phase, in order to evaluate changes in the intensities of GluA1 and LC3 via immunohistochemistry

The animals' freezing behaviour was assessed online via a photobeam detection system that detected immobility periods >1s. The freezing score was calculated as percentage of total time spent freezing during context exposure and CS presentations

(Albrecht et al. 2010; Laxmi, Stork, and Pape 2003). The boxes were cleaned with 70% Ethanol between each mouse.

3.3.5. Tissue processing

Mice were anesthetized with a ketamine (80 mg/ml)/xylazine (6 mg/ml) mixture at ~1 mg/kg body weight and were transcardially perfused with around 50ml of PBS followed by 50ml of 4% PFA in PBS. Brains were then removed and post-fixed in the same 4% PFA/PBS solution for 24h, followed by cryoprotection in 30% sucrose in PBS at 4°C. After 48h of cryoprotection in the 30%sucrose/PBS solution, brains were snap frozen either in dry-ice or in methylbutane cooled with liquid nitrogen. 30μm thick coronal sections were prepared in a cryomicrotome (Leica) and were then stored free-floating in 0.02% sodium azide in PBS for further processing and use.

3.3.6. Immunohistochemistry

- 10mM trisodium citrate (pH 6.0)
- 0.1M Phosphate buffer (PB);
- Blocking solution: 10% donkey serum plus 0.3% Triton X in PBS;
- Secondary antibody solution: 2% bovine serum albumin (BSA) plus 0.3% Triton X in PBS;
- DAPI: 100nM working solution in dH$_2$O

For GluA1 staining (Cell Signalling # 13185S, 1:200), the slices were washed four times in 0.1M PB for 5min, followed by a 1h incubation in the blocking solution. Right after, the GluA1 primary antibody, prepared in the blocking solution, was applied on the slices. The incubation lasted 24h at 4°C thumbling. Afterwards, the slices were washed three times in PBS and then the secondary antibody was applied. The incubation was over night at 4°C thumbling. Lastly, slices were washed three times in PBS, followed by a 5min incubation with DAPI, prepared in dH$_2$O. After the last three washing steps, slices were mounted on super frost object slides in PBS. The mounted slices were led airdry for 30mins and were then embedded with immune mount. A coverslip was applied and, again, led airdry. Slides were stored at 4°C.

For LC3 staining (Cell Signaling #12741S, 1:250), an antigen retrieval phase preceded the aforementioned protocol: slices were incubated for 30min at 80°C in 10mM trisodium citrate (pH 6.0). Afterwards, the slices underwent the exact previously described protocol.

For the animals that received the NPY infusion and for the ones that were injected with the DREADD virus the A488 donkey anti rabbit (Invitrogen) in a dilution of 1:1000 (Invitrogen) was used. For the animals that were injected with the NPY KD virus the A555 donkey anti rabbit (Invitrogen) in a dilution of 1:1000 was used.

Stainings were performed on two dorsal hippocampal sections per animal, to obtain a total of four dorsal hippocampi per animal per staining.

3.3.7. IHC image analysis

For the quantitative analysis of the IHC staining intensities, fluorescent photomicrographs of the dorsal dentate gyrus of the hippocampus were taken with an epifluorescence microscope (Leica) at 10x magnification and analysed with the open-source image processing software Fiji. Please note that the brightness and contrast of immunofluorescence signals were not adjusted in FIJI in order to allow a quantitative analysis of the intensities. A scale was set for all the pictures and then each picture was manually segmented in order to define the different areas of interest of the dorsal hippocampus and obtain the different intensities by area (Fig. 4).
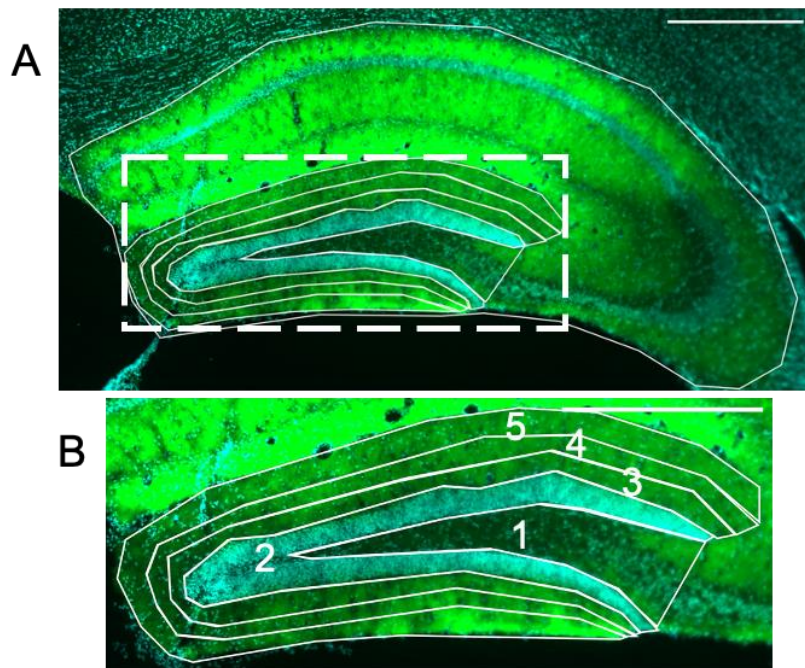
Figure 4. Example picture of GluA1 IHC staining in the dorsal hippocampus with segmented areas used for the intensity analysis.
(A) Representative picture of GluA1 staining with segmentation of the different areas of interest. (B) Inlet showing the dentate gyrus formation with segmentation of the different areas further used for the intensity analysis: 1. hilus, 2. dentate gyrus: granule cells layer, 3. proximal molecular layer or inner portion of the granule cells dendrites; 4. medial molecular layer or medial portion of the granule cells dendrites; 5. outer portion of the granule cells dendrites or distal molecular layer. Scale bar: 500 µM

The areas were manually segmented according to the fundamental neuroanatomical organization described by Scharfmann and colleagues (2013). The areas' intensities of one picture were then normalized by the intensity of the whole dorsal hippocampus for that single picture. For statistical comparison, the normalized intensities for each subarea were averaged over 4 hippocampi obtained for each animal.

For the quantitative analysis of the hM4Di viral infection, fluorescent photomicrographs of the positive infected cells were taken under an epifluorescence microscope (Leica) at 40x magnification and analysed with the open-source image processing software FIJI. In this case, after having set a scale for all the pictures, the soma of the positive infected cells were manually segmented and the intensity of the segmented area was analysed. A minimum of 5 soma per animal were analysed. For statistical comparison, these intensity values were then averaged, and the averaged values were normalised over the CTR group of its own batch.

3.4.   Statistics

All statistical analysis was executed with SPSSStatistics (version 26). Data were first checked for normality using Shapiro-Wilk normality test. For normally distributed data, Student's t-test or one-way ANOVA was performed. For data that does not pass the normality test, Mann-Whitney U-test or Kruskal-Wallis test was used. Two-way ANOVA or three-way ANOVA were used when respectively two factors or three factors were compared. When applicable, post-hoc comparisons were performed with Fisher's LSD test. Targeted comparisons after 2-way ANOVA were performed by using Student's t-test. Significance levels were assumed with * = $p \leq 0.05$, ** = $p \leq 0.01$, *** = $p \leq 0.001$.

4. Results

4.1.   Inducing autophagy in neurons

Researches are showing how neuropsychiatric disorders present a downregulation of autophagy (Sumitomo et al. 2018; Yan et al. 2018) and the induction of autophagy seems to be required during memory formation as well as during fear memory destabilization in an auditory fear reconsolidation mice model (Glatigny et al. 2019b; Shehata et al. 2018). Since NPY is released during stress in the hippocampus where it might play an anxiolytic action (Raza *et al.*, 2017) and it was recently proven to increase autophagy in hypothalamic and cortical primary neuronal cultures (Ferreira-Marques et al. 2016; Aveleira, Botelho, and Cavadas 2015), it was selected as experimental treatment to investigate into synaptic markers and their autophagy-mediated regulation during fear memories formation.

4.1.1. Cortical neurons

At first, to confirm the treatment used in the aforementioned paper from Aveleira and colleagues (2015), rat cortical cocultures mature neurons (DIV21) were treated with 100nM NPY for 6h, after which cells were lysed for WB analysis of the two most common autophagy markers p62 and LC3 (Fig. 5). It was possible to confirm a decrease in the levels of p62, that might suggest an increase in the degradation rate, namely a potential increase in autophagy (Fig. 5 C; 2-way ANOVA: NPY x CQ $F_{(1,20)}=3.527$, p=0.079, NPY effect $F_{(1,20)}=0.517$, p=0.483, CQ effect $F_{(1,20)}=7.347$, p=0.015; Student's t-test: CTR vs NPY t=2.604, df=8, p=0.031; CTR CQ vs NPY CQ t=-0.669, df=8, p=0.523). Furthermore, the increase in the ratio of the LC3-II over LC3-I form can give an idea of the amount of autophagosomes formation at a given point, i.e. the consequent increase in autophagy. However, changes in autophagy might be difficult to observe in neurons due to its high efficiency and flux, and also the interpretation of the markers p62 and LC3 might be misleading, as an increase in the LC3-II/LC3-I ratio might represent either an increase in the autophagosomes formation or a block in the autophagic flux, the LC3-II over LC3-I net flux changes was analysed with and without the use of chloroquine (CQ). CQ is an autophagy blocker that blocks the autophagic flux by affecting the fusion of autophagosomes with lysosomes (Mauthe et al. 2018) (Fig. 5 B; Student's t-test: t=-2.977, df=8, p=0.018) and it allows the formation of autophagosomes that then accumulates, since they cannot complete the last step of

autophagy where the material inside the autophagosomes is degraded, along with LC3-II and p62. To evaluate the increase in autophagy produced by the 6h NPY treatment, CQ was to the cells and it was verified that the increase in the LC3-II over LC3-I is more when the cells receive a combination of NPY+CQ, compared to the CTR+CQ alone (Fig. 5 B and D; 2-way ANOVA: NPY x CQ $F_{(1,20)}=8.96$, $p=0.009$, NPY effect $F_{(1,20)}=10.675$, $p=0.005$, CQ effect $F_{(1,20)}=39.953$, $p<0.0001$; Student's t-test: CTR vs NPY $t=-0.557$, $df=8$, $p=0.593$; CTR CQ vs NPY CQ $t=-3.229$, $df=8$, $p=0.012$). Taken all these evidences together, it was possible to confirm that the 100nM 6h NPY treatment is able to produce an increase in the autophagy levels of cortical primary cocultures of neurons.
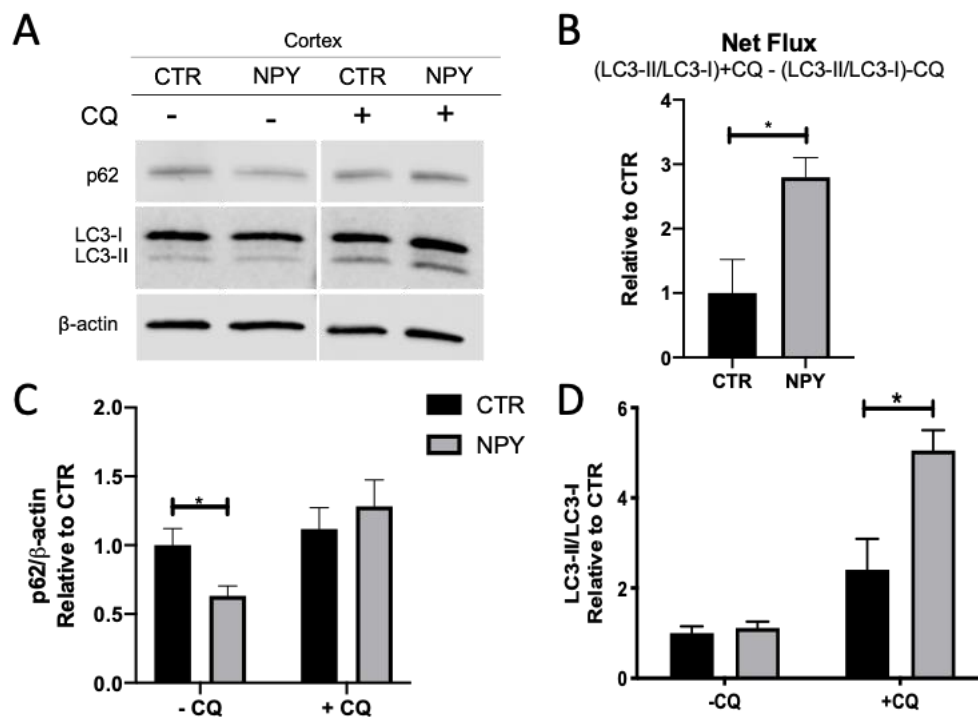
Figure 5. **NPY enhances autophagy in cortical primary neuronal co-cultures.**
To induce autophagy, mature rat differentiated cortical primary neural cells (DIV21) were exposed to NPY (100 nM) for 6h in the absence or presence of chloroquine (50 µM; CQ) for 4h, to block lysosomal degradation of autophagosomes, and cells were then lysed. (A-D) Western blotting analysis of LC3-II/LC3-I and p62. (A) Representative immunoblot pictures, white bands between densitometry pictures show that the bands come from different position on the same blot. (B) LC3-II/LC3-I net flux was determined by subtracting the densitometric value of LC3-II/LC3-I amount in samples non-treated with chloroquine ((LC3B-II/LC3-I) − CQ) from the corresponding sample treated with chloroquine ((LC3-II/LC3-I) + CQ). Cortical cultures show an increase of LC3 net-flux and a decrease of p62 upon NPY treatment indicating autophagy induction. Data are means + SEM. *P < 0.05 significantly different from CTR. Exp=4, n ≥ 3.

4.1.2. Hippocampal neurons

After testing the efficacy of the NPY treatment in increasing autophagy in the routinely used cortical primary neuronal culture, the 100nM NPY treatment was used on DIV21 hippocampal primary neuronal cocultures, since it is known that NPY is released in the hippocampus during a fear conditioning paradigm where it regulates the context salience (Raza et al., 2017). In order to verify the NPY effect on hippocampal autophagy, neurons were lysed 6h after the NPY addition to the wells and the autophagic markers p62 and LC3, as well as the LC3-II over LC3-I net flux, with and without CQ, were analysed (Fig. 7). Even if it is not possible to see an increase in the LC3-II over LC3-I ratio (Fig. 7 D; 2-way ANOVA: NPY x CQ $F_{(1,18)}=0.614$, $p=0.446$, NPY effect $F_{(1,18)}=2.078$, $p=0.171$, CQ effect $F_{(1,18)}=17.129$, $p<0.0001$; Student's t-test: CTR vs NPY $t=-0.784$, df=8, $p=0.476$; CTR CQ vs NPY CQ $t=-1.127$, df=8, $p=0.303$), the increase in autophagy can be very well appreciated by looking at the increase in the net flux when cells are treated with NPY and the autophagic flux is blocked with CQ (Fig. 7 B; Paired sample t-test: $t=-8.444$, df=3, $p=0.003$). Also, NPY-treated neurons show a decrease in p62 in the CTR vs NPY conditions (Fig. 7 C; 2-way ANOVA: NPY x CQ $F_{(1,18)}=1.454$, $p=0.248$, NPY effect $F_{(1,18)}=0.001$, $p=0.973$, CQ effect $F_{(1,18)}=2.694$, $p=0.123$; Student's t-test: CTR vs NPY $t=2.536$, df=8, $p=0.035$; CTR CQ vs NPY CQ $t=-0.564$, df=8, $p=0.593$). The 6h 100nM NPY treatment induces an increase in autophagy in hippocampal primary neuronal cultures as well.
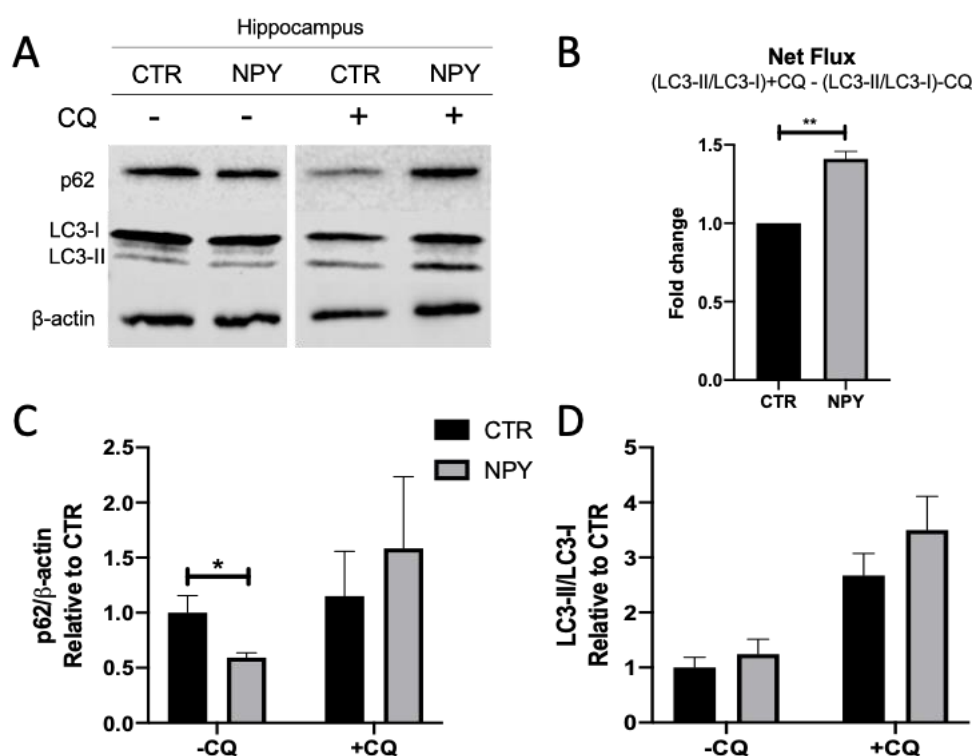
Results

<u>**Figure 6.**</u> **NPY enhances autophagy in hippocampal primary neuronal cultures.**
To induce autophagy, mature rat differentiated hippocampal primary neural cells (DIV21) were exposed to NPY (100 nM) for 6h in the absence or presence of chloroquine (50 µM; CQ) for 4h, to block lysosomal degradation of autophagosomes, and cells were then lysed. (A–D) Western blotting analysis of LC3-II/LC3- I and p62. (A) Representative immunoblot pictures, white bands between densitometry pictures show that the bands come different position on the same blot. (B) LC3-II/LC3-I net flux was determined by subtracting the densitometric value of LC3-II/LC3-I amount in samples non-treated with chloroquine ((LC3B-II/LC3-I) − CQ) from the corresponding sample treated with chloroquine ((LC3-II/LC3-I) + CQ). Both hippocampal and cortical cultures show an increase of LC3 net-flux and a decrease of p62 upon NPY treatment indicating autophagy induction. Data are means + SEM. $P < 0.05$, **$P < 0.01$ significantly different from CTR. Exp=4, n ≥ 3.

The formation of autophagosomes is tightly regulated in neurons, as it is the autophagosomes motility (Hollenbeck, 1993; Maday, Wallace and Holzbaur, 2012; Maday and Holzbaur, 2014): autophagosomes that form distally in the axon migrate towards the soma, where they are confined, while the movement of autophagosomes in dendrites is oscillatory along the dendritic shaft (Maday and Holzbaur, 2014; 2016). To further confirm the increase in autophagy seen via WB, the somatic accumulation of autophagosomes was verified via immunocytochemistry (ICC). The 100nM NPY treatment was applied on DIV21 hippocampal primary neuronal cocultures for 6h, cells were fixed and the LC3 puncta in the soma of the neurons were counted (Fig. 8; Mann-Whitney U, U=671, p=0.003). The application of NPY is inducing an increase in the LC3 puncta compared to the control, a result that along with the WB data is confirming that the NPY treatment is able to increase autophagy and that the autophagosomes accumulate in the soma of the neurons.
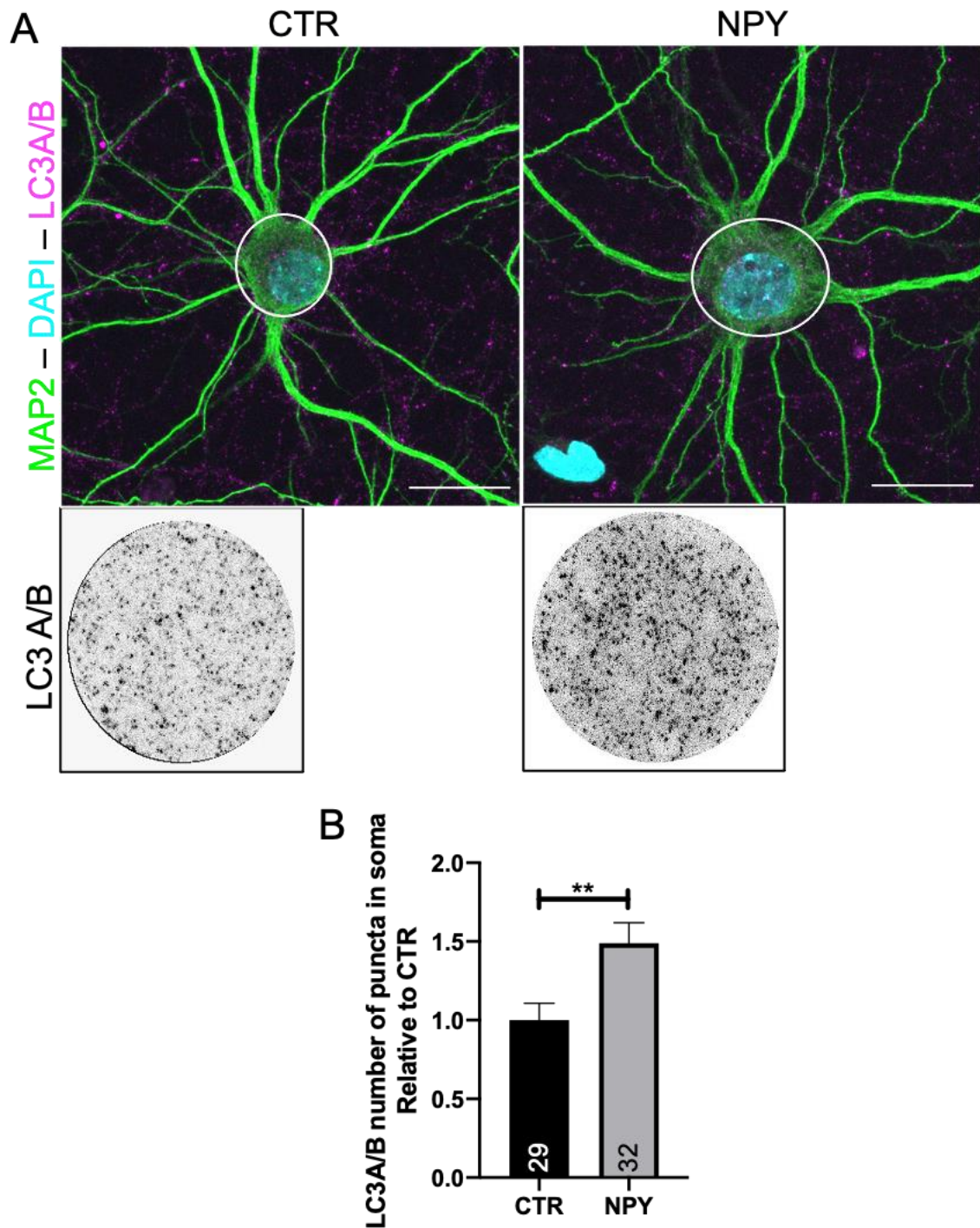
Figure 7. **NPY increases LC3 puncta in the soma of hippocampal primary neuronal cultures.**

To induce autophagy, mature rat differentiated hippocampal primary neural cells (DIV21) were exposed to NPY (100 nM) for 6h and cells were then fixed. (A) Representative pictures of LC3 A/B immunoreactivity in hippocampal rat primary cultures (DIV21) exposed to NPY for 6h. (B) Puncta analysis of LC3 A/B immunoreactivity, insets show increased LC3 puncta in the magnified soma in NPY treated neurons. Scale bar: 20 µM. Data are means + SEM. **P < 0.01 significantly different from control. Exp=3, 10 cells/exp group.

Results

4.1.3. The long-lasting NPY-induced autophagy increase

In order to verify the effects of this NPY-induced increase in autophagy in synapses, at first, it was investigated if the increase was long-lasting and, if long-lasting, for how long. To do so, DIV21 cortical primary neuronal cocultures were treated with NPY 100nM for 6h. Next, the medium was completely removed and replaced with freshly prepared half-conditioned medium and the cells were left in the incubator for 24h or 48h after the medium change, after which the cells were lysed. The common autophagic marker p62 and LC3 were analysed via WB (Fig. 8). The NPY 6h treatment is able to produce a long-lasting increase in autophagy that lasts up to 24h after the medium change (Fig. 8 B; Student's t-test: t=-2.753, df=12, p=0.018; and C; Mann-Whitney U: U=35, p=0.209) and that it goes then back to normal levels 48h after the medium change (Fig. 8 E; Student's t-test: t=-0.26, df=12, p=0.799; and F; Student's t-test: t=1.235, df=12, p=0.253).
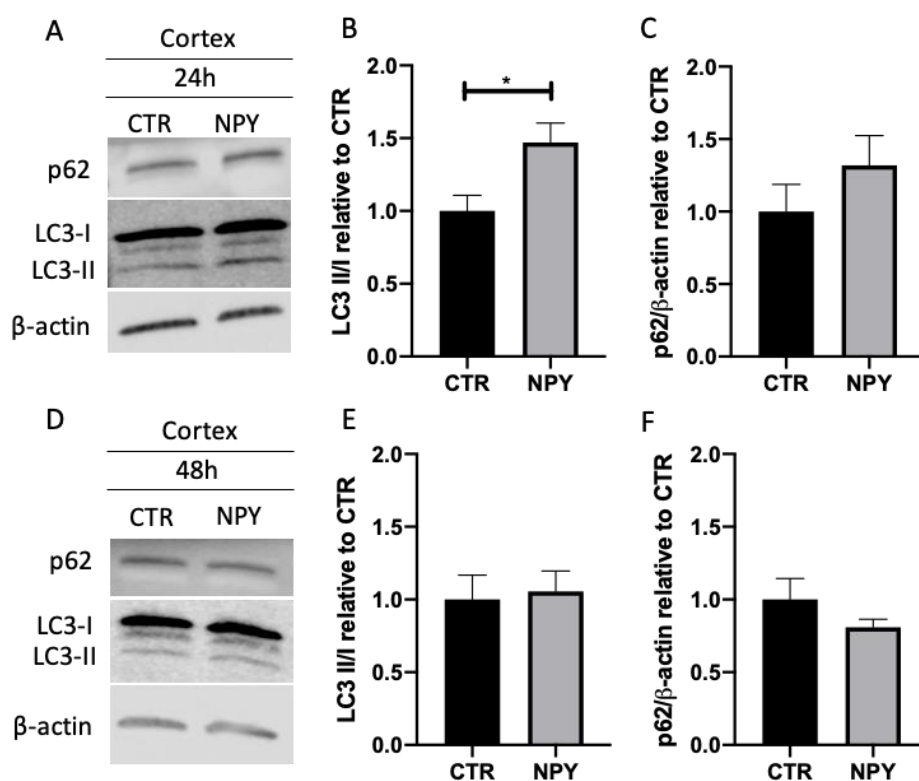
Figure 8. Autophagy levels stay high 24h after the 6h NPY exposure and they decrease 48h later.

Mature rat differentiated cortical primary neural cells (DIV21) were exposed to NPY (100 nM) for 6h. The medium was changed after the 6h NPY exposure and the neurons were lysed 24h or 48h after the medium change. (A and D) Representative immunoblot pictures. (A-C) Immunoblot analysis of LC3-II/LC3-I and p62 24h after 6h of NPY exposure. (D-F) Immunoblot analysis of LC3-II/LC3-I and p62 48h after 6h of NPY exposure. (G) Schematic of the long-lasting autophagy activation after 6h NPY treatment. Data are means + SEM. *P < 0.05, significantly different from control. Exp=3, n=4

Results

To verify if the effect is dependent on protein expression changes, the protein synthesis was blocked using cycloheximide (CHX) (355µM), a protein synthesis inhibitor in eukaryotes. CHX effects on autophagy have been controversial (Abeliovich et al. 2000; Takeshige et al. 1992; Papadopoulos and Pfeifer 1986), however it should be taken into account that blocking the protein synthesis reduces the consumption of amino acids, thus increasing the availability of intracellular amino acids, a positive regulator of mTOR that suppresses autophagy (Beugnet et al. 2003; Vabulas and Hartl 2005). When blocking the protein synthesis there is a drastic decrease in the p62 levels for both the CTR and NPY conditions, when treated with CHX. This was expected, as p62 is degraded along with the cargo it tags and having the protein synthesis inhibited via the use of CHX, the p62 levels cannot be replenished. (Fig 9 B; 2-way ANOVA: NPY x CHX $F_{(1,12)}=0.201$, p=0.666, NPY effect $F_{(1,12)}=0.699$, p=0.427, CHX effect $F_{(1,12)}=52.193$, p<0.0001; Student's t-test: CTR vs NPY t=-0.672, df=4, p=0.539; CTR CQ vs NPY CQ t=-0.664, df=4, p=0.543). However, when analysing LC3 levels, it is possible to appreciate a trend into an increase when cells are treated with NPY, even when the protein synthesis is blocked (Fig. 9 C; 2-way ANOVA: NPY x CHX $F_{(1,12)}=0.094$, p=0.766, NPY effect $F_{(1,12)}=3.442$, p=0.101, CHX effect $F_{(1,12)}=0.326$, p=0.584; Student's test: CTR vs NPY t=-1.351, df=4, p=0.248; CTR CQ vs NPY CQ t=-1.29, df=4, p=0.267). Even though the NPY effect has a significance of only 0.101, the data indicate that, despite the availability of amino acids that should prevent an increase in autophagy, the NPY treatments is determining a tendency into an increase in the LC3-II over LC3-I, i.e. in the formation of autophagosomes. This tendency might be comparable to the ones observed in Fig. 5 and Fig. 6, where the use of NPY alone, without a blocker of autophagy flux such as CQ, is not able to produce a statistically significant effect on autophagy viewable via WB (as seen as well in the experiments from Aveleira et al. (2014) and Ferreira-Marques et al. (2016)).

Results
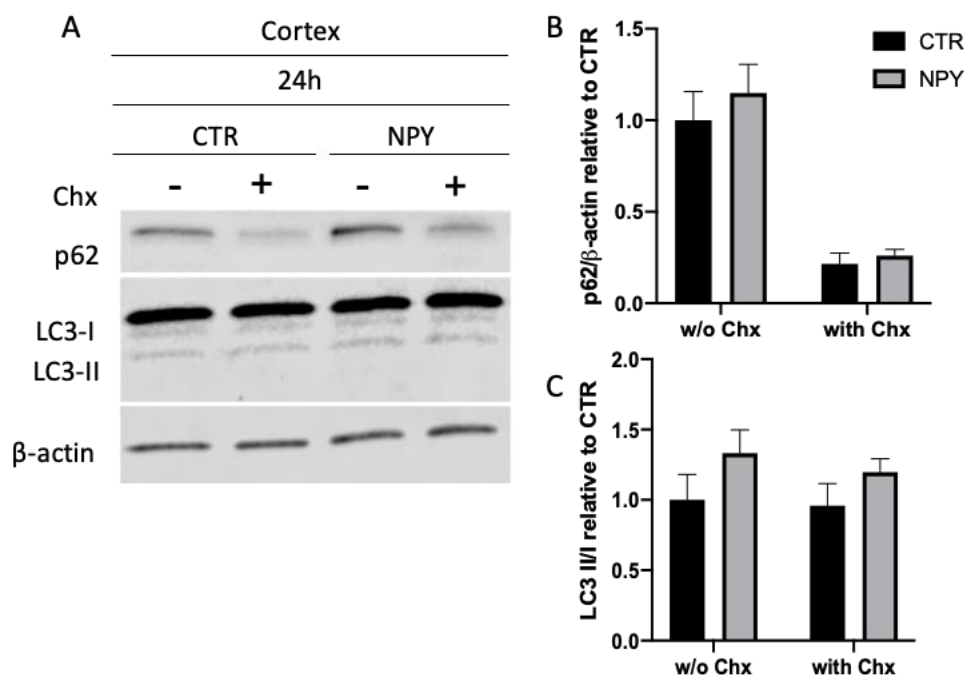
Figure 9. Autophagy levels stay high 24h after the 6h NPY exposure even after blocking protein synthesis.
Rat differentiated cortical primary neural cells (DIV21) were exposed to NPY (100 nM) and cycloheximide (CHX) (355µM) for 6h and cells were then lysed. The medium was changed after this 6h exposure and the neurons were lysed 24h after the medium change. (A-B) Representative picture of western blotting analysis of LC3-II/LC3-I and p62 24h after 6h of NPY and CHX exposure: blocking the protein synthesis with CHX during the NPY exposure does not prevent the increase in autophagy. Data are means + SEM. Exp=4, n=4.

4.2.   NPY effect on synaptic markers

Knowing the fundamental role that autophagy plays in neurons, not only as a quality control system, but also in shaping synapses and during synaptic signalling, changes in synaptic markers produced by the NPY-induced increase in autophagy were investigated. Rat differentiated cortical primary neural cells (DIV21) were treated with 100nM NPY for 6h, after which cells were lysed and it was performed a screening for several different synaptic markers via WBs (Fig. 10). Synaptic markers were selected based on previous works showing how autophagy can shape synapses either on the pre- or post-synaptic side: from spine pruning (Tang et al. 2014) to synaptic vesicles number (Okerlund et al. 2017) in the axons, from degradation of synaptic scaffolding proteins (Nikoletopoulou et al., 2017) to internalization of ionotropic receptors in the dendrites (Rowland et al., 2006; Shehata et al., 2012). No statistically significant changes were induced after 6h of NPY treatment (GluA1: Mann-Whitney U: U=132, p=0.423; NMDAR1: Student's t-test: t=-0.208, df=22, p=0.837; GABA-A: Student's t-

Results

test: t=0.195, df=22, p=0.847; VGlut: Student's t-test: t=0.727, df=30, p=0.473; VGat: Student's t-test: t=-0.471, df=30, p=0.641; GAD65: Student's t-test: t=0.406, df=30, p=0.688; GABA Transp: Student's t-test: t=0.202, df=22, p=0.842; EAAT3: Student's t-test: t=0.577, df=23, p=0.569; Synaptophysin: Student's t-test: t=-0.673, df=22, p=0.508).
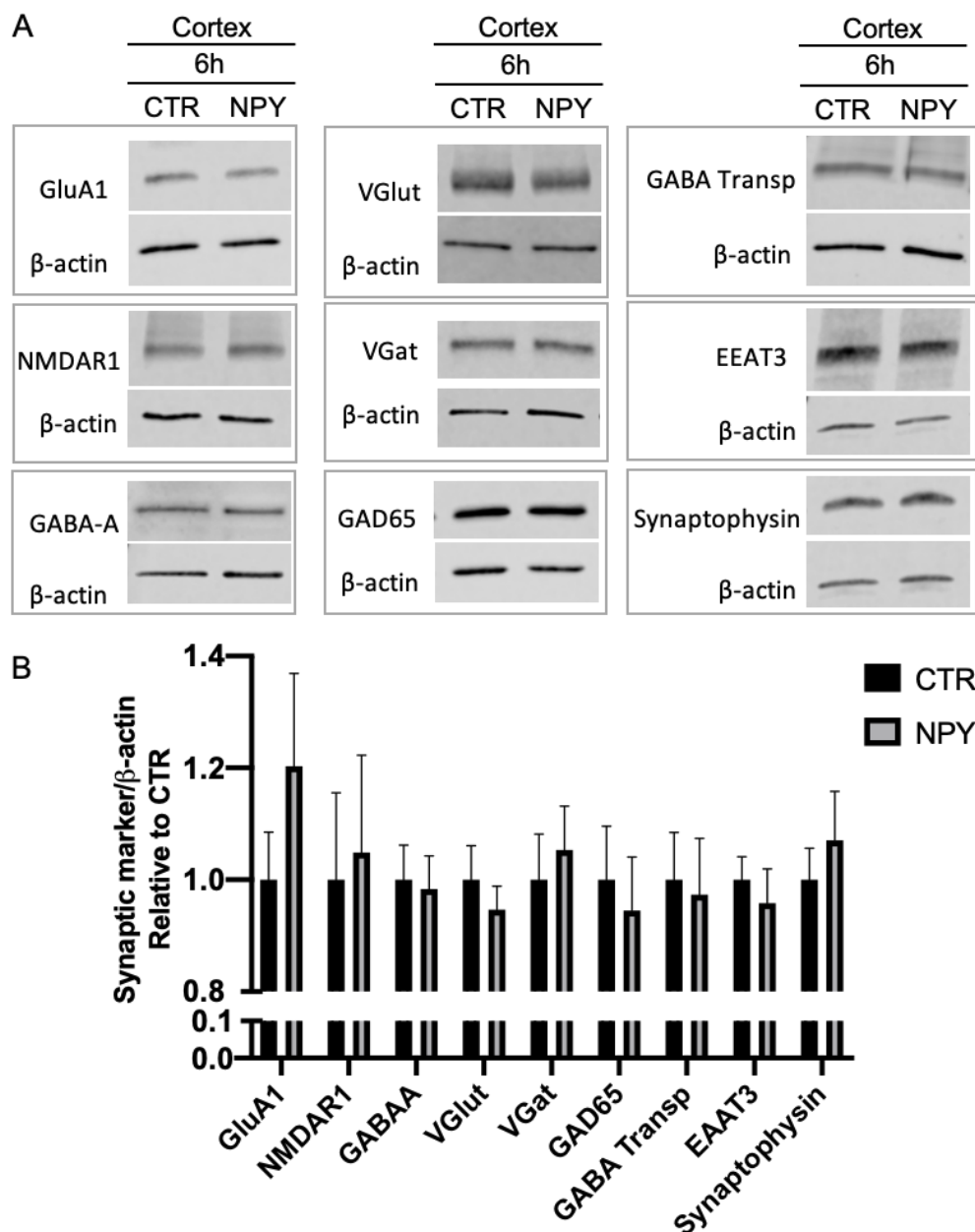
Figure 10. NPY does not affect synaptic markers.

Rat differentiated cortical primary neural cells (DIV21) were exposed to NPY (100 nM) for 6h and cells were lysed. (A) Representative immunoblot pictures. (B) Immunoblot analysis of several synaptic markers, showing no statistical differences between control and NPY treatment. Data are means + SEM. Exp ≥ 4, n=5.

4.3. NPY effect on the GluA1 subunit of the AMPA receptor

Even if no statistically significant changes were seen after 6h of NPY treatment, the tendency increase in GluA1 receptor was further investigated due to the work of Shehata et al., showing that chemical LTD increases autophagy in neurons and this increase was promoting internalization and degradation of AMPA receptors (Shehata et al. 2012). Since the effect on the GluA1 receptor detected with the NPY treatment was contrasting with the aforementioned paper by Shehata, it was taken a closer look into this tendency into an increase of this GluA1 subunit of AMPA receptor and rat differentiated hippocampal primary neural cells (DIV21) were treated with 100nM NPY for 6h, after which the cells were fixed and stained, in order to pinpoint the location of this tendency increase of GluA1 (Fig. 11). Pictures were then analysed by counting the GluA1 puncta in two different compartments of the cell: the soma (Fig. 11 B; Mann-Whitney U: U=874, p=0.04) or the first 50µm of the neuron's main dendrite (Fig 11 C; Mann-Whitney U: U=617, p=0.349). Indeed, GluA1 puncta accumulate more in the soma of the NPY-treated cells compared to control conditions, but this increase was not accompanied by a reduction in the GluA1 puncta in the dendrites, as it would have been expected according to the aforementioned paper by Shehata and colleagues.
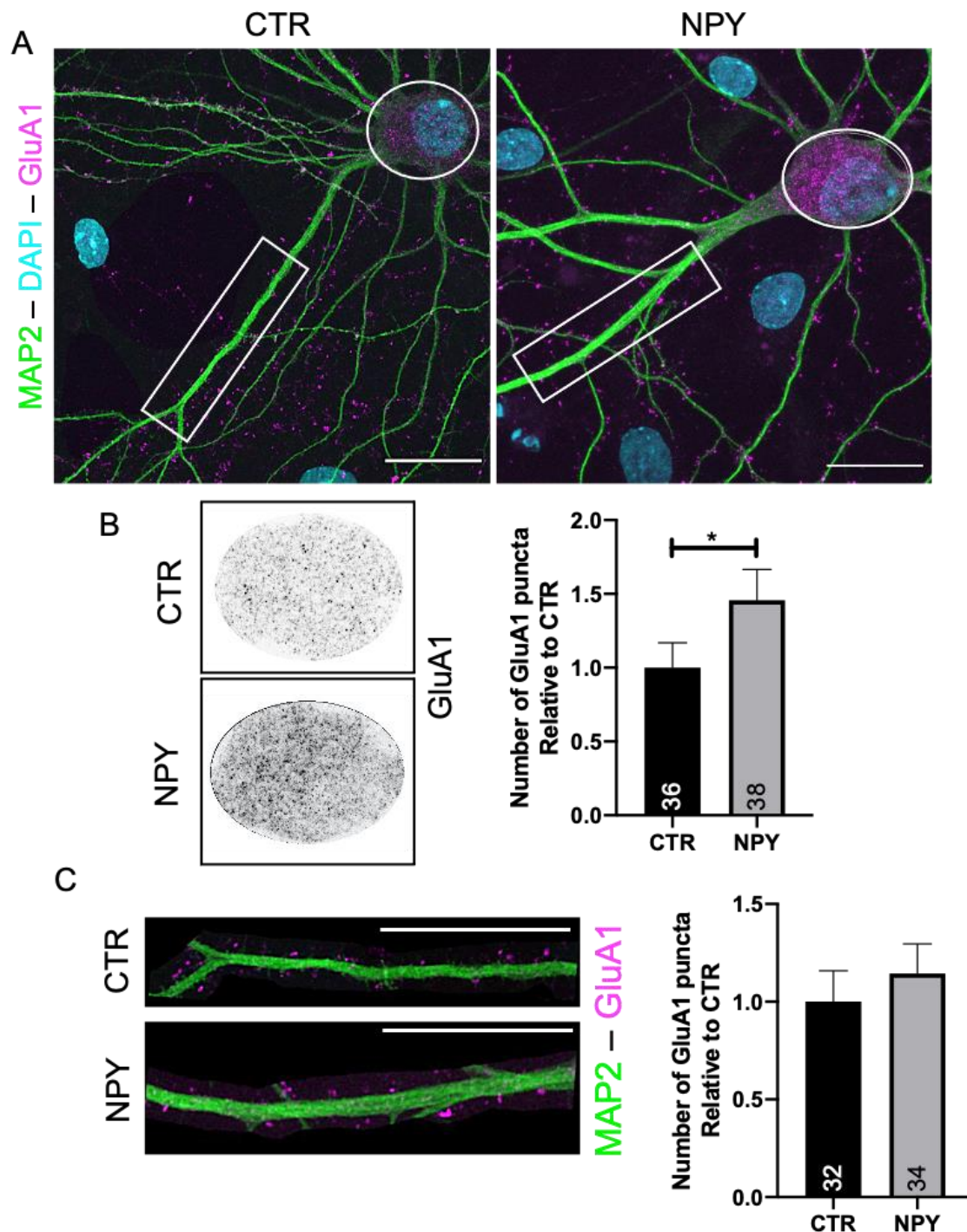
Figure 11. **NPY enhances GluA1 puncta in the soma of hippocampal primary neuronal cultures after the 6h NPY exposure.**

Rat differentiated hippocampal primary neural cells (DIV21) were exposed to NPY (100 nM) for 6h and were then fixed. (A) Representative pictures of GluA1-MAP2-DAPI immunocytochemistry in hippocampal rat primary cultures (DIV21) exposed to NPY for 6h. Insets show increased GluA1 puncta in the magnified soma of the NPY treated neurons. (B-C) Insets showing the immunoreactivity for GluA1 in magnified soma and first 50µm of neurons' main dendrite. (B) Puncta analysis of GluA1 immunoreactivity in soma and (C) in the first 50µm of neurons' main dendrite. Data are mean + SEM. Scale bar, 20 µM. *P < 0.05 significantly different from CTR. Exp=3, minimum 10 cells/exp group.

4.3.1. GluA1 puncta accumulation in the soma of neurons

In the previously mentioned paper by Shehata et al. (2012) it is hypothesised that AMPA receptors are engulfed into endocytic vesicles that might then either be recycled back to the membrane or directed to fuse with autophagosomes in order to direct the receptors into lysosomes for degradation: increasing the number of autophagosomes would trap more AMPA receptors and direct them to degradation (Shehata et al., 2012). However, the NPY treatment is determining an accumulation of GluA1 puncta in the soma that is not accompanied by a reduction of the puncta in the dendrites. Therefore, in order to verify if the GluA1 puncta increase is due to the relocation of GluA1 puncta in the soma via autophagosomes, at first an increase in autophagy was induced using the 100nM NPY treatment. Then, autophagy was blocked it in its last stage, that is the degradation of autophagosomes, by using CQ, to verify if this block would induce an accumulation of GluA1 puncta compared to the control treated only with CQ (Fig. 12). Indeed, the block of autophagy in its last stage, just before the fusion of autophagosomes with lysosomes that promotes their degradation, seem to determine an accumulation of GluA1 puncta in the soma of the neurons, that is statistically significant compared to the control (Fig. 12 B; 2-way ANOVA: NPY x CQ $F(1,180)=0.26$, $p=0.611$; NPY $F(1,180)=13.225$, $p<0.0001$; CQ $F(1,180)=16.347$, $p<0.0001$). In the dendrite it is possible to appreciate an interaction between the NPY treatment and the block of autophagy via CQ in the dendrites, where it is possible to see a decrease in the number of puncta in the dendrite, probably due to their shuffling towards the soma (Fig. 12 C; 2-way ANOVA: NPY x CQ $F(1,124)=5.933$, $p=0.016$; NPY $F(1,124)=0.103$, $p=0.749$; CQ $F(1,124)=1.328$, $p=0.251$).
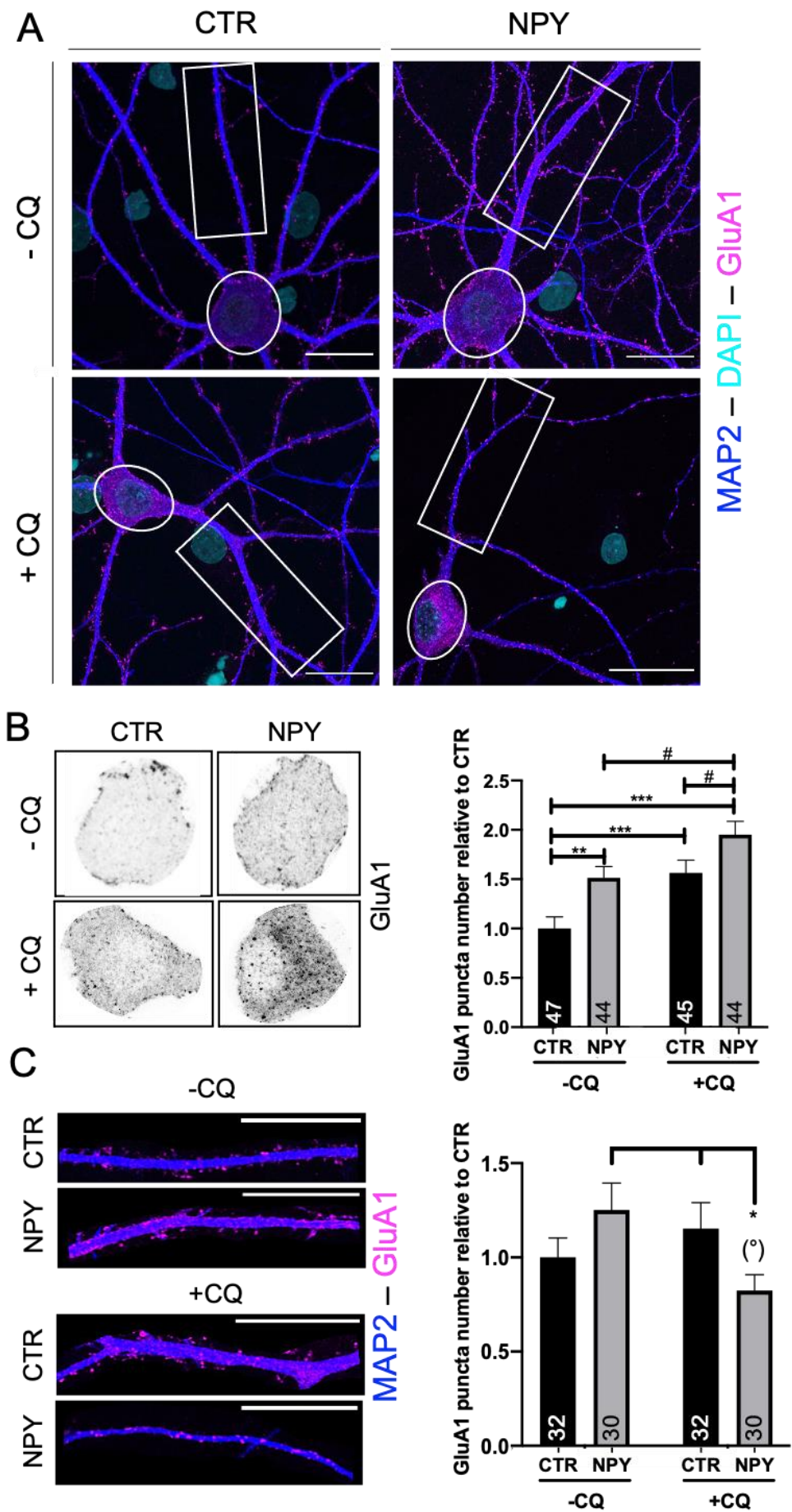
Results

Figure 12. **Blocking the last stage of autophagy with CQ determines an accumulation of GluA1 puncta in the soma of hippocampal rat primary neuronal culture after the 6h NPY exposure.**

Rat differentiated hippocampal primary neural cells (DIV21) were exposed to NPY (100 nM) for 6h in the absence or presence of chloroquine (50 μM; CQ) for 4h, to block lysosomal degradation of autophagosomes, and cells were then fixed. (A) Representative pictures of GluA1-MAP2-DAPI immunoreactivity in hippocampal rat primary culture (DIV21) exposed to NPY for 6h in the absence or presence of chloroquine. (B-C) Insets showing the immunoreactivity for GluA1 in magnified soma and first 50 μm of neurons' main dendrite. (B) Puncta analysis of GluA1 immunoreactivity in soma (**$P<0.01$, ***$P<0.0001$ versus CTR - CQ, #$P<0.05$ versus NPY +CQ) and (C) in the first 50 μm of neurons' main dendrite (*$P<0.05$ versus NPY -CQ, (°) $P=0.054$ versus CTR +CQ). Scale bar, 20 μM. Data are means + SEM. Exp=4, minimum 10 cells/exp group.

Therefore, to better understand the role of autophagy in this GluA1 puncta accumulation in the soma, autophagy was blocked in the first stages, preventing the formation of autophagic vesicles, by using a lentivirus containing a short hairpin (sh) RNA against ATG5, one of the autophagic protein involved in the autophagosomes elongation step of the autophagosome vesicles formation.

At first, to verify if the shRNA lentivirus against ATG5 was effective in knocking down ATG5 and, consequently, decreasing autophagy, rat differentiated cortical primary neural cells (DIV14) were infected with the lentivirus containing the shRNA and the cells were allowed to express the shRNA for one week (up until DIV21). Cells were then treated with 100nM NPY for 6h, before being lysed, and the autophagy markers were analysed via WB (Fig.13). The virus is effective in knocking down the ATG5 levels (Fig. 13 B; 2-way ANOVA: NPY x shATG5 $F(1,12)=0$, $p=0.989$, NPY effect $F(1,12)=0.166$, $p=0.694$, shATG5 effect $F(1,12)=10.146$, $p=0.013$) and, consequently, lentivirus containing the ATG5 shRNA inhibits autophagy, as it can be appreciated by the accumulation of p62 (Fig.13 C; 2-way ANOVA: NPY x shATG5 $F(1,12)=0.41$, $p=0.534$, NPY effect $F(1,12)=0.123$, $p=0.731$, shATG5 effect $F(1,12)=17.798$, $p=0.001$), but particularly from the loss of effect in the LC3-II/LC3-I ratio when cells are treated with NPY but were infected with the shATG5 (Fig. 13 D; 2-way ANOVA: NPY x shATG5 $F(1,12)=4.781$, $p=0.049$, NPY effect $F(1,12)=1.271$, $p=0.282$, shATG5 effect $F(1,12)=4.415$, $p=0.057$).
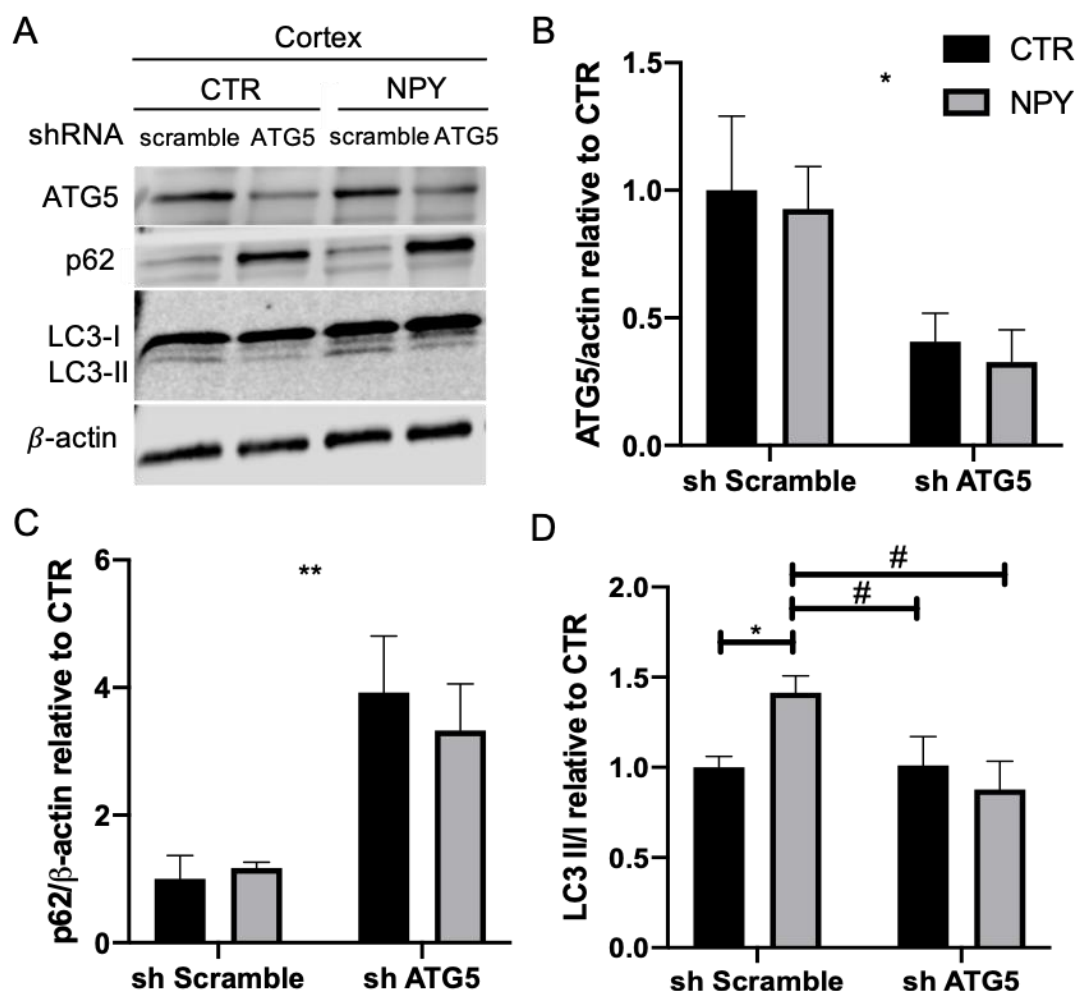
Figure 13. **Blocking autophagy using an shATG5 lentivirus blocks the NPY induced increase in autophagy.**

The use of an shRNA against ATG5 prevents the increase in autophagy determined by the 100nM NPY 6h treatment. Rat differentiated cortical primary neural cells (DIV14) were infected with a shATG5 lentivirus and respective shScramble control. At DIV21, neurons were exposed to NPY (100 nM) for 6h, after which cells were lysed. (A) Representative immunoblot pictures of ATG5, p62 and LC3-I/LC3-II. (B and C) Immunoblot analysis of ATG5 and the autophagic markers p62 and LC3-I/LC3-II; *p<0.05 shATG5 effect in B; **p<0.01 shATG5 effect in C; *P<0.05 versus CTR shScramble; #P<0.05 versus NPY shScramble in D. Data are means + SEM. Exp=4, n≥3.

After seen that the shATG5 lentivirus is able to decrease the protein levels of ATG5 and, consequently, decreasing autophagy, with or without the NPY treatment, the shRNA lentivirus against ATG5 was used to block autophagy at the first stage in order to verify if the accumulation of GluA1 puncta seen when treating cells with both NPY and CQ is prevented by halting the formation of autophagosomes (Fig. 14). Indeed, the block of autophagy in the first stage, that prevents the formation of autophagosomes, is halting the accumulation of GluA1 puncta in the soma of neurons

(Fig. 14 B). These data allow for speculations on the possibility that the GluA1 puncta seen when blocking the autophagy at its last stage, that blocks the fusion of autophagosomes with lysosomes by using CQ, might be due to a relocation of autophagosomes towards the soma of neurons into autophagic vesicles, as previously hypothesised by Shehata as well (Shehata et al., 2012). However, even if we block autophagy, there is still a slight tendency into an increase in the number of GluA1 puncta in the soma, compared to the CTR that was infected with shRNA against ATG5 (Fig. 14 B; 2-way ANOVA: NPY x virus $F_{(1,130)}=1.513$, $p=0.221$; NPY $F_{(1,130)}=8.171$, $p=0.005$; virus $F_{(1,130)}=0$, $p=0.999$; CTR shScramble versus NPY shScramble: Mann-Whitney U $U=833.5$, $p=0.017$; CTR shATG5 versus NPY shATG5: Mann Whitney U $U=499.5$, $p=0.32$).
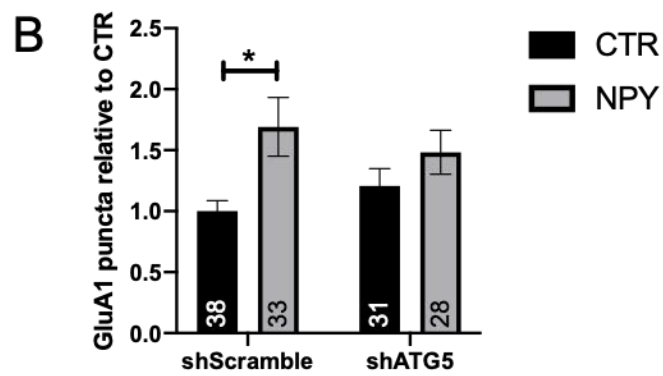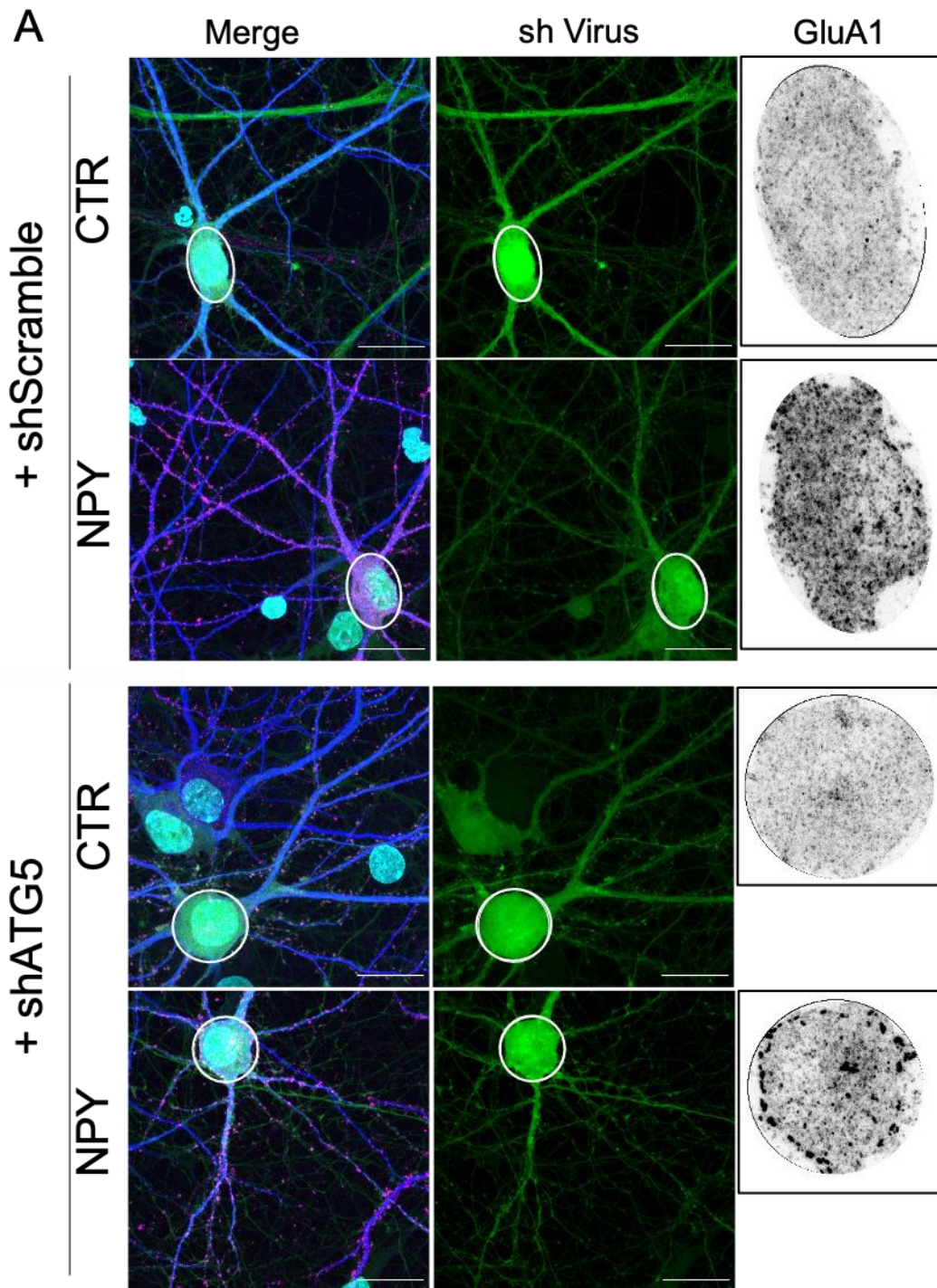
Results

Figure 14. **Preventing the formation of autophagosome blocks the accumulation of GluA1 puncta in the soma of hippocampal neurons despite the 6h NPY exposure.**

Blocking autophagy at the first step using a shATG5 lentivirus, thus preventing the formation of autophagosome, halts the accumulation of GluA1 puncta in the soma of hippocampal rat primary neuronal culture after the 6h NPY exposure. Rat differentiated hippocampal primary neural cells (DIV14) were infected with a shATG5 lentivirus and respective shScramble control. At DIV21, neurons were exposed to NPY (100 nM) for 6h and cells were then fixed. (A) Representative pictures of GluA1-Map2-DAPI immunoreactivity in hippocampal rat primary culture (DIV21) exposed to NPY for 6h. Insets showing the immunoreactivity for GluA1 in magnified soma. (B) Puncta analysis of GluA1 immunoreactivity in soma. Scale bar, 20 µM. Data are means + SEM. *P<0.05 versus CTR shScramble. Exp=3, minimum 10 cells/exp group.

In order to further investigate the slight increase of total GluA1 seen via WB after the 6h NPY treatment, as well as the slight enhancement of puncta seen in the soma of NPY treated neurons even when autophagosomes cannot form and autophagy is blocked, neurons were treated with NPY in combination with actinomycin D, a transcription inhibitor that inhibits new RNA synthesis by intercalating into the DNA, thereby blocking nearly all transcription in a dose-dependent manner (C. Y. A. Chen, Ezzeddine, and Shyu 2008; Perry and Kelley 1970). Therefore, DIV21 rat hippocampal neuronal cocultures were treated with or without 30 µM actinomycin D 5min before the 100nM NPY for 6h, after which cells were fixed and stained (Fig. 15). While the use of DMSO and actinomycin D in the control groups show a similar GluA1 puncta count, proving that these treatments are not interfering with basal GluA1 puncta, the pre-treatment of neurons with actinomycin in the NPY-treated group is blocking the accumulation of GluA1 puncta in the soma (Fig. 15 B; 2-way ANOVA: NPY x actinomycin $F_{(1,138)}=4.254$, p=0.041; NPY $F_{(1,138)}=0.339$, p=0.561; actinomycin $F_{(1,138)}=7.13$, p=0.009), determining a decrease in the GluA1 puncta compared to the CTR + actinomycin D. However, it is interesting to notice that this effect is not present in the main dendrite, where the GluA1 puncta are the same as the control (Fig. 15 C; 2-way ANOVA: NPY x actinomycin $F_{(1,120)}=0.008$, p=0.931; NPY $F_{(1,120)}=1.414$, p=0.237; actinomycin $F_{(1,120)}=2.255$, p=0.136). Knowing that dendrites contain mRNAs and the machinery for protein synthesis (Hafner et al. 2019), these data seem to go in the direction of locally synthesised GluA1.
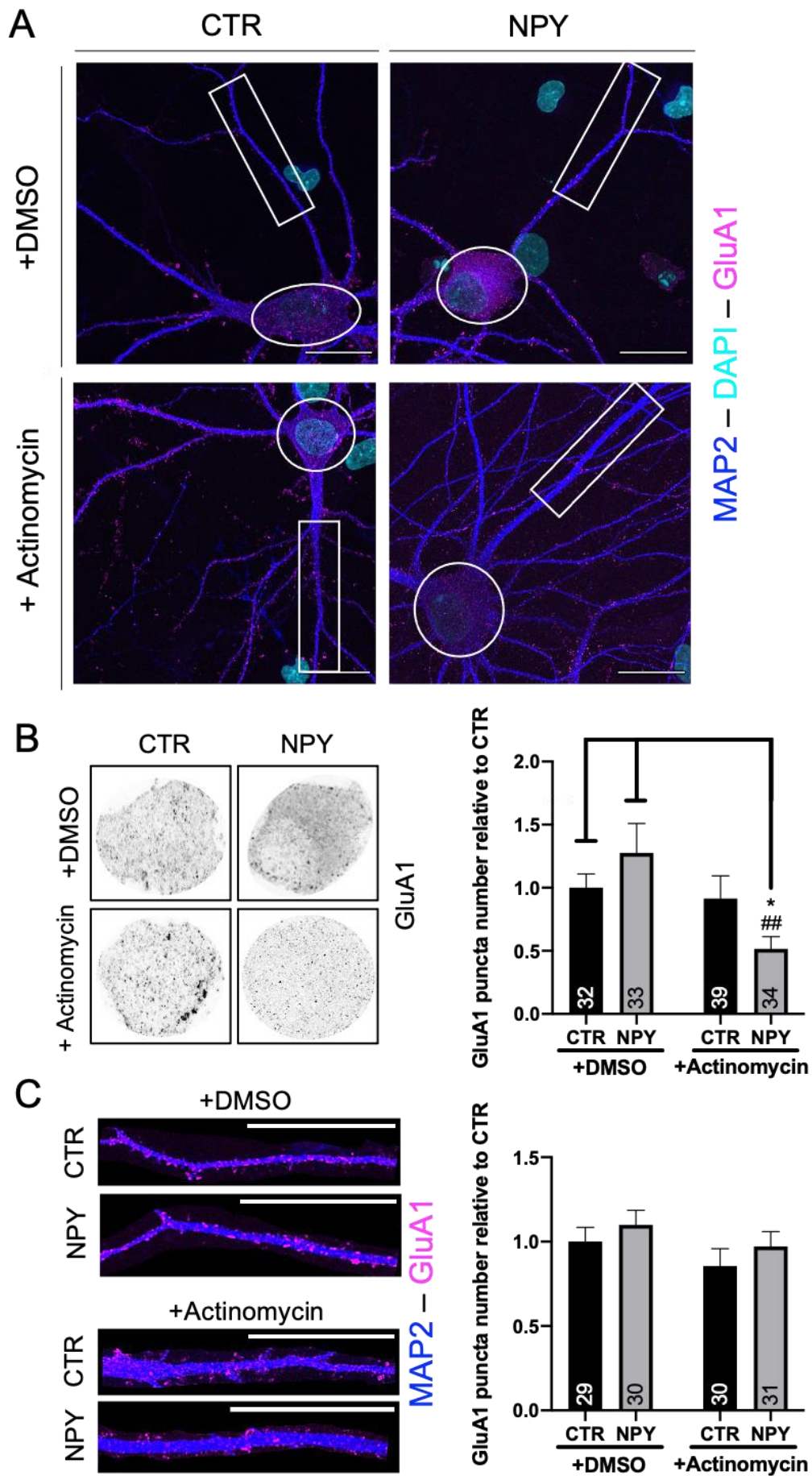
Results

Figure 15. **Blocking the RNA transcriptase with alfa-actinomycin decreases GluA1 puncta in the soma of NPY treated cells but not in the main dendrite.**
Rat differentiated hippocampal primary neural cells (DIV21) were exposed to NPY (100 nM) for 6h in the absence or presence of actinomycin (30 μM, added 5min before NPY) for 6h and cells were then fixed. The control group was treated with pure DMSO, the solvent in which actinomycin is diluted. (A) Representative pictures of GluA1-MAP2-DAPI immunoreactivity in hippocampal rat primary culture (DIV21) exposed to NPY for 6h in the absence or presence of actinomycin. (B-C) Insets showing the immunoreactivity for GluA1 in magnified soma and first 50 μm of neurons' main dendrite. (B) Puncta analysis of GluA1 immunoreactivity in soma and (C) in the first 50μm of neurons' main dendrite. Scale bar, 20 μM. Data are means + SEM. *P < 0.05 versus CTR+DMSO; ##P<0.001 versus NPY+DMSO. Exp=3.

Aveleira et al. (2014) demonstrated that NPY is inducing an increase in autophagy via the coordinated activation of PI3K, MEK/ERK and PKA signalling. These kinases are important in several pathway that span from cell growth and proliferation, to cell differentiation and migration (Nagashima et al. 2015). In particular, ERK has a role in protein synthesis and late-phase LTP (Costa-Mattioli et al. 2009; Kelleher, Govindarajan, and Tonegawa 2004): the activation of ERK is involved in trafficking of existing AMPARs, but it can as well determine the downstream signalling pathways, which in turn initiate new protein synthesis of GluA1 during non-physiological conditions (Liu et al. 2020). In order to evaluate if the NPY treatment has an effect on GluA1 mRNA transcription as well and understand if NPY is regulating GluA1 via increasing its mRNA transcription, at first, the phosphorylation of ERK1/2 time-course during the 6h NPY treatment was investigated (Fig. 16). Despite knowing that NPY activates autophagy via PI3K, MEK/ERK and PKA signalling (as previously seen by Aveleira and colleagues (2014)), the time-course of the phosphorylated form of ERK1/2 did not show any statistically significant difference compared to the control condition (Fig.16; 1h: Student's t-test: t=-1.12, df=8, p=0.295; 3h: Student's t-test: t=-0.622, df=6, p=0.557; 6h: Student's t-test: t=-0.069, df=8, p=0.947).
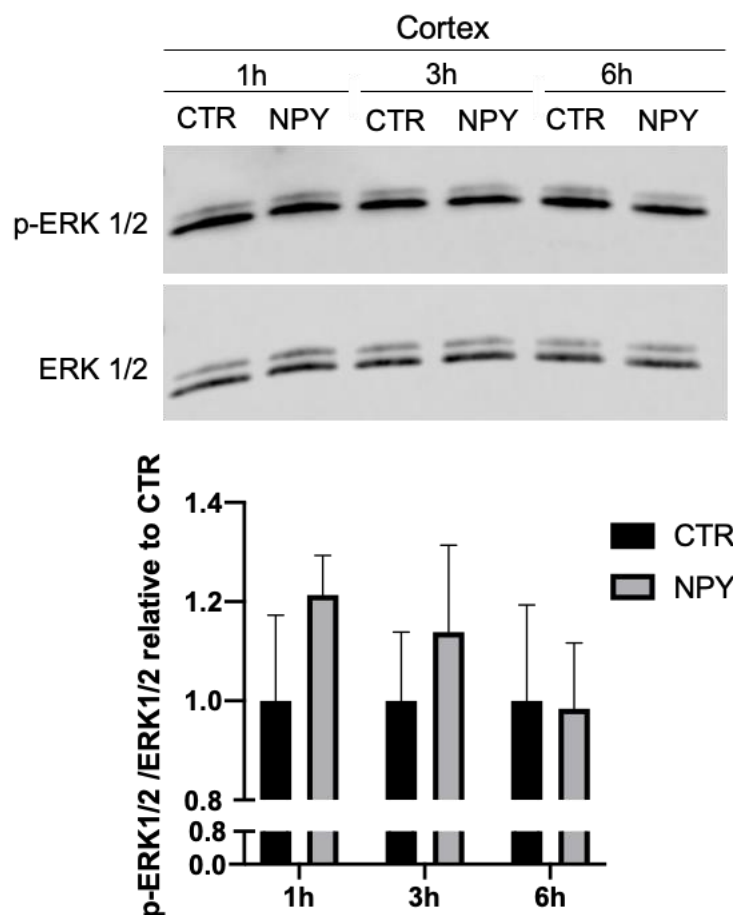
Figure 16. **1h of NPY treatment increases the phosphorylation levels of ERK 1/2.**
Rat differentiated cortical primary neural cells (DIV21) were exposed to NPY (100 nM) for 1h, 3h or 6h and cells were then lysed. At 1h after NPY addition to the medium, p-ERK 1/2 levels show a tendency into an increase compared to the CTR and the phosphorylation increase tendency shows a descending trend over the time points analysed. Representatives immunoblot pictures and immunoblot analysis of p-ERK1/2 and ERK1/2. Exp=3, n=3.

Also, the mRNA levels of GluA1 in DIV21 rat cortical neuronal cocultures were investigated, analysing the relative Gria1 mRNA levels via quantitative reverse transcription polymerase chain reaction (qRT-PCR) over the 6h NPY treatment time course (Fig.17; 1h: Student's t-test: t=-0.19, df=10, p=0.853; 3h: Student's t-test: t=-0.279, df=4, p=0.794; 6h: Student's t-test: t=-0.098, df=6, p=0.925). The NPY treatment is not changing the Gria1 mRNA levels during the 6h time-course.
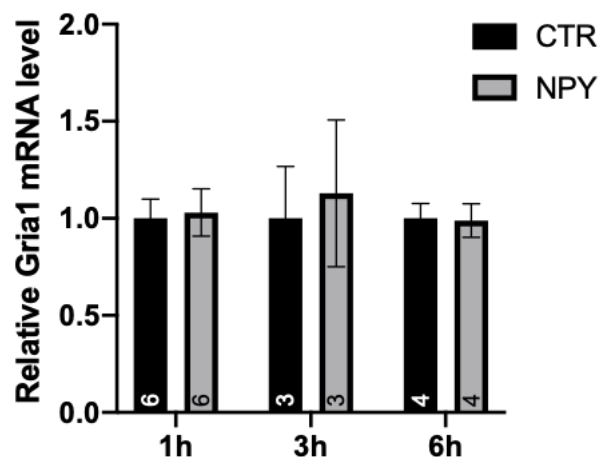
Figure 17. NPY treatment does not increase Gria1 mRNA levels.
Fold changes in Gria1 mRNA expression tested by qRT-PCR in rat differentiated cortical primary neural cells (DIV21) exposed to NPY (100 nM). Total RNA was isolated at 1h, 3h or 6h NPY treatment and used for qRT-PCR analysis of Gria1 gene normalized to GAPDH. Values are expressed as mean fold change relative to control. Error bars show ± SEM. Experiments number in bars.

Despite the lack of changes in the Gria1 levels, it is known that both excitatory and inhibitory presynaptic terminals contain the machinery for protein synthesis, from poly (A)$^+$ mRNA to ribosomal proteins and rRNA, as exhaustively demonstrated by Hafner et al (2019), and among the most enriched transcripts in excitatory synapses there are the ones from the AMPA neurotransmitter family (Hafner et al. 2019). To further investigate the effect seen in the dendrite, where there is no decrease in the GluA1 puncta, nor when the cells are treated with NPY (Fig. 10), nor when there is the pre-treatment with actinomycin D (Fig. 15), the protein synthesis was blocked using cycloheximide. DIV21 rat hippocampal cocultures were treated with the 100nM NPY treatment in combination with 355µM CHX for 6h, after which cells were fixed and stained (Fig. 18). After careful analysis of the data, one point worth mentioning is the variable effect observed when cells are treated with NPY in combination with DMSO, when comparing the different values obtained in Fig. 16 and Fig.18 for the same experimental groups in different sets of experiments: it is known that DMSO, a widely used polar solvent for various pharmacological agents, might have some biological effects on neurons. Reports show that DMSO might produce widespread neuronal apoptosis (Hanslick et al. 2009), neurotoxicity (Bauwens et al. 2005; Windrum and Morris 2003) or even the block of block Na$^+$, K$^+$ and Ca^{++} currents (Ogura et al. 1995). Also, a recent study showed how the use of DMSO in mouse preimplantation embryos is able to induce an increase in the expression of autophagy related genes (Kang et

al. 2017). Nevertheless, neurons resulted viable during the microscopy examination and the concentration of DMSO used in these experiments is lower than the ones described in the aforementioned papers. However, this evidence left space for speculations on possible differences in autophagy between the NPY and DMSO experimental groups that will be further investigated. Nonetheless, as expected, the block of the protein synthesis via the use of CHX is massively decreasing the number of GluA1 puncta in the soma of both the control and the NPY treated conditions (Fig. 18 B; 2-way ANOVA: NPY x CHX $F_{(1,135)}=12.995$, $p<0.0001$; NPY $F_{(1,135)}=8.001$, $p=0.005$; CHX $F_{(1,135)}=67.579$, $p<0.0001$), as the soma is the main neuronal compartment where protein synthesis is carried on. Intriguingly, the block of protein synthesis is decreasing the GluA1 puncta only in the dendrite of the neurons treated by the combination of NPY and CHX (Fig.18 C; 2-way ANOVA: NPY x CHX $F_{(1,124)}=2.954$, $p=0.088$; NPY $F_{(1,124)}=1.65$, $p=0.201$; CHX $F_{(1,124)}=9.223$, $p=0.003$), showing that NPY is promoting the removal of GluA1 puncta from the synapses that cannot be replaced by the local dendritic synthesis of GluA1 when the protein synthesis is blocked with cycloheximide.
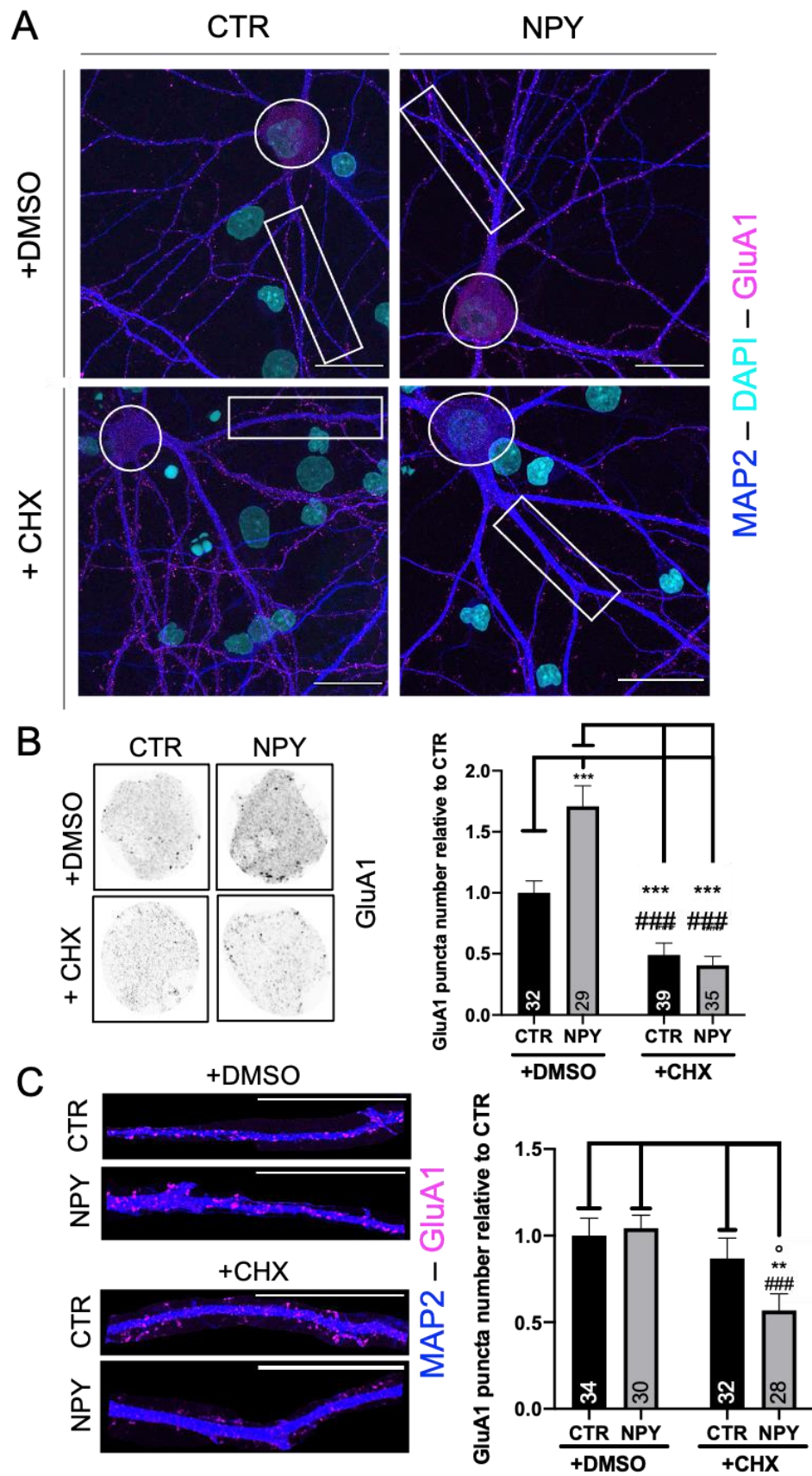
Results

Results

Figure 18. **Blocking the protein synthesis with cycloheximide (CHX) decreases GluA1 puncta in the dendrite of NPY treated neurons.**

Rat differentiated hippocampal primary neural cells (DIV21) were exposed to NPY (100 nM) for 6h in the presence or absence of CHX (355 µM) for 6h. Pure DMSO was used to dilute CHX and, therefore, the diluent was used in the experimental groups that did not receive CHX, as a control. The block of protein synthesis induced by CHX is decreasing GluA1 puncta in the soma of both CTR and NPY treated neurons. However, in the first 50µm of neurons' main dendrite, CHX decreases GluA1 puncta only if the cells are treated with NPY. (A) Representative pictures of GluA1-Map2-DAPI immunoreactivity in hippocampal rat primary culture (DIV21) exposed to NPY for 6h in the absence or presence of CHX. (B-C) Insets showing the immunoreactivity for GluA1 in magnified soma and first 50µm of neurons' main dendrite. (B) Puncta analysis of GluA1 immunoreactivity in soma and (C) in the first 50µm of neurons' main dendrite. Scale bar, 20 µM. Data are means + SEM.**P<0.01, ***P<0.001 versus CTR+DMSO; ###P<0.001 versus NPY+DMSO; °P<0.05 versus CTR+CHX. Exp=3

4.3.2. NPY effect on GluA1 puncta at the synapses

Taken together, these data are pointing towards an NPY-induced removal of GluA1 subunit of AMPA receptor from the synapses. To explore this hypothesis, it was employed an antibody capable of recognising the amino acid residues of the extracellular N-terminus. This antibody can therefore be used to recognize the potential GluA1 subunit sitting at the membrane, meaning that this receptor could be potentially establishing an active synapse, as it is in the location for forming the post-synaptic side of an active synapse. At first, DIV21 rat hippocampal primary cocultures were treated with 100nM NPY for 6h. Then, following the staining protocol from Altmuller et al. (2017), the external portion recognizing GluA1 antibody was added to the medium 30 minutes before the end of the 6h treatment, in order to evaluate if the GluA1 is moving away from the membranes, and consequently from the potential synapses. Neurons were then fixed and further stained with MAP2, in order to identify the dendrites (Fig. 19). As expected, the NPY treatment is statistically decreasing the number of external GluA1 puncta in the main dendrite in the NPY treating condition (Fig. 19 B; Mann-Whitney U: U=168.5, p<0.0001).
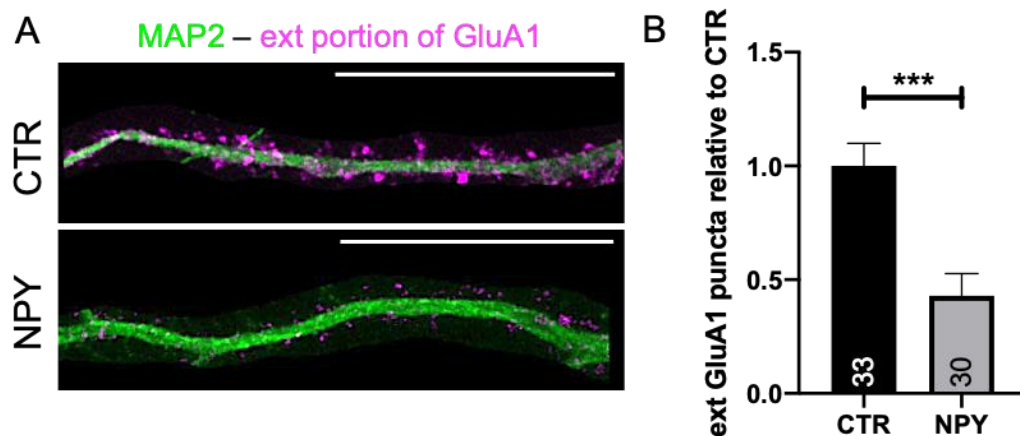
Figure 19. **NPY decreases the external GluA1 puncta in the dendrite.**

Rat differentiated hippocampal primary neural cells (DIV21) were exposed to NPY (100 nM) for 6h and 30 minutes before fixation, an external GluA1 antibody was added to the medium for the live staining. The NPY treatment statistically decrease the number of external GluA1 puncta in the first 50µm of neurons' main dendrite. (A) Representative pictures of external GluA1 portion-Map2 immunoreactivity in hippocampal rat primary culture (DIV21) exposed to NPY for 6h. (B) Puncta analysis of GluA1 immunoreactivity in the first 50µm of neurons' main dendrite. Scale bar, 25 µM. Data are means + SEM. ***P<0.001 versus CTR. Exp=3.

4.3.2.1. NPY decreases the number of VGlut-ext. GluA1 colocalizing puncta

Consequently, to further validate these data and obtain a closer look at the changes in the synapses, the same experimental settings described in 4.3.2 were repeated, this time adding a pre-synaptic marker, VGlut, during the post-fixation staining, in order to evaluate changes in the pre-synaptic – post-synaptic marker association, that could loosely relate to a possible active synapse, as the two areas could potentially contain all the elements necessary and sufficient to have an active synapse (Fig. 20). As expected, there is a decrease in the number of co-localizing VGlut-GluA1 puncta (Fig. 20 B; Mann-Whitney U: number U=413.5, p=0.044; intensity U=426, p=0.063), that is not accompanied by a decrease in the number of VGlut puncta (Fig. 20 C; Mann-Whitney U: U=578.5, p=0.99). These data are pointing towards a NPY-induced reorganization of the post-synaptic side.

Results
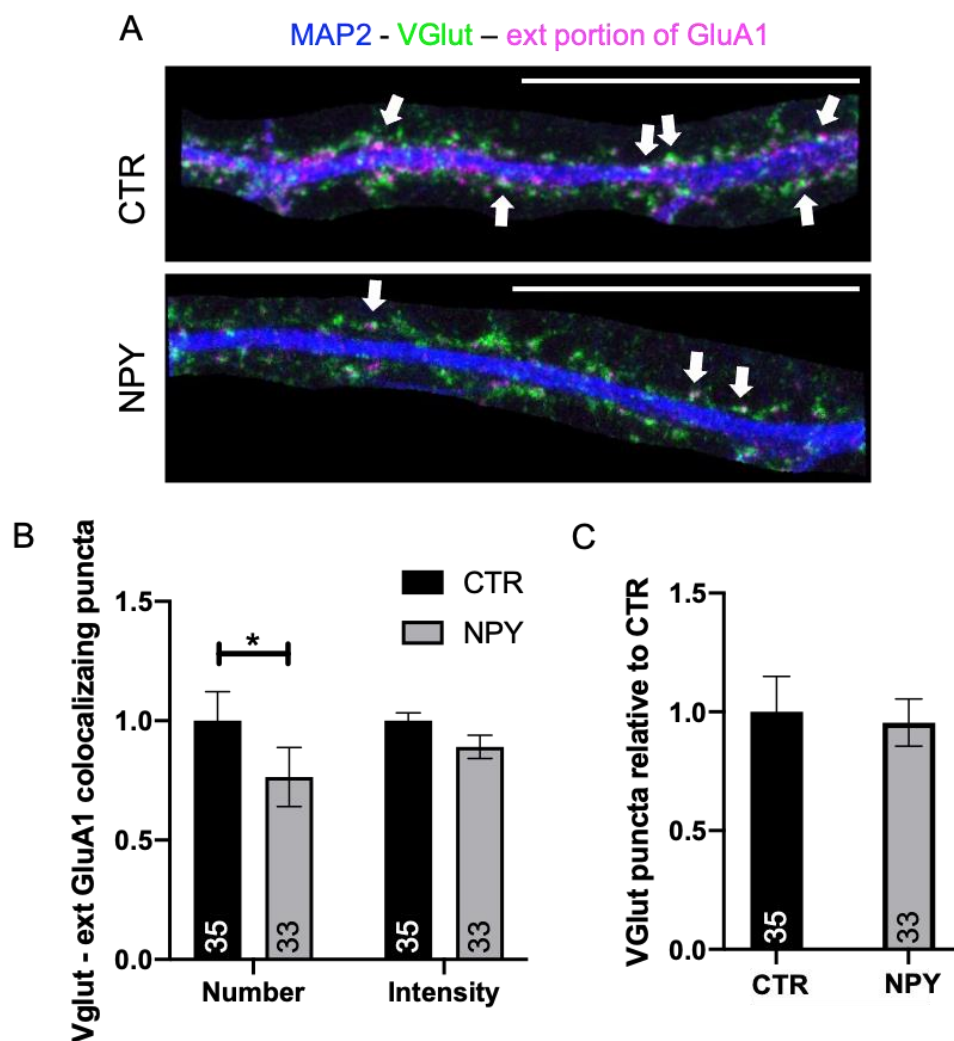
Figure 20. NPY decreases the number of co-localizing VGlut-GluA1, without decreasing the number of VGlut puncta.

Rat differentiated hippocampal primary neural cells (DIV21) were exposed to NPY (100 nM) for 6h and cells were then fixed. (A) Representative pictures of external GluA1 portion-VGlut-Map2 immunoreactivity in hippocampal rat primary culture. White arrows show the colocalizing puncta. (B) Analysis of co-localizing number of puncta and intensity of the co-localization in the first 50μm of neurons' main dendrite. (C) Puncta analysis of VGlut immunoreactivity in the first 50μm of neurons' main dendrite. Scale bar, 25 μM. Data are means + SEM. *$P < 0.05$ versus CTR. Exp=3.

4.3.2.2. NPY increases the number of GluA1-Shank2 colocalizing puncta

In order to further evaluate NPY-induced changes in the dendrites, it was used the GluA1 antibody that recognizes the total endogenous levels of AMPA Receptor 1 (GluA1) protein, in combination with another post-synaptic marker, Shank2. Shank2 is a scaffold protein at the neuronal post-synaptic density (PSD) (Grabrucker et al. 2011), where, together with the other shank protein family members, it plays a critical

role in PSD assembly and functioning of excitatory synapses (Boeckers et al. 1999). Therefore, DIV21 rat hippocampal primary cocultures were treated with 100nM NPY for 6h, after which cells were fixed and stained (Fig. 21). Interestingly, the GluA1 puncta show an increase in the co-localization with Shank2 (Fig. 21 B; Mann-Whitney U: number U=648, p=0.017; intensity U=467, p=0.877), that is accompanied by a strong tendency into an increase in the Shank2 puncta (Fig. 21 C; Mann-Whitney U: U=597, p=0.051).
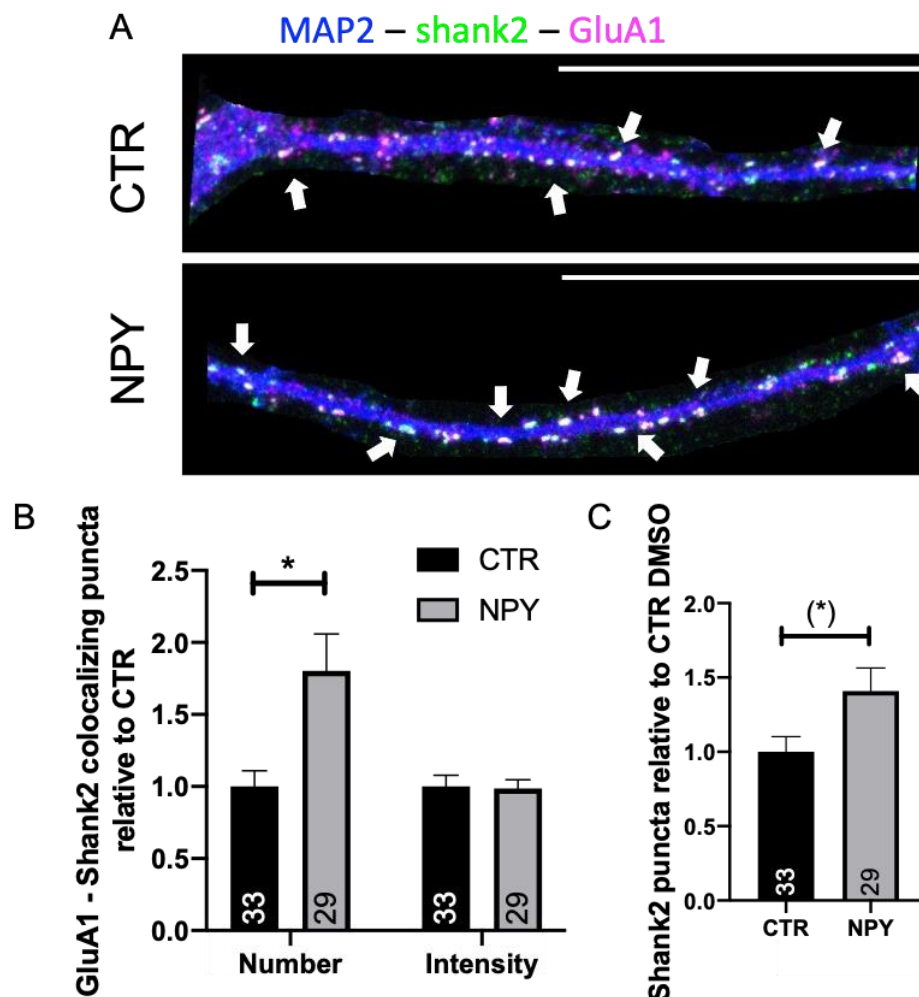
Figure 21. **NPY is increasing the number of co-localizing GluA1-shank2 puncta.**
Rat differentiated hippocampal primary neural cells (DIV21) were exposed to NPY (100 nM) for 6h and cells were then fixed. NPY is promoting the colocalization of GluA1 with shank2, while also showing a trend in increasing the number of shank2 puncta. (A) Representative pictures of GluA1-shank2-Map2 immunoreactivity in hippocampal rat primary culture. White arrows show the colocalizing puncta. (B) Analysis of co-localizing number of puncta and intensity of the co-localization in the first 50µm of neurons' main dendrite. (C) Puncta analysis of shank2 immunoreactivity in the first 50µm of neurons' main dendrite. Scale bar, 25 µM. Data are means + SEM. **P<0.01; (*)p=0.051 versus CTR. Exp=3.

Results

4.3.3. The concomitant block of autophagy and protein synthesis prevents the NPY-effect on GluA1 puncta

To better identify if GluA1 is shuffled in autophagosomes during this possible reorganization, autophagy was blocked again using the shATG5 lentivirus and it was verified what is happening in the dendrite when autophagy is stopped at its first step, the formation of the autophagosomes. Accordingly, rat differentiated hippocampal primary neural cells were infected at DIV14 with the lentivirus containing the shATG5 and the respective shScramble control and allowed the cells to express the shRNA for one week, up until DIV21. Neurons were then treated with 100nM NPY for 6h, after which cells were fixed and stained (Fig. 22). Interestingly, even if autophagosomes cannot be formed due to the use of the shATG5 lentivirus, we still see a tendency into an increase in the GluA1 puncta in the dendrite, in both the control and the NPY treated condition when using the shATG5 lentivirus (Fig. 22 B; 2-way ANOVA: NPY x virus $F_{(1,124)}=0.457$, $p=0.5$; NPY $F_{(1,124)}=81.617$, $p=0.206$; virus $F_{(1,124)}=2.474$, $p=0.118$; CTR shScramble VS NPY shScramble: $t=-2.113$, $df=62$, $p=0.039$; CTR shATG5 VS NPY shATG5: $t=-0.383$, $df=58$, $p=0.703$).
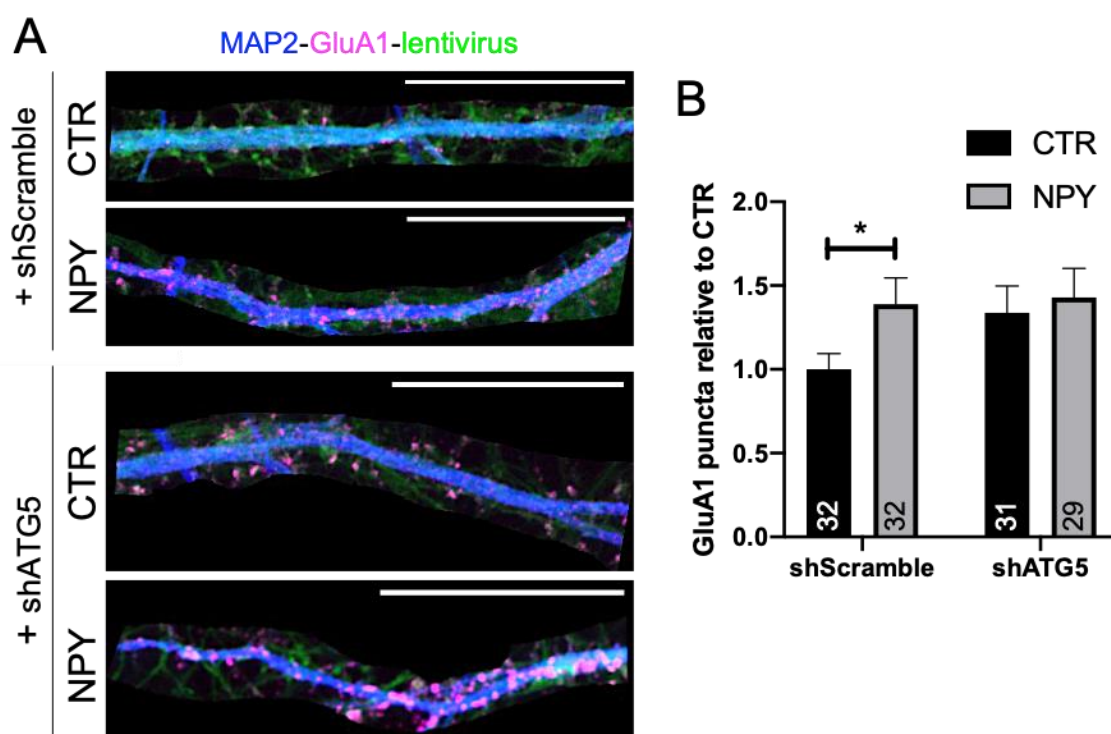
Results

Blocking autophagy by preventing the formation of autophagosomes by using a shATG5 lentivirus determines a slight increase in the GluA1 puncta in both the CTR and NPY treated condition. Rat differentiated hippocampal primary neural cells (DIV14) were infected with a shATG5 lentivirus and respective shScramble control. At DIV21, neurons were exposed to NPY (100 nM) for 6h and cells were then fixed. (A) Representative pictures of GluA1-Map2 immunoreactivity in hippocampal rat primary culture (DIV21) exposed to NPY for 6h in the first 50μm of neurons' main dendrite. (B) Puncta analysis of GluA1 immunoreactivity in the first 50μm of neurons' main dendrite. *$p<0.05$ VS CTR shScramble. Data are means + SEM. Scale bar, 25 μM. Exp=3.

These data leave space for speculation as the block of autophagy in the first step, i.e. the block of the formation of autophagic vesicles, might halt the normal recycle of GluA1 that takes place routinely in cells, therefore leading to an accumulation in both the CTR and NPY condition. Consequently, the increase seen when cells are treated with NPY might be depending on the possibly newly synthesised GluA1 subunit. In order to better understand the aforementioned increase in GluA1 and its relation to autophagy and protein synthesis, the previously described experimental conditions were repeated, this time blocking the protein synthesis as well with CHX during the 6h NPY treatment, to investigate if the effect seen is due to a combination of autophagy and newly produced GluA1 (Fig. 23). Indeed, it was possible to see that neurons infected with the lentivirus containing the shScramble sequence are reproducing the same pattern already seen in Fig. 19, when blocking the protein synthesis: a GluA1 puncta decrease only in the dendrite of the neurons treated by the combination of NPY and CHX (Fig. 23 B). However, this pattern is halted when cells are infected with the shATG5 lentivirus: indeed, the impossibility of the cells to form autophagosomes determines a slight tendency into an increase in the NPY+DMSO control condition (Fig. 23 B), as seen already in Fig. 22. However, when the neurons are infected with the shATG5 and then treated with NPY in combination with CHX, the cells do not show a decrease in the GluA1 puncta (Fig. 23 B; 3-way ANOVA: NPY x virus x CHX $F_{(1,247)}=5.751$, $p=0.017$; NPY $F_{(1,247)}=2.866$, $p=0.092$; virus $F_{(1,247)}=0.405$, $p=0.525$; CHX $F_{(1,247)}=7.302$, $p=0.007$; NPY x virus $F_{(1,247)}=1.312$, $p=0.253$; CHX x NPY $F_{(1,247)}=5.68$, $p=0.018$; CHX x virus $F_{(1,247)}=3.047$, $p=0.082$; CTR shScramble + DMSO VS NPY shScramble + DMSO: $t=-2.237$, df=60, $p=0.029$; NPY shScramble + DMSO VS CTR shScramble + CHX: $t=1.913$, df:59, $p=0.041$; NPY shScramble + DMSO VS NPY shScramble

Results

+ CHX: t=3.638, df=60, p=0.001; CTR shScramble + CHX VS NPY shScramble + CHX: t=1.723, df=59, p=0.05). These data show that NPY seems to promote the reorganization of GluA1 via autophagy and a subsequent GluA1 local synthesis.
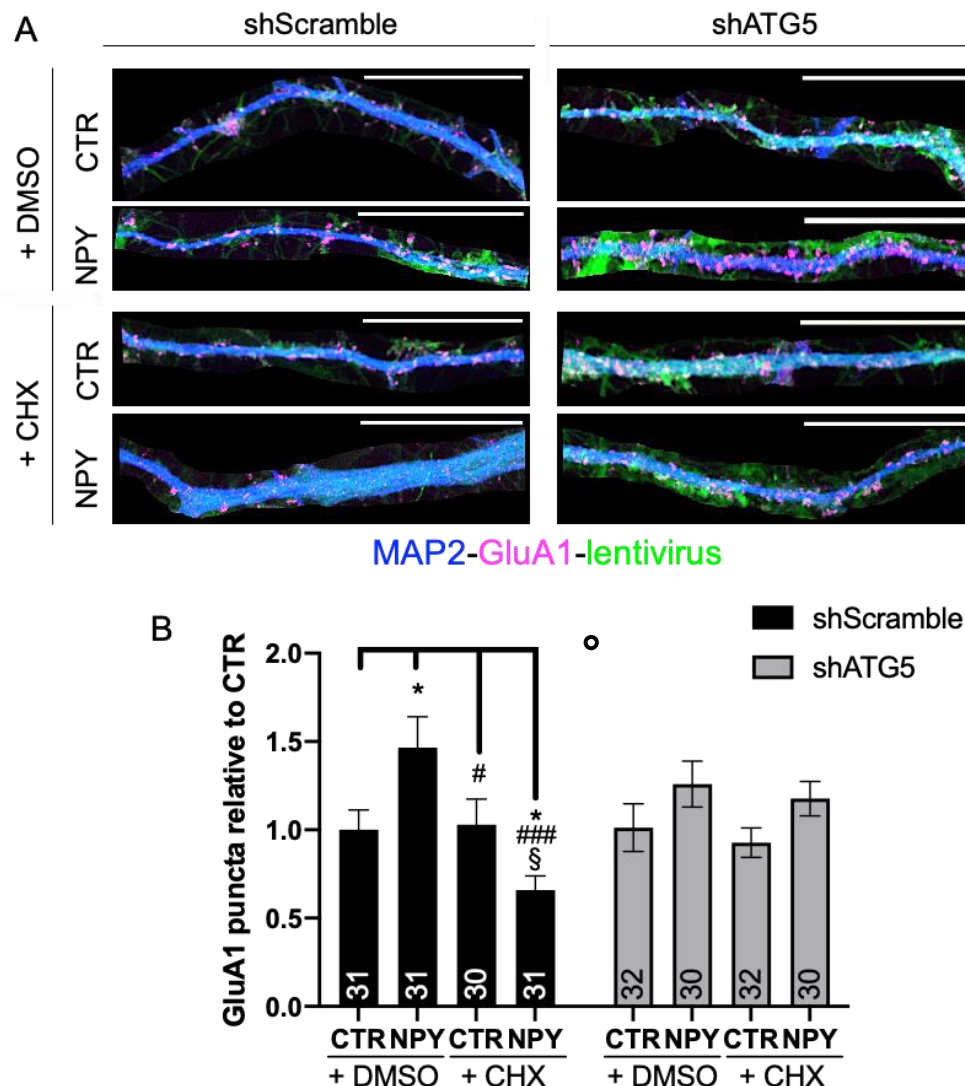
Figure 23. **Blocking autophagy and protein synthesis prevents the decrease of GluA1 puncta in the main dendrite.**

Blocking autophagy at the first step, using a shATG5 lentivirus, thus preventing the formation of autophagosome, and blocking protein synthesis using CHX prevents the decrease in the GluA1 puncta that is determined by the block of protein synthesis with CHX. Rat differentiated hippocampal primary neural cells (DIV14) were infected with a shATG5 lentivirus and respective shScramble control. At DIV21, neurons were exposed to NPY (100 nM) for 6h, with or without CHX (355 µM), and cells were then fixed. Pure DMSO was used to dilute CHX and, therefore, the diluent was used in the experimental groups that did not receive CHX, as a control. (A) Representative pictures of GluA1-Map2 immunoreactivity in hippocampal rat primary culture (DIV21) in the first 50µm of neurons' main dendrite. (B) Puncta analysis of GluA1 immunoreactivity in the first 50µm of neurons' main dendrite. Scale bar, 25 µM. °P<0.05 NPY x virus x CHX effect; *P<0.05 versus CTR+DMSO shScramble; #P<0.05, ##P<0.01 versus NPY+DMSO shScramble; °P<0.05 versus CTR+CHX shScramble. Data are means + SEM. Exp=3.

Results

4.4.　　　The long-lasting changes in GluA1

Knowing that the autophagy effect induced by the 6h NPY treatment is lasting for up to 24h after the medium change, it was further investigated if the changes seen in the GluA1 subunit of the AMPA receptor are as long-lasting as the autophagic ones. Consequently, repeating the experiment described in 4.1.3., DIV21 cortical primary neuronal cocultures were treated with NPY 100nM for 6h. Next, the medium was completely removed and replaced with freshly prepared half-conditioned medium and the cells were left in the incubator for 24h or 48h after the medium change, after which the cells were lysed. The GluA1 subunit of the AMPA receptor was then analysed via WB (Fig. 24). Interestingly, it was possible to see an effect of the 6h NPY treatment on the GluA1 protein levels 24h after the medium change (Fig. 24 A; Paired sample test: $t=-4.376$, $df=6$, $p=0.005$). On the other hand, the increase in the GluA1 levels at 24h goes back to control levels 48h after the 6h NPY treatment and subsequent medium change (Fig. 24 B; Paired sample test: $t=-0.15$, $df=14$, $p=0.885$).
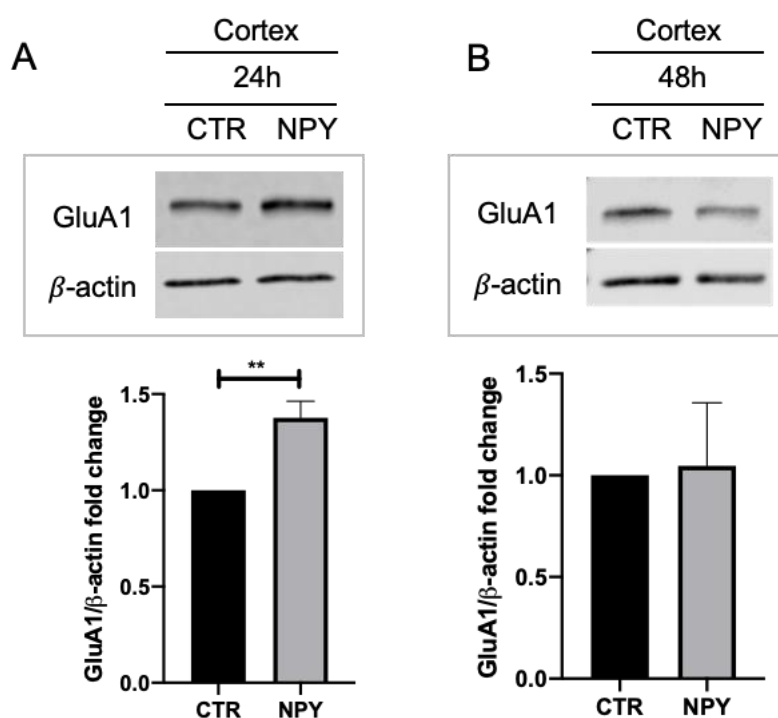
Figure 24. **The 6h NPY treatment increases the GluA1 protein levels 24h after the medium change.**
Rat differentiated cortical primary neural cells (DIV21) were exposed to NPY (100 nM) for 6h, after which the medium was changed, and cells were then lysed 24h or 48h after the medium change. NPY is promoting the increase of GluA1 for up to 24h. (A) Representative immunoblot pictures and immunoblot analysis of GluA1 24h after the medium exchange. (D) Representative immunoblot pictures and immunoblot analysis of GluA1 48h after the medium exchange. Data are means + SEM. **$P<0.01$ versus CTR. Exp=4, n=4.

Results

Two other neuronal receptors were analysed, to investigate if the NPY effect 24h after the medium change is specific for the GluA1 subunit receptor or if there are changes in other receptors as well (Fig. 25). The effect seems to be specific for the GluA1 subunit of the AMPA receptor, as nor GABA A, an inhibitory receptor, nor NMDAR1, another excitatory receptor, seem to show any changes 24h after the 6h NPY treatment and subsequent medium change (Fig. 25 A; Student's t-test: t=1.051, df=6, p=0.334; and B; Student's t-test: t=-0.547, df=6, p=0.604).
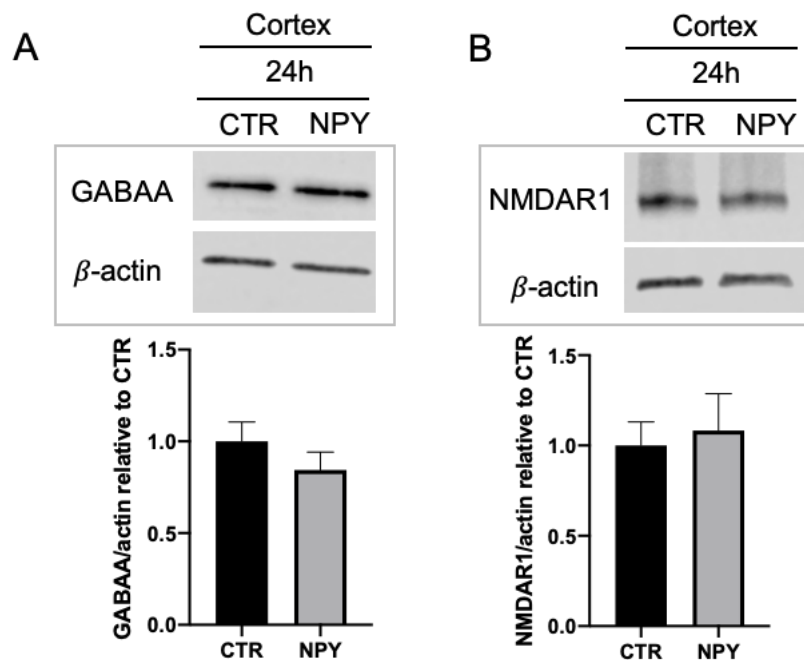
Figure 25. **The 6h NPY treatment does not increase GABAA or NMDAR1 protein levels.**
Rat differentiated cortical primary neural cells (DIV21) were exposed to NPY (100 nM) for 6h, after which the medium was changed, and cells were then lysed 24h after the medium change. NPY does not change GABAA nor NMDAR1 protein levels 24h after medium change. (A) Representative immunoblot pictures and immunoblot analysis of GABAA and (B) NMDAR1 after the medium exchange. Data are means + SEM. *P<0.05 versus CTR. Exp=4, n=4.

4.4.1. The NPY-induced autophagy increases GluA1 levels 24h post-stimulation

To further confirm and evaluate if the increase seen in GluA1 protein levels 24h after the 6h NPY treatment is due to the increase in autophagy induced by NPY, autophagy was blocked at the first step either using wortmannin (WRT), an inhibitor of PI3K that blocks the autophagic sequestration (Edward F.C. Blommaart et al. 1997) during the 6h NPY treatment or the previously mentioned shATG5 lentivirus (Fig. 26). As expected, the block of autophagy, either pharmacologically using WRT (Fig. 26 A; 2-way ANOVA: NPY x WRT $F_{(1,12)}=0.808$, p=0.395; NPY $(1,12)=3.218$, p=0.111; WRT

Results

F(1,12)=8.376, p=0.02) or more specifically and precisely with the sh-lentivirus against ATG5 (Fig. 26 B; 2-way ANOVA: NPY x virus F(1,12)=1.045, p=0.327; NPY (1,12)=4.762, p=0.05; virus F(1,12)=4.67, p=0.052), is preventing the GluA1 increase 24h after the medium change.
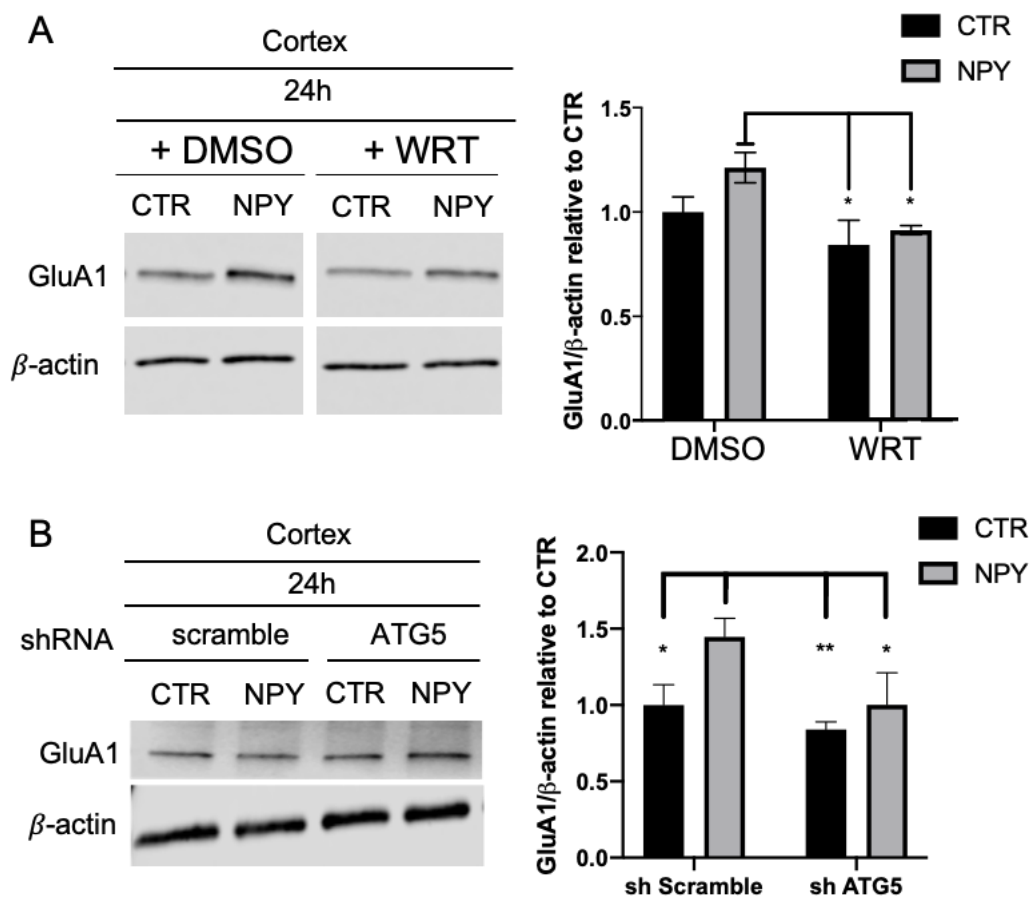
Figure 26. **Blocking autophagy with wortmannin (WRT) or the shATG5 lentivirus during the NPY 6h treatment prevents the increase in GluA1 24h after the medium change.**
(A) WRT is preventing the increase of GluA1. Rat differentiated cortical primary neural cells (DIV21) were exposed to NPY (100 nM) for 6h with or without WRT (1 μM), after which the medium was changed, and cells were then lysed 24h after the medium change. Pure DMSO was used to dilute WRT and, therefore, the diluent was used in the experimental groups that did not receive WRT, as a control. Representative immunoblot pictures and immunoblot analysis of GluA1 24h after the medium exchange. White bands between densitometry pictures show that the bands come from different position on the same blot. (B) Rat differentiated cortical primary neural cells (DIV14) were infected with a shATG5 lentivirus and respective shScramble control. At DIV21, neurons were exposed to NPY (100 nM) for 6h after which the medium was changed, and cells were then lysed 24h after the medium change. Data are means + SEM. *P<0.05 versus NPY+DMSO in (A). *P<0.05 and **P<0.01 versus NPY shScramble in (B). Exp=4, n=4.

Moreover, the effect seems to be induced by autophagy, as the UPS system, the other quality control system used by cells to recycle its components for cellular homeostasis, is not affected by the NPY treatment already right after the 6h NPY treatment (Fig. 27; Student's t-test: t=0.332, df=10, p=0.747).
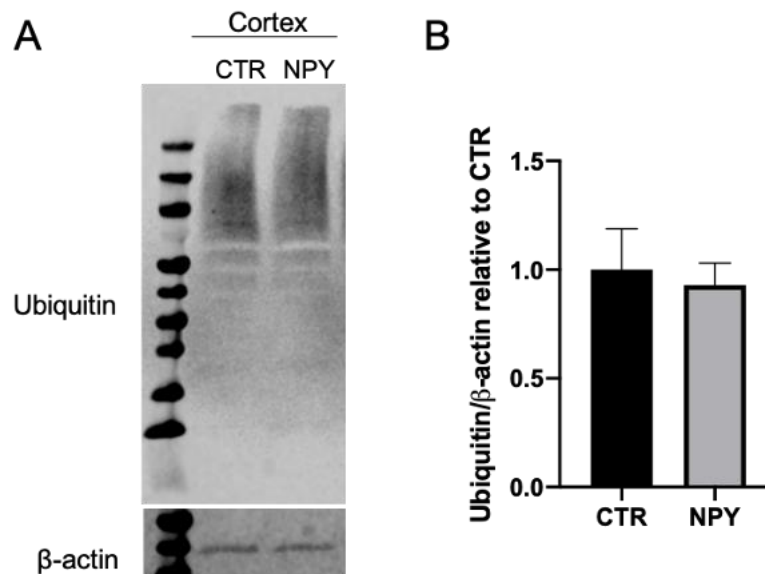
Figure 27.NPY does not increase the ubiquitination of proteins.
Mature rat differentiated cortical primary neural cells (DIV21) were exposed to NPY (100 nM) for 6h and cells were then lysed. (A-B) Immunoblotting analysis of Ubiquitin. The 6h NPY treatment does not increase the ubiquitination. (A) Representative immunoblot pictures. Data are means + SEM. Exp=4, n ≥ 3.

4.4.2. NPY is increasing the GluA1 puncta in the main dendrite 24h after the 6h stimulation

In order to pinpoint the exact location of the GluA1 increase, DIV21 rat hippocampal primary cocultures were treated with 100nM NPY for 6h, after which the medium was removed and substituted with freshly prepared half-conditioned medium. The cells were then put back in the incubator for 24h, after which cells were fixed and stained for GluA1 (Fig. 28). Differently to what it was possible to see directly after the 6h of NPY treatment in Fig.11, there are no changes in the soma of the neurons treated with NPY (Fig. 28 B; Mann-Whitney U: U=436, p=0.413), while it is possible to see an increase of the GluA1 puncta in the first 50µm of neurons' main dendrite 24h after the 6h NPY treatment and subsequent medium change (Fig. 28 C; Student's t-test: t=-2.157, df=61, p=0.035).

Results
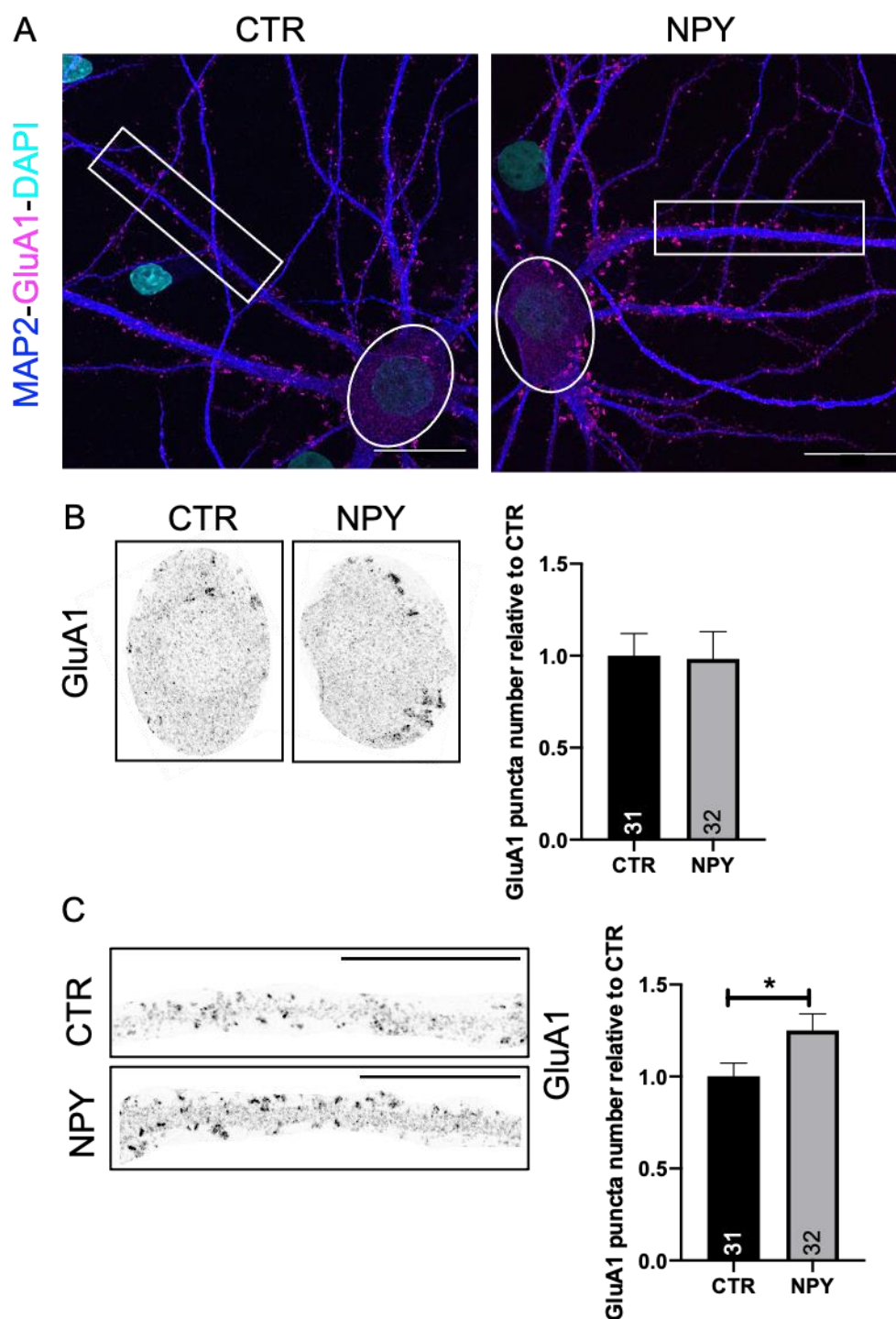
Figure 28. **The 6h NPY treatment enhances GluA1 puncta in the dendrite of hippocampal primary neuronal cultures 24h after the medium change.**

Rat differentiated cortical primary neural cells (DIV21) were exposed to NPY (100 nM) for 6h after which the medium was changed, and cells were then fixed 24h after the medium change. (A) Representative pictures of GluA1-Map2-DAPI immunocytochemistry. Insets show increased GluA1 puncta in the magnified soma of the NPY treated neurons. (B-C) Insets showing the immunoreactivity for GluA1 in magnified soma and first 50μm of neurons' main dendrite. (B) Puncta analysis of GluA1 immunoreactivity in soma and (C) in the first 50μm of neurons' main dendrite. Scale bar, 20 μM. Data are means + SEM. *P < 0.05 significantly different from CTR. Exp=3.

Results

Indeed, it seems that the NPY treatment is producing a rearrangement of the GluA1 puncta that are now shuffled towards the synapses. Therefore, to get a closer look into this phenomenon, the previously mentioned experiment was repeated, but this time the cells were live stained with the GluA1 antibody recognising the amino acid residues of the extracellular N-terminus already mentioned in section 4.3.2.1. Accordingly, to investigate this hypothesis, at first, DIV21 rat hippocampal primary cocultures were treated with 100nM NPY for 6h. Then, once more, the medium was removed and substituted with freshly prepared half-conditioned medium and the cells back were put back in the incubator for 24h. On the next day, following the staining protocol from Altmuller et al. (2017), the external portion recognizing GluA1 antibody was added to the medium 30 minutes before the end of the 24h post medium change and the neurons were then fixed and further stained with MAP2, in order to identify the dendrites (Fig. 29). Indeed, these data seem to show that the increase in the GluA1 puncta in the main dendrite seen in Fig. 28 might be due to an increase in the GluA1 portion sitting at the synapse (Fig. 28 B; Mann-whitney U: U=732.5, p=0.016).
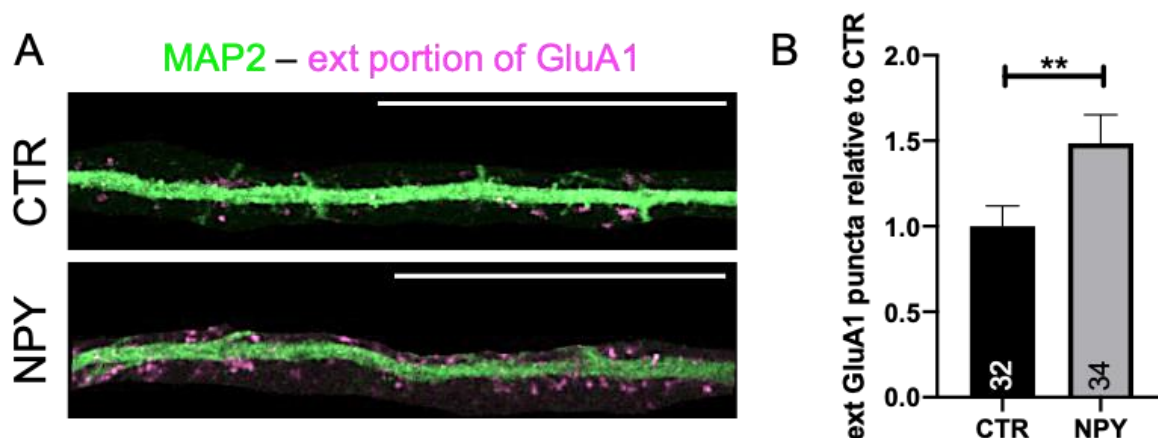
Figure 29. **The 6h NPY treatment increases the external GluA1 puncta in the dendrite 24h after the medium change.**
Rat differentiated hippocampal primary neural cells (DIV21) were exposed to NPY (100 nM) for 6h, after which the medium was change and cells were then fixed 24h after the medium change. 30 minutes before fixation, an external GluA1 antibody was added to the medium for the live staining. The NPY treatment statistically increase the number of external GluA1 puncta in the first 50µm of neurons' main dendrite. (A) Representative pictures of external GluA1 portion-Map2 immunoreactivity in hippocampal rat primary culture (DIV21) exposed to NPY for 6h. (B) Puncta analysis of GluA1 immunoreactivity in the first 50µm of neurons' main dendrite. Scale bar, 25 µM. Data are means + SEM. **P<0.01 versus CTR. Exp=3.

Results

4.4.2.1. NPY is not modifying the number of GluA1 colocalization

To further investigate the increase of GluA1 puncta (both the total and the external portion GluA1 puncta), the number of GluA1 puncta colocalization with a pre-synaptic and a post-synaptic marker was evaluated. At first, the same experiment performed in Fig. 29 was repeated, but this time the neurons were stained for VGlut as well, post fixation (Fig. 30). Interestingly, these data show that despite the increase of the external GluA1 puncta, these puncta do not colocalize more with the presynaptic marker VGlut (Fig. 30 B; Mann-Whitney U: number U=730.5, p=0.477; intensity U=602, p=0.48), neither there are changes in the number of VGlut (Fig. 30 C; Student's t-test: t=-0.869, df=71, p=0.388).
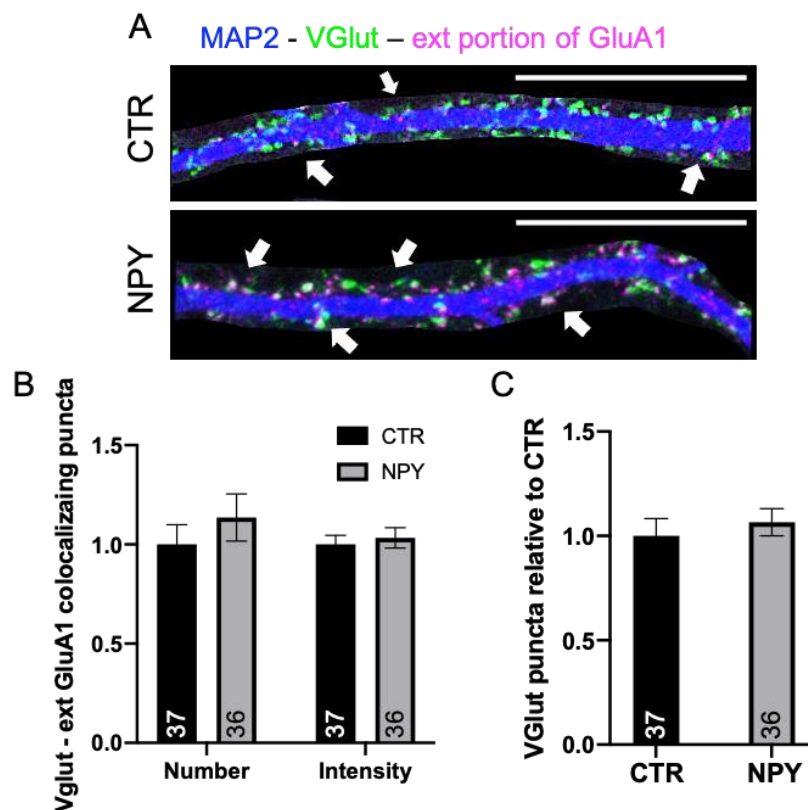
Figure 30. **The 6h NPY treatment does not affect the number of colocalizing GluA1-VGlut puncta in the dendrite 24h after the medium change.**
Rat differentiated hippocampal primary neural cells (DIV21) were exposed to NPY (100 nM) for 6h, after which the medium was change and cells were then fixed 24h after the medium change. 30 minutes before fixation, an external GluA1 antibody was added to the medium for the live staining. (A) Representative pictures of external GluA1 portion-VGlut-Map2 immunoreactivity in hippocampal rat primary culture. White arrows show some of the colocalizing puncta. (B) Analysis of co-localizing number of puncta and intensity of the co-localization in the first 50µm of neurons' main dendrite. (C) Puncta analysis of VGlut immunoreactivity in the first 50µm of neurons' main dendrite. Scale bar: 25 µM. Data are means + SEM. Exp=3.

Results

Consequently, to visualize if the NPY treatment is inducing changes on the post-synaptic side, in this case it was used the antibody recognizing the total GluA1, paired with, Shank2, a post-synaptic marker. DIV21 rat hippocampal primary cocultures were treated with 100nM NPY for 6h. Then, the medium was completely removed and substituted with freshly prepared half-conditioned medium and the cells were left in the incubator for 24h. On the next day, the cells were fixed and stained after fixation with the GluA1 antibody recognizing the total GluA1, paired with MAP2 and Shank2 antibodies (Fig. 30). On the post-synaptic side as well, NPY is not inducing any statistically significant changes (Fig. 30 B; Mann-Whitney U: number U=545, p=0.36; intensity U=455, p=0.725; and C; Mann-Whitney U: U=519.5, p=0.747).
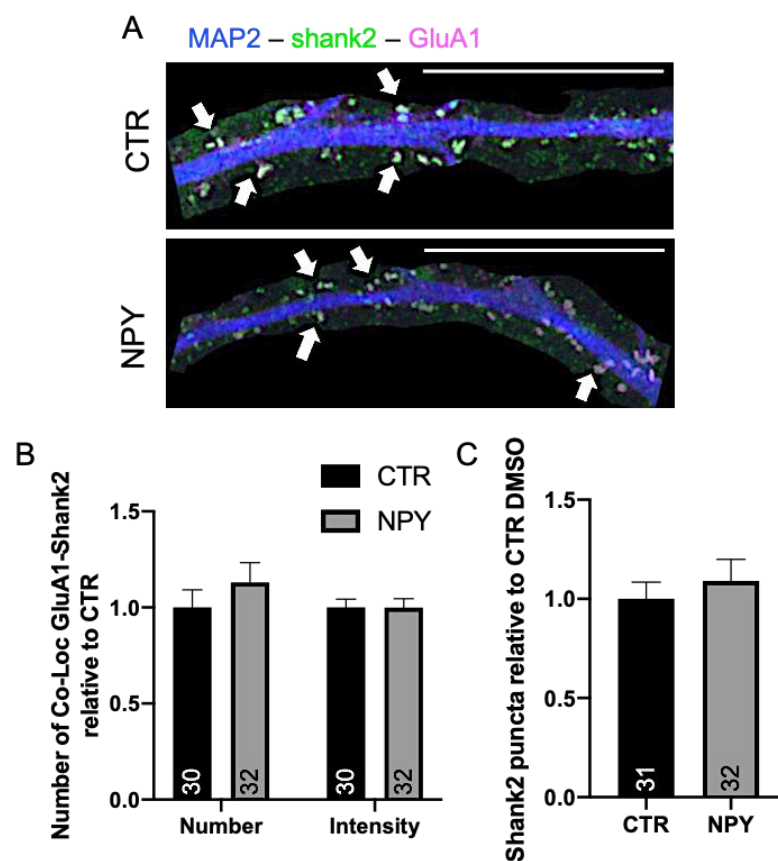
Figure 31. **The 6h NPY treatment does not affect the number of colocalizing GluA1-Shank2 puncta in the dendrite 24h after the medium change.**
Rat differentiated hippocampal primary neural cells (DIV21) were exposed to NPY (100 nM) for 6h, after which the medium was change and cells were then fixed 24h after the medium change. (A) Representative pictures of GluA1-Shank2-Map2 immunoreactivity in hippocampal rat primary culture. White arrows show some of the colocalizing puncta. (B) Analysis of co-localizing number of puncta and intensity of the co-localization in the first 50µm of neurons' main dendrite. (C) Puncta analysis of Shank2 immunoreactivity in the first 50µm of neurons' main dendrite. Scale bar: 25 µM. Data are means + SEM. Exp=3.

4.5.   The NPY effect on mice hippocampus

As previously described in the introduction of this thesis, the FC model could be used to activate some of the key brain areas involved in PTSD, along with the inducement of trigger-induced persistent and exaggerated learned fear. Moreover, it is known that, *in vivo*, NPY is released by the HIPP cells in the hippocampus during fear conditioning: Raza et al. (2017) demonstrated that during stressful aversive learning, such as the Pavlovian FC protocol performed in the aforementioned paper, cholinergic neurons from the septum activate at the same time HIPP cells (the major population of NPY positive interneurons in the dentate gyrus (DG), where they have a role in the adjustment of memory salience by releasing NPY) and granule cells. However, the cholinergic activation of HIPP cells prompts the release of NPY from HIPP cells, which binds to Y1 receptors on the granule cells, that in turns attenuates their activity and regulates the context salience in a background context fear conditioning paradigm.

4.5.1. NPY effect on mice dDG 6h after infusion

At first, the effect NPY has *in vivo* on both GluA1 and LC3 at 6h was evaluated histologically, knowing that, for example, in the cell culture there is an increase in autophagy that is accompanied by an accumulation of LC3 puncta in the soma of the neurons already 6h after the treatment. To do so, Prof. Dr. Dr. Anne Albrecht infused NPY (0.15 mg/ml) in the dDG of young adult mice that were then sacrificed 6h after NPY-infusion, to evaluate regional changes in the intensity of GluA1 and LC3 IHC stainings in the dDG, following the *in vitro* timeline. At first, the focus was on the autophagy marker LC3 and the IHC performed on the dDG slices aimed at evaluating changes in the intensities displayed 6h after the infusion of NPY, mimicking the NPY treatment performed on the hippocampal cell cultures (Fig. 32). As expected, visualising changes in the autophagy levels of neurons *in vivo* can be difficult, as autophagy has a high flux and efficiency that, even if perturbed, is difficult to see and in contrast to cell culture experiments, blocking the autophagic flux with CQ is not conceivable in the intact brain (Fig. 32 G; Student's t-test: Hilus: $t=-0.486$, $df=10$, $p=0.637$; Granule cell layer (GCL): $t=-1.292$, $df=10$, $p=0.225$; Inner portion of the granule cells' dendrites or inner molecular layer (IML): $t=-1.395$, $df=10$, $p=0.193$; Medial portion of the granule cells'

dendrites or middle molecular layer (MML): t=-1.473, df=10, p=0.171; Distal portion of the granule cells' dendrites or outer molecular layer (OML) t=-0.339, df=10, p=0.741).
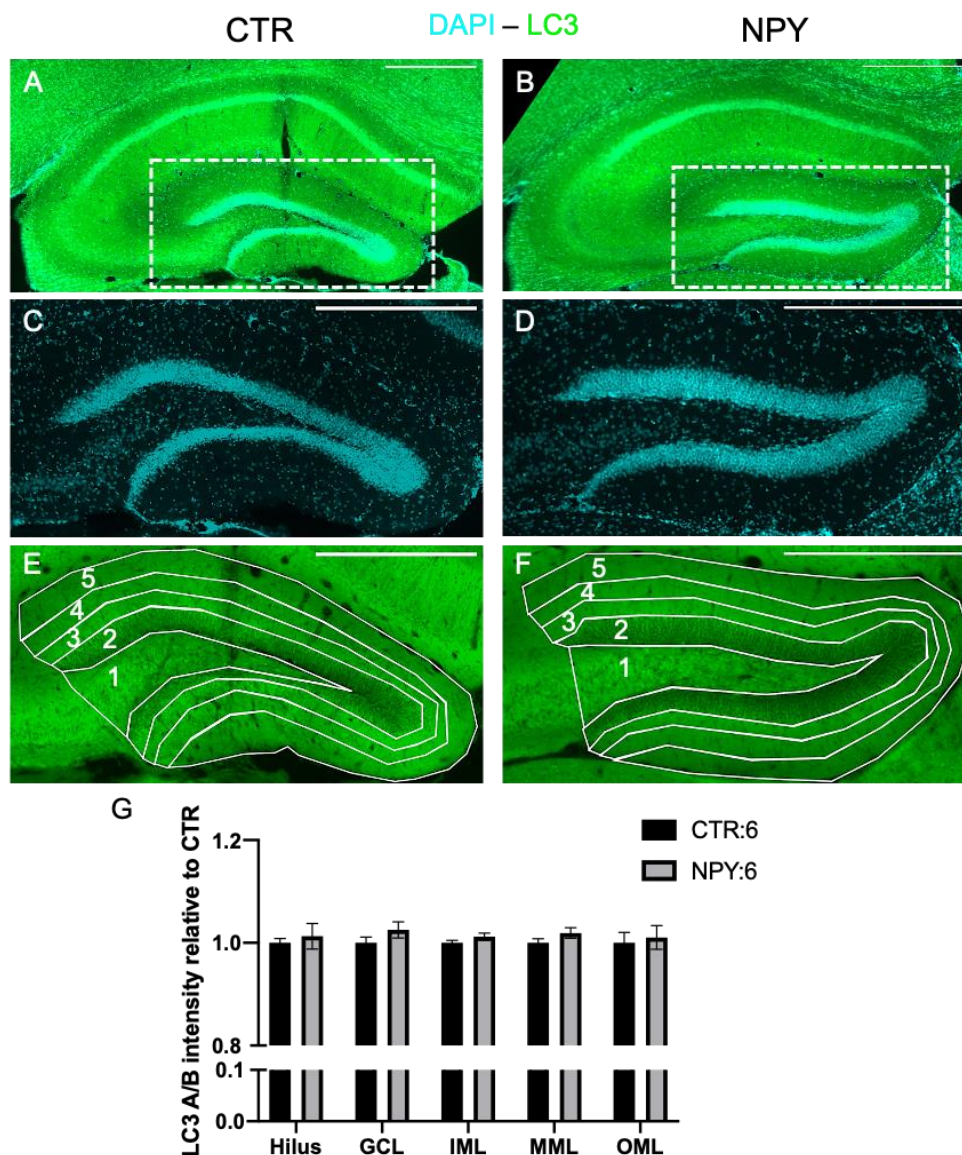
Figure 32. **The infusion of NPY in the dorsal dentate gyrus does not produce any changes in the LC3 intensity in the dDG, 6h after the NPY infusion.**
Young adult mice were infused with 1ul/side of NPY (0.15mg/ml) or saline delivered over 4 min. The injection cannula was left in position for additional 2 min before withdrawal to minimize dragging of the injected liquid along the injection tract. The animals were the left undisturbed for 6h after the injection and the brains were then perfused.
(A-B) Representative pictures of LC3-DAPI immunoreactivity in the dorsal hippocampus of mice infused with NPY or saline as a control. (C-D) Insets show DAPI immunoreactivity in the magnified dorsal dentate gyrus. (E-F) Insets show LC3 immunoreactivity in the magnified dorsal dentate gyrus, with a schematic of the different areas' segmentation used to analyse the LC3 intensity; 1. hilus, 2. DG: granule cells layer (GCL), 3. proximal portion of the granule cells dendrites or inner molecular layer (IML); 4. medial portion middle of the granule cells dendrites or middle molecular layer (MML); 5. distal portion of the granule cells' dendrites or outer molecular layer (OML). (G) Quantification of the LC3 intensity in the dDG divided per area analysed. Scale bar: 500 µM. Data are shown as mean ± SEM.

Results

Despite this lack of changes in the autophagy levels, slices were stained for GluA1, in order to verify if the accumulation of GluA1 puncta in the soma seen in the cell culture (see Fig. 11) can be seen in the animals 6h after NPY infusion as well (Fig. 32). Differently to my previous findings in the cell culture, where the 6h NPY treatment produces an accumulation of GluA1 puncta in the soma of neurons (seen via ICC in Fig. 11), the infusion of NPY *in vivo* is determining an increase in the intensity of GluA1 in the distal part of the granule cell dendrites, as well as an interaction between the NPY infusion and the dendritic portion analysed, as the more distal we move across the dendritic portion, the more the GluA1 intensity increases (Fig. 32 G; Student's t-test, Hilus: $t=1.348$, $df=10$, $p=0.207$; Granule cell layer (GCL): $t=1.438$, $df=10$, $p=0.181$; Inner portion of the granule cells' dendrites or inner molecular layer (IML): $t=1.024$, $df=10$, $p=0.33$; Medial portion of the granule cells' dendrites or middle molecular layer (MML): $t=-0.173$, $df=10$, $p=0.866$; Distal portion of the granule cells' dendrites or outer molecular layer (OML): $t=-2.787$, $df=10$, $p=0.019$; repeated measures ANOVA with a Greenhouse-Geisser correction NPY x dendritic portion effect: $F_{(1.226, 12.261)}=8.495$, $p=0.01$). However, as the evidences from the cell culture show, already at 6h there is tendency into an increase in the general GluA1 protein levels (seen via WB in Fig. 10), as well as a beginning of GluA1 accumulation in the dendrites of hippocampal neurons (as seen via ICC in Fig. 11).
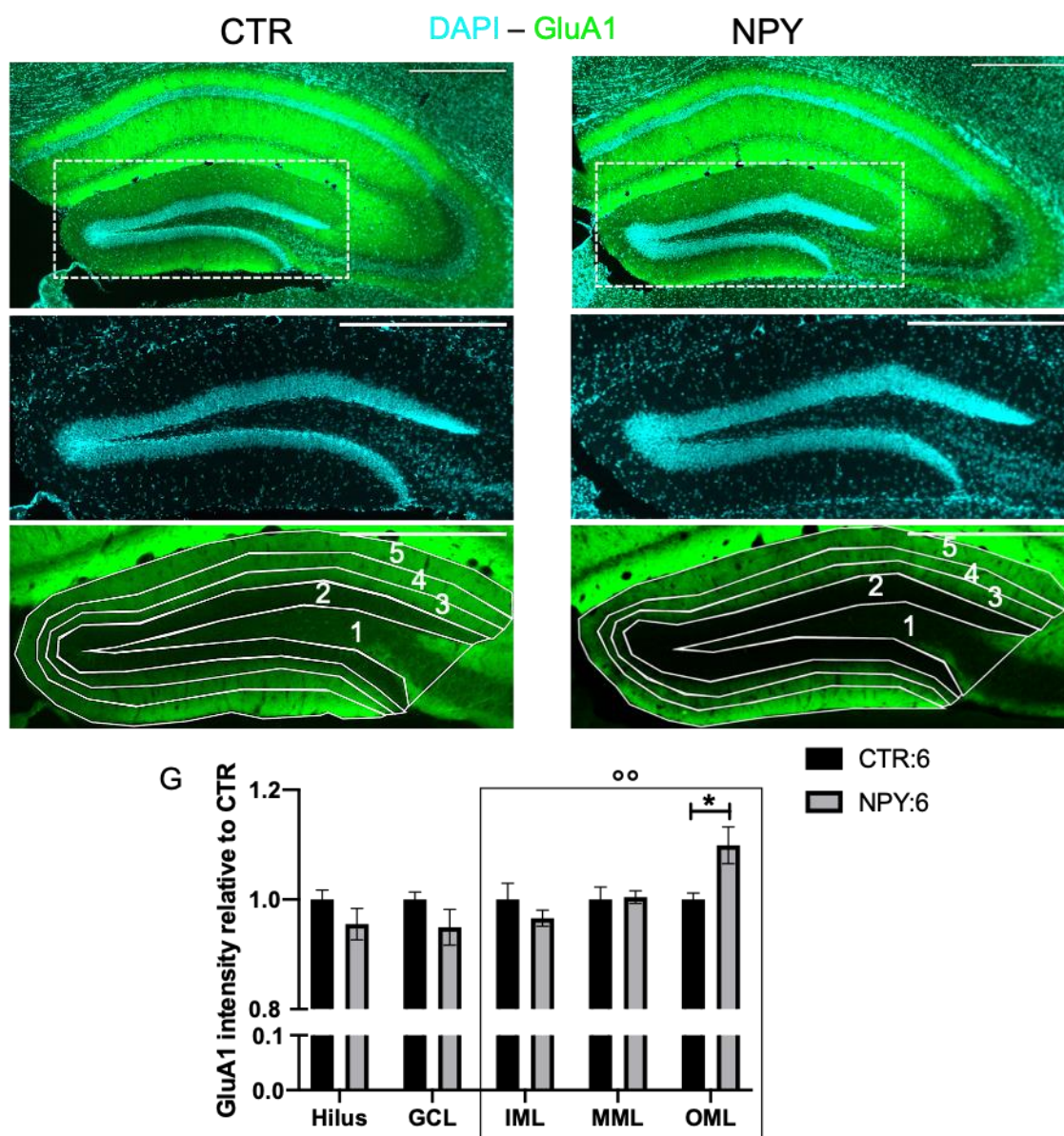
Figure 33. **The infusion of NPY in the dorsal dentate gyrus determines an increase of GluA1 intensity in the outer portion of the dendrites of the granule cells, 6h after the NPY infusion.**

Young adult mice were infused with 1ul/side of NPY (0.15mg/ml) or saline delivered over 4 min. The injection cannula was left in position for additional 2 min before withdrawal to minimize dragging of the injected liquid along the injection tract. The animals were then left undisturbed for 6h after the injection and the brains were then perfused.

(A-B) Representative pictures of GluA1-DAPI immunoreactivity in the dorsal hippocampus of mice infused with NPY or saline as a control. (C-D) Insets show DAPI immunoreactivity in the magnified dorsal dentate gyrus. (E-F) Insets show GluA1 immunoreactivity in the magnified dorsal dentate gyrus, with a schematic of the different areas' segmentation used to analyse the GluA1 intensity; 1. hilus, 2. DG: granule cells layer (GCL), 3. proximal portion of the granule cells dendrites or inner molecular layer (IML); 4. medial portion middle of the granule cells dendrites or molecular layer (MML); 5. distal portion of the granule cells' dendrites or outer molecular layer (OML). (G) Quantification of the GluA1 intensity in the dDG divided per area analysed. Scale bar: 500 µM. °°p=0.01 NPY x dendritic portion effect; *p<0.05 VS CTR. Data are shown as mean ± SEM.

4.5.2. NPY effect on mice dDG 24h after infusion

To further investigate the effect NPY has in the dDG of mice, the findings and timeline of the cell culture was followed. From the data collected in the cell culture, NPY is able to produce an increase in autophagy that continues to stay high, compared to CTR conditions, 24h after the 6h NPY treatment. Consequently, animals were sacrificed 24h after the NPY infusion in the dDG and IHC was performed, at first, to analyse the autophagy marker LC3 (Fig. 34). Intriguingly, it was possible to detect an increase in the LC3 intensity in the hilus of the NPY infused animals 24h after the infusion, even if an increase in the soma of the granule cell layer of the dDG was expected as well (Fig. 34 G; Student's t-test: Hilus: $t=-2.233$, $df=10$, $p=0.05$; Granule cell layer (GCL): $t=-0.147$, $df=10$, $p=0.886$; Inner portion of the granule cells' dendrites or inner molecular layer (IML): $t=-1.125$, $df=10$, $p=0.287$; Medial portion of the granule cells' dendrites or middle molecular layer (MML): $t=-0.784$, $df=10$, $p=0.451$; Distal portion of the granule cells' dendrites or outer molecular layer (OML): $t=-0.192$, $df=10$, $p=0.852$). These data might be in accordance with the ones collected from the cell culture, as in Fig. 8 it is possible to detect an increase in autophagy via WB 24h after the NPY treatment, as seen via the LC3-II over LC3-I ratio. However, this *in vivo* finding of an increase in the LC3 intensity in the hilus might possibly point towards an autoregulation of HIPP cells, as these cells are in the hilus and release NPY on to the granule cells, regulating the salience of the background context during a FC paradigm (Raza et al, 2017).
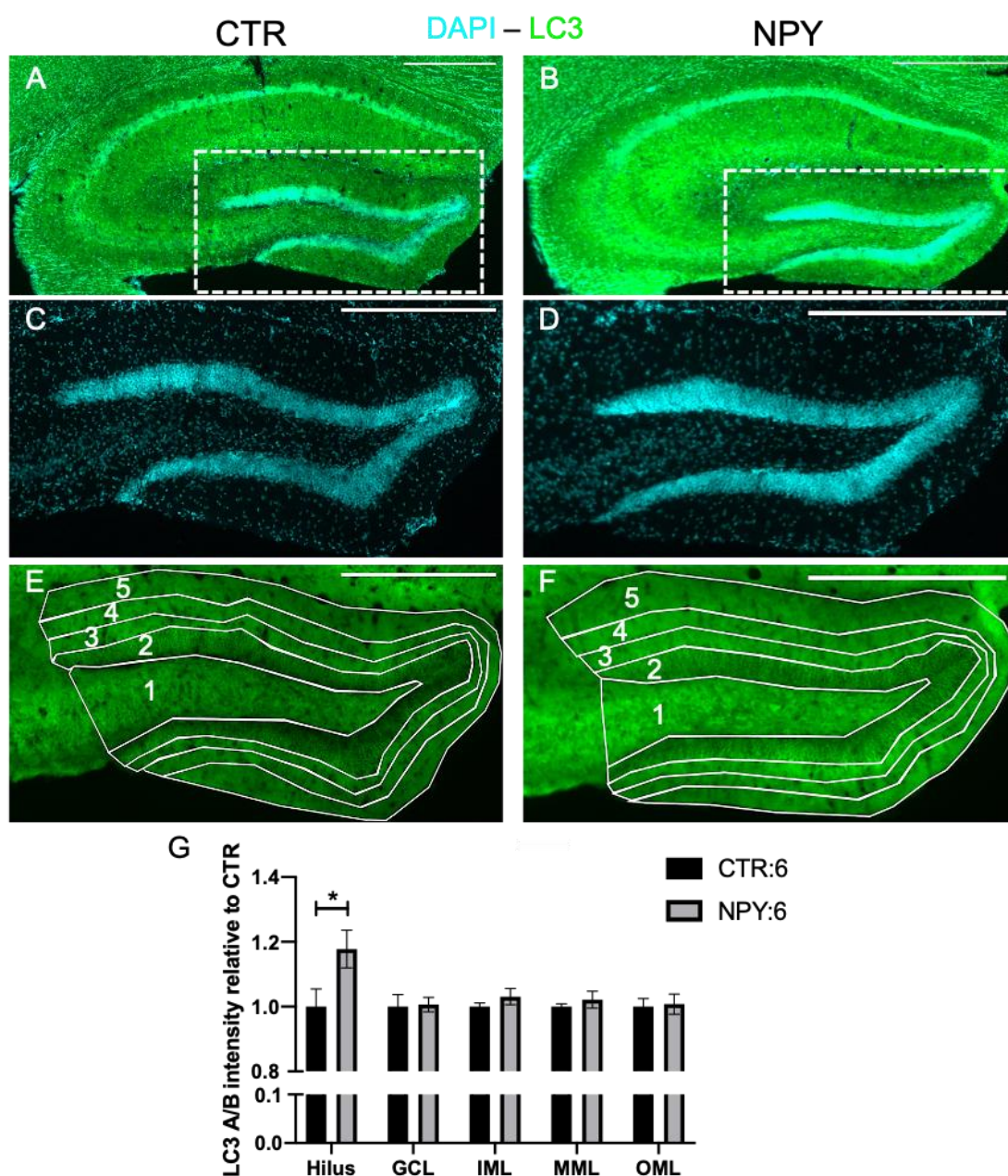
Figure 34. The infusion of NPY in the dorsal dentate gyrus statistically increase the LC3 intensity in the hilus of the dDG, 24h after the NPY infusion.

Young adult mice were infused with 1ul/side of NPY (0.15mg/ml) or saline delivered over 4 min. The injection cannula was left in position for additional 2 min before withdrawal to minimize dragging of the injected liquid along the injection tract. The animals were the left undisturbed for 6h after the injection and the brains were then perfused. (A-B) Representative pictures of LC3-DAPI immunoreactivity in the dorsal hippocampus of mice infused with NPY or saline as a control. (C-D) Insets show DAPI immunoreactivity in the magnified dorsal dentate gyrus. (E-F) Insets show LC3 immunoreactivity in the magnified dorsal dentate gyrus, with a schematic of the different areas' segmentation used to analyse the LC3 intensity; 1. hilus, 2. DG: granule cells layer (GCL), 3. proximal portion of the granule cells dendrites or inner molecular layer (IML); 4. medial portion middle of the granule cells dendrites or molecular layer (MML); 5. distal portion of the granule cells' dendrites or outer molecular layer (OML). Quantification of the LC3 intensity in the dDG divided per area analysed. Scale bar: 500 µM. *$p < 0.05$ VS CTR. Data are shown as mean ± SEM.

Results

dDg slices of animals perfused 24h after the NPY infusion were stained for GluA1 as well (Fig. 35). As expected, the 24h time point shows a general tendency into an increase in all the areas of the dDG analysed, with a statistically NPY significant effect in the dendritic portion of the granule cells and a statistically significant increase in the outer molecular layer, which contains the distal dendrites of granule cells (Fig. 35 G; repeated measures ANOVA NPY effect $F(1,10)= 6.819$, $p=0.026$; Student's t-test, Hilus: $t=-1.582$, $df=10$, $p=0.145$; Granule cell layer (GCL): $t=-2.201$, $df=10$, $p=0.052$; Inner portion of the granule cells' dendrites or inner molecular layer (IML): $t=-1.961$, $df=10$, $p=0.078$; Medial portion of the granule cells' dendrites or middle molecular layer (MML): $t=-1.658$, $df=10$, $p=0.128$; Distal portion of the granule cells' dendrites or outer molecular layer (OML): $t=-2.583$, $df=10$, $p=0.027$). These observations are completely in accordance with the cell culture data, where 24h after the 6h NPY treatment it is possible to see an increase in the protein levels of GluA1 (detected via WB in Fig. 24), but also an increase in the GluA1 positive puncta in the dendrites (detected via ICC in Fig. 28).
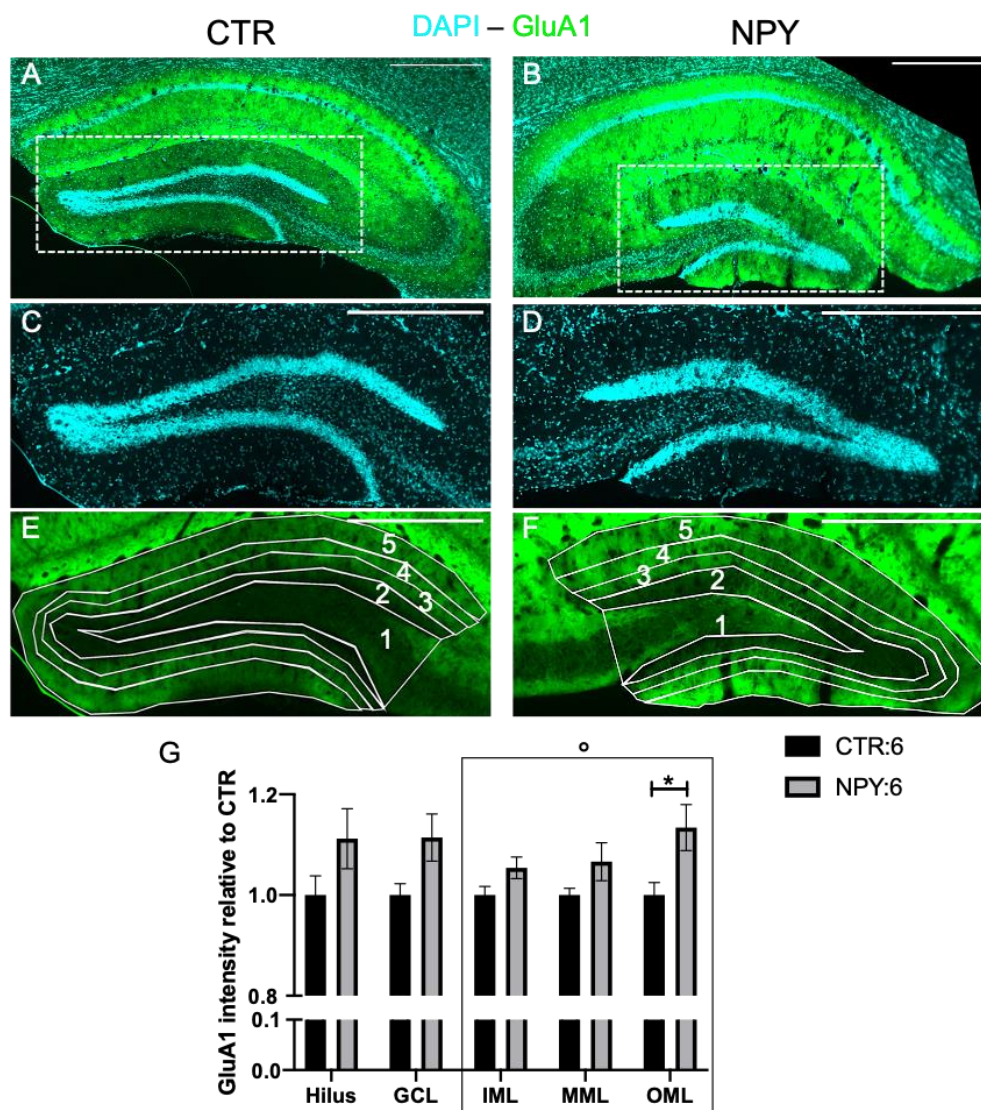
Figure 35. **The infusion of NPY in the dorsal dentate gyrus determines a general tendency in an increase of GluA1 intensity in the whole dDG, with a statistically significant increase in the outer portion of the dendrites of the granule cells, 24h after the NPY infusion.**
Young adult mice were infused with 1ul/side of NPY (0.15mg/ml) or saline delivered over 4 min. The injection cannula was left in position for additional 2 min before withdrawal to minimize dragging of the injected liquid along the injection tract. The animals were the left undisturbed for 24h after the injection and the brains were then perfused.
(A-B) Representative pictures of GluA1-DAPI immunoreactivity in the dorsal hippocampus of mice infused with NPY or saline as a control. (C-D) Insets show DAPI immunoreactivity in the magnified dorsal dentate gyrus. (E-F) Insets show GluA1 immunoreactivity in the magnified dorsal dentate gyrus, with a schematic of the different areas' segmentation used to analyse the GluA1 intensity; 1. hilus, 2. DG: granule cells layer (GCL), 3. proximal portion of the granule cells dendrites or inner molecular layer (IML); 4. medial portion middle of the granule cells dendrites or molecular layer (MML); 5. distal portion of the granule cells' dendrites or outer molecular layer (OML). (G) Quantification of the GluA1 intensity in the dDG divided per area analysed. Scale bar: 500 µM.°p<0.05 NPY effect; *p<0.05 vs CTR. Data are shown as mean ± SEM.

4.6.   The stress effect on GluA1 in the dDG

Raza and colleagues demonstrated that NPY is released by the HIPP cells in the hilus onto the granule cells in the granule cell layer of the dDG during a Pavlovian fear conditioning paradigm (Raza et al, 2017). Therefore, instead of pharmacologically infusing NPY, the same fear conditioning protocol was used as a mean to allow the endogenous release of NPY in the dDG. This paradigm was used in order to evaluate how the endogenous NPY affects the autophagy and GluA1 levels 24h after the stressful event, the time point that showed a peak into the changes induced by the NPY, as the results from both the *in vitro* and the *in vivo* experiments suggest. Viral constructs and transgenic mice to constitutively knock down (KD) NPY or conditionally inactivating HIPP cells, the source of NPY release during FC according to Raza et al., 2017, were used in order to pinpoint molecular changes induced by NPY in different regions of the dDG.

4.6.1. The constitutive KD of NPY in the dDG

At first, it was investigated the constitutional KD of NPY positive interneurons in the hilus of the dDG is modifying the IHC intensity of GluA1 and the autophagy marker LC3, after subjecting the mice to a FC protocol that involves either the delivery of three-foot shocks paired to a tone (as described in Raza et al., 2017) or no foot shocks after the tone (Fig. 36 A). It was then evaluated the time the animals spent freezing as

an output of their fear levels in the 2 minutes before the first CS (Fig. 36 B; 2-way ANOVA: virus x FC effect $F_{(1,28)}=0.371$, p=0.548; virus effect $F_{(1, 28)}=0.414$, p=0.525; FC effect $F_{(1,28)}=6.614$, p=0.016) and in the 2 minutes after the last CS (Fig. 36 C; 2-way ANOVA: virus x FC effect $F_{(1,28)}=0.021$, p=0.887; virus effect $F_{(1, 28)}=0.162$, p=0.69; FC effect $F_{(1,28)}=0.001$, p=0.98), as well as the delta freezing between the pretraining and post-training freezing time was calculated in order to verify if the animals learnt during the paradigm and acquired the fear memory (Fig. 36 D). The delta freezing increases for the tone+shock groups, but the tone control group shows some delta freezing as well, that might indicate a condition of pre-existing stress that is not due to the behavioural paradigm used, as these animals did not receive any foot shock during their sham FC training (Fig. 36 D; 2-way ANOVA: virus x FC effect $F_{(1,28)}=0.272$, p=0.606; virus effect $F_{(1, 28)}=0.726$, p=0.401; FC effect $F_{(1,28)}=2.099$, p=0.158). This last finding could be in accordance with the significance found for the FC effect in the pre-train analysis (Fig. 36 B), as up until that point, the 2 minutes before the first CS, the experimental groups were handled and received the exact same procedures. Nevertheless, the animals that did receive the three-foot shocks show a tendency into an increase in the freezing time that could potentially represent the acquisition of a fear memory due to the foot shocks received during the behavioural training and these data need to be further explored and confirmed.

Results
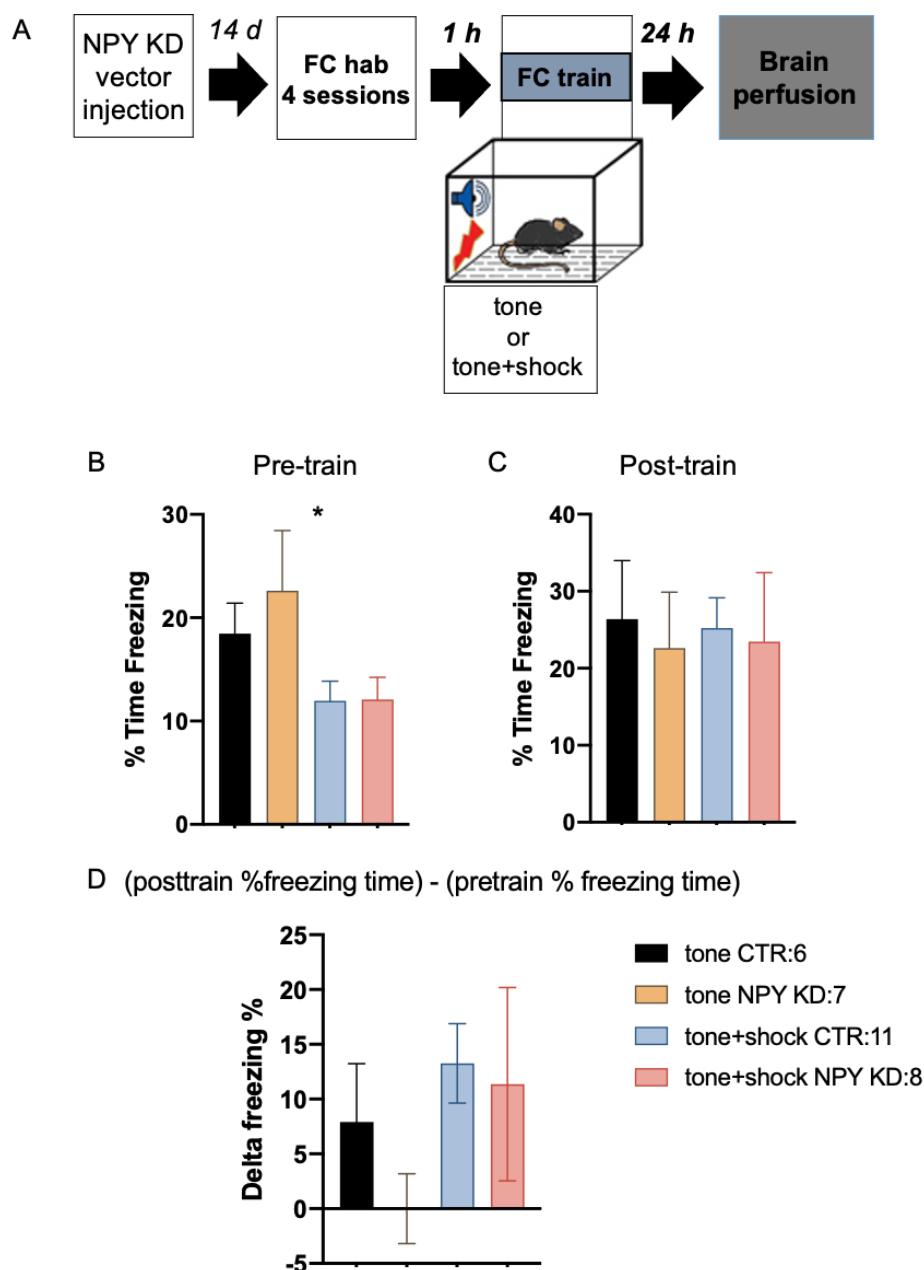
Figure 36. **The constitutional inactivation of NPY positive interneurons in the hilus of the dDG does not produce behavioural difference during a fear conditioning paradigm, either with or without foot shock.**

(A) Young adult mice underwent surgery 2 weeks before the fear conditioning paradigm exposure in order to inject a vector able to KD NPY positive interneurons in the hilus constitutionally. The animal underwent through 2 days of habituation with 2 sessions per day (one in the morning and one in the afternoon). On the third day the animals received the fear conditioning training, either with or without the foot shock. The brains were then perfused 24h after the fear conditioning training. (B) Percentage time freezing during the two minutes before the first CS. (C) Percentage time freezing during the two minutes after the last CS. (D) Delta percentage time freezing calculated as the difference between the time spent freezing the two minutes after the last conditioned stimulus (Post-train) and the time spent freezing the two minutes before the first conditioned stimulus (Pre-train). *$p < 0.05$ FC effect. Data are shown as mean ± SEM.

Results

Animals were then sacrificed 24h after the FC training and the dDG was further analysed via IHC to investigate changes in autophagy or GluA1 (Fig. 37). As seen previously in both the *in vitro* and *in vivo* results presented, NPY is increasing autophagy. The LC3 intensity analysis revealed a NPY KD effect across all the area analysed (Fig. 37 E; 2-way ANOVA: hilus: FC x virus $F_{(1,32)}=0.033$, p=0.857; FC $F_{(1,32)}=0.001$, p=0.982; virus $F_{(2,32)}=11.358$, p<0.0001. Granule cell layer (GCL): FC x virus $F_{(1,32)}= 0.001$, p=0.979; FC $F_{(1,32)}=0.018$, p=0.894; virus $F_{(2,32)}=11.882$, p<0.0001. Inner portion of the granule cells' dendrites or inner molecular layer (IML): FC x virus $F_{(1,32)}=1.441$, p=0.24; FC $F_{(1,32)}=0$, p=0.985; virus $F_{(2,32)}=3.492$, p=0.045. Medial portion of the granule cells' dendrites or middle molecular layer (MML): FC x virus $F_{(1,32)}=1.063$, p=0.312; FC $F_{(1,32)}=0.001$, p=0.976; virus $F_{(2,32)}=5.705$, p=0.009; Distal portion of the granule cells' dendrites or outer molecular layer (OML): FC x virus $F_{(1,32)}= 0.116$, p=0.736; FC $F_{(1,32)}=0.018$, p=0. 893; virus $F_{(2,32)}=6.716$, p=0.004). In particular, these data show that when animals receive only the tone, LC3 intensity seems to be lower than the tone CTR group in the hilus and in the soma of the granule cell layer, while in the dendrites of the granule cells the LC3 intensity seems to be similar to the tone CTR group, if not slightly higher (Fig. 37 E). On the other hand, when animals receive the tone and the foot shocks, the LC3 intensity increases in the hilus and in the soma of the granule cell layer compared to the tone + shock CTR group, while the LC3 intensity seems to decrease in the more distal portions of the granule cell dendrites (Fig. 37 E).
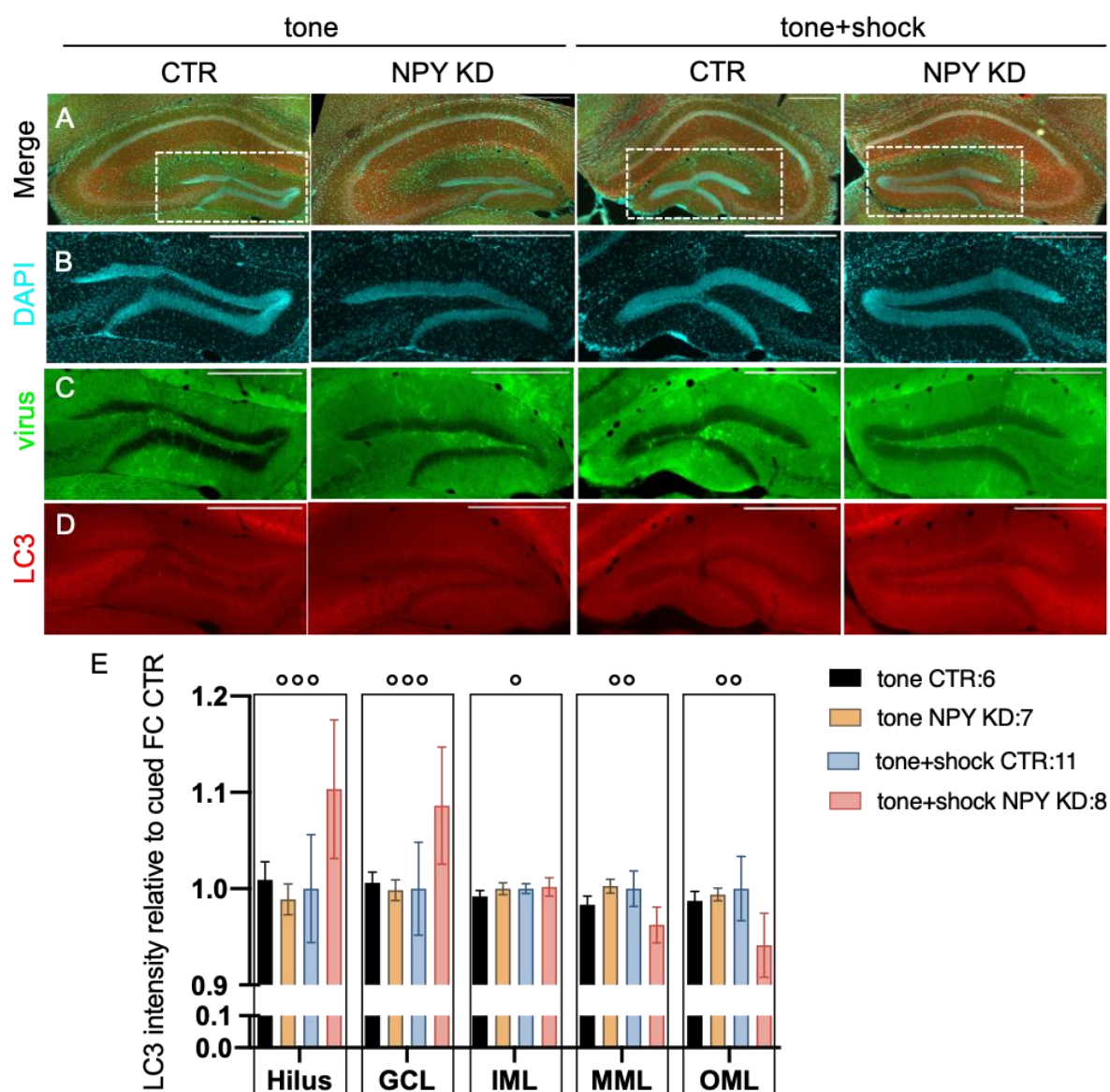
Figure 37. **The NPY KD has an effect on the LC3 intensity in the dDG.**
(row A) Representative merge pictures of the dDG of animals sacrificed 24h after FC training showing immunoreactivity to LC3 and DAPI staining with inlets showing the area of interest, dDG, further analysed. (row B) Zoom of the dDG nuclear DAPI staining, used for visualization of cell bodies. (row C) Zoom of the dDG viral expression of NPY KD viral construct tagged with GFP-tag. (row D) Zoom of LC3 immunoreactivity in the dDG, further segmented and analysed as described in 3.3.8. (E) Quantification of the LC3 intensity in the dDG divided per area analysed. Scale bar: 100 µM. °$p < 0.05$, °°$p < 0.01$, °°°$p < 0.001$ NPY KD effect. Data are shown as mean ± SEM.

Results

The dDG slices were then analysed for the intensity of GluA1 (Fig. 38). The GluA1 intensity shows a statistically significant interaction between the NPY KD and the FC training protocol used in the proximal portion of the dendrites of the granule cells: the constitutional KD of NPY is determining an increase in the GluA1 intensity in the animals that receive only the tone during the sham FC training, an increase that is also shown by the tone + shock CTR group, while the tone+ shock NPY KD group shows a decrease (Fig. 38 E; 2-way ANOVA: Hilus, FC x virus $F_{(1,32)}=0.122$, p=0.729; FC $F_{(1,32)}=0.159$, p=0.693; virus $F_{(1,32)}=0.987$, p=0.329; Granule cell layer (GCL): FC x virus $F_{(1,32)}=2.741$, p=0.109; FC $F_{(1,32)}=1.031$, p=0.319; virus $F_{(1,32)}=3.181$, p=0.085; Inner portion of the granule cells' dendrites or inner molecular layer (IML): FC x virus $F_{(1,32)}=5.491$, p=0.026; FC $F_{(1,32)}=0.01$, p=0.92; virus $F_{(1,32)}=0.293$, p=0.593; Medial portion of the granule cells' dendrites or middle molecular layer (MML): FC x virus $F_{(1,32)}=3.782$, p=0.062; FC $F_{(1,32)}=0.005$, p=0.943; virus $F_{(1,32)}=0.024$, p=0.878; Distal portion of the granule cells' dendrites or outer molecular layer (OML): FC x virus $F_{(1,32)}=2.447$, p=0.129; FC $F_{(1,32)}=0.034$, p=0. 856; virus $F_{(1,32)}=0.954$, p=0.337). This finding might show that animals that do not undergo through a stressful episode but have NPY KD have high levels of GluA1. On the other hand, animals that receive the three-foot shocks show higher levels of GluA1, but the NPY KD during stress decreases these levels. It seems like stress is increasing GluA1, but when the endogenous NPY is less present, it is not driving the increase, that might be protective.
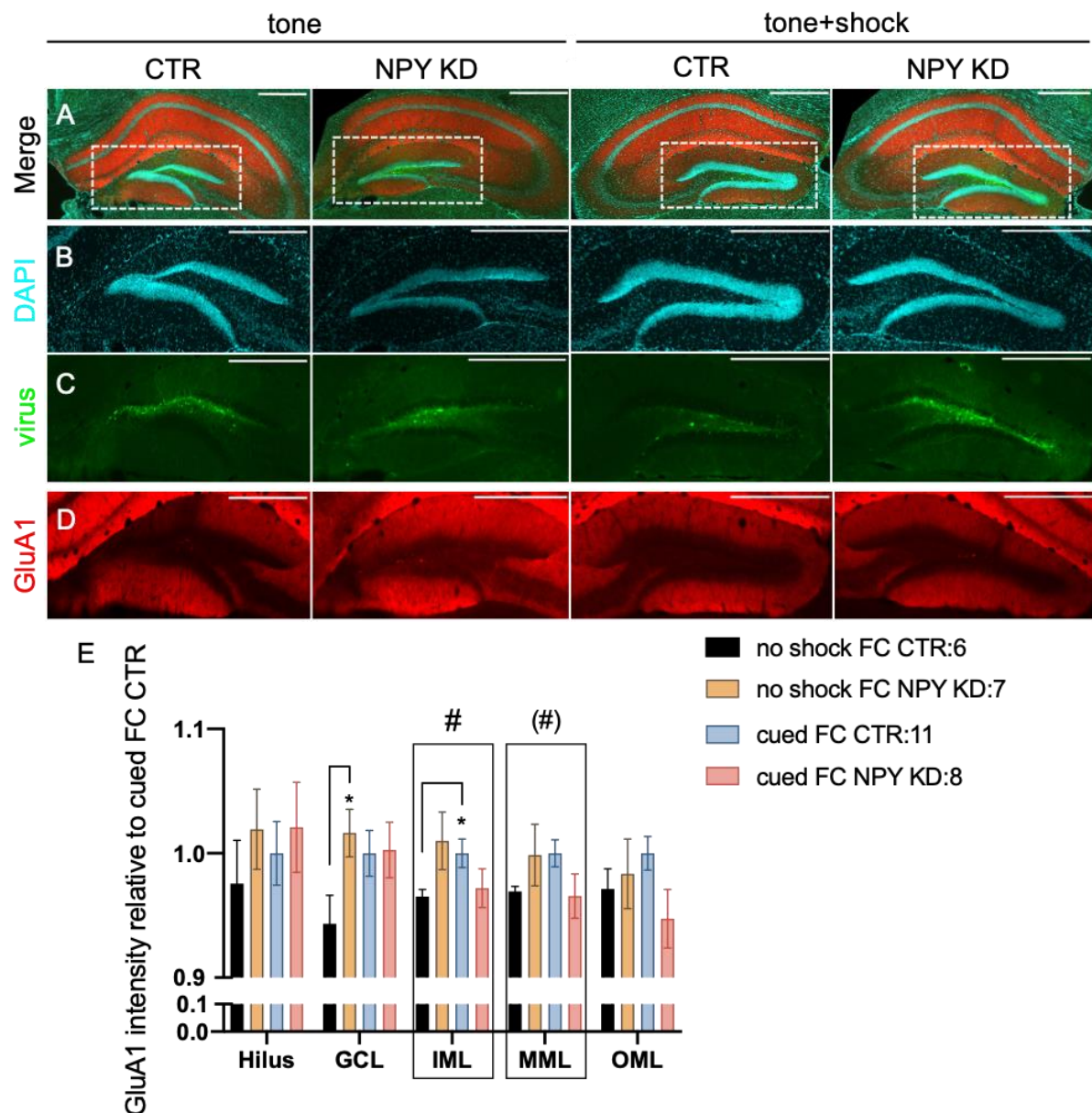
Figure 38. The NPY KD of positive interneurons in the dDG shows an interaction with the FC paradigm in the GluA1 intensity in the proximal part of the granule cells dendrite, and a strong tendency into an interaction in the medial part as well.

(row A) Representative merge pictures of the dDG of animals sacrificed 24h after FC training showing immunoreactivity to GluA1 and DAPI staining with inlets showing the area of interest, dDG, further analysed. (row B) Zoom of the dDG nuclearDAPI staining, used for visualization of cell bodies. (row C) Zoom of the dDG viral expression of NPY KD viral construct tagged with GFP. (row D) Zoom of GluA1 immunoreactivity in the dDG, further segmented and analysed as described in 3.3.8.(E) Quantification of the GluA1 intensity in the dDG divided per area analysed. Scale bar: 500 µM. #$p<0.05$, (#)$p=0.062$, NPY KD x FC protocol effect; *$p<0.05$ VS tone CTR. Data are shown as mean ± SEM.

4.6.2. The conditional inactivation of HIPP cells in the dDG

As some compensatory mechanisms might come into play when KD constitutionally a protein, it was used a different strategy and HIPP cells releasing NPY interneurons in the hilus of the dDG were conditionally inactivated only before the FC training, in order to block the aforementioned compensatory mechanisms and be able to see how the animals behave during the previously described FC paradigm and not having the chance to release NPY. Statin-Cre mice were used (as previously described by Raza et al, 2017). These mice express the CRE recombinase under the promoter of the neuropeptide somatostatin (Statin-Cre mice). When the chemo genetic vector AAV-hSyn-DIO-hM4Di-mCherry is injected in the dDG of the adult animals, it causes the somatostatin-positive cells to express an inactivating artificial receptor (DREADD). The subsequent injection of an artificial ligand (CNO) allows to artificially inactivate the neurons, therefore blocking the release of NPY. Using this elegant system, HIPP cells were silenced 1h before the FC training via i.p. injection of 10 mg/kg body weight of CNO (Fig. 39 A) and the freezing behaviour of the mice during the FC protocol was then quantified, once more, the time the animals spent freezing as an output of their fear levels in the 2 minutes before the first CS (Fig. 39 B; 2-way ANOVA: virus x FC effect $F_{(1,26)}=0.868$, p=0.36; virus effect $F_{(1, 26)}=0.78$, p=0.385; FC effect $F_{(1,26)}=0.014$, p=0.908) and in the 2 minutes after the last CS (Fig. 39 C; 2-way ANOVA: virus x FC effect $F_{(1,26)}=0.176$, p=0.678; virus effect $F_{(1, 26)}=0.013$, p=0.911; FC effect $F_{(1,26)}=0.675$, p=0.419) along with the delta freezing, as previously described in 4.6.1. (Fig. 39 D; 2-way ANOVA: virus x FC effect $F_{(1,26)}=0.259$, p=0.615; virus effect $F_{(1, 26)}=0.629$, p=0.435; FC effect $F_{(1,28)}=0.599$, p=0.446). In this case, no statistically significant differences were found, as the variability among groups is important and these data might show a high state of pre-existing anxiety in the animals, that should be further investigated. However, the findings presented might show an increased sensitization of the tone hM4Di group, as these mice are already showing high levels of delta freezing even without receiving the foot shock (Fig. 39 B).

Results
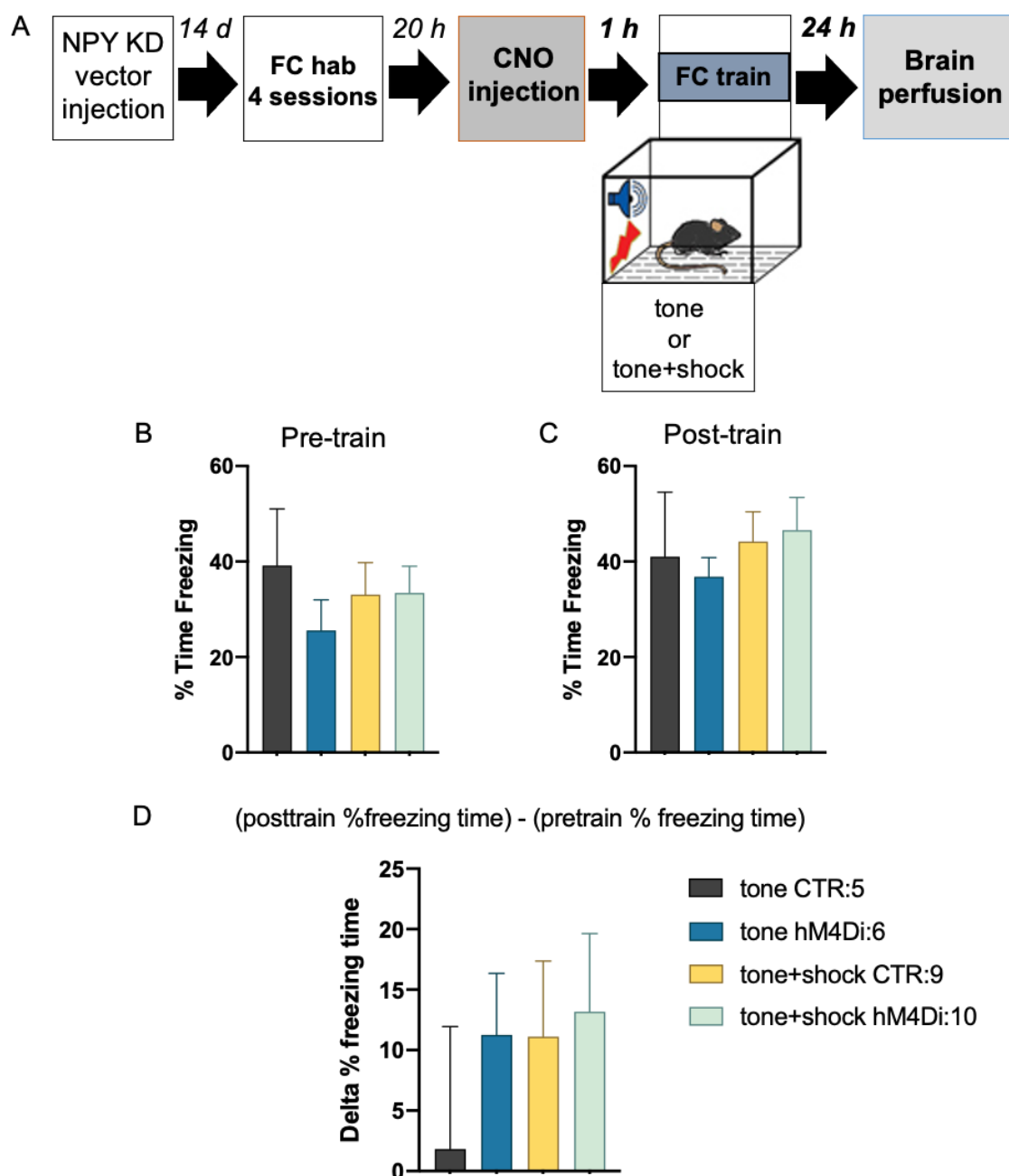
Figure 39. **The conditional inactivation of NPY positive interneurons in the hilus 1h before fear conditioning training is not statistically affecting the freezing time.**
(A) Schematics of the fear conditioning protocol used to stimulate NPY release in the dDG. Briefly, young adult statin-Cre mice were operated to inject a DREADD vector able to inhibit NPY positive interneurons in the hilus of the dDG 2 weeks before the fear conditioning paradigm exposure. Mice were left undisturbed in order to allow the expression of the virus. Then, the animal went through 2 days of habituation with 2 sessions per day (one in the morning and one in the afternoon). 1h before the fear conditioning training, the animals were injected with CNO in order to inactivate NPY-positive interneurons in the hilus. The brains were then perfused 24h after the fear conditioning training. (B) Percentage time freezing during the two minutes before the first CS. (C) Percentage time freezing during the two minutes after the last CS. (D) Percentage time freezing during the last session of habituation (Habituation), the two minutes before the first conditioned stimulus (Pre-train) and the two minutes after the training (Post-train). Data are shown as mean ± SEM.

Results

Mice were sacrificed 24h after the FC training and the IHC intensity of GluA1 and LC3, as a possible output for autophagy changes, were analysed. At first, the focus was on the LC3 staining (Fig. 40). Interestingly, inactivating NPY positive interneurons in the hilus of the dDG is decreasing LC3 intensity across all the areas analysed, but especially in the granule cells' dendritic portion irrespectively of the FC protocol performed (Fig. 40 E; Dendritic portion: repeated measures ANOVA hM4Di viral vector effect: $F_{(1,25)}=4.632$, p=0.041). In particular, this result becomes statistically significant in the outer portion of the molecular layer, where the silencing of NPY effect is maximum (Fig. 40 E; 2-way ANOVA: Hilus: FC x virus $F_{(1, 29)}=0.339$, p=0.566; FC $F_{(1,29)}=0$, p=0.992; virus $F_{(1,29)}= 2.879$, p=0.102; Granule cell layer (GCL): FC x virus $F_{(1,29)}= 0.097$, p=0.758; FC $F_{(1,29)}=0.518$, p=0.478; virus $F_{(1,29)}=3.456$, p=0.075; Inner portion of the granule cells' dendrites or inner molecular layer (IML): FC x virus $F_{(1,29)}= 0.095$, p=0.761; FC $F_{(1,29)}=0.34$, p=0.565; virus $F_{(1,29)}=2.459$, p=0.129; Medial portion of the granule cells' dendrites or middle molecular layer (MML): FC x virus $F_{(1,29)}=0.026$, p=0.873; FC $F_{(1,29)}=0.401$, p=0.533; virus $F_{(1,32)}=3.464$, p=0.075; Distal portion of the granule cells' dendrites or outer molecular layer (OML): FC x virus $F_{(1,29)}=0.978$, p=0.332; FC $F_{(1,29)}=3.023$, p=0. 094; virus $F_{(1,29)}=4.903$, p=0.036). In the distal portion of the granule cells' dendrites, it is observable a statistically significant decrease in the tone+shock hM4Di group compared to the tone+shock CTR, as well as both groups that received the tone only (Fig. 40 E; Student's t-test: tone CTR VS tone+shock hM4Di t=-3.174, df=12, p=0.008; tone hM4Di VS tone+shock hM4Di t=-2.083, df=14, p=0.056; tone+shock CTR VS tone+shock hM4Di t=3.041, df=17, p=0.007). The observable LC3 intensity decrease across all the areas analysed for the hM4Di group of animals is of particular interest, especially when observing the decrease in the hilus, where the silenced NPY positive interneurons are (Fig. 39 E).
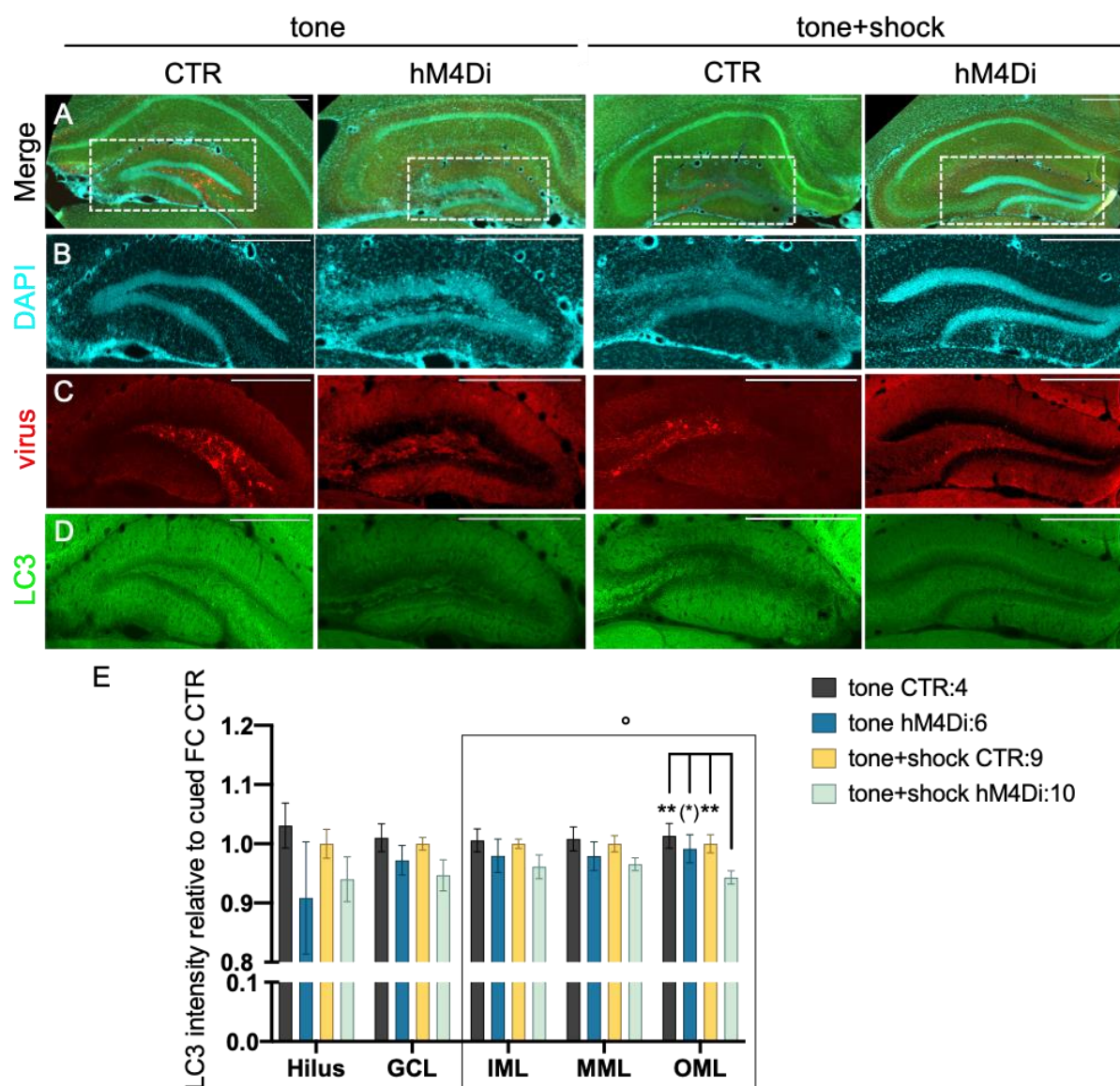
Figure 40. **The silencing of NPY positive interneurons via hM4Di viral vector in the dDG 1h before FC is statistically affecting LC3 intensity in the distal portion of the granule cells' dendrites.**

(row A) Representative merge pictures of the dDG of animals sacrificed 24h after FC training showing immunoreactivity to LC3 and DAPI staining with inlets showing the area of interest, dDG, further analysed. (row B) Zoom of the dDG nuclear DAPI staining, used for visualization of cell bodies. (row C) Zoom of the dDG viral expression of the h4MDi viral construct tagged with mCherry-tag. (row D) Zoom of LC3 immunoreactivity in the dDG, further segmented and analysed as described in 3.3.8. (E) Quantification of the LC3 intensity in the dDG divided per area analysed. Scale bar: 100 µM. °p<0.05 hM4Di viral vector effect; **p<0.01, p<0.05, (*)p=0.056 VS tone+shock hM4Di. Data are shown as mean ± SEM.

Results

Then, GluA1 intensities were analysed (Fig. 41): in this case, no statistically significant differences were found (Fig. 41 E; 2-way ANOVA: Hilus, FC x virus $F_{(1, 29)}=1.422$, p=0.244; FC $F_{(1,29)}=0.201$, p=0.658; virus $F_{(1,29)}= 1.739$, p=0.199; Granule cell layer (GCL): FC x virus $F_{(1,29)}= 0.432$, p=0.517; FC $F_{(1,29)}=0.035$, p=0.854; virus $F_{(1,29)}=0.246$, p=0.624; Inner portion of the granule cells' dendrites or inner molecular layer (IML): FC x virus $F_{(1,29)}= 0.337$, p=0.567; FC $F_{(1,29)}=0.256$, p=0.617; virus $F_{(1,29)}=1.317$, p=0.262; Medial portion of the granule cells' dendrites or middle molecular layer (MML): FC x virus $F_{(1,29)}=0$, p=0.993; FC $F_{(1,29)}=0.756$, p=0.393; virus $F_{(1,32)}=1.095$, p=0.305; Distal portion of the granule cells' dendrites or outer molecular layer (OML): FC x virus $F_{(1,29)}=0.671$, p=0.421; FC $F_{(1,29)}=0.933$, p=0. 329; virus $F_{(1,29)}=1.316$, p=0.262). However, it was possible to observe a general tendency into an increase in the GluA1 intensity across all the areas analysed for the tone hM4Di group, that is statistically significant in the medial portion of the molecular layer when compared with the tone+shock CTR group (Fig. 41 E; Student's t-test: Inner portion of the granule cells' dendrites: t=-1.635, df=13, p=0.126; Medial portion of the granule cells' dendrites: t=-2.161, df=13, p=0.05; Distal portion of the granule cells' dendrites: t=-1.985, df=13, p=0.069). Once more, the dDG hilus of the tone hM4Di group is showing a decrease in intensity that leaves space for speculations on a possible autoregulation effect of the NPY positive interneurons.
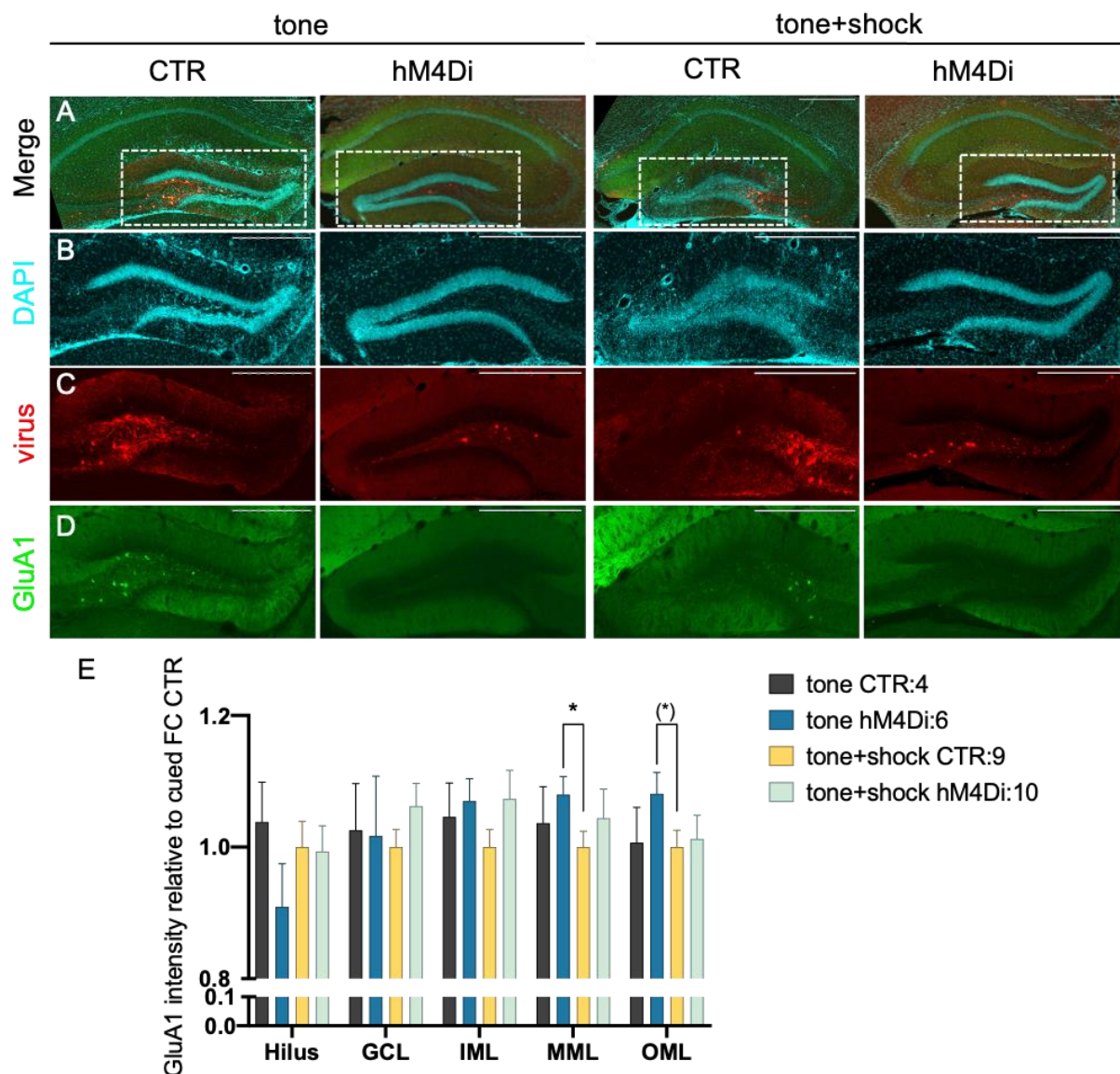
Figure 41. **The silencing of NPY positive interneurons in the dDG 1h before FC determines an increase in the GluA1 intensity when animals receive the tone only.**
(row A) Representative merge pictures of the dDG of animals sacrificed 24h after FC training showing immunoreactivity to GluA1 and DAPI staining with inlets showing the area of interest, dDG, further analysed. (row B) Zoom of the dDG nuclear DAPI staining, used for visualization of cell bodies. (row C) Zoom of the dDG viral expression of the h4MDi viral construct tagged with mCherry-tag. (row D) Zoom of GluA1 immunoreactivity in the dDG, further segmented and analysed as described in 3.3.8. (E) Quantification of the GluA1 intensity in the dDG divided per area analysed. Scale bar: 100 μM. $p < 0.05$, (*)$p = 0.069$ VS tone+shock CTR. Data are shown as mean ± SEM.

4.6.3. NPY positive interneurons in the hilus of the dDG

The results presented in 4.6.2 left space for speculations about a possible autoregulation of NPY positive interneurons of the dDG. Indeed, the data presented in the previous chapter might somehow be contrasting in certain aspects with the results obtained from the *in vitro* experiments. Apart from an obvious degree of complexity that the animal as a whole organism has in comparison with a much simpler culture of neurons in a dish, the possibility that the conditional inactivation of NPY positive interneurons might have an effect on themselves arose and needed further exploring. Therefore, to further investigate into this hypothesis, the LC3 and GluA1 IHC stainings in the NPY positive interneurons were investigated, using the mCherry signal as a way to manually segment the infected cells and measure the intensity signals in the soma of these neurons.

As it can be seen in Fig. 42, the inactivation of the aforementioned neurons has a statistically significant effect: the silencing of the NPY positive interneurons 1h before the FC training is producing a decrease in the LC3 intensities, independently of the FC protocol, i.e. when they receive the tone only or the tone + shock, compared to the control injected animals (Fig. 42 C; 2-way ANOVA: FC x virus $F_{(1,29)}=1.124$, $p=0.299$; FC $F_{(1,29)}=0.075$, $p=0.787$; virus $F_{(1,29)}=5.482$, $p=0.027$). These data might further confirm that the decrease in LC3 intensity seen in the hilus in Fig. 40 might be due to the decrease in the NPY positive interneurons themselves, therefore pointing towards an autoregulation of these cells, that in the lack of the endogenous NPY might decrease their own autophagy.
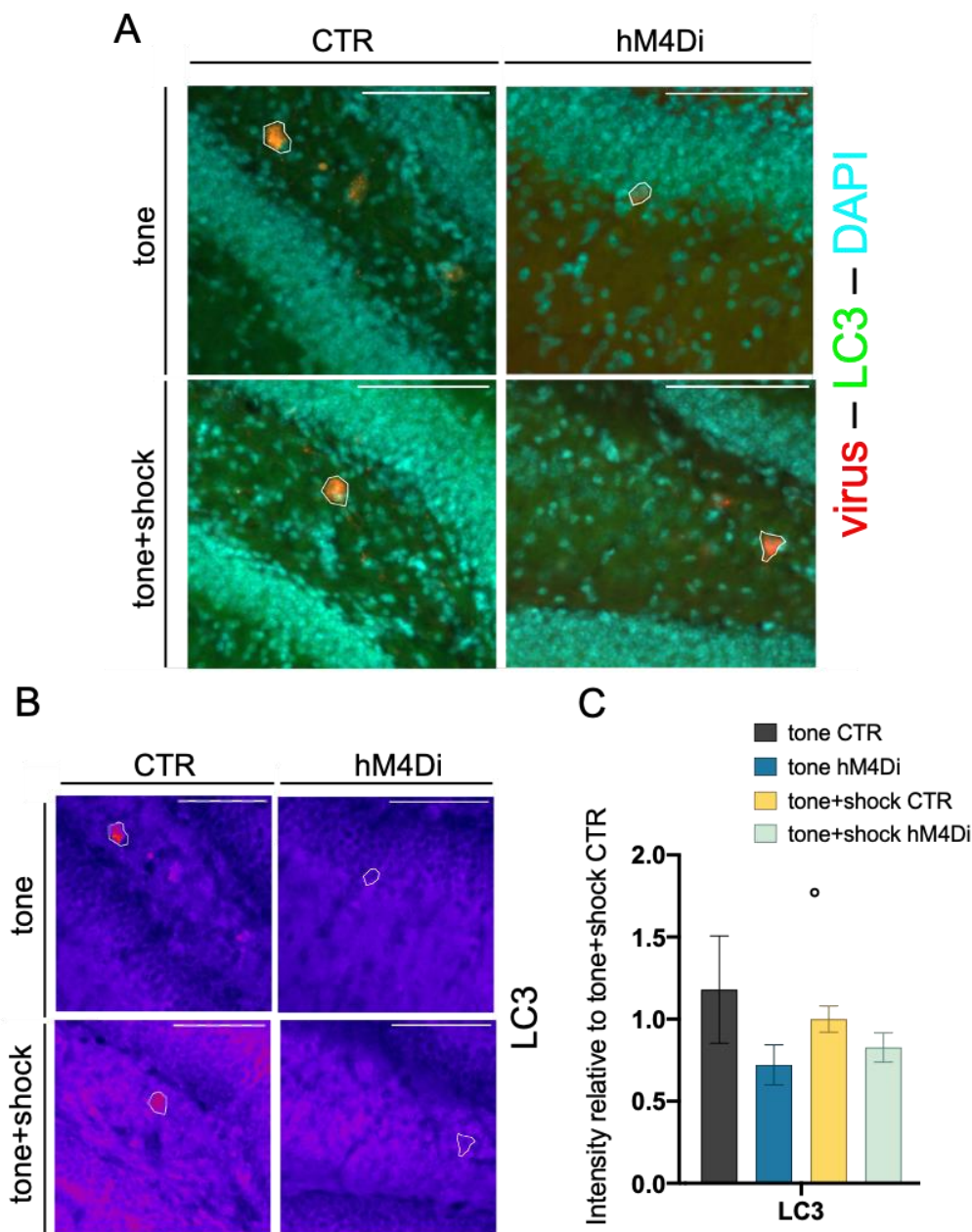
Figure 42. **The LC3 intensity of NPY positive interneurons in the hilus of the dDG show an interaction between their inactivation via hM4Di viral vector and the FC protocol used.**

(A) Merge pictures of LC3 and DAPI immunoreactivity in NPY positive interneurons tagged with mCherry, that have been manually segmented as shown in the pictures. (B) Fire pictures of LC3 immunoreactivity in NPY positive interneurons. (C) Quantification of the LC3 intensity in the NPY positive interneurons. Scale bar: 100 μM. °p<0.05 hM4Di viral vector effect. Data are shown as mean ± SEM.

Results

The GluA1 intensity in the same NPY positive interneurons were analysed as well and, surprisingly, it was possible to see a decrease in the GluA1 intensity in these same neurons (Fig. 43): the hM4Di viral vector is decreasing the GluA1 intensity as well and, once more, it does it irrespectively of the FC training received (Fig. 43 C; 2-way ANOVA: FC x virus $F_{(1,29)}=1.235$, p=0.277; FC $F_{(1,29)}=2.155$, p=0.155; virus $F_{(1,29)}=7.01$, p=0.014) and this decrease is maximum in the tone hM4Di group when compared to the CTR injected animals (Fig. 43 C; Student's t-test: tone CTR VS tone hM4Di: t=-4.576, df=8, p=0.002; tone+shock CTR VS tone hM4Di: t=8.608, df=13, p<0.001). In the light of the evidences collected when using the conditional silencing of NPY positive interneurons, it is possible to speculate that the decrease in both GluA1 and LC3 intensity might represent an automodulation of the NPY positive interneurons of the dDG hilus, that could in turn explain the sensitization arose when analysing the delta freezing of these animals (in Fig. 39). On the other hand, when animals receive the foot shocks, but have the hM4Di viral vector, the decrease of GluA1 intensity is not as marked and this might be a mechanism arising to help the animals to cope with the formation of the fear memory (Fig. 43 C; Student's t-test: tone CTR VS tone+shock hM4Di: t=-0.567, df=12, p=0.581; tone+shock CTR VS tone+shock hM4Di: t=1.14, df=17, p=0.27).
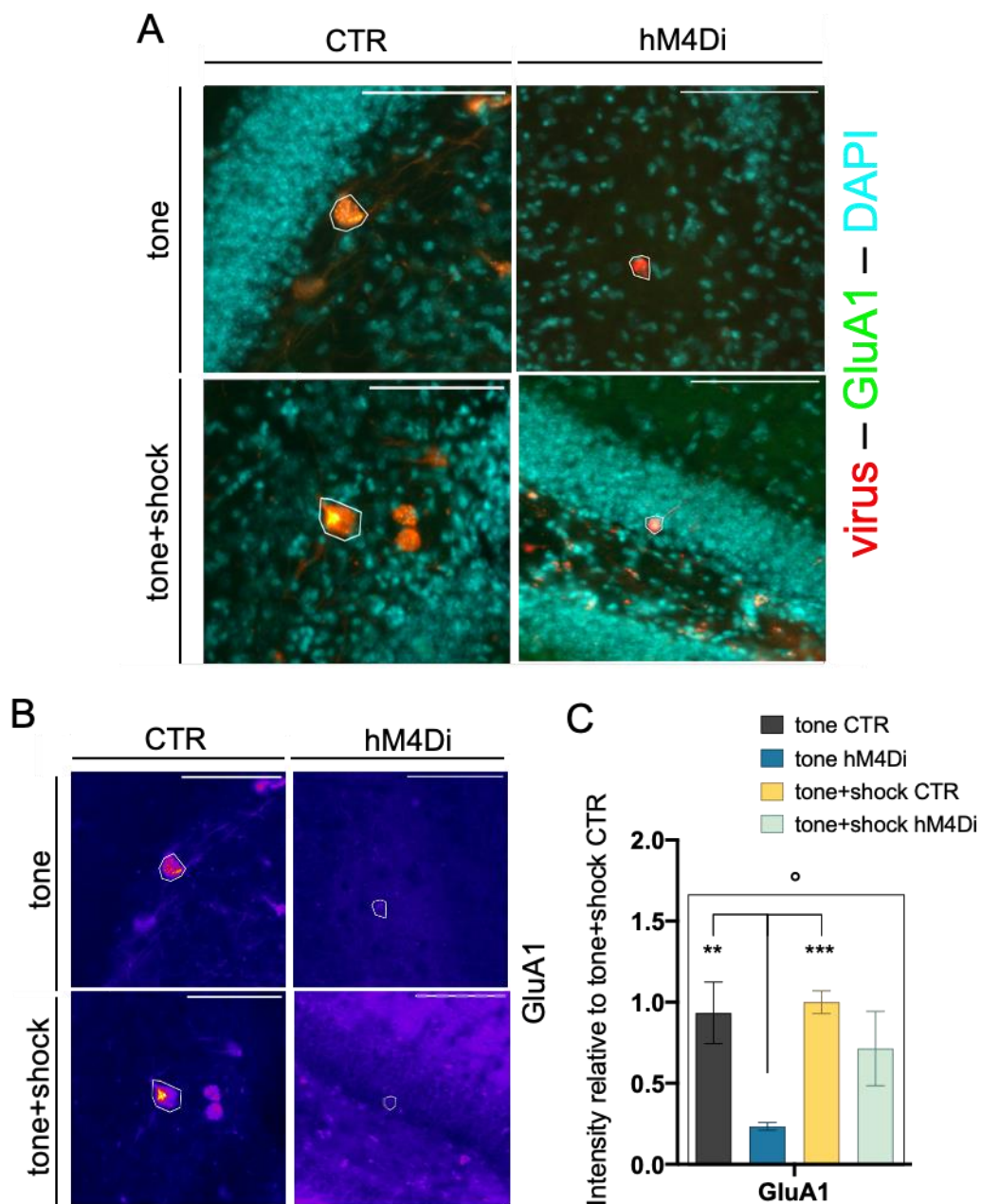
Figure 43. <u>**NPY positive interneurons in the hilus of the dDG that were inactivated 1h before FC training show a statistically significant decrease in the GluA1 intensity in the animals that did not receive a foot shock.**</u>

(A) Merge pictures of GluA1 and DAPI immunoreactivity in NPY positive interneurons tagged with mCherry, that have been manually segmented as shown in the pictures. (B) Fire pictures of GluA1 immunoreactivity in NPY positive interneurons. (C) Quantification of the GluA1 intensity in the NPY positive interneurons. Scale bar: 100 µM. °p<0.05 hM4Di viral vector effect; ***p<0.001, **p<0.05 VS tone hM4Di. Data are shown as mean ± SEM.

5. Discussion

NPY has a well-established anxiolytic role during stressful conditions (Heilig *et al.*, 1989; Śmiałowska *et al.*, 2007, Raza *et al.*, 2017) and it was recently demonstrated that it also increases neuronal autophagy *in vitro* and *in vivo* (Aveleira et al. 2014; Ferreira-Marques et al. 2016), a cellular process that is a strong modulator of pre- and postsynaptic neuronal plasticity. The role of autophagy has considerably changed over the years and autophagy is now considered not only a fundamental physiological process that ensures homeostasis in the cells, but it is now believed to play a pivotal role in pathologies as well (Galluzzi, Bravo-San Pedro, et al. 2017; Levine and Kroemer 2008). In particular, neuronal autophagy is unveiling new and more complex functions, that are not only related to homeostatic adjustments or quality control system for non-functional cellular components: autophagy regulation seems to control and be controlled by synaptic transmission as well. For example, already in 2012, Shehata and colleagues demonstrated how chemical LTD, induced by KCl depolarization, is able to promote autophagy in primary hippocampal neurons via NMDA receptors and this in turn decreases the protein level of AMPA receptor. More recently, Glatigny and colleagues (2019) were able to show that autophagy has a pivotal role during presentation of novel stimuli and once more Shehata and colleagues demonstrated how autophagy can destabilise the fear memory formed during an auditory fear reconsolidation behavioural paradigm and it can contribute to its erasure (Shehata et al. 2018). These evidences allowed for speculations on the role of NPY as a possible synaptic factor linking experience driven synaptic plasticity and autophagy in the framework of stress and anxiety: the release of NPY could induce autophagy that would in turn modulate synaptic plasticity, thereby contributing to behavioural stress resilience *in vivo*.

The data presented in this thesis further confirmed that NPY increases autophagy in cortical neurons and it proved that NPY can increase autophagy in hippocampal neurons as well. This effect on autophagy is lasting up to 24h after the stimulation and it goes back to control levels at 48h post-stimulation. The target affected by this increased autophagy is the GluA1 subunit of AMPA receptor, that already 6h after the stimulation is removed from the synapses and starts to accumulate in the soma of neurons. The NPY effect on GluA1 seems to be produced by a concomitance of events, as the contemporary block of autophagy and protein synthesis during the NPY

Discussion

stimulation prevent the previously described effects. Results of this modulation can be further appreciated 24h post-stimulation, when the GluA1 levels reach their maximum, although the subunit of AMPA receptor does not sit the synapses that have a presynaptic side. When tested *in vivo*, the infusion of NPY in the dDG of mice is able to reproduce similar effects to the ones obtained *in vitro* on GluA1 levels, with an increase in GluA1 intensities that starts already 6h post infusion in the more distal portion of the granule cells' dendrites, up to a general increase in all the areas of the dDG analysed 24h post-infusion. However, the NPY effect on autophagy seen *in* vitro was difficult to spot *in vivo*, due to the nature of neuronal autophagy, that even under strong autophagy induction conditions such as inhibitors of the mTOR kinase pathway like rapamycin (E. F.C. Blommaart et al. 1995; Sabers et al. 1995) and nutrient deprivation (Barber et al. 2001; Vander Haar et al. 2007), shows an unperturbed efficiency, as the fusion of autophagosomes with lysosomes is highly active in these cells (Boland et al. 2008). The use of a FC paradigm that stimulates the endogenous release of NPY from the NPY releasing cells in the hilus on to the dendrites of the granule cells in the molecular layer of the dDG, as previously described by Raza and colleagues (2017), did not provide exhaustive results as the variability across animals is still high, even though there seems to be a general tendency into an increase in the GluA1 levels when the animals receive the tone+shock during the behavioural protocol, in particular in the KD experimental setting. However, the viral manipulations that allowed for the constitutional KD of NPY showed that compensatory mechanisms come into play when constitutionally KD NPY, therefore producing contrasting results with the ones obtained *in vitro*: when NPY is KD, GluA1 intensity increases when animals receive the tone only, so during a non-stressful event, while when animals receive the tone paired with the shock, GluA1 intensity goes down. On the other hand, when NPY releasing cells are inactivated just before the FC training, it is possible to see an opposite effect in the hilus and soma of the granule cells, compared to the constitutional KD, but there is still an increase in the GluA1 intensity across the different portion of the dendrites of granule cells, irrespectively of the FC protocol used. These latter results might possibly be explained when analysing the NPY releasing cells in the hilus: indeed, the viral manipulation seems to show that these cells might autoregulate themselves: in the lack of endogenous NPY release, there is a decrease in both the LC3 and GluA1 intensities, that could in turn determine a further lack of

modulation in the circuit that might dysregulate the whole system in place for the animals to cope during a stressful event.

5.1. NPY is inducing autophagy in cortical and hippocampal neurons

As NPY is one of the most abundant neuropeptides in the brain and plays a role in regulating emotional memory formation in the hippocampus, it was selected for its promising results in increasing autophagy in order to evaluate the molecular mechanisms underlying its action on the hippocampus. At first, it was verified if the protocol employed by Aveleira et al. (2014) is a stable system that can be used to induce autophagy in neurons: NPY is indeed able to induce autophagy in cortical primary neuronal cultures, as previously described in Ferreira-Marques et al. (2016), and the same protocol can increase autophagy in hippocampal primary neuronal cultures. NPY seems to promote autophagy in different areas of the brain, as the previously mentioned researches show the NPY-induced increase in autophagy in both hypothalamic and cortical neurons, and it was possible to demonstrate the same induction of autophagy in yet another brain area, the hippocampus. Autophagy in neurons is tightly regulated on a spatial level, as the motility of autophagosomes changes, depending on the site where they formed (Ariosa and Klionsky 2016; Vassiliki Nikoletopoulou and Tavernarakis 2018). In order to identify where autophagy is exerting its effect in the neurons after its induction with NPY, hippocampal cultures were stained for LC3, a protein that is incorporated into the budding autophagosomes and remains associated with them until degradation (Evans at al., 2018). Consistent with other researches (Maday and Holzbaur 2014, 2016), LC3 puncta accumulate in the soma of neurons, the primary site of protein synthesis, in order to facilitate the recycling of degradation products for new and constitutive biosynthesis. Moreover, a surprising result obtained while further investigating the effect of NPY on autophagy, is the 24h long-lasting effect increase that goes back to control level 48h after the NPY stimulation. Such an effect seems to be independent from the availability of amino acids, as the concomitant block of protein synthesis during NPY stimulation that reduces the consumption of amino acids, thus increasing the availability of intracellular amino acids, a positive regulator of mTOR that suppresses autophagy (Beugnet et al. 2003; Vabulas and Hartl 2005) should prevent the 24h autophagy effect, but it was not

the case. This surprising effect could possibly be explained by looking at the NPY receptor signalling: NPY receptors belong to GPCR family and evidences show that these receptors might have a signalling that can be rapidly inhibited after prolonged agonist exposure, such as the β_2-adrenoceptor (Ferguson and Caron 1998; Van Riper and Bevan 1991). However, the speed of the signalling termination seems to be dependent on the receptor type (see Holliday, Michel, and Cox 2011 for an overview) and such a long-lasting effect should be further and deeply investigated as it would be crucial pinpointing which of the NPY receptor is actually determining the prolonged autophagy increase and how, as the different NPY receptors have different effects on behaviour. For example, while the Y1 receptor activation promotes an anxiolytic effect (Primeaux et al. 2005; Molosh et al. 2013; Sørensen et al. 2004), the Y2 receptor activation produces an anxiogenic effect (Caberlotto, Fuxe, and Hurd 2000; Sajdyk et al. 2002). Already Aveleira et al. (2014) explored which receptor was involved in the initial autophagy increase after 6h of NPY stimulation in hypothalamic rat primary co-cultures, but the results obtained by using antagonists of the Y1, Y2 or Y5 receptor showed that all of them are implied in this phenomenon, therefore leaving space for a more focused research that would eventually differentiate which receptor is inducing such and effect and how on a signalling level. Yet, the NPY 24h long-lasting autophagy increase that goes back to control levels 48h after medium change might be one of the beneficial factors producing the phenomena further presented in this thesis (Fig. 44).
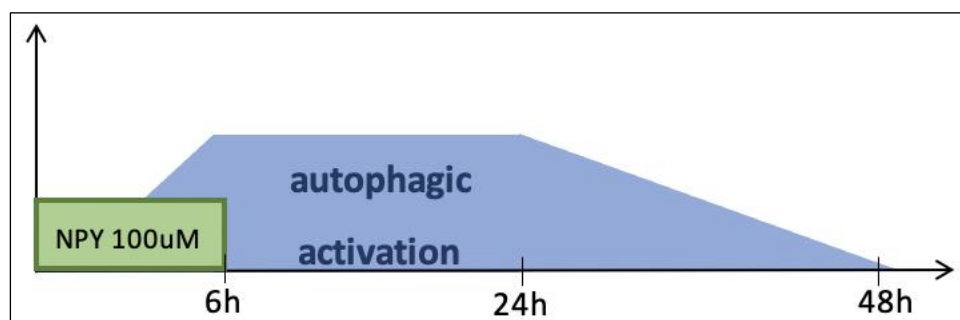
Figure 44. **Schematics of the long-lasting NPY effect on neuronal autophagy.**

5.2.   NPY-induced autophagy regulates GluA1 subunit of AMPA receptor

NPY has a well-established role as anxiolytic compound that is physiologically recruited to cope with stress (Heilig et al. 1989; Reichmann and Holzer 2016): its

Discussion

behavioural effect can be particularly appreciated, for example, when it is applied intranasally and it effectively treats anxiety after a single prolonged stress in rats (Serova et al. 2019), or when it is knocked down after underwater trauma and the number of affected, anxious animals is increased (Regev-Tsur et al. 2020). Knowing such NPY effects on behaviour and having a stable protocol that is able to induce autophagy even up to 24h after the stimulation, several synaptic markers were investigated for autophagy-induced changes after NPY stimulation. Indeed, more and more researches are showing how autophagy can shape synapses either on the pre- or post-synaptic side: from spine pruning (Tang et al. 2014) to synaptic vesicles number (Okerlund et al. 2017) in the axons, from degradation of synaptic scaffolding proteins (Nikoletopoulou et al., 2017) to internalization of ionotropic receptors in the dendrites (Rowland et al., 2006; Shehata et al., 2012). After the 6h NPY-treatment, none of the synaptic markers analysed, that were chosen based on previous works showing changes induced by an autophagy related modulation, are showing any statistically significant difference, despite the increase in autophagy seen at this time point. However, knowing that the increase in autophagy induced via chemical LTD by Shehata et al. (2012) is affecting the GluA1 receptor via engulfment into autophagosomes, this subunit of the AMPA receptor was further investigated: staining primary hippocampal neuronal co-cultures, it was possible to spatially discriminate the location of the increase tendency seen via WB and locate it in the soma of neurons, an opposite effect compared to the one previously described by Shehata and colleagues. In order to further investigate the NPY effect on the GluA1 puncta and verify its relationship to autophagy, autophagy was blocked at the last stage using CQ, to block the fusion of the autophagosomes with lysosomes producing an accumulation of autophagic vesicles, and in the first stage, the autophagosomes formation, using an shATG5 lentivirus able to decrease the protein levels of ATG5 and therefore decrease the formation of the autophagic vesicles. While the block of autophagy at the last stage using CQ is inducing an accumulation of GluA1 puncta in the soma of neurons that is more when neurons are treated with NPY, the block of autophagy in the first step that prevents the formation of the autophagic vesicles is blocking the NPY effect on GluA1 puncta. Indeed, these findings seem to be in line with the work by Shehata et al. (2012), that shows how GluA1 is engulfed in endocytic vesicles, after stimulation of autophagy, that afterwards either can or cannot be directed to lysosomes for degradation, as well as the aforementioned knowledge about the

Discussion

motility of autophagosomes towards the soma (Holliday, Michel, and Cox 2011), that generally converge to the somatic portion of neurons, all suggesting the possibility of GluA1 being engulfed into autophagosomes that are then shuffled towards the soma of neurons.

   Nevertheless, when blocking the formation of autophagosomes, it is still possible to see a slight increase in the GluA1 puncta in the soma of neurons when cells are treated with NPY. To understand how NPY is determining this effect on GluA1 puncta even when autophagy cannot start, at first hippocampal neurons were treated with actinomycin D, a transcription inhibitor that inhibits new mRNA synthesis in a dose dependent manner by intercalating into the DNA, thereby blocking nearly all transcription (Chen, Ezzeddine, and Shyu 2008; Perry and Kelley 1970). Interestingly, while the decrease in the GluA1 puncta in the soma was statistically significant in the group treated with both NPY and RNA synthesis inhibitor, compared to the control treated with actinomycin only, in the dendrites of hippocampal cells the puncta remained unchanged across all experimental groups. This evidence arising from the soma can be once more related to the degradation of GluA1 puncta in the autophagosomes. Indeed, as already mentioned above, the autophagosomes are shuffled from the dendrites to the soma, where they then fuse with lysosomes and can degrade their content. Guo et al. (2015) already demonstrated the half-life of the GluA1 mRNA is around 4.5h (Guo et al. 2015) and, consequently, the decrease seen in the soma might be related to the degradation of the GluA1 present into the autophagosomes plus the depletion of the mRNA pool present in there that cannot be transcribed anymore due to the actinomycin blockage. In order to verify if the increase in the GluA1 puncta can be related to an increase in the mRNA of GluA1, ERK phosphorylation time-course was investigated during the 6h NPY treatment. Aveleira et al. (2014) showed that NPY is able to activate the ERK pathway to induce autophagy and this, combined with the knowledge that the majority of ERK1/2 can be found in the nucleus 10min to 20min post activation (R. H. Chen, Sarnecki, and Blenis 1992), might lead to the idea that NPY could somehow promote an increase in the mRNA transcription of Gria1, GluA1 gene, that will be then translated into protein. It is already known that ERK plays a role in protein synthesis and late-phase LTP (Costa-Mattioli et al. 2009; Kelleher, Govindarajan, and Tonegawa 2004) and its activation is involved in trafficking of existing AMPARs, but it can as well determine the downstream signalling pathways, which in turn initiate new protein synthesis of GluA1 during non-

physiological conditions (Liu et al. 2020). However, it was not possible to detect any differences in in the phosphorylated form of ERK over the 6h time-course of the NPY stimulation, as well as in the Gria1 levels by qRT-PC. However, to further confirm the results obtained and explore in more details what effect NPY has on GluA1 puncta in the dendrite, where it seems that the block of RNA synthesis is not determining a decrease in the GluA1 puncta, cells were treated with CHX, a blocker of protein synthesis in eukaryotes: while the GluA1 puncta dramatically decreased in the soma when cells are treated with CHX (with or without the NPY treatment), in the dendrite the GluA1 puncta decrease only when NPY is applied in combination to CHX. It is very well known that both excitatory and inhibitory presynaptic terminals contain the machinery for protein synthesis, from poly $(A)^+$ mRNA to ribosomal proteins and rRNA, as exhaustively demonstrated by Hafner et al (2019), and among the most enriched transcripts in excitatory synapses there are the ones from the AMPA neurotransmitter family (Hafner et al. 2019). Therefore, the blockage of the protein synthesis during the 6h NPY stimulation, might allow for speculations on a possible role for NPY as reorganizer of GluA1 subunit of AMPA receptor. These experiments will fit into the aforementioned work by Shehata and colleagues (2012), where they hypothesise that the increase in autophagy determined via chemical-LTD would in turn increase the number of autophagosomes and consequently imbalance the recycling endosomes entrapment or lysosomal degradation of the GluA1 subunit of AMPA receptor. Indeed, from the evidences collected in this thesis, it seems like the GluA1 subunit is removed from the synapses via autophagosomes, that are then directed to the soma of the neurons (where they can either be degraded or later shuffled back to the dendrites) and then replaced by newly synthesised ones. This process is suppressed when the protein synthesis is blocked, leaving only space for the engulfment of GluA1 in autophagosomes that are moved away from the main dendrite and that cannot be replace by the local synthesis of new GluA1 when the protein synthesis is blocked with CHX (Fig. 45).

Discussion
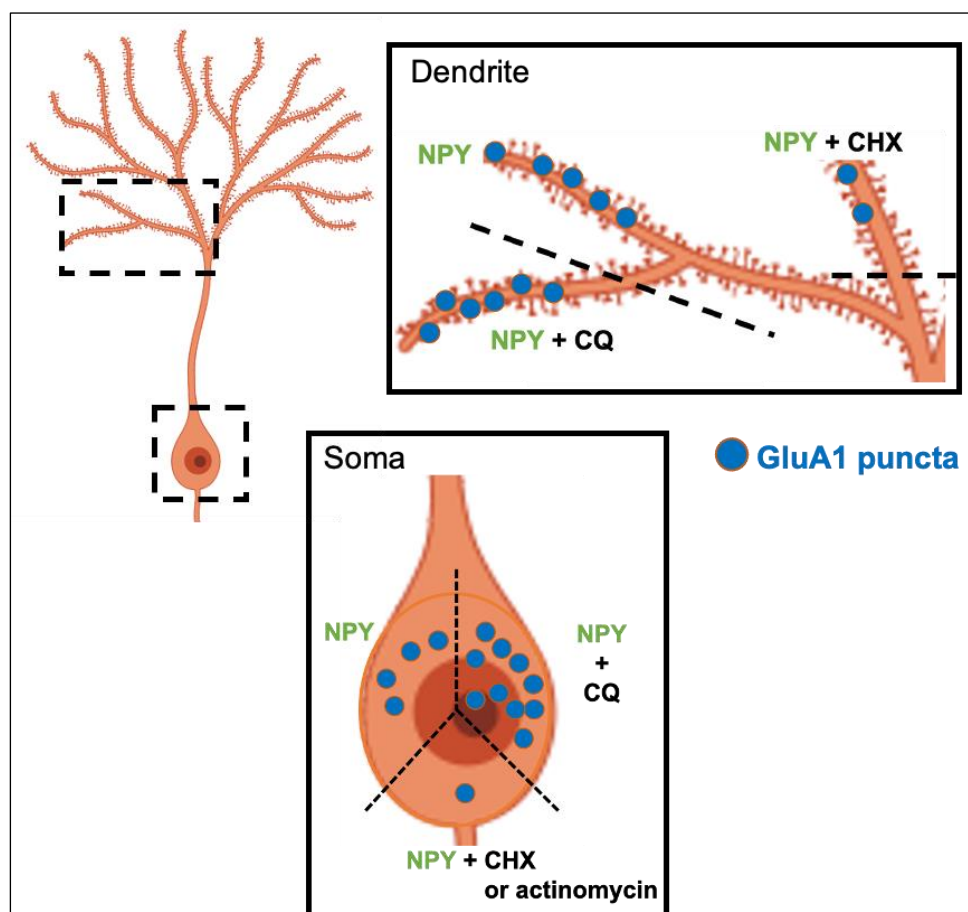
Figure 45. **Schematics of GluA1 puncta changes due to the 6h NPY treatment.**
<u>Soma</u>: the 6h NPY treatment seems to promote an increase of GluA1 puncta in the soma of hippocampal neurons; when autophagy is arrested via CQ, the GluA1 puncta accumulate in the soma; on the other hand, when the RNA transcription or the protein synthesis translation are inhibited (via actinomycin or CHX respectively), GluA1 puncta significantly decrease.
<u>Dendrite</u>: the 6h NPY treatment only shows a slight tendency into increasing GluA1 puncta; this increase is slightly more pronounced when the autophagy is halted with CQ; on the other hand, inhibiting the protein translation via CHX is significantly decreasing the GluA1 puncta.

In order to verify the aforementioned hypothesis and further investigate if GluA1 is removed from the synapses, it was used an antibody able to recognise its extracellular portion. This antibody showed that the 6h NPY treatment is promoting the removal of the GluA1 subunit of the AMPA receptor from the synapses and, consequently, the decrease in the number of pre-synaptic – post-synaptic colocalization. Indeed, a functional synapse needs a pre-synaptic and post-synaptic compartment and as GluA1 is a subunit of the excitatory AMPA receptor, the pre-synaptic marker selected was VGlut, that refills synaptic vesicles with glutamate. Interestingly, while the number of colocalising VGlut – extracellular GluA1 is decreasing, the number of VGlut puncta is the same as the control, allowing for speculation on the fact that NPY seems to have

Discussion

an effect in decreasing the number of potentially functional synapses, but it appears to be a specific post-synaptic effect and on GluA1. Indeed, there seems to be a reorganization of the synapses on the post-synaptic side, where GluA1 appears to be removed from the synapses. The evaluation of GluA1/Shank2 colocalization was performed in order to investigate how NPY is exerting its effect on the post-synaptic side. Shank2 belongs to the Shank proteins family, that are constituents of the post-synaptic density in excitatory spines and are involved in a wide range of synaptic processes (Sheng and Kim 2000). In particular, Shank proteins coordinate actin dynamics, connect the endocytic machinery and calcium signalling, but, more importantly, they are involved in the scaffold of ionotropic and metabotropic receptors (Du et al. 1998; Hwang et al. 2005; Lu et al. 2007; Naisbitt et al. 1999; Verpelli et al. 2011). In particular, Shank2 seems to be critical for AMPA recruitment, as the loss of Shank2 resulted in reduced GluA1 levels and reduced AMPA receptor function (Wegener et al. 2018). The analysis of the colocalising GluA1-Shank2 puncta revealed an increase in the colocalization of these two proteins, that is as well accompanied by a strong tendency into an increase in the Shank2 puncta. These data are in line with those from Uchino et al. (2006), that show how Shank2 interacts with the cytoplasmic tail of GluA1 and this interaction could possibly be involved in AMPAR trafficking (Uchino et al. 2006), therefore pointing once more to the hypothesis that the NPY treatment might lead to a reorganization of AMPA receptors. It is well known that exocytosis and endocytosis of AMPARs play critical roles in LTP and LTD (Anggono and Huganir 2012; Kessels and Malinow 2009) and together with the knowledge that chemical LTD produces the internalization of GluA1 subunit of AMPA receptor (Shehata et al. 2012), this thesis might provide an additional mechanism through which hippocampal neurons traffic this subunit of AMPA receptor, as this ionotropic receptor is only functional when sitting at the synapse and when a pre-synaptic site is in close distance. Indeed, study shows that Shank2 participates in pathways that regulate activity-dependent transcription and translation and, as well, it suppresses excess dendritogenesis during the development and enables acute activity-dependent extension (Santini and Klann 2014; Zaslavsky et al. 2019). These changes in the synapses seem to be a concomitant effect of the increase in autophagy, that engulfs the GluA1 present on the membranes into autophagosomes possibly via Shank2, and the local protein synthesis, that substitutes the missing GluA1 puncta with newly formed ones. In order to confirm this hypothesis, both autophagy and protein synthesis

were blocked. In accordance with our previous results, blocking the protein synthesis when autophagosomes cannot be formed due to the shlentivirus mediated ATG5 KD prevents the decrease in the GluA1 seen in the shScramble condition. This result provides further evidence on NPY regulation of GluA1 expression via autophagy. It is indeed a not so uncommon phenomenon the concomitant activation of protein degradation and synthesis, as it could be seen, for example, in the case of the secreted amyloid precursor protein-alpha that facilitates LTP through cellular processes involving both trafficking of AMPA and NMDA receptors to the extrasynaptic cell surface and de novo protein synthesis, among which there was GluA1 as one of the upregulated proteins (Mockett et al. 2019). Moreover, mTOR that is a well-known regulator of protein turn-over in neurons by functioning at the intersection between protein synthesis and degradation, is not involved in the NPY-induced autophagy, i.e. mTOR is not inhibited as demonstrated by Aveleira and colleagues (2014), thus pointing on a concomitance of effects on both protein synthesis and degradation determined by the NPY application.

5.3.   The long-lasting changes in GluA1

Knowing that NPY can elicit a 24h increase in autophagy, the GluA1 levels were checked as well 24h after the medium change. Surprisingly, the increase in GluA1 subunit seen via WB is statistically significant 24h after the 6h NPY treatment and medium change. Moreover, this increase seems to autoregulate as it goes back to control levels 48h after the medium change, but it also seems specific for this subunit of the AMPA receptor, as the other excitatory receptor subunit NMDAR1 or the inhibitory subunit GABAA do not seem to be affected again by the NPY stimulation. Once more, the NPY effect on GluA1 is lost when the autophagy is not functional during the NPY treatment, either via a pharmacological approach using WRT or via the use of the aforementioned shATG5 lentivirus. When analysing the spatial distribution of the GluA1 puncta 24h after the NPY stimulation, they seem to be redistributed to the dendrites of the neurons and they seem to be sitting on the synapses, allowing for speculations on a possible increase on the potentially functional synapses. However, after analysing the colocalization, either the pre-synaptic – post-synaptic markers, with VGlut and the external GluA1 antibody, or the post-synaptic – post-synaptic markers, with GluA1 and Shank2, it was not possible to see any

Discussion

differences with respect to the CTR condition. Consequently, this might be interpreted in the light of a re-organization of GluA1 puncta 24h after the NPY stimulation, that might be sitting on the membrane of the neurons, possibly ready to be used, but still not functional as they do not seem to have a pre-synaptic connection yet. AMPARs are highly mobile and undergo both constitutive and activity-dependent trafficking to the synapse as well as recycling and degradation, and in particular it is widely accepted that LTP in the hippocampus requires an increase in AMPA receptors within the synapses (Wu et al. 2017). Here, it is described a possible mechanism, through which the GluA1 subunit of AMPA receptor is trafficked to and from the synapses after NPY stimulation. Studies showed how AMPA receptor is recruited to the spines inducing increases in CA1 spine density (Middei et al. 2012) and the positive correlation between GluA1 intensity at the spine and shaft and spine size after whisker stimulation (Zhang et al. 2015). Evidences show that the insertion of GluA1 at the synapses requires neuronal activity and it is a multistep process: its insertion starts at extrasynaptic sites and its traffic is associated with scaffold proteins and enzymes that control its synaptic entry, localization and removal (Boehm et al. 2006; Ehlers 2000; Makino and Malinow 2009). NPY might be the initiator of a process through which GluA1 is removed from the synapses during the 6h application, to then be shuffled back to the membranes 24h after the stimulation, in order to be sitting at the membranes and be used for a potential LTP induction. Studies on addiction already show long-lasting changes in GluA1 subunit of AMPA receptor after a single drug application: for example, a single injection of amphetamine in rats determines increases specifically in GluA1 in the nucleus accumbens (NAc) 2h post-injections (Nelson et al. 2009), as well as cocaine injections that promotes an increase in GluA1 24h after the administration always in the NAc (Ferrario, Li, and Wolf 2011). Acute stress as well can modulate the GluA1 subunit of the AMPA receptor: for example in the PFC, an acute foot shock stress modulates GluA1 via phosphorylation on the serine site responsible for LTP, in order to rapidly and transiently activate AMPA receptor-mediated synaptic currents (Bonini et al. 2016), or via an increase in the surface protein levels that seem to last until 24h (Yuen et al. 2009). The studies presented above show that relative brief events such as exposure to acute stressors or one-time cocaine or amphetamine administration have a lasting impact on AMPA function. The results from this *in vitro* study now suggest that NPY could evoke similar effects via autophagy, with possible consequences for hippocampal plasticity *in vivo.*

Discussion

Indeed, these data allow for speculation on a possible strategy used by animals during stressful conditions: the release of NPY during stress in the hippocampus might promotes an increase of autophagy, that determines an increase in the formation of autophagosomes. The autophagosomes seem to engulf the GluA1 subunit of AMPA receptors, that are consequently removed from synapses and shuffled to the soma. At the same time, the removal of GluA1 subunit of AMPA receptors is stimulating the production of new GluA1, production that happens both in the soma of the neurons and in the synapses, where local translation takes place and where there are GluA1 mRNA ready-to-use. These changes are starting to take place while NPY is still stimulating the neurons, but they become particularly evident 24h after the removal of NPY, when there is an increase in the GluA1 puncta in the synapses, that does not seem to be accompanied by an increase in colocalization with a pre-synaptic marker, a characteristic that is required to consider a synapse structurally ready to function (Fig. 46).
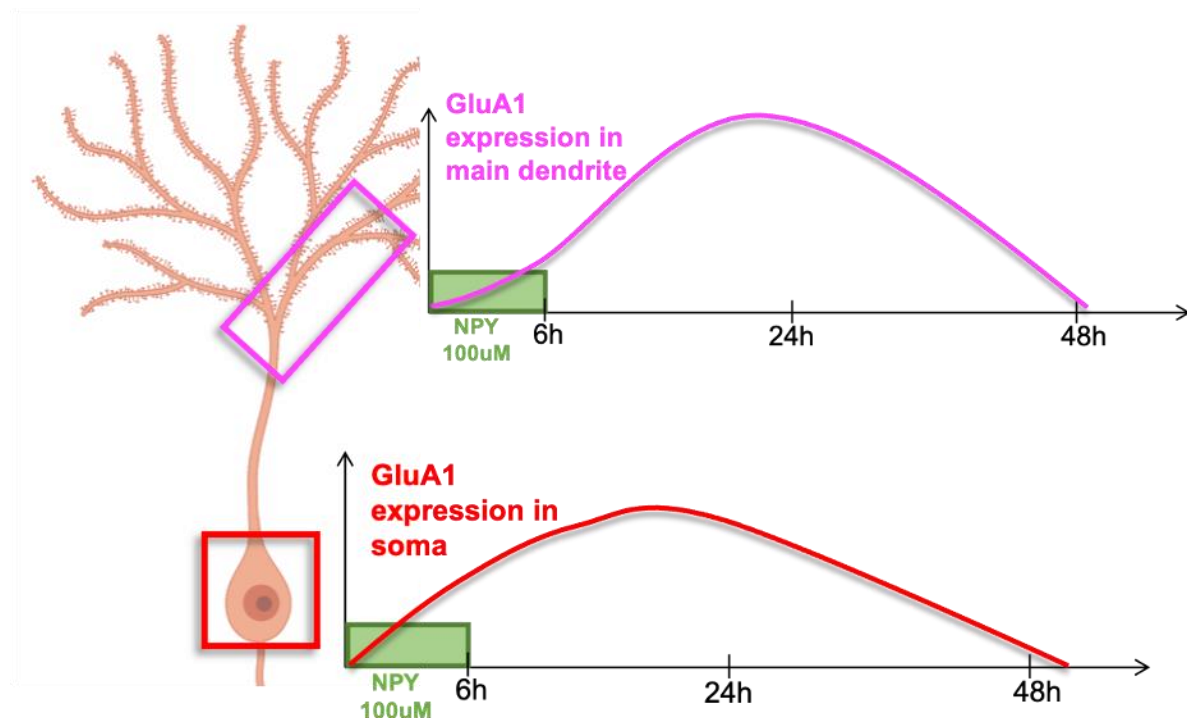
Figure 46. **Schematic of the proposed changes in GluA1 expression over the time course of NPY stimulation and autophagy activation.**

These results need to be further investigated, as the changes in GluA1 in the synapses during the 6h NPY treatment or 24h after the NPY stimulation should determine variations in the electrophysiological responses of neurons, such as modifications of LTP by investigating on hippocampal plasticity models, that could be

better evaluated either *in vitro* via whole-cell patch-clamp in hippocampal primary neuronal cultures or *ex vivo* recordings from hippocampal slices, in order to have an activity read-out of such changes in the GluA1 subunit of AMPA receptor. Also, further studies should characterise the significance of this synaptic pool of available GluA1 24h after NPY stimulation, as for example, another stimulation, such as chemical-LTP, might determine an increase in the colocalization of pre-synaptic – post-synaptic markers and, consequently, an increase in potentially functional synapses compared to the non-stimulated cells.

5.4. The *in vivo* NPY effect in the hippocampus

NPY is released in the hippocampus during stress and it has a well-known role as anxiolytic compound, as well as having antidepressant properties (Heilig et al. 1989; Reichmann and Holzer 2016). Particularly fascinating is the role of NPY during contextual fear memory formation, where the release of NPY controls the excitability of the granule cells in the DG. This modulation via the NPY releasing cells allows for a control on the formation of aversive memory and thus could be a mechanism used by resilient individual against PTSD (Raza et al. 2017). Therefore, to find out if the NPY released in the hippocampus is exerting the same effect seen *in vitro* in the hippocampal cell culture, young adult mice received bilateral infusions of NPY in the dDG and both autophagy and GluA1 were analysed in the dorsal hippocampus 6h or 24h post-infusions. As expected, the 6h post-infusion time point does not show any differences in the LC3 intensities compared with the saline group. This finding is in line with previous researches showing difficulties in visualising changes in autophagy markers due to the high efficiency and flux of neuronal autophagy (Boland et al. 2008; Mizushima et al. 2004; Nixon et al. 2005). Even though ATG proteins, that are essential for autophagic delivery of cargo to the vacuole, are highly expressed in rodent brains, autophagic activity markers are low compared with other tissues and detecting autophagy has been particularly challenging in neurons compared to other cell types, since autophagic vesicles are difficult to visualise by electron microscopy or even when fluorescent reporters are used (Mizushima et al. 2004; Nixon et al. 2005). Moreover, even under strong autophagy induction conditions such as inhibitors of the mTOR kinase pathway like rapamycin (Blommaart et al. 1995; Sabers et al. 1995) and nutrient deprivation (Barber et al. 2001; Vander Haar et al. 2007), the

efficiency of neuronal autophagy is not perturbed, as the fusion of autophagosomes with lysosomes is highly active in these cells (Boland et al. 2008). However, the GluA1 intensity levels show an interaction between the NPY infusion and the dendritic portion analysed, as the more distal we move across the dendritic portion, the more the GluA1 intensity increases. This reaches the peak in the most distal portion of the dendrites of the granule cells, that shows higher GluA1 intensity compared to the CTR group and it might be in line with the previously described *in vitro* findings. On the other hand, when analysing the 24h post infusion time point, the GluA1 intensity levels show a general tendency for an increase in all the analysed areas: from the hilus, that contains the nuclei of the NPY positive interneurons involved in the aforementioned regulation of aversive memory formation, to the granule cells, involved in the actual formation of these memories, both in the soma region and the different segments of their dendrites, where, once more, the more distal region shows a significant increase. LC3 levels instead are higher only in the hilus, possibly showing either presynaptic autophagy, as the LC3 intensity coming from the axons of the granule cells, i.e. the mossy fibers, that are crossing in this area would be caught with the setup of this intensity analysis (Andres-Alonso et al. 2019), or some modulation effects in this same area, that might as well involve the previously discussed NPY positive interneurons, therefore possibly hinting to an NPY auto-modulation.

5.5. The *in vivo* stress effect on GluA1 in dDG

In vivo as well, the NPY stimulation seems to promote the increase in autophagy and GluA1 in the dorsal hippocampus, in accordance with our observations in the hippocampal primary neuronal co-cultures. However, in order to investigate the effect of the endogenous NPY *in vivo*, the behavioural paradigm established by Raza et al. (2017) was used to induce NPY release in the dorsal hippocampus. Indeed, as already described above, in this paradigm NPY is released from NPY positive interneurons on to the granule cells, during a Pavlonian FC task, where it controls the formation of aversive memories. Knowing that the maximum effect on autophagy and GluA1 intensities occurs 24h after the NPY stimulation (for both the *in vitro* and *in vivo* experimental conditions seen in this thesis), animals were sacrificed exactly 24h after the FC training, that was carried either with the tone alone or with the tone paired with three foot shocks, in order to provide some of the animals with the stressful experience

that should induce the release of NPY. Also, NPY was either constitutionally KD, via the use of a shlentiviral vector that has a KD efficacy of 25% as demonstrated by Regev-Tsur and colleagues (2020), or the NPY-releasing cells in the hilus were transiently silenced using statin-Cre mice and a DREADD lentiviral vector that can be activated via injecting CNO 1h before the FC training, as previously described by Raza et al. (2017), in order to unmask possible modulatory NPY effect on the two phenomena of interest: autophagy and GluA1.

As far as it concerns autophagy, the difficulties in visualising changes seem to come into play once more, as differences among groups were not significant and animals show a high variability. However, in the constitutional NPY KD set of experiments, the LC3 intensity analysis revealed an effect of the KD of NPY itself across all the areas analysed independently of the FC protocol received. On the other hand, when NPY releasing cells are transiently silenced 1h before the FC training, the LC3 intensity analysis showed once more an effect of the viral manipulation alone across the dendritic portions of the granule cells, that is maximum in the outer part of the molecular layer, where the animals that receive the tone and the foot shocks have lower levels of LC3 intensity compared to both the CTR groups (either injected with the hM4Di or the mCherry vector alone). The observed effect is opposite compared to the one previously seen one, when NPY is constitutionally KD, hinting towards compensatory effects that might arise during the constitutional KD and that are unmasked when the NPY-releasing cells are inactivated just 1h before receiving the FC training. This is in line with previous reports that show how autophagy can be modulated by stress itself, such as chronic cold exposure that can induce neuronal autophagy in mice hippocampus (Qu et al. 2017; Xu et al. 2019), as well as chronic restrain stress or the application of corticosterone (Woo et al. 2018). However, it must be considered that the freezing levels recorder during the FC training are very high and with quite some variability among animals, even for the groups that received the tone alone: this might show that even these animals that receive the tone only were stressed to some level. However, it is worth noticing that the group that had the NPY-releasing neurons inactivated before the FC training, but received the tone only, shows similar freezing levels as the groups that received the tone paired with the foot shocks: these data should be further investigated, as they might be interpreted in the light of a sensitization due to the tone exposure only. Nevertheless, the *in vivo* data presented in this thesis seem to be in accordance with the previously discussed *in vitro* and *in*

Discussion

vivo results and this can be appreciated when looking at the silencing of the NPY-releasing 1h before FC training set of experiments, as compensatory phenomena do not come into play: when NPY is not released by the cells in the hilus (independently of the FC protocol used) the LC3 intensity levels are lower compared to the control groups. Indeed, the lack of NPY seems to determine a decrease in autophagy (see figure Fig. 47 for a summary of the effects produced by the different viral manipulation and FC groups used).

When analysing the GluA1 intensity, the evidences collected show opposite effects, whether NPY is constitutionally KD or the NPY-releasing cells in the hilus are transiently inactivated. Data show that stress by itself is increasing the GluA1 intensity in the inner portion of the granule cell dendrites. When NPY is KD, the GluA1 intensity goes up in the soma of the granule cell when the animals receive the tone only, but this time it was possible to appreciate an interaction between the KD of NPY and the FC protocol used in the proximal portion of the granule cell dendrites, with a pattern that repeats itself across the outer sections, even if not significant. It appears that, if the animals receive the tone only, the constitutional KD of NPY determines a general increase in the GluA1 intensity levels across all the areas segmented. However, when stress comes into play in the form of foot shocks paired with the tone and NPY is KD, the GluA1 levels show an increase in the hilus and soma of the granule cells, while at the same time, they decrease across all sections of the granule cells dendrites, to almost reach the tone only control levels. On the other hand, when analysing the GluA1 intensity in the transient silencing of the NPY-releasing neurons in the hilus set of experiments, the animals that receive the viral manipulation but the tone only, have higher GluA1 intensity levels compared to the CTR group that received the tone paired with the foot shocks: this result is statistically significant in the medial portion of the granule cell dendrites, but it shows a repeated pattern in the other portions of the dendrites as well, despite not being significant (see figure Fig. 47 for a summary of the effects produced by the different viral manipulation and FC groups used).

Discussion
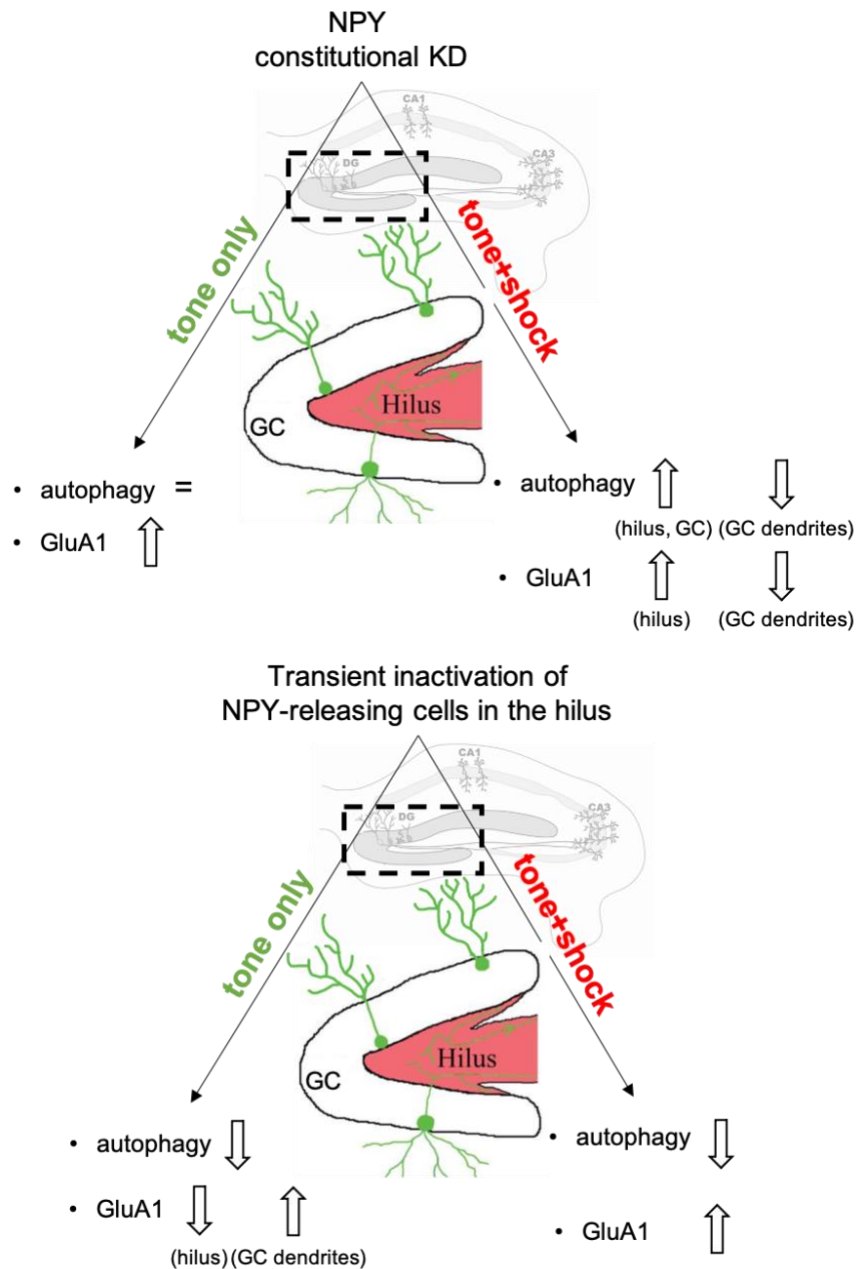
Figure 47. **Summary of the different viral manipulation used to either KD NPY or transiently inactivate NPY releasing cells in the dDG and the effects on autophagy and GluA1 intensity levels.**

The data collected from the transient inactivation of NPY-releasing cells in the hilus showed a tendency into a decrease in both LC3 and GluA1 intensities in the hilus and knowing that the NPY positive interneurons that release NPY on the granule cells have their soma in that area, using the viral fluorescent signal as a marker for those cells, it was investigated in these same neurons the possible autophagy and GluA1 modulation elicited by stress and/or the silencing of these same cells itself. Indeed, as far as it concerns the LC3 intensity levels, a statistically significant factor is the viral

Discussion

manipulation: the inactivation of the NPY positive interneurons via DREADD virus is decreasing the autophagy levels in these cells, independently of the tone or tone+shock group. Moreover, when analysing the GluA1 levels, the viral manipulation itself has a statistically significant effect, and it was also possible to see a statistically significant decrease in the tone only group that has silenced the NPY positive interneurons, compared to the tone only and tone+shock CTR groups. This finding can support the idea of an NPY regulation of NPY positive interneurons, which could possibly be carried out via the Y2 receptor, that has a presynaptic localization and can in turn act as an autoreceptor (Reichmann and Holzer 2016). Nevertheless, the silencing of NPY-releasing cells in the hilus when the animals receive the tone only is decreasing GluA1 in these same cells. Consequently, these neurons might be less excitable and, therefore, even less prone to release NPY, creating a negative feedback that can in turn affect the granule cells during the aversive memory formation. However, when the stressful event is present, i.e. the tone is paired with the foot shock, these NPY releasing cells are somehow trying to rescue the lack of NPY signalling in these same cells, as from the data collected the GluA1 levels are higher for the hM4Di tone+shock group.

These data might be interpreted in the light of the well-known anxiolytic effect of NPY (Primeaux et al. 2005; Molosh et al. 2013; Sørensen et al. 2004). NPY is a resilience factor during stress exposure, as several human studies on resilient soldiers demonstrated: their plasma and serum have higher levels of NPY compared to soldiers that developed PTSD (Charles A. Morgan et al. 2000; Reijnen et al. 2018). Conversely, the absence of NPY via KO in mice produces a strong phenotype that has increased acquisition of conditioned fear (Verma et al. 2012), and even the KD of NPY via shlentivirus with only 25% of efficiency, significantly reduced the prevalence of resilient animals (Regev-Tsur et al. 2020). This is particularly true in the dorsal hippocampus, where NPY plays a role in the emotional memory formation (raza et al. 2017). NPY is inducing autophagy, as already demonstrated by Aveleira et al. (2014), Ferreira-Marques et al. (2016), as well as from the experiments in this thesis, and more and more papers are pointing towards a beneficial role of an increased autophagy in neuropsychopathologies (J. Fu et al. 2017; Gulbins et al. 2018; Zhai et al. 2018). Moreover, autophagy seems to play a pivotal role in shaping activity-dependent synaptic plasticity: on one hand, synaptic activity stimulates autophagy that in turn promotes memory formation via the production of dendritic spines (Glatigny et

al. 2019a), on the other hand, the increase in autophagy might be helpful in erasing reconsolidation-resistant fear memory (Shehata et al. 2018). From the evidences collected in this thesis, it is possible to speculate that NPY might exert its beneficial effect during stressful events via an increase in autophagy. This increase might in turn act on the GluA1 levels in order to promote resilience via the long-lasting changes observed both *in vitro* and *in vivo*, where we see a removal of GluA1 from the synapses during the NPY stimulation and a subsequent increase 24h post NPY application in hippocampal neurons. Indeed, stress can modulate AMPA receptors and their trafficking: CORT, as well as *in vivo* protocols that induce stress, can promote an increase in the membrane mobility of GluA2-containing AMPA receptors during bi-directional synaptic plasticity (Conboy and Sandi 2010; Groc, Choquet, and Chaouloff 2008; Martin et al. 2009). In these experiments, it was possible to see a long-lasting reorganization of AMPA receptor, induced by NPY, that eventually determine an increase in the number of AMPA receptors sitting at the membranes, yet not co-localizing with a pre-synaptic end. This interesting finding could be partially appreciated via *in vivo* experiments as well: if on one hand the KD of NPY is determining results that are contrasting with the *in vitro* finding, as the 25% KD efficiency can either determine compensatory effects such as an increase in the receptor expression that should be eventually further investigated, the transient silencing of the NPY-releasing cells in the hilus is determining a decrease in the GluA1 intensities across all the areas analysed in the dDG. This decrease might as well be dependent on an autoregulation of the NPY-releasing cells, where the absence of NPY could create a negative feedback that decreases these cells' excitability as well. These results leave space for speculations on the effects of this GluA1 reorganization that might exert on memory retrieval, that need to be further explored.

6. Future perspectives and closing remarks

The results obtained for the NPY-mediated autophagy modulation of GluA1 are in line with the knowledge that neuronal stimulation, not only induces autophagy, but its consequent increase impacts synaptic function as well (Shehata et al. 2012). As already mentioned, GluA1 is a ionotropic receptor that plays a role in LTP (Granger et al. 2013; Lu et al. 2009) and it can be modulated by stress (Qu et al. 2017; Xu et al. 2019). However, the behavioural implications of this modulation elicited via NPY are still to be explored.

More work needs to be done to find out exactly how NPY is modulating autophagy, but particularly, GluA1 in the dorsal hippocampus, as data are hinting to a complex regulation of these two players *in vivo* and yet no behavioural effect was seen, despite the trends in autophagy and GluA1 changes collected from this analysis. This was not surprising, as the time point chosen for the animal perfusion, 24h after the FC training, coincided with a possible first retrieval session and the behavioural effects were expected during the retrieval sessions (as already seen in the paper by Raza and colleagues (2017)). Moreover, to better understand the electrophysiological changes that could eventually arise from this NPY-induced GluA1 reorganization, *ex vivo* organotypic brain slices cultures of the hippocampus could be investigated by applying LTP and LTD protocols at the different time points analysed in this thesis and evaluate the changes that might arise from the removal and/or the insertion of GluA1 promoted by NPY in the membrane. Also, the use of *ex vivo* organotypic brain slices cultures could help elucidate on a spatial resolution level and in a properly developed hippocampal structure, yet without the complexity of a whole organism, which of the NPY receptors is activated in this phenomenon, as the NPY receptors present regional differences in the dDG that might determine different effects, e.g. the Y2 receptor is discretely distributed in the hippocampus and it is usually an autoreceptor that inhibits the release of NPY and other neurotransmitters (Caberlotto et al., 2000; King et al., 1999, 2000; Martire et al., 1995), while the Y1 has a higher distribution in the different areas of the hippocampus and a post-synaptic localization (Dumont et al. 1998; Kishi et al. 2005; Larsen et al. 1993). Yet, the autoregulating 24h long-lasting NPY-induced autophagy increase that goes back to control levels 48h after medium change and that in turn controls the reorganization of GluA1 subunit of AMPA receptor might have

unexplored beneficial effects that could be further investigated to be eventually exploited as possible therapy for psychiatric disorders.

Perhaps the increase seen in GluA1 24h after the NPY application might require another stimulation, such as retrieval sessions after the foot shocks in a FC behavioural protocol that should mimic a reminder of a traumatic experience in humans. Recently, Shehata et al. (2018) reported how autophagy contributes to contextual memory destabilization in the hippocampus, that correlates with AMPA receptor degradation in the spines of the contextual memory-ensemble cells (Shehata et al. 2018). Indeed, the data presented in this thesis might show how NPY could be the main player of this phenomenon. The retrieval sessions might be used to see the possible protective effect of NPY demonstrated in the work by Raza et al. (2017), where NPY is controlling the formation of aversive memory by adjusting the strength of the context memory. Many tools can be used to verify the hypothesised potentially beneficial behavioural effects deriving from the increase in GluA1 elicited by NPY, such as CNQX, a pharmacological competitive AMPA receptor antagonist, or a lentiviral vector containing a sh against GluA1, in order to prevent the increase in this AMPA receptor subunit levels and observe the differences that might arise. Also, to further confirm *in vivo* if the NPY-induced GluA1 increase is determined by the increase in autophagy that, in the beginning, is promoting the engulfment of GluA1 in autophagosomes as seen from the *in vitro* data of this thesis, another sh lentivirus targeting the ATG5 protein *in vivo* should be tested. Indeed, the confirmation that the GluA1 effect provoked by NPY could be induced by an increase in autophagy could give powerful insights into new strategies to be investigated and later used for the treatment of people with PTSD.

Such a characterisation of the NPY effect on autophagy and GluA1, both *in vitro* and *in vivo*, is once more unmasking the complex role of this neuropeptide in the brain and possibly unveiling its target, the GluA1 subunit of AMPA receptor, and how it is exerting its anxiolytic effect in the hippocampus, via the induction of autophagy. Therefore, the discover of this NPY modulation induced by a stressful event, as it might be this particular FC behavioural paradigm or other stress exposures such as PTSD models, anxiety tests, models of depression and so on, and obtained via an increase in autophagy can have interesting and potentially advantageous implications that can be eventually used as a starting point in the search for new targets for PTSD therapies.

Bibliography

Abeliovich, Hagai, William A. Dunn, John Kim, and Daniel J. Klionsky. 2000. "Dissection of Autophagosome Biogenesis into Distinct Nucleation and Expansion Steps." *Journal of Cell Biology* 151 (5): 1025–33. https://doi.org/10.1083/jcb.151.5.1025.

Albrecht, Anne, Jorge Ricardo Bergado-Acosta, Hans Christian Pape, and Oliver Stork. 2010. "Role of the Neural Cell Adhesion Molecule (NCAM) in Amygdalo-Hippocampal Interactions and Salience Determination of Contextual Fear Memory." *International Journal of Neuropsychopharmacology* 13 (5): 661–74. https://doi.org/10.1017/S1461145709991106.

Albrecht, Anne, Sebastian Ivens, Ismini E. Papageorgiou, Gürsel Çalışkan, Nasrin Saiepour, Wolfgang Brück, Gal Richter-Levin, Uwe Heinemann, and Oliver Stork. 2016. "Shifts in Excitatory/Inhibitory Balance by Juvenile Stress: A Role for Neuron-Astrocyte Interaction in the Dentate Gyrus." *Glia* 64 (6): n/a-n/a. https://doi.org/10.1002/glia.22970.

Amaral, David G., Helen E. Scharfman, and Pierre Lavenex. 2007. "The Dentate Gyrus: Fundamental Neuroanatomical Organization (Dentate Gyrus for Dummies)." *Progress in Brain Research*. Elsevier. https://doi.org/10.1016/S0079-6123(07)63001-5.

American Psychiatric Association. 2013. "Anxiety Disorders." *Diagnostic and Statistical Manual of Mental Disorders* 5th ed. https://doi.org/https://doi.org/10.1176/appi.books.9780890425596.dsm05.

Anand, Kuljeet, and Vikas Dhikav. 2012. "Hippocampus in Health and Disease: An Overview." *Annals of Indian Academy of Neurology*. Wolters Kluwer -- Medknow Publications. https://doi.org/10.4103/0972-2327.104323.

Andres-Alonso, Maria, Mohamed Raafet Ammar, Ioana Butnaru, Guilherme M. Gomes, Gustavo Acuña Sanhueza, Rajeev Raman, Ping An Yuanxiang, et al. 2019. "SIPA1L2 Controls Trafficking and Local Signaling of TrkB-Containing Amphisomes at Presynaptic Terminals." *Nature Communications* 10 (1): 1–17. https://doi.org/10.1038/s41467-019-13224-z.

Anggono, Victor, and Richard L. Huganir. 2012. "Regulation of AMPA Receptor Trafficking and Synaptic Plasticity." *Current Opinion in Neurobiology*. Elsevier Current Trends. https://doi.org/10.1016/j.conb.2011.12.006.

Ardi, Z., A. Richter-Levin, L. Xu, X. Cao, H. Volkmer, O. Stork, and G. Richter-Levin. 2019. "The Role of the GABAA Receptor Alpha 1 Subunit in the Ventral Hippocampus in Stress Resilience." *Scientific Reports* 9 (1). https://doi.org/10.1038/s41598-019-49824-4.

Ardi, Ziv, Anne Albrecht, Alon Richter-Levin, Rinki Saha, and Gal Richter-Levin. 2016. "Behavioral Profiling as a Translational Approach in an Animal Model of Posttraumatic Stress Disorder." *Neurobiology of Disease* 88 (April): 139–47. https://doi.org/10.1016/j.nbd.2016.01.012.

Ariosa, Aileen R., and Daniel J. Klionsky. 2016. "Autophagy Core Machinery: Overcoming Spatial Barriers in Neurons." *Journal of Molecular Medicine* 94 (11): 1217–27. https://doi.org/10.1007/s00109-016-1461-9.

Ashford, T. P., and K. R. Porter. 1962. "CYTOPLASMIC COMPONENTS IN HEPATIC CELL LYSOSOMES." *The Journal of Cell Biology* 12 (1): 198–202. https://doi.org/10.1083/jcb.12.1.198.

Aveleira, Célia A, Mariana Botelho, Sara Carmo-Silva, Jorge F Pascoal, Marisa Ferreira-Marques, Clévio Nóbrega, Luísa Cortes, et al. 2014. "Neuropeptide Y Stimulates Autophagy in Hypothalamic Neurons." *PNAS* 112 (13): 1642–51. https://doi.org/10.1073/pnas.1416609112.

Aveleira, Célia A, Mariana Botelho, and Cláudia Cavadas. 2015. "NPY/Neuropeptide Y Enhances Autophagy in the Hypothalamus: A Mechanism to Delay Aging?" *Autophagy* 11 (8): 1431–33. https://doi.org/10.1080/15548627.2015.1062202.

Bacchi, Fabrizio, Aleksander A. Mathé, Patricia Jiménez, Luigi Stasi, Roberto Arban, Philip Gerrard, and Laura Caberlotto. 2006. "Anxiolytic-like Effect of the Selective Neuropeptide Y Y2 Receptor Antagonist BIIE0246 in the Elevated plus-Maze." *Peptides* 27 (12): 3202–7. https://doi.org/10.1016/j.peptides.2006.07.020.

Bibliography

Bannerman, D. M., M. Grubb, R. M.J. Deacon, B. K. Yee, J. Feldon, and J. N.P. Rawlins. 2003. "Ventral Hippocampal Lesions Affect Anxiety but Not Spatial Learning." *Behavioural Brain Research* 139 (1–2): 197–213. https://doi.org/10.1016/S0166-4328(02)00268-1.

Bannerman, D. M., J. N.P. Rawlins, S. B. McHugh, R. M.J. Deacon, B. K. Yee, T. Bast, W. N. Zhang, H. H.J. Pothuizen, and J. Feldon. 2004. "Regional Dissociations within the Hippocampus - Memory and Anxiety." *Neuroscience and Biobehavioral Reviews*. Neurosci Biobehav Rev. https://doi.org/10.1016/j.neubiorev.2004.03.004.

Barber, Alistair J., Makoto Nakamura, Ellen B. Wolpert, Chad E.N. Reiter, Gail M. Seigel, David A. Antonetti, and Thomas W. Gardner. 2001. "Insulin Rescues Retinal Neurons from Apoptosis by a Phosphatidylinositol 3-Kinase/Akt-Mediated Mechanism That Reduces the Activation of Caspase-3." *Journal of Biological Chemistry* 276 (35): 32814–21. https://doi.org/10.1074/jbc.M104738200.

Barlow, D.H. 2002. "Anxiety and Its Disorders: The Nature and Treatment of Anxiety and Panic." Guilford Press. 2002. https://psycnet.apa.org/record/2001-05896-000.

Bartanusz, V., J. M. Aubry, S. Pagliusi, D. Jezova, J. Baffi, and J. Z. Kiss. 1995. "Stress-Induced Changes in Messenger RNA Levels of N-Methyl-d-Aspartate and AMPA Receptor Subunits in Selected Regions of the Rat Hippocampus and Hypothalamus." *Neuroscience* 66 (2): 247–52. https://doi.org/10.1016/0306-4522(95)00084-V.

Bauwens, Deborah, Philippe Hantson, Pierre François Laterre, Lucienne Michaux, Dominique Latinne, Marianne De Tourtchaninoff, Guy Cosnard, and Danielle Hernalsteen. 2005. "Recurrent Seizure and Sustained Encephalopathy Associated with Dimethylsulfoxide-Preserved Stem Cell Infusion." *Leukemia and Lymphoma* 46 (11): 1671–74. https://doi.org/10.1080/10428190500235611.

Beattie, Eric C., Reed C. Carroll, Xiang Yu, Wade Morishita, Hiroki Yasuda, Mark Von Zastrow, and Robert C. Malenka. 2000. "Regulation of AMPA Receptor Endocytosis by a Signaling Mechanism Shared with LTD." *Nature Neuroscience* 3 (12): 1291–1300. https://doi.org/10.1038/81823.

Beugnet, Anne, Andrew R. Tee, Peter M. Taylor, and Christopher G. Proud. 2003. "Regulation of Targets of MTOR (Mammalian Target of Rapamycin) Signalling by Intracellular Amino Acid Availability." *Biochemical Journal* 372 (2): 555–66. https://doi.org/10.1042/BJ20021266.

Bhukel, Anuradha, Christine Brigitte Beuschel, Marta Maglione, Martin Lehmann, Gabor Juhász, Frank Madeo, and Stephan J Sigrist. 2019. "Autophagy within the Mushroom Body Protects from Synapse Aging in a Non-Cell Autonomous Manner." https://doi.org/10.1038/s41467-019-09262-2.

Bingol, Baris. 2018. "Autophagy and Lysosomal Pathways in Nervous System Disorders." *Molecular and Cellular Neuroscience*, May. https://doi.org/10.1016/J.MCN.2018.04.009.

Bjørkøy, Geir, Trond Lamark, Andreas Brech, Heidi Outzen, Maria Perander, Aud Overvatn, Harald Stenmark, and Terje Johansen. 2005. "P62/SQSTM1 Forms Protein Aggregates Degraded by Autophagy and Has a Protective Effect on Huntingtin-Induced Cell Death." *The Journal of Cell Biology* 171 (4): 603–14. https://doi.org/10.1083/jcb.200507002.

Bliss, T. V.P., and G. L. Collingridge. 1993. "A Synaptic Model of Memory: Long-Term Potentiation in the Hippocampus." *Nature*. Nature. https://doi.org/10.1038/361031a0.

Blommaart, E. F.C., J. J.F.P. Luiken, P. J.E. Blommaart, G. M. Van Woerkom, and A. J. Meijer. 1995. "Phosphorylation of Ribosomal Protein S6 Is Inhibitory for Autophagy in Isolated Rat Hepatocytes." *Journal of Biological Chemistry* 270 (5): 2320–26. https://doi.org/10.1074/jbc.270.5.2320.

Blommaart, Edward F.C., Ulrike Krause, Jacques P.M. Schellens, Heleen Vreeling-Sindelárová, and Alfred J. Meijer. 1997. "The Phosphatidylinositol 3-Kinase Inhibitors Wortmannin and LY294002 Inhibit in Isolated Rat Hepatocytes." *European Journal of Biochemistry* 243 (1–2): 240–46. https://doi.org/10.1111/j.1432-1033.1997.0240a.x.

Boeckers, Tobias M., Michael R. Kreutz, Carsten Winter, Werner Zuschratter, Karl Heinz Smalla, Lydia Sanmarti-Vila, Heike Wex, et al. 1999. "Proline-Rich Synapse-Associated Protein-1/Cortactin Binding Protein 1 (ProSAP1/CortBP1) Is a PDZ-Domain Protein

Highly Enriched in the Postsynaptic Density." *Journal of Neuroscience* 19 (15): 6506–18. https://doi.org/10.1523/jneurosci.19-15-06506.1999.

Boehm, Jannic, Myoung Goo Kang, Richard C. Johnson, Jose Esteban, Richard L. Huganir, and Roberto Malinow. 2006. "Synaptic Incorporation of AMPA Receptors during LTP Is Controlled by a PKC Phosphorylation Site on GluR1." *Neuron* 51 (2): 213–25. https://doi.org/10.1016/j.neuron.2006.06.013.

Boland, Barry, Asok Kumar, Sooyeon Lee, Frances M. Platt, Jerzy Wegiel, W. Haung Yu, and Ralph A. Nixon. 2008. "Autophagy Induction and Autophagosome Clearance in Neurons: Relationship to Autophagic Pathology in Alzheimer's Disease." *Journal of Neuroscience* 28 (27): 6926–37. https://doi.org/10.1523/JNEUROSCI.0800-08.2008.

Bommel, Bas, Anja Konietzny, Oliver Kobler, Julia Bär, and Marina Mikhaylova. 2019. "F-actin Patches Associated with Glutamatergic Synapses Control Positioning of Dendritic Lysosomes." *The EMBO Journal* 38 (15). https://doi.org/10.15252/embj.2018101183.

Bonini, Daniela, Cristina Mora, Paolo Tornese, Nathalie Sala, Alice Filippini, Luca La Via, Marco Milanese, et al. 2016. "Acute Footshock Stress Induces Time-Dependent Modifications of AMPA / NMDA Protein Expression and AMPA Phosphorylation" 2016.

Brinkmann, Kerstin, Michael Schell, Thorsten Hoppe, and Hamid Kashkar. 2015. "Regulation of the DNA Damage Response by Ubiquitin Conjugation." *Frontiers in Genetics.* Frontiers Media S.A. https://doi.org/10.3389/fgene.2015.00098.

Brunello, Nicoletta, Jonathan R.T. Davidson, Martin Deahl, Ron C. Kessler, Julien Mendlewicz, Giorgio Racagni, Arieh Y. Shalev, and Joseph Zohar. 2001. "Posttraumatic Stress Disorder: Diagnosis and Epidemiology, Comorbidity and Social Consequences, Biology and Treatment." *Neuropsychobiology* 43 (3): 150–62. https://doi.org/10.1159/000054884.

Caberlotto, L, K Fuxe, and Y L Hurd. 2000. "Characterization of NPY MRNA-Expressing Cells in the Human Brain: Co-Localization with Y2 but Not Y1 MRNA in the Cerebral Cortex, Hippocampus, Amygdala, and Striatum." *Journal of Chemical Neuroanatomy* 20 (3–4): 327–37. http://www.ncbi.nlm.nih.gov/pubmed/11207429.

Calabrese, Francesca, Gianluigi Guidotti, Raffaella Molteni, Giorgio Racagni, Michele Mancini, and Marco Andrea Riva. 2012. "Stress-Induced Changes of Hippocampal NMDA Receptors: Modulation by Duloxetine Treatment." *PLoS ONE* 7 (5). https://doi.org/10.1371/journal.pone.0037916.

Calandreau, Ludovic, Robert Jaffard, and Aline Desmedt. 2007. "Dissociated Roles for the Lateral and Medial Septum in Elemental and Contextual Fear Conditioning." *Learning and Memory* 14 (6): 422–29. https://doi.org/10.1101/lm.531407.

Callis, Judy. 2014. "The Ubiquitination Machinery of the Ubiquitin System." *The Arabidopsis Book* 12: e0174. https://doi.org/10.1199/tab.0174.

Carroll, Reed C., Eric C. Beattie, Mark Von Zastrow, and Robert C. Malenka. 2001. "Role of AMPA Receptor Endocytosis in Synaptic Plasticity." *Nature Reviews Neuroscience.* Nat Rev Neurosci. https://doi.org/10.1038/35072500.

Carvalho, Marcele Regine de, Marcia Rozenthal, and Antonio Nardi. 2009. "The Fear Circuitry in Panic Disorder and Its Modulation by Cognitive-Behaviour Therapy Interventions." *World Journal of Biological Psychiatry* 11 (2 Pt 2): 1–11. https://doi.org/10.1080/15622970903178176.

Catalani, E., C. De Palma, C. Perrotta, and D. Cervia. 2017. "Current Evidence for a Role of Neuropeptides in the Regulation of Autophagy." *BioMed Research International* 2017. https://doi.org/10.1155/2017/5856071.

Caudal, Dorian, Bill P. Godsil, François Mailliet, Damien Bergerot, and Thérèse M. Jay. 2010. "Acute Stress Induces Contrasting Changes in AMPA Receptor Subunit Phosphorylation within the Prefrontal Cortex, Amygdala and Hippocampus." Edited by Ted M. Dawson. *PLoS ONE* 5 (12): e15282. https://doi.org/10.1371/journal.pone.0015282.

Chan, E. Y. 2009. "MTORC1 Phosphorylates the ULK1-MAtg13-FIP200 Autophagy Regulatory Complex." *Science Signaling* 2 (84): pe51–pe51. https://doi.org/10.1126/scisignal.284pe51.

Chen, Chyi Ying A., Nader Ezzeddine, and Ann Bin Shyu. 2008. "Chapter 17 Messenger RNA

Bibliography

Half-Life Measurements in Mammalian Cells." *Methods in Enzymology*. NIH Public Access. https://doi.org/10.1016/S0076-6879(08)02617-7.

Chen, R H, C Sarnecki, and J Blenis. 1992. "Nuclear Localization and Regulation of Erk- and Rsk-Encoded Protein Kinases." *Molecular and Cellular Biology* 12 (3): 915–27. https://doi.org/10.1128/mcb.12.3.915.

Cheng, Xiu-Tang, Bing Zhou, Mei-Yao Lin, Qian Cai, and Zu-Hang Sheng. 2015. "Axonal Autophagosomes Recruit Dynein for Retrograde Transport through Fusion with Late Endosomes." *The Journal of Cell Biology* 209 (3): 377–86. https://doi.org/10.1083/jcb.201412046.

Chiang, H L, S R Terlecky, C P Plant, and J F Dice. 1989. "A Role for a 70-Kilodalton Heat Shock Protein in Lysosomal Degradation of Intracellular Proteins." *Science (New York, N.Y.)* 246 (4928): 382–85. https://doi.org/10.1126/SCIENCE.2799391.

Chilcoat, Howard D., and Naomi Breslau. 1998. "Posttraumatic Stress Disorder and Drug Disorders: Testing Causal Pathways." *Archives of General Psychiatry* 55 (10): 913–17. https://doi.org/10.1001/archpsyc.55.10.913.

Chrousos, George P. 2009. "Stress and Disorders of the Stress System." *Nat. Rev. Endocrinol* 5 (2): 374–81. https://doi.org/10.1038/nrendo.2009.106.

Cohen-Kaplan, Victoria, Ido Livneh, Noa Avni, Bertrand Fabre, Tamar Ziv, Yong Tae Kwon, and Aaron Ciechanover. 2016. "P62- and Ubiquitin-Dependent Stress-Induced Autophagy of the Mammalian 26S Proteasome." *Proceedings of the National Academy of Sciences of the United States of America* 113 (47): E7490–99. https://doi.org/10.1073/pnas.1615455113.

Cohen, Hagit, Tianmin Liu, Nitsan Kozlovsky, Zeev Kaplan, Joseph Zohar, and Aleksander A. Mathé. 2012. "The Neuropeptide y (NPY)-Ergic System Is Associated with Behavioral Resilience to Stress Exposure in an Animal Model of Post-Traumatic Stress Disorder." *Neuropsychopharmacology* 37 (2): 350–63. https://doi.org/10.1038/npp.2011.230.

Collingridge, Graham L., Richard W. Olsen, John Peters, and Michael Spedding. 2009. "A Nomenclature for Ligand-Gated Ion Channels." *Neuropharmacology* 56 (1): 2–5. https://doi.org/10.1016/j.neuropharm.2008.06.063.

Conboy, Lisa, and Carmen Sandi. 2010. "Stress at Learning Facilitates Memory Formation by Regulating Ampa Receptor Trafficking through a Glucocorticoid Action." *Neuropsychopharmacology* 35 (3): 674–85. https://doi.org/10.1038/npp.2009.172.

Corcoran, Cheryl, Elaine Walker, Rebecca Huot, Vijay Mittal, Kevin Tessner, Lisa Kestler, and Dolores Malaspina. 2003. "The Stress Cascade and Schizophrenia: Etiology and Onset." In *Schizophrenia Bulletin*, 29:671–92. DHHS Public Health Service. https://doi.org/10.1093/oxfordjournals.schbul.a007038.

Costa-Mattioli, Mauro, Wayne S. Sossin, Eric Klann, and Nahum Sonenberg. 2009. "Translational Control of Long-Lasting Synaptic Plasticity and Memory." *Neuron*. Neuron. https://doi.org/10.1016/j.neuron.2008.10.055.

Czéh, Boldizsár, Zsófia K. Kalangyáné Varga, Kim Henningsen, Gábor L. Kovács, Attila Miseta, and Ove Wiborg. 2015. "Chronic Stress Reduces the Number of GABAergic Interneurons in the Adult Rat Hippocampus, Dorsal-Ventral and Region-Specific Differences." *Hippocampus* 25 (3): 393–405. https://doi.org/10.1002/hipo.22382.

Diamond, David M., M. Catherine Bennett, Monika Fleshner, and Gregory M. Rose. 1992. "Inverted-U Relationship between the Level of Peripheral Corticosterone and the Magnitude of Hippocampal Primed Burst Potentiation." *Hippocampus* 2 (4): 421–30. https://doi.org/10.1002/hipo.450020409.

Dikic, Ivan, and Zvulun Elazar. 2018. "Mechanism and Medical Implications of Mammalian Autophagy." *Nature Reviews Molecular Cell Biology* 19 (6): 1–16. https://doi.org/10.1038/s41580-018-0003-4.

Du, Yunrui, Scott A. Weed, Wen-Cheng Xiong, Trudy D. Marshall, and J. Thomas Parsons. 1998. "Identification of a Novel Cortactin SH3 Domain-Binding Protein and Its Localization to Growth Cones of Cultured Neurons." *Molecular and Cellular Biology* 18 (10): 5838–51. https://doi.org/10.1128/mcb.18.10.5838.

Dumont, Yvan, Danielle Jacques, Pascale Bouchard, and Rémi Quirion. 1998. "Species

Bibliography

Differences in the Expression and Distribution of the Neuropeptide Y Y1, Y2, Y4, and Y5 Receptors in Rodents, Guinea Pig, and Primates Brains." *Journal of Comparative Neurology* 402 (3): 372–84. https://doi.org/10.1002/(SICI)1096-9861(19981221)402:3<372::AID-CNE6>3.0.CO;2-2.

Eccles, J. C. 1959. "EXCITATORY AND INHIBITORY SYNAPTIC ACTION." *Annals of the New York Academy of Sciences* 81 (2): 247–64. https://doi.org/10.1111/j.1749-6632.1959.tb49312.x.

Ehlers, Michael D. 2000. "Reinsertion or Degradation of AMPA Receptors Determined by Activity-Dependent Endocytic Sorting." *Neuron* 28 (2): 511–25. https://doi.org/10.1016/S0896-6273(00)00129-X.

———. 2003. "Activity Level Controls Postsynaptic Composition and Signaling via the Ubiquitin-Proteasome System." *Nature Neuroscience* 6 (3): 231–42. https://doi.org/10.1038/nn1013.

Engert, Florian, and Toblas Bonhoeffer. 1999. "Dendritic Spine Changes Associated with Hippocampal Long-Term Synaptic Plasticity." *Nature* 399 (6731): 66–70. https://doi.org/10.1038/19978.

Etkin, Amit, and Tor D. Wager. 2007. "Functional Neuroimaging of Anxiety: A Meta-Ana Lysis of Emotional Processing in PTSD, Social Anxiety Disorder, and Specific Phobia." *American Journal of Psychiatry*. Am J Psychiatry. https://doi.org/10.1176/appi.ajp.2007.07030504.

Evans, Tracey, Robert Button, Oleg Anichtchik, and Shouqing Luo. 2018. "Visualization and Measurement of Multiple Components of the Autophagy Flux Tracey." *Methods in Molecular Biology*, no. 1341: 257–84. https://doi.org/10.1007/7651_2018_168.

Fanselow, Michael S., and Hong Wei Dong. 2010. "Are the Dorsal and Ventral Hippocampus Functionally Distinct Structures?" *Neuron*. Elsevier. https://doi.org/10.1016/j.neuron.2009.11.031.

Farré, Jean-Claude, and Suresh Subramani. 2004. "Peroxisome Turnover by Micropexophagy: An Autophagy-Related Process." *Trends in Cell Biology* 14 (9): 515–23. https://doi.org/10.1016/j.tcb.2004.07.014.

Farzi, A., F. Reichmann, and P. Holzer. 2015. "The Homeostatic Role of Neuropeptide Y in Immune Function and Its Impact on Mood and Behaviour." *Acta Physiologica* 213 (3): 603–27. https://doi.org/10.1111/apha.12445.

Ferguson, Stephen S.G., and Marc G. Caron. 1998. "G Protein-Coupled Receptor Adaptation Mechanisms." *Seminars in Cell and Developmental Biology* 9 (2): 119–27. https://doi.org/10.1006/scdb.1997.0216.

Fernandes, Ana Clara, Valerie Uytterhoeven, Sabine Kuenen, Yu Chun Wang, Jan R. Slabbaert, Jef Swerts, Jaroslaw Kasprowicz, Stein Aerts, and Patrik Verstreken. 2014. "Reduced Synaptic Vesicle Protein Degradation at Lysosomes Curbs TBC1D24/Sky-Induced Neurodegeneration." *Journal of Cell Biology* 207 (4): 453–62. https://doi.org/10.1083/jcb.201406026.

Ferrario, Carrie R., Xuan Li, and Marina E. Wolf. 2011. "Effects of Acute Cocaine or Dopamine Receptor Agonists on AMPA Receptor Distribution in the Rat Nucleus Accumbens." *Synapse* 65 (1): 54–63. https://doi.org/10.1002/syn.20823.

Ferreira-Marques, Marisa, Célia A Aveleira, Sara Carmo-Silva, Mariana Botelho, Luís Pereira de Almeida, and Cláudia Cavadas. 2016. "Caloric Restriction Stimulates Autophagy in Rat Cortical Neurons through Neuropeptide Y and Ghrelin Receptors Activation." *Aging* 8 (7): 1470–84. https://doi.org/10.18632/aging.100996.

Flood, J F, M L Baker, E N Hernandez, and J E Morley. 1989. "Modulation of Memory Processing by Neuropeptide Y Varies with Brain Injection Site." *Brain Research* 503 (1): 73–82. http://www.ncbi.nlm.nih.gov/pubmed/2611661.

Foster, Michael, and Sir Charles Scott Sherrington. 1897. "A Textbook of Physiology. With C.S. Sherrington. Part 3. The Central Nervous System. (EBook, 1897) [WorldCat.Org]." 1897. https://www.worldcat.org/title/textbook-of-physiology-with-cs-sherrington-part-3-the-central-nervous-system/oclc/1045302366.

Francati, V., E. Vermetten, and J. D. Bremner. 2007. "Functional Neuroimaging Studies in

Posttraumatic Stress Disorder: Review of Current Methods and Findings." *Depression and Anxiety*. NIH Public Access. https://doi.org/10.1002/da.20208.

Fu, Jingxuan, Hui Wang, Jing Gao, Mei Yu, Rubin Wang, Zhuo Yang, and Tao Zhang. 2017. "Rapamycin Effectively Impedes Melamine-Induced Impairments of Cognition and Synaptic Plasticity in Wistar Rats." *Molecular Neurobiology* 54 (2): 819–32. https://doi.org/10.1007/s12035-016-9687-7.

Fu, Meng-Meng, Jeffrey J Nirschl, and Erika L F Holzbaur. 2014. "LC3 Binding to the Scaffolding Protein JIP1 Regulates Processive Dynein-Driven Transport of Autophagosomes." *Developmental Cell* 29 (5): 577–90. https://doi.org/10.1016/j.devcel.2014.04.015.

Furuya, Norihiko, Jie Yu, Maya Byfield, Sophie Pattingre, and Beth Levine. 2005. "The Evolutionarily Conserved Domain of Beclin 1 Is Required for Vps34 Binding, Autophagy, and Tumor Suppressor Function." *Autophagy* 1 (1): 46–52. https://doi.org/10.4161/auto.1.1.1542.

Galluzzi, Lorenzo, Eric H Baehrecke, Andrea Ballabio, Patricia Boya, José Manuel Bravo-San Pedro, Francesco Cecconi, Augustine M Choi, et al. 2017. "Molecular Definitions of Autophagy and Related Processes." *The EMBO Journal* 36 (13): 1811–36. https://doi.org/10.15252/embj.201796697.

Galluzzi, Lorenzo, José Manuel Bravo-San Pedro, Beth Levine, Douglas R. Green, and Guido Kroemer. 2017. "Pharmacological Modulation of Autophagy: Therapeutic Potential and Persisting Obstacles." *Nature Reviews Drug Discovery* 16 (7): 487–511. https://doi.org/10.1038/nrd.2017.22.

Gassen, Nils C., Jakob Hartmann, Mathias V. Schmidt, and Theo Rein. 2015. "FKBP5/FKBP51 Enhances Autophagy to Synergize with Antidepressant Action." *Autophagy* 11 (3): 578–80. https://doi.org/10.1080/15548627.2015.1017224.

Gassen, Nils C., and Theo Rein. 2019. "Is There a Role of Autophagy in Depression and Antidepressant Action?" *Frontiers in Psychiatry* 10 (May): 337. https://doi.org/10.3389/fpsyt.2019.00337.

Ghavami, Saeid, Shahla Shojaei, Behzad Yeganeh, Sudharsana R. Ande, Jaganmohan R. Jangamreddy, Maryam Mehrpour, Jonas Christoffersson, et al. 2014. "Autophagy and Apoptosis Dysfunction in Neurodegenerative Disorders." *Progress in Neurobiology* 112 (January): 24–49. https://doi.org/10.1016/j.pneurobio.2013.10.004.

Giesbrecht, Chantelle J., James P. Mackay, Heika B. Silveira, Janice H. Urban, and William F. Colmers. 2010. "Countervailing Modulation of Ihby Neuropeptide Y and Corticotrophin-Releasing Factor in Basolateral Amygdala as a Possible Mechanism for Their Effects on Stress-Related Behaviors." *Journal of Neuroscience* 30 (50): 16970–82. https://doi.org/10.1523/JNEUROSCI.2306-10.2010.

Gilbertson, Mark W., Martha E. Shenton, Aleksandra Ciszewski, Kiyoto Kasai, Natasha B. Lasko, Scott P. Orr, and Roger K. Pitman. 2002. "Smaller Hippocampal Volume Predicts Pathologic Vulnerability to Psychological Trauma." *Nature Neuroscience* 5 (11): 1242–47. https://doi.org/10.1038/nn958.

Glatigny, Mélissa, Stéphanie Moriceau, Manon Rivagorda, Mariana Ramos-Brossier, Anna C. Nascimbeni, Fabien Lante, Mary R. Shanley, et al. 2019a. "Autophagy Is Required for Memory Formation and Reverses Age-Related Memory Decline." *Current Biology* 29 (3): 435-448.e8. https://doi.org/10.1016/j.cub.2018.12.021.

———. 2019b. "Autophagy Is Required for Memory Formation and Reverses Age-Related Memory Decline." *Current Biology* 29 (3): 435-448.e8. https://doi.org/10.1016/j.cub.2018.12.021.

Gonçalves, Joana, Carlos F. Ribeiro, João O. Malva, and Ana P. Silva. 2012. "Protective Role of NeuropeptideY Y 2 Receptors in Cell Death and Microglial Response Following Methamphetamine Injury." *European Journal of Neuroscience* 36 (9): 3173–83. https://doi.org/10.1111/j.1460-9568.2012.08232.x.

Goo, Marisa S., Laura Sancho, Natalia Slepak, Daniela Boassa, Thomas J. Deerinck, Mark H. Ellisman, Brenda L. Bloodgood, and Gentry N. Patrick. 2017. "Activity-Dependent Trafficking of Lysosomes in Dendrites and Dendritic Spines." *Journal of Cell Biology* 216

Bibliography

(8): 2499–2513. https://doi.org/10.1083/jcb.201704068.

Grabrucker, Andreas M., Michael J. Schmeisser, Michael Schoen, and Tobias M. Boeckers. 2011. "Postsynaptic ProSAP/Shank Scaffolds in the Cross-Hair of Synaptopathies." *Trends in Cell Biology*. Trends Cell Biol. https://doi.org/10.1016/j.tcb.2011.07.003.

Gray, E. G. 1959. "Electron Microscopy of Synaptic Contacts on Dendrite Spines of the Cerebral Cortex." *Nature* 183 (4675): 1592–93. https://doi.org/10.1038/1831592a0.

Grillon, Christian. 2002. "Startle Reactivity and Anxiety Disorders: Aversive Conditioning, Context, and Neurobiology." *Biological Psychiatry*. Biol Psychiatry. https://doi.org/10.1016/S0006-3223(02)01665-7.

Grillon, Christian, Charles A. Morgan, Michael Davis, and Steven M. Southwick. 1998. "Effects of Experimental Context and Explicit Threat Cues on Acoustic Startle in Vietnam Veterans with Posttraumatic Stress Disorder." *Biological Psychiatry* 44 (10): 1027–36. https://doi.org/10.1016/S0006-3223(98)00034-1.

Groc, Laurent, Daniel Choquet, and Francis Chaouloff. 2008. "The Stress Hormone Corticosterone Conditions AMPAR Surface Trafficking and Synaptic Potentiation." *Nature Neuroscience* 11 (8): 868–70. https://doi.org/10.1038/nn.2150.

Groll, Michael, and Robert Huber. 2004. "Inhibitors of the Eukaryotic 20S Proteasome Core Particle: A Structural Approach." *Biochimica et Biophysica Acta - Molecular Cell Research*. Biochim Biophys Acta. https://doi.org/10.1016/j.bbamcr.2004.09.025.

Gulbins, Anne, Fabian Schumacher, Katrin Anne Becker, Barbara Wilker, Matthias Soddemann, Francesco Boldrin, Christian P. Müller, et al. 2018. "Antidepressants Act by Inducing Autophagy Controlled by Sphingomyelin–Ceramide." *Molecular Psychiatry* 23 (12): 2324–46. https://doi.org/10.1038/s41380-018-0090-9.

Guo, Weixiang, Eric D Polich, Juan Su, Feifei Wang, Guangfu Wang, and Xinyu Zhao Correspondence. 2015. "Fragile X Proteins FMRP and FXR2P Control Synaptic GluA1 Expression and Neuronal Maturation via Distinct Mechanisms." *Cell Reports* 11: 1651–66. https://doi.org/10.1016/j.celrep.2015.05.013.

Haar, Emilie Vander, Seong il Lee, Sricharan Bandhakavi, Timothy J. Griffin, and Do Hyung Kim. 2007. "Insulin Signalling to MTOR Mediated by the Akt/PKB Substrate PRAS40." *Nature Cell Biology* 9 (3): 316–23. https://doi.org/10.1038/ncb1547.

Hadad-Ophir, Osnat, Anne Albrecht, Oliver Stork, and Gal Richter-Levin. 2014. "Amygdala Activation and GABAergic Gene Expression in Hippocampal Sub-Regions at the Interplay of Stress and Spatial Learning." *Frontiers in Behavioral Neuroscience* 8 (JAN). https://doi.org/10.3389/fnbeh.2014.00003.

Hafner, Anne Sophie, Paul G. Donlin-Asp, Beulah Leitch, Etienne Herzog, and Erin M. Schuman. 2019. "Local Protein Synthesis Is a Ubiquitous Feature of Neuronal Pre- And Postsynaptic Compartments." *Science* 364 (6441). https://doi.org/10.1126/science.aau3644.

Hanslick, JL, K Lau, KK Noguchi, … JW Olney - Neurobiology of, and Undefined 2009. 2009. "Dimethyl Sulfoxide (DMSO) Produces Widespread Apoptosis in the Developing Central Nervous System." *Elsevier*. https://www.sciencedirect.com/science/article/pii/S0969996108002830.

Hara, Taichi, Kenji Nakamura, Makoto Matsui, Akitsugu Yamamoto, Yohko Nakahara, Rika Suzuki-Migishima, Minesuke Yokoyama, et al. 2006. "Suppression of Basal Autophagy in Neural Cells Causes Neurodegenerative Disease in Mice." *Nature* 441 (7095): 885–89. https://doi.org/10.1038/nature04724.

Harding, T. M. 1995. "Isolation and Characterization of Yeast Mutants in the Cytoplasm to Vacuole Protein Targeting Pathway." *The Journal of Cell Biology* 131 (3): 591–602. https://doi.org/10.1083/jcb.131.3.591.

Hawley, Darby F., Kristin Morch, Brian R. Christie, and J. Leigh Leasure. 2012. "Differential Response of Hippocampal Subregions to Stress and Learning." *PLoS ONE* 7 (12). https://doi.org/10.1371/journal.pone.0053126.

Hayashi, Takashi, and Richard L. Huganir. 2004. "Tyrosine Phosphorylation and Regulation of the AMPA Receptor by Src Family Tyrosine Kinases." *Journal of Neuroscience* 24 (27): 6152–60. https://doi.org/10.1523/JNEUROSCI.0799-04.2004.

Bibliography

He, Congcong, and Daniel J Klionsky. 2009. "Regulation Mechanisms and Signaling Pathways of Autophagy." *Annual Review of Genetics* 43: 67–93. https://doi.org/10.1146/annurev-genet-102808-114910.

Heilig, M, B Söderpalm, J A Engel, and E Widerlöv. 1989. "Centrally Administered Neuropeptide Y (NPY) Produces Anxiolytic-like Effects in Animal Anxiety Models." *Psychopharmacology* 98 (4): 524–29. http://www.ncbi.nlm.nih.gov/pubmed/2570434.

Helenius, A, I Mellman, D Wall, A Hubbard - Trends in Biochemical Sciences, and undefined 1983. 1983. "Endosomes." *Elsevier*. https://www.sciencedirect.com/science/article/pii/096800048390350X.

Hernandez, Daniela, Ciara A. Torres, Wanda Setlik, Carolina Cebrián, Eugene V. Mosharov, Guomei Tang, Hsiao Chun Cheng, et al. 2012. "Regulation of Presynaptic Neurotransmission by Macroautophagy." *Neuron* 74 (2): 277–84. https://doi.org/10.1016/j.neuron.2012.02.020.

Hirling, H. 2009. "Endosomal Trafficking of AMPA-Type Glutamate Receptors." *Neuroscience*. Pergamon. https://doi.org/10.1016/j.neuroscience.2008.02.057.

Hollenbeck, P J. 1993. "Products of Endocytosis and Autophagy Are Retrieved from Axons by Regulated Retrograde Organelle Transport." *The Journal of Cell Biology* 121 (2): 305–15. http://www.ncbi.nlm.nih.gov/pubmed/7682217.

Holliday, N. D., M. C. Michel, and H. M. Cox. 2011. "NPY Receptor Subtypes and Their Signal Transduction," 45–73. https://doi.org/10.1007/978-3-642-18764-3_3.

Hollmann, Michael, and Stephen Heinemann. 1994. "Cloned Glutamate Receptors." *Annual Review of Neuroscience*. Annual Reviews Inc. https://doi.org/10.1146/annurev.ne.17.030194.000335.

Holzer, Peter, Florian Reichmann, and Aitak Farzi. 2012. "Neuropeptide Y, Peptide YY and Pancreatic Polypeptide in the Gut-Brain Axis." *Neuropeptides* 46 (6): 261–74. https://doi.org/10.1016/j.npep.2012.08.005.

Huganir, Richard L., and Roger A. Nicoll. 2013. "AMPARs and Synaptic Plasticity: The Last 25 Years." *Neuron*. Neuron. https://doi.org/10.1016/j.neuron.2013.10.025.

Hwang, Jong Ik, Soo Kim Hyeon, Ran Lee Jae, Eunjoon Kim, Ho Ryu Sung, and Pann Ghill Suh. 2005. "The Interaction of Phospholipase C-B3 with Shank2 Regulates MGluR-Mediated Calcium Signal." *Journal of Biological Chemistry* 280 (13): 12467–73. https://doi.org/10.1074/jbc.M410740200.

Kang, Min Hee, Joydeep Das, Sangiliyandi Gurunathan, Hwan Woo Park, Hyuk Song, Chankyu Park, and Jin Hoi Kim. 2017. "The Cytotoxic Effects of Dimethyl Sulfoxide in Mouse Preimplantation Embryos: A Mechanistic Study." *Theranostics* 7 (19): 4735–52. https://doi.org/10.7150/thno.21662.

Kar, Nilamadhab. 2011. "Cognitive Behavioral Therapy for the Treatment of Post-Traumatic Stress Disorder: A Review." *Neuropsychiatric Disease and Treatment*. Neuropsychiatr Dis Treat. https://doi.org/10.2147/NDT.S10389.

Kara, N. Z., L. Toker, G. Agam, G. W. Anderson, R. H. Belmaker, and H. Einat. 2013. "Trehalose Induced Antidepressant-like Effects and Autophagy Enhancement in Mice." *Psychopharmacology* 229 (2): 367–75. https://doi.org/10.1007/s00213-013-3119-4.

Kask, Ants, Jaanus Harro, Stephan von Hörsten, John P. Redrobe, Yvan Dumont, and Rémi Quirion. 2002. "The Neurocircuitry and Receptor Subtypes Mediating Anxiolytic-like Effects of Neuropeptide Y." *Neuroscience & Biobehavioral Reviews* 26 (3): 259–83. https://doi.org/10.1016/S0149-7634(01)00066-5.

Kaur, Jasvinder, and Jayanta Debnath. 2015. "Autophagy at the Crossroads of Catabolism and Anabolism." *Nature Reviews Molecular Cell Biology* 16 (8): 461–72. https://doi.org/10.1038/nrm4024.

Kelleher, Raymond J., Arvind Govindarajan, and Susumu Tonegawa. 2004. "Translational Regulatory Mechanisms in Persistent Forms of Synaptic Plasticity." *Neuron*. Neuron. https://doi.org/10.1016/j.neuron.2004.09.013.

Kennedy, M. B. 2000. "Signal-Processing Machines at the Postsynaptic Density." *Science*. Science. https://doi.org/10.1126/science.290.5492.750.

Kessels, Helmut W., and Roberto Malinow. 2009. "Synaptic AMPA Receptor Plasticity and

Bibliography

Behavior." *Neuron*. Cell Press. https://doi.org/10.1016/j.neuron.2009.01.015.

Kessler, Ronald C., Amanda Sonnega, Evelyn Bromet, Michael Hughes, and Christopher B. Nelson. 1995. "Posttraumatic Stress Disorder in the National Comorbidity Survey." *Archives of General Psychiatry* 52 (12): 1048–60. https://doi.org/10.1001/archpsyc.1995.03950240066012.

Kessler, Ronald C., Tat Chiu Wai, Olga Demler, and Ellen E. Walters. 2005. "Prevalence, Severity, and Comorbidity of 12-Month DSM-IV Disorders in the National Comorbidity Survey Replication." *Archives of General Psychiatry*. NIH Public Access. https://doi.org/10.1001/archpsyc.62.6.617.

Kim, Joungmok, Young Chul Kim, Chong Fang, Ryan C. Russell, Jeong Hee Kim, Weiliang Fan, Rong Liu, Qing Zhong, and Kun-Liang Guan. 2013. "Differential Regulation of Distinct Vps34 Complexes by AMPK in Nutrient Stress and Autophagy." *Cell* 152 (1–2): 290–303. https://doi.org/10.1016/J.CELL.2012.12.016.

Kimura, Shunsuke, Takeshi Noda, and Tamotsu Yoshimori. 2008. "Dynein-Dependent Movement of Autophagosomes Mediates Efficient Encounters with Lysosomes." *Cell Structure and Function* 33 (1): 109–22. https://doi.org/10.1247/csf.08005.

Kishi, Toshiro, Carl J. Aschkenasi, Brian J. Choi, Marisol E. Lopez, Charlotte E. Lee, Hongyan Liu, Anthony N. Hollenberg, Jeffrey M. Friedman, and Joel K. Elmquist. 2005. "Neuropeptide Y Y1 Receptor MRNA in Rodent Brain: Distribution and Colocalization with Melanocortin-4 Receptor." *Journal of Comparative Neurology* 482 (3): 217–43. https://doi.org/10.1002/cne.20432.

Klionsky, D, Lotta Agholme, Maria Agnello, Patrizia Agostinis, Julio A Aguirre-ghiso, Hyung Jun Ahn, Ouardia Ait-mohamed, et al. 2016. "Guidelines for the Use and Interpretation of Assays for Monitoring Autophagy." *Autophagy* 8 (April): 445–544. https://doi.org/10.4161/auto.19496.

Klionsky, Daniel J. 2007. "Autophagy: From Phenomenology to Molecular Understanding in Less than a Decade." *Nature Reviews Molecular Cell Biology* 8 (11): 931–37. https://doi.org/10.1038/nrm2245.

Klionsky, Daniel J, Eric H Baehrecke, John H Brumell, Charleen T Chu, Patrice Codogno, Ana Marie Cuervo, Jayanta Debnath, et al. 2011. "A Comprehensive Glossary of Autophagy-Related Molecules and Processes (2nd Edition)." *Autophagy* 7 (11): 1273–94. https://doi.org/10.4161/auto.7.11.17661.

Kobayashi, Toshihide, Espen Stang, Karen S. Fang, Philippe De Moerloose, Robert G. Parton, and Jean Gruenberg. 1998. "A Lipid Associated with the Antiphospholipid Syndrome Regulates Endosome Structure and Function." *Nature* 392 (6672): 193–97. https://doi.org/10.1038/32440.

Komatsu, Masaaki, Satoshi Waguri, Tomoki Chiba, Shigeo Murata, Jun Ichi Iwata, Isei Tanida, Takashi Ueno, et al. 2006. "Loss of Autophagy in the Central Nervous System Causes Neurodegeneration in Mice." *Nature* 441 (7095): 880–84. https://doi.org/10.1038/nature04723.

Kornhuber, Johannes, and Iulia Zoicas. 2019. "Neuropeptide Y Reduces Expression of Social Fear via Simultaneous Activation of Y1 and Y2 Receptors." *Journal of Psychopharmacology* 33 (12): 1533–39. https://doi.org/10.1177/0269881119862529.

Kozarić-Kovačić, Dragica. 2008. "Psychopharmacotherapy of Posttraumatic Stress Disorder." *Croatian Medical Journal*. Croat Med J. https://doi.org/10.3325/cmj.2008.4.459.

Kraft, Claudine, and Sascha Martens. 2012. "Mechanisms and Regulation of Autophagosome Formation." *Current Opinion in Cell Biology* 24 (4): 496–501. https://doi.org/10.1016/J.CEB.2012.05.001.

Kropf, Michel, Guillaume Rey, Liliane Glauser, Karina Kulangara, Kai Johnsson, and Harald Hirling. 2008. "Subunit-Specific Surface Mobility of Differentially Labeled AMPA Receptor Subunits." *European Journal of Cell Biology* 87 (10): 763–78. https://doi.org/10.1016/j.ejcb.2008.02.014.

Kulkarni, Aditi, Jessica Chen, Sandra Maday, Juan Burrone, and Erika Holzbaur. 2018. "Neuronal Autophagy and Intercellular Regulation of Homeostasis in the Brain." *Current Opinion in Neurobiology* 51: 29–36. https://doi.org/10.1016/j.conb.2018.02.008.

Bibliography

Kumari, V., H. Kaviani, P. W. Raven, J. A. Gray, and S. A. Checkley. 2001. "Enhanced Startle Reactions to Acoustic Stimuli in Patients with Obsessive-Compulsive Disorder." *American Journal of Psychiatry* 158 (1): 134–36. https://doi.org/10.1176/appi.ajp.158.1.134.

Lamb, Christopher A., Tamotsu Yoshimori, and Sharon A. Tooze. 2013. "The Autophagosome: Origins Unknown, Biogenesis Complex." *Nature Reviews Molecular Cell Biology* 14 (12): 759–74. https://doi.org/10.1038/nrm3696.

Laplante, M., and D. M. Sabatini. 2013. "Regulation of MTORC1 and Its Impact on Gene Expression at a Glance." *Journal of Cell Science* 126 (8): 1713–19. https://doi.org/10.1242/jcs.125773.

Larsen, Philip J., Søren P. Sheikh, Cherine R. Jakobsen, Thue W. Schwartz, and Jens D. Mikkelsen. 1993. "Regional Distribution of Putative NPY Y1 Receptors and Neurons Expressing Y1 MRNA in Forebrain Areas of the Rat Central Nervous System." *European Journal of Neuroscience* 5 (12): 1622–37. https://doi.org/10.1111/j.1460-9568.1993.tb00231.x.

Laxmi, T. Rao, Oliver Stork, and Hans Christian Pape. 2003. "Generalisation of Conditioned Fear and Its Behavioural Expression in Mice." *Behavioural Brain Research* 145 (1–2): 89–98. https://doi.org/10.1016/S0166-4328(03)00101-3.

Lee, Inah, and Raymond P. Kesner. 2004. "Different Contributions of Dorsal Hippocampal Subregios to Emory Acquisation and Retrieval in Contextual Fear-Conditioning." *Hippocampus* 14 (3): 301–10. https://doi.org/10.1002/hipo.10177.

Levine, Beth, and Guido Kroemer. 2008. "Autophagy in the Pathogenesis of Disease." *Cell*. Elsevier. https://doi.org/10.1016/j.cell.2007.12.018.

Li, Nanxin, Boyoung Lee, Rong Jian Liu, Mounira Banasr, Jason M. Dwyer, Masaaki Iwata, Xiao Yuan Li, George Aghajanian, and Ronald S. Duman. 2010. "MTOR-Dependent Synapse Formation Underlies the Rapid Antidepressant Effects of NMDA Antagonists." *Science* 329 (5994): 959–64. https://doi.org/10.1126/science.1190287.

Liang, Xiao Huan, Saadiya Jackson, Matthew Seaman, Kristy Brown, Bettina Kempkes, Hanina Hibshoosh, and Beth Levine. 1999. "Induction of Autophagy and Inhibition of Tumorigenesis by Beclin 1." *Nature* 402 (6762): 672–76. https://doi.org/10.1038/45257.

Lippai, Mónika, and Zsuzsanna Szatmári. 2017. "Autophagy—from Molecular Mechanisms to Clinical Relevance." *Cell Biology and Toxicology* 33 (2): 145–68. https://doi.org/10.1007/s10565-016-9374-5.

Liu, An, Hong Ji, Qiaoyun Ren, Yanghong Meng, Haiwang Zhang, Graham Collingride, Wei Xie, and Zhengping Jia. 2020. "The Requirement of the C-Terminal Domain of GluA1 in Different Forms of Long-Term Potentiation in the Hippocampus Is Age-Dependent." *Frontiers in Synaptic Neuroscience* 12 (October): 50. https://doi.org/10.3389/fnsyn.2020.588785.

Livak, Kenneth J, and Thomas D Schmittgen. 2001. "Analysis of Relative Gene Expression Data Using Real-Time Quantitative PCR and the 2 C T Method." *METHODS* 25: 402–8. https://doi.org/10.1006/meth.2001.1262.

Lois, Carlos, Elizabeth J. Hong, Shirley Pease, Eric J. Brown, and David Baltimore. 2002. "Germline Transmission and Tissue-Specific Expression of Transgenes Delivered by Lentiviral Vectors." *Science* 295 (5556): 868–72. https://doi.org/10.1126/science.1067081.

Lu, Jiuyi, Thomas D. Helton, Thomas A. Blanpied, Bence Rácz, Thomas M. Newpher, Richard J. Weinberg, and Michael D. Ehlers. 2007. "Postsynaptic Positioning of Endocytic Zones and AMPA Receptor Cycling by Physical Coupling of Dynamin-3 to Homer." *Neuron* 55 (6): 874–89. https://doi.org/10.1016/j.neuron.2007.06.041.

Maday, Sandra, and Erika L F Holzbaur. 2014. "Autophagosome Biogenesis in Primary Neurons Follows an Ordered and Spatially Regulated Pathway." *Developmental Cell* 30 (1): 71–85. https://doi.org/10.1016/j.devcel.2014.06.001.

———. 2016. "Compartment-Specific Regulation of Autophagy in Primary Neurons." *The Journal of Neuroscience : The Official Journal of the Society for Neuroscience* 36 (22): 5933–45. https://doi.org/10.1523/JNEUROSCI.4401-15.2016.

Bibliography

Maday, Sandra, Karen E Wallace, and Erika L F Holzbaur. 2012. "Autophagosomes Initiate Distally and Mature during Transport toward the Cell Soma in Primary Neurons." *The Journal of Cell Biology* 196 (4): 407–17. https://doi.org/10.1083/jcb.201106120.

Maggio, Nicola, and Menahem Segal. 2007. "Striking Variations in Corticosteroid Modulation of Long-Term Potentiation along the Septotemporal Axis of the Hippocampus." *Journal of Neuroscience* 27 (21): 5757–65. https://doi.org/10.1523/JNEUROSCI.0155-07.2007.

Maglione, Marta, Gaga Kochlamazashvili, Tobias Eisenberg, Bence Rácz, Eva Michael, David Toppe, Alexander Stumpf, et al. 2019. "Spermidine Protects from Age-Related Synaptic Alterations at Hippocampal Mossy Fiber-CA3 Synapses." *Scientific Reports* 9 (1). https://doi.org/10.1038/s41598-019-56133-3.

Makino, Hiroshi, and Roberto Malinow. 2009. "AMPA Receptor Incorporation into Synapses during LTP: The Role of Lateral Movement and Exocytosis." *Neuron* 64 (3): 381–90. https://doi.org/10.1016/j.neuron.2009.08.035.

Malinow, Roberto, and Robert C. Malenka. 2002. "AMPA Receptor Trafficking and Synaptic Plasticity." *Annual Review of Neuroscience*. Annu Rev Neurosci. https://doi.org/10.1146/annurev.neuro.25.112701.142758.

Malva, J O, S Xapelli, S Baptista, J Valero, F Agasse, R Ferreira, and A P Silva. 2012. "Multifaces of Neuropeptide Y in the Brain--Neuroprotection, Neurogenesis and Neuroinflammation." *Neuropeptides* 46 (6): 299–308. https://doi.org/10.1016/j.npep.2012.09.001.

Maren, S. 2001. "Nuerobiology of Pavlovian Fear Conditioning." *Annual Review of Neuroscience*. Annu Rev Neurosci. https://doi.org/10.1146/annurev.neuro.24.1.897.

Marle, Hein J.F. van, Erno J. Hermans, Shaozheng Qin, and Guillén Fernández. 2009. "From Specificity to Sensitivity: How Acute Stress Affects Amygdala Processing of Biologically Salient Stimuli." *Biological Psychiatry* 66 (7): 649–55. https://doi.org/10.1016/j.biopsych.2009.05.014.

Martin, Stéphane, Jeremy M. Henley, David Holman, Ming Zhou, Olof Wiegert, Myrrhe van Spronsena, Marian Joëls, Casper C. Hoogenraad, and Harmen J. Krugers. 2009. "Corticosterone Alters AMPAR Mobility and Facilitates Bidirectional Synaptic Plasticity." *PLoS ONE* 4 (3). https://doi.org/10.1371/journal.pone.0004714.

Matsuo, Naoki, Leon Reijmers, and Mark Mayford. 2008. "Spine-Type-Specific Recruitment of Newly Synthesized AMPA Receptors with Learning." *Science* 319 (5866): 1104–7. https://doi.org/10.1126/science.1149967.

Matsuzaki, Masanori, Graham C.R. Ellis-Davies, Tomomi Nemoto, Yasushi Miyashita, Masamitsu Iino, and Haruo Kasai. 2001. "Dendritic Spine Geometry Is Critical for AMPA Receptor Expression in Hippocampal CA1 Pyramidal Neurons." *Nature Neuroscience* 4 (11): 1086–92. https://doi.org/10.1038/nn736.

Mauthe, Mario, Idil Orhon, Cecilia Rocchi, Xingdong Zhou, Morten Luhr, Kerst Jan Hijlkema, Robert P. Coppes, Nikolai Engedal, Muriel Mari, and Fulvio Reggiori. 2018. "Chloroquine Inhibits Autophagic Flux by Decreasing Autophagosome-Lysosome Fusion." *Autophagy* 14 (8): 1435–55. https://doi.org/10.1080/15548627.2018.1474314.

Maxfield, Frederick R., and Timothy E. McGraw. 2004. "Endocytic Recycling." *Nature Reviews Molecular Cell Biology*. Nat Rev Mol Cell Biol. https://doi.org/10.1038/nrm1315.

Mayer, Mark L., and Neali Armstrong. 2004. "Structure and Function of Glutamate Receptor Ion Channels." *Annual Review of Physiology*. Annu Rev Physiol. https://doi.org/10.1146/annurev.physiol.66.050802.084104.

Mayer, Mark L., Gary L. Westbrook, and Peter B. Guthrie. 1984. "Voltage-Dependent Block by Mg2+ of NMDA Responses in Spinal Cord Neurones." *Nature* 309 (5965): 261–63. https://doi.org/10.1038/309261a0.

McEwen, B. S., E. A. Gould, and R. R. Sakai. 1992. "The Vulnerability of the Hippocampus to Protective and Destructive Effects of Glucocorticoids in Relation to Stress." In *British Journal of Psychiatry*, 160:18–24. Cambridge University Press. https://doi.org/10.1192/s0007125000296645.

McHugh, Thomas J., Matthew W. Jones, Jennifer J. Quinn, Nina Balthasar, Roberto Coppari, Joel K. Elmquist, Bradford B. Lowell, Michael S. Fanselow, Matthew A. Wilson, and

Bibliography

Susumu Tonegawa. 2007. "Dentate Gyrus NMDA Receptors Mediate Rapid Pattern Separation in the Hippocampal Network." *Science* 317 (5834): 94–99. https://doi.org/10.1126/science.1140263.

Mello, Patricia, Gustavo Silva, Julia Donat, and Christian Kristensen. 2013. "An Update on the Efficacy of Cognitive-Behavioral Therapy, Cognitive Therapy, and Exposure Therapy for Posttraumatic Stress Disorder." *International Journal of Psychiatry in Medicine* 46 (4): 339–57. https://doi.org/10.2190/PM.46.4.b.

Menzies, Fiona M., Angeleen Fleming, Andrea Caricasole, Carla F. Bento, Stephen P. Andrews, Avraham Ashkenazi, Jens Füllgrabe, et al. 2017. "Autophagy and Neurodegeneration: Pathogenic Mechanisms and Therapeutic Opportunities." *Neuron* 93 (5): 1015–34. https://doi.org/10.1016/j.neuron.2017.01.022.

Mercer, Carol A., Alagammai Kaliappan, and Patrick B. Dennis. 2009. "A Novel, Human Atg13 Binding Protein, Atg101, Interacts with ULK1 and Is Essential for Macroautophagy." *Autophagy* 5 (5): 649–62. https://doi.org/10.4161/auto.5.5.8249.

Miao, Xue Rong, Qian Bo Chen, Kai Wei, Kun Ming Tao, and Zhi Jie Lu. 2018. "Posttraumatic Stress Disorder: From Diagnosis to Prevention 11 Medical and Health Sciences 1117 Public Health and Health Services 11 Medical and Health Sciences 1103 Clinical Sciences Alexander V. Libin." *Military Medical Research*. BioMed Central Ltd. https://doi.org/10.1186/s40779-018-0179-0.

Middei, Silvia, Alida Spalloni, Patrizia Longone, Christopher Pittenger, Shane M. O'Mara, Hélène Marie, and Martine Ammassari-Teule. 2012. "CREB Selectively Controls Learning-Induced Structural Remodeling of Neurons." *Learning and Memory* 19 (8): 330–36. https://doi.org/10.1101/lm.025817.112.

Mijaljica, Dalibor, Mark Prescott, and Rodney J Devenish. 2012. "The Intriguing Life of Autophagosomes." *International Journal of Molecular Sciences* 13 (3): 3618–35. https://doi.org/10.3390/ijms13033618.

Miracco, Clelia, Elena Cosci, Giuseppe Oliveri, Pietro Luzi, Lorenzo Pacenti, Irene Monciatti, Susanna Mannucci, et al. 2007. "Protein and MRNA Expression of Autophagy Gene Beclin 1 in Human Brain Tumours." *International Journal of Oncology* 30 (2): 429–36. https://doi.org/10.3892/ijo.30.2.429.

Mizushima, Noboru. 2007. "Autophagy: Process and Function." *Genes and Development*. https://doi.org/10.1101/gad.1599207.

Mizushima, Noboru, and Masaaki Komatsu. 2011. "Autophagy: Renovation of Cells and Tissues." *Cell* 147 (4): 728–41. https://doi.org/10.1016/J.CELL.2011.10.026.

Mizushima, Noboru, Akitsugu Yamamoto, Makoto Matsui, Tamotsu Yoshimori, and Yoshinori Ohsumi. 2004. "In Vivo Analysis of Autophagy in Response to Nutrient Starvation Using Transgenic Mice Expressing a Fluorescent Autophagosome Marker." *Molecular Biology of the Cell* 15 (3): 1101–11. https://doi.org/10.1091/mbc.E03-09-0704.

Mizushima, Noboru, Tamotsu Yoshimori, and Yoshinori Ohsumi. 2011. "The Role of Atg Proteins in Autophagosome Formation." *Annual Review of Cell and Developmental Biology* 27 (1): 107–32. https://doi.org/10.1146/annurev-cellbio-092910-154005.

Mizushima, Noboru, Tamotsu Yoshimorim, and Beth Levine. 2010. "Methods in Mammalian Autophagy Research." *Cell*. https://doi.org/10.1016/j.cell.2010.01.028.

Mockett, Bruce G, Diane Guévremont, Megan K Elder, Karen D Parfitt, Katie Peppercorn, Jodi Morrissey, Anurag Singh, et al. 2019. "Cellular/Molecular Glutamate Receptor Trafficking and Protein Synthesis Mediate the Facilitation of LTP by Secreted Amyloid Precursor Protein-Alpha." https://doi.org/10.1523/JNEUROSCI.1826-18.2019.

Molosh, Andrei I, Tammy J Sajdyk, William A Truitt, Weiguo Zhu, Gerry S Oxford, and Anantha Shekhar. 2013. "NPY Y1 Receptors Differentially Modulate GABAA and NMDA Receptors via Divergent Signal-Transduction Pathways to Reduce Excitability of Amygdala Neurons." *Neuropsychopharmacology* 38 (7): 1352–64. https://doi.org/10.1038/npp.2013.33.

Morgan, C. A., Christian Grillon, Steven M. Southwick, Michael Davis, and Dennis S. Charney. 1995. "Fear-Potentiated Startle in Posttraumatic Stress Disorder." *Biological Psychiatry* 38 (6): 378–85. https://doi.org/10.1016/0006-3223(94)00321-S.

Bibliography

Morgan, Charles A., Sheila Wang, Steven M. Southwick, Ann Rasmusson, Gary Hazlett, Richard L. Hauger, and Dennis S. Charney. 2000. "Plasma Neuropeptide-Y Concentrations in Humans Exposed to Military Survival Training." *Biological Psychiatry* 47 (10): 902–9. https://doi.org/10.1016/S0006-3223(99)00239-5.

Mortimore, Glenn E., and Charles M. Schworer. 1977. "Induction of Autophagy by Amino-Acid Deprivation in Perfused Rat Liver." *Nature* 270 (5633): 174–76. https://doi.org/10.1038/270174a0.

Moser, E., M. B. Moser, and P. Andersen. 1993. "Spatial Learning Impairment Parallels the Magnitude of Dorsal Hippocampal Lesions, but Is Hardly Present Following Ventral Lesions." *Journal of Neuroscience* 13 (9): 3916–25. https://doi.org/10.1523/jneurosci.13-09-03916.1993.

Moser, May Britt, and Edvard I. Moser. 1998. "Functional Differentiation in the Hippocampus." *Hippocampus*. John Wiley & Sons, Ltd. https://doi.org/10.1002/(SICI)1098-1063(1998)8:6<608::AID-HIPO3>3.0.CO;2-7.

Murrow, Lyndsay, and Jayanta Debnath. 2013. "Autophagy as a Stress-Response and Quality-Control Mechanism: Implications for Cell Injury and Human Disease." *Annual Review of Pathology* 8 (January): 105–37. https://doi.org/10.1146/annurev-pathol-020712-163918.

Nagashima, Takeshi, Norihiko Inoue, Noriko Yumoto, Yuko Saeki, Shigeyuki Magi, Natalia Volinsky, Alexander Sorkin, Boris N. Kholodenko, and Mariko Okada-Hatakeyama. 2015. "Feedforward Regulation of MRNA Stability by Prolonged Extracellular Signal-Regulated Kinase Activity." *FEBS Journal*. Blackwell Publishing Ltd. https://doi.org/10.1111/febs.13172.

Naisbitt, Scott, Kim Eunjoon, Jian Cheng Tu, Bo Xiao, Carlo Sala, Juli Valtschanoff, Richard J. Weinberg, Paul F. Worley, and Morgan Sheng. 1999. "Shank, a Novel Family of Postsynaptic Density Proteins That Binds to the NMDA Receptor/PSD-95/GKAP Complex and Cortactin." *Neuron* 23 (3): 569–82. https://doi.org/10.1016/S0896-6273(00)80809-0.

Nakajima, Masaharu, Akio Inui, Akihiro Asakawa, Kazuhiro Momose, Naohiko Ueno, Arata Teranishi, Shigeaki Baba, and Masato Kasuga. 1998. "Neuropeptide Y Produces Anxiety via Y2-Type Receptors." *Peptides* 19 (2): 359–63. https://doi.org/10.1016/S0196-9781(97)00298-2.

Nakatogawa, Hitoshi. 2013. "Two Ubiquitin-like Conjugation Systems That Mediate Membrane Formation during Autophagy." *Essays In Biochemistry* 55 (September): 39–50. https://doi.org/10.1042/bse0550039.

Nelson, Christopher L., Michael Milovanovic, Joseph B. Wetter, Kerstin A. Ford, and Marina E. Wolf. 2009. "Behavioral Sensitization to Amphetamine Is Not Accompanied by Changes in Glutamate Receptor Surface Expression in the Rat Nucleus Accumbens." *Journal of Neurochemistry* 109 (1): 35–51. https://doi.org/10.1111/j.1471-4159.2009.05911.x.

Nikoletopoulou, V, M-E Papandreou, and N Tavernarakis. 2015. "Autophagy in the Physiology and Pathology of the Central Nervous System." *Cell Death and Differentiation* 22 (3): 398–407. https://doi.org/10.1038/cdd.2014.204.

Nikoletopoulou, Vassiliki, Kyriaki Sidiropoulou, Emmanouela Kallergi, Yannis Dalezios, and Nektarios Tavernarakis. 2017. "Modulation of Autophagy by BDNF Underlies Synaptic Plasticity." *Cell Metabolism* 26 (1): 230-242.e5. https://doi.org/10.1016/j.cmet.2017.06.005.

Nikoletopoulou, Vassiliki, and Nektarios Tavernarakis. 2018. "Regulation and Roles of Autophagy at Synapses." *Trends in Cell Biology*, May. https://doi.org/10.1016/j.tcb.2018.03.006.

Nixon, Ralph A., Jerzy Wegiel, Asok Kumar, Wai Haung Yu, Corrinne Peterhoff, Anne Cataldo, and Ana Maria Cuervo. 2005. "Extensive Involvement of Autophagy in Alzheimer Disease: An Immuno-Electron Microscopy Study." *Journal of Neuropathology and Experimental Neurology* 64 (2): 113–22. https://doi.org/10.1093/jnen/64.2.113.

Nowak, L., P. Bregestovski, P. Ascher, A. Herbet, and A. Prochiantz. 1984. "Magnesium Gates

Bibliography

Glutamate-Activated Channels in Mouse Central Neurones." *Nature* 307 (5950): 462–65. https://doi.org/10.1038/307462a0.

Ogura, T, LM Shuba, TF McDonald - Journal of Pharmacology And, and Undefined 1995. 1995. "Action Potentials, Ionic Currents and Cell Water in Guinea Pig Ventricular Preparations Exposed to Dimethyl Sulfoxide." *ASPET*. https://jpet.aspetjournals.org/content/273/3/1273.short.

Ohsumi, Yoshinori. 2001. "Molecular Dissection of Autophagy: Two Ubiquitin-like Systems." *Nature Reviews Molecular Cell Biology* 2 (3): 211–16. https://doi.org/10.1038/35056522.

Okerlund, Nathan D., Richard J. Reimer, Katharina Schneider, Sergio Leal-Ortiz, Carolina Montenegro-Venegas, Sally A. Kim, Loren C. Garner, Eckart D. Gundelfinger, Richard J. Reimer, and Craig C. Garner. 2017. "Bassoon Controls Presynaptic Autophagy through Atg5." *Neuron* 93 (4): 897-913.e7. https://doi.org/10.1016/j.neuron.2017.01.026.

Olson, T S, S R Terlecky, and J F Dice. 1991. "Targeting Specific Proteins for Lysosomal Proteolysis." *Biomedica Biochimica Acta* 50 (4–6): 393–97. http://www.ncbi.nlm.nih.gov/pubmed/1801703.

Pankiv, Serhiy, Terje Høyvarde Clausen, Trond Lamark, Andreas Brech, Jack Ansgar Bruun, Heidi Outzen, Aud Øvervatn, Geir Bjørkøy, and Terje Johansen. 2007. "P62/SQSTM1 Binds Directly to Atg8/LC3 to Facilitate Degradation of Ubiquitinated Protein Aggregates by Autophagy*[S]." *Journal of Biological Chemistry* 282 (33): 24131–45. https://doi.org/10.1074/jbc.M702824200.

Papadopoulos, T., and U. Pfeifer. 1986. "Regression of Rat Liver Autophagic Vacuoles by Locally Applied Cycloheximide." *Laboratory Investigation* 54 (1): 100–107. https://europepmc.org/article/med/3941538.

Park, Mikyoung, Esther C. Penick, Jeffrey G. Edwards, Julie A. Kauer, and Michael D. Ehlers. 2004. "Recycling Endosomes Supply AMPA Receptors for LTP." *Science* 305 (5692): 1972–75. https://doi.org/10.1126/science.1102026.

Parzych, Katherine R., and Daniel J. Klionsky. 2014. "An Overview of Autophagy: Morphology, Mechanism, and Regulation." *Antioxidants & Redox Signaling* 20 (3): 460–73. https://doi.org/10.1089/ars.2013.5371.

Passafaro, Maria, Valentin Piãch, and Morgan Sheng. 2001. "Subunit-Specific Temporal and Spatial Patterns of AMPA Receptor Exocytosis in Hippocampal Neurons." *Nature Neuroscience* 4 (9): 917–26. https://doi.org/10.1038/nn0901-917.

Perry, Robert P., and Dawn E. Kelley. 1970. "Inhibition of RNA Synthesis by Actinomycin D: Characteristic Dose-response of Different RNA Species." *Journal of Cellular Physiology* 76 (2): 127–39. https://doi.org/10.1002/jcp.1040760202.

Phelps, Elizabeth A. 2004. "Human Emotion and Memory: Interactions of the Amygdala and Hippocampal Complex." *Current Opinion in Neurobiology*. Curr Opin Neurobiol. https://doi.org/10.1016/j.conb.2004.03.015.

Phillips, RG, and JE LeDoux. 1994. "Lesions of the Dorsal Hippocampal Formation Interfere with Background but Not Foreground Contextual Fear Conditioning." *Learn Mem.* 1 (1): 34–44.

Pickel, Virginia, and Menahem Segal. 2013. *The Synapse: Structure and Function. The Synapse: Structure and Function.* Elsevier Inc. https://doi.org/10.1016/C2013-0-12631-1.

Piper, Robert C., and David J. Katzmann. 2007. "Biogenesis and Function of Multivesicular Bodies." *Annual Review of Cell and Developmental Biology*. Annu Rev Cell Dev Biol. https://doi.org/10.1146/annurev.cellbio.23.090506.123319.

Primeaux, Stefany D, Steven P Wilson, Michael C Cusick, David A York, and Marlene A Wilson. 2005. "Effects of Altered Amygdalar Neuropeptide Y Expression on Anxiety-Related Behaviors." *Neuropsychopharmacology* 30 (9): 1589–97. https://doi.org/10.1038/sj.npp.1300705.

Purves, Dale, George J Augustine, David Fitzpatrick, Lawrence C Katz, Anthony-Samuel LaMantia, James O McNamara, and S Mark Williams. 2001. "The Initial Differentiation of Neurons and Glia." https://www.ncbi.nlm.nih.gov/books/NBK11144/.

Qu, Ting Ting, Jie Xin Deng, Rui Ling Li, Zhan Jun Cui, Xiao Qing Wang, Lai Wang, and Jin

Bibliography

Bo Deng. 2017. "Stress Injuries and Autophagy in Mouse Hippocampus after Chronic Cold Exposure." *Neural Regeneration Research* 12 (3): 440–46. https://doi.org/10.4103/1673-5374.202932.

R. G. M. Morris, P. Garrud, J. N. P. Rawlins, and J. O'Keefe. 1982. "Place Navigation Impaired in Rats with Hippocampal Lesions." *Nature* 297 (June): 681–83. https://www.nature.com/articles/297681a0.pdf.

Ragen, Benjamin J., Jordan Seidel, Christine Chollak, Robert H. Pietrzak, and Alexander Neumeister. 2015. "Investigational Drugs under Development for the Treatment of PTSD." *Expert Opinion on Investigational Drugs*. Informa Healthcare. https://doi.org/10.1517/13543784.2015.1020109.

Rasmusson, Ann M, and Suzanne L Pineles. 2018. "Neurotransmitter, Peptide, and Steroid Hormone Abnormalities in PTSD: Biological Endophenotypes Relevant to Treatment." *Current Psychiatry Reports* 20 (52). https://doi.org/10.1007/s11920-018-0908-9.

Raza, Syed Ahsan, Anne Albrecht, Gürsel Çalışkan, Bettina Müller, Yunus Emre Demiray, Susann Ludewig, Susanne Meis, et al. 2017. "HIPP Neurons in the Dentate Gyrus Mediate the Cholinergic Modulation of Background Context Memory Salience." *Nature Communications* 8 (189). https://doi.org/10.1038/s41467-017-00205-3.

Regev-Tsur, Stav, Yunus Emre Demiray, Kuldeep Tripathi, Oliver Stork, Gal Richter-Levin, and Anne Albrecht. 2020. "Region-Specific Involvement of Interneuron Subpopulations in Trauma-Related Pathology and Resilience." *Neurobiology of Disease* 143 (September). https://doi.org/10.1016/j.nbd.2020.104974.

Reichmann, Florian, and Peter Holzer. 2016. "Neuropeptide Y: A Stressful Review." *Neuropeptides* 55: 99–109. https://doi.org/10.1016/j.npep.2015.09.008.

Reijnen, Alieke, Elbert Geuze, Iris Eekhout, Adam X. Maihofer, Caroline M. Nievergelt, Dewleen G. Baker, and Eric Vermetten. 2018. "Biological Profiling of Plasma Neuropeptide Y in Relation to Posttraumatic Stress Symptoms in Two Combat Cohorts." *Biological Psychology* 134 (April): 72–79. https://doi.org/10.1016/j.biopsycho.2018.02.008.

Reisel, D., D. M. Bannerman, W. B. Schmitt, R. M.J. Deacon, J. Flint, T. Borchardt, P. H. Seeburg, and J. N.P. Rawlins. 2002. "Spatial Memory Dissociations in Mice Lacking GluR1." *Nature Neuroscience* 5 (9): 868–73. https://doi.org/10.1038/nn910.

Rescorla, RA, and AR Wagner. 1972. "A Theory of Pavlovian Conditioning: Variations in the Effectiveness of Reinforcement and Nonreinforcement." A. H. Black & W. F. Prokasy (Eds.),Classical Conditioning II. New York: Appleton-Century-Crofts. 1972. https://scholar.google.com/scholar_lookup?title=Classical conditioning II&pages=64-99&publication_year=1972&author=Rescorla%2CR. A.&author=Wagner%2CA. R.

Riper, D. A. Van, and J. A. Bevan. 1991. "Evidence That Neuropeptide Y and Norepinephrine Mediate Electrical Field-Stimulated Vasoconstriction of Rabbit Middle Cerebral Artery." *Circulation Research* 68 (2): 568–77. https://doi.org/10.1161/01.RES.68.2.568.

Rubino, Mariantonietta, Marta Miaczynska, Roger Lippé, and Marino Zerial. 2000. "Selective Membrane Recruitment of EEA1 Suggests a Role in Directional Transport of Clathrin-Coated Vesicles to Early Endosomes." *Journal of Biological Chemistry* 275 (6): 3745–48. https://doi.org/10.1074/jbc.275.6.3745.

Rudy, Jerry W. 2009. "Context Representations, Context Functions, and the Parahippocampal- Hippocampal System." *Learning and Memory*. Learn Mem. https://doi.org/10.1101/lm.1494409.

Rumpel, Simon, Joseph LeDoux, Anthony Zador, and Roberto Malinow. 2005. "Postsynaptic Receptor Trafficking Underlying a Form of Associative Learning." *Science* 308 (5718): 83–88. https://doi.org/10.1126/science.1103944.

Russell, Ryan C., Ye Tian, Haixin Yuan, Hyun Woo Park, Yu-Yun Chang, Joungmok Kim, Haerin Kim, Thomas P. Neufeld, Andrew Dillin, and Kun-Liang Guan. 2013. "ULK1 Induces Autophagy by Phosphorylating Beclin-1 and Activating VPS34 Lipid Kinase." *Nature Cell Biology* 15 (7): 741–50. https://doi.org/10.1038/ncb2757.

Sabers, C. J., M. M. Martin, G. J. Brunn, J. M. Williams, F. J. Dumont, G. Wiederrecht, and R. T. Abraham. 1995. "Isolation of a Protein Target of the FKBP12-Rapamycin Complex in

Bibliography

Mammalian Cells." *Journal of Biological Chemistry* 270 (2): 815–22. https://doi.org/10.1074/jbc.270.2.815.

Sajdyk, Tammy J., Douglas A. Schober, David L. Smiley, and Donald R. Gehlert. 2002. "Neuropeptide Y-Y2 Receptors Mediate Anxiety in the Amygdala." *Pharmacology Biochemistry and Behavior* 71 (3): 419–23. https://doi.org/10.1016/S0091-3057(01)00679-7.

Santini, Emanuela, and Eric Klann. 2014. "Reciprocal Signaling between Translational Control Pathways and Synaptic Proteins in Autism Spectrum Disorders." *Science Signaling*. American Association for the Advancement of Science. https://doi.org/10.1126/scisignal.2005832.

Sarkar, Sovan, Janet E. Davies, Zebo Huang, Alan Tunnacliffe, and David C. Rubinsztein. 2007. "Trehalose, a Novel MTOR-Independent Autophagy Enhancer, Accelerates the Clearance of Mutant Huntingtin and α-Synuclein." *Journal of Biological Chemistry* 282 (8): 5641–52. https://doi.org/10.1074/jbc.M609532200.

Satoo, Kenji, Nobuo N Noda, Hiroyuki Kumeta, Yuko Fujioka, Noboru Mizushima, Yoshinori Ohsumi, and Fuyuhiko Inagaki. 2009. "The Structure of Atg4B–LC3 Complex Reveals the Mechanism of LC3 Processing and Delipidation during Autophagy." *The EMBO Journal* 28 (9): 1341–50. https://doi.org/10.1038/emboj.2009.80.

Scharfman, Helen E., and Catherine E. Myers. 2013. "Hilar Mossy Cells of the Dentate Gyrus: A Historical Perspective." *Frontiers in Neural Circuits* 6 (DEC): 106. https://doi.org/10.3389/fncir.2012.00106.

Schultz, Christian, and Maren Engelhardt. 2014. "Anatomy of the Hippocampal Formation." In *The Hippocampus in Clinical Neuroscience*, 34:6–17. S. Karger AG. https://doi.org/10.1159/000360925.

Schwarz, Lindsay A., Benjamin J. Hall, and Gentry N. Patrick. 2010. "Activity-Dependent Ubiquitination of GluA1 Mediates a Distinct AMPA Receptor Endocytosis and Sorting Pathway." *Journal of Neuroscience* 30 (49): 16718–29. https://doi.org/10.1523/JNEUROSCI.3686-10.2010.

Serova, Lidia I, Chiso Nwokafor, Elisabeth J Van, Beverly A S Reyes, Xiaoping Lin, and Esther L Sabban. 2019. "Single Prolonged Stress PTSD Model Triggers Progressive Severity of Anxiety , Altered Gene Expression in Locus Coeruleus And." *European Neuropsychopharmacology*, 1–11. https://doi.org/10.1016/j.euroneuro.2019.02.010.

Sheehan, Patricia, Mei Zhu, Anne Beskow, Cyndel Vollmer, and Clarissa L. Waites. 2016. "Activity-Dependent Degradation of Synaptic Vesicle Proteins Requires Rab35 and the ESCRT Pathway." *Journal of Neuroscience* 36 (33): 8668–86. https://doi.org/10.1523/JNEUROSCI.0725-16.2016.

Shehata, Mohammad, Kareem Abdou, Kiriko Choko, Mina Matsuo, Hirofumi Nishizono, and Kaoru Inokuchi. 2018. "Autophagy Enhances Memory Erasure through Synaptic Destabilization." *The Journal of Neuroscience* 38 (15): 3505–17. https://doi.org/10.1523/JNEUROSCI.3505-17.2018.

Shehata, Mohammad, Hiroyuki Matsumura, Reiko Okubo-Suzuki, Noriaki Ohkawa, and Kaoru Inokuchi. 2012. "Neuronal Stimulation Induces Autophagy in Hippocampal Neurons That Is Involved in AMPA Receptor Degradation after Chemical Long-Term Depression." https://doi.org/10.1523/JNEUROSCI.4533-11.2012.

Sheng, Morgan, and Eunjoon Kim. 2000. "The Shank Family of Scaffold Proteins." *Journal of Cell Science* 113 (11): 1851–56.

Shi, Song Hai, Yasunori Hayashi, José A. Esteban, and Roberto Malinow. 2001. "Subunit-Specific Rules Governing AMPA Receptor Trafficking to Synapses in Hippocampal Pyramidal Neurons." *Cell* 105 (3): 331–43. https://doi.org/10.1016/S0092-8674(01)00321-X.

Shimobayashi, Mitsugu, and Michael N. Hall. 2014. "Making New Contacts: The MTOR Network in Metabolism and Signalling Crosstalk." *Nature Reviews Molecular Cell Biology* 15 (3): 155–62. https://doi.org/10.1038/nrm3757.

Shintani, T., N Mizushima, Y Ogawa, A Matsuura, T Noda, and Y Ohsumi. 1999. "Apg10p, a Novel Protein-Conjugating Enzyme Essential for Autophagy in Yeast." *The EMBO*

Journal 18 (19): 5234–41. https://doi.org/10.1093/emboj/18.19.5234.

Shpilka, Tomer, Hilla Weidberg, Shmuel Pietrokovski, and Zvulun Elazar. 2011. "Atg8: An Autophagy-Related Ubiquitin-like Protein Family." *Genome Biology* 12 (7): 226. https://doi.org/10.1186/gb-2011-12-7-226.

Śmiałowska, Maria, Joanna M Wierońska, Helena Domin, and Barbara Zięba. 2007. "The Effect of Intrahippocampal Injection of Group II and III Metobotropic Glutamate Receptor Agonists on Anxiety; the Role of Neuropeptide Y." *Neuropsychopharmacology* 32 (6): 1242–50. https://doi.org/10.1038/sj.npp.1301258.

Sørensen, Gunnar, Camilla Lindberg, Gitta Wörtwein, Tom G. Bolwig, and David P.D. Woldbye. 2004. "Differential Roles for Neuropeptide Y Y1 and Y5 Receptors in Anxiety and Sedation." *Journal of Neuroscience Research* 77 (5): 723–29. https://doi.org/10.1002/jnr.20200.

Sossa, K. G., B. L. Court, and R. C. Carroll. 2006. "NMDA Receptors Mediate Calcium-Dependent, Bidirectional Changes in Dendritic PICK1 Clustering." *Molecular and Cellular Neuroscience* 31 (3): 574–85. https://doi.org/10.1016/j.mcn.2005.11.011.

Sumitomo, Akiko, Hiroshi Yukitake, Kazuko Hirai, Kouta Horike, Keisho Ueta, Youjin Chung, Eiji Warabi, et al. 2018. "Ulk2 Controls Cortical Excitatory-Inhibitory Balance via Autophagic Regulation of P62 and GABAA Receptor Trafficking in Pyramidal Neurons." *Human Molecular Genetics* 27 (18): 3165–76. https://doi.org/10.1093/hmg/ddy219.

Takeshige, K., M. Baba, S. Tsuboi, T. Noda, and Y. Ohsumi. 1992. "Autophagy in Yeast Demonstrated with Proteinase-Deficient Mutants and Conditions for Its Induction." *Journal of Cell Biology* 119 (2): 301–12. https://doi.org/10.1083/jcb.119.2.301.

Tanaka, Yoshitaka, Gundula Guhde, Anke Suter, Eeva Liisa Eskelinen, Dieter Hartmann, Renate Lüllmann-Rauch, Paul M.L. Janssen, Judith Blanz, Kurt Von Figura, and Paul Saftig. 2000. "Accumulation of Autophagic Vacuoles and Cardiomyopathy LAMP-2-Deficient Mice." *Nature* 406 (6798): 902–6. https://doi.org/10.1038/35022595.

Tang, Guomei, Kathryn Gudsnuk, Sheng-Han Kuo, Marisa L. Cotrina, Gorazd Rosoklija, Alexander Sosunov, Mark S. Sonders, et al. 2014. "Loss of MTOR-Dependent Macroautophagy Causes Autistic-like Synaptic Pruning Deficits." *Neuron* 83 (5): 1131–43. https://doi.org/10.1016/j.neuron.2014.07.040.

Tanida, Isei, Noboru Mizushima, Miho Kiyooka, Mariko Ohsumi, Takashi Ueno, Yoshinori Ohsumi, and Eiki Kominami. 1999. "Apg7p/Cvt2p: A Novel Protein-Activating Enzyme Essential for Autophagy." Edited by Randy W. Schekman. *Molecular Biology of the Cell* 10 (5): 1367–79. https://doi.org/10.1091/mbc.10.5.1367.

Thumm, M., R. Egner, B. Koch, M. Schlumpberger, M. Straub, M. Veenhuis, and D.H. Wolf. 1994. "Isolation of Autophagocytosis Mutants of Saccharomyces Cerevisiae." *FEBS Letters* 349 (2): 275–80. https://doi.org/10.1016/0014-5793(94)00672-5.

Todde, Virginia, Marten Veenhuis, and Ida J. van der Klei. 2009. "Autophagy: Principles and Significance in Health and Disease." *Biochimica et Biophysica Acta (BBA) - Molecular Basis of Disease* 1792 (1): 3–13. https://doi.org/10.1016/J.BBADIS.2008.10.016.

Tsigos, Constantine, Ioannis Kyrou, Eva Kassi, and George P Chrousos. 2000. *Stress, Endocrine Physiology and Pathophysiology*. *Endotext*. MDText.com, Inc. http://www.ncbi.nlm.nih.gov/pubmed/25905226.

Tsukada, Miki, and Yoshinori Ohsumi. 1993. "Isolation and Characterization of Autophagy-Defective Mutants of Saccharomyces Cerevisiae." *FEBS Letters* 333 (1–2): 169–74. https://doi.org/10.1016/0014-5793(93)80398-E.

Tsuriel, Shlomo, Ran Geva, Pedro Zamorano, Thomas Dresbach, Tobias Boeckers, Eckart D. Gundelfinger, Craig C. Garner, and Noam E. Ziv. 2006. "Local Sharing as a Predominant Determinant of Synaptic Matrix Molecular Dynamics." *PLoS Biology* 4 (9): 1572–87. https://doi.org/10.1371/journal.pbio.0040271.

Uchino, Shigeo, Hidenori Wada, Shizuyo Honda, Yasuko Nakamura, Yumiko Ondo, Takayoshi Uchiyama, Moe Tsutsumi, Eri Suzuki, Takae Hirasawa, and Shinichi Kohsaka. 2006. "Direct Interaction of Post-Synaptic Density-95/Dlg/ZO-1 Domain-Containing Synaptic Molecule Shank3 with GluR1 Alpha-Amino-3-Hydroxy-5-Methyl-4-Isoxazole Propionic Acid Receptor." *Journal of Neurochemistry* 97 (4): 1203–14.

https://doi.org/10.1111/j.1471-4159.2006.03831.x.

Uytterhoeven, Valerie, Sabine Kuenen, Jaroslaw Kasprowicz, Katarzyna Miskiewicz, and Patrik Verstreken. 2011. "Loss of Skywalker Reveals Synaptic Endosomes as Sorting Stations for Synaptic Vesicle Proteins." *Cell* 145 (1): 117–32. https://doi.org/10.1016/j.cell.2011.02.039.

Vabulas, Ramunas M., and F. Ulrich Hartl. 2005. "Cell Biology: Protein Synthesis upon Acute Nutrient Restriction Relies on Proteasome Function." *Science* 310 (5756): 1960–63. https://doi.org/10.1126/science.1121925.

Verma, D., R. O. Tasan, H. Herzog, and G. Sperk. 2012. "NPY Controls Fear Conditioning and Fear Extinction by Combined Action on Y 1 and Y 2 Receptors." *British Journal of Pharmacology* 166 (4): 1461–73. https://doi.org/10.1111/j.1476-5381.2012.01872.x.

Verpelli, Chiara, Elena Dvoretskova, Cinzia Vicidomini, Francesca Rossi, Michela Chiappalone, Michael Schoen, Bruno Di Stefano, et al. 2011. "Importance of Shank3 Protein in Regulating Metabotropic Glutamate Receptor 5 (MGluR5) Expression and Signaling at Synapses." *Journal of Biological Chemistry* 286 (40): 34839–50. https://doi.org/10.1074/jbc.M111.258384.

Vouimba, Rose Marie, Dan Yaniv, David Diamond, and Gal Richter-Levin. 2004. "Effects of Inescapable Stress on LTP in the Amygdala versus the Dentate Gyrus of Freely Behaving Rats." *European Journal of Neuroscience* 19 (7): 1887–94. https://doi.org/10.1111/j.1460-9568.2004.03294.x.

Waites, Clarissa L, Sergio A Leal-Ortiz, Nathan Okerlund, Hannah Dalke, Anna Fejtova, Wilko D Altrock, Eckart D Gundelfinger, and Craig C Garner. 2013. "Bassoon and Piccolo Maintain Synapse Integrity by Regulating Protein Ubiquitination and Degradation." *The EMBO Journal* 32 (7): 954–69. https://doi.org/10.1038/emboj.2013.27.

Wegener, Stephanie, Arne Buschler, A. Vanessa Stempel, Sukjae J. Kang, Chae Seok Lim, Bong Kiun Kaang, Sarah A. Shoichet, Denise Manahan-Vaughan, and Dietmar Schmitz. 2018. "Defective Synapse Maturation and Enhanced Synaptic Plasticity in Shank2 Δex7–/– Mice." *ENeuro* 5 (3). https://doi.org/10.1523/ENEURO.0398-17.2018.

Weidberg, Hilla, Elena Shvets, and Zvulun Elazar. 2011. "Biogenesis and Cargo Selectivity of Autophagosomes." *Annual Review of Biochemistry* 80 (1): 125–56. https://doi.org/10.1146/annurev-biochem-052709-094552.

Wenthold, Robert J., Ronald S. Petralia, Jaroslav Blahos, and Andrew S. Niedzielski. 1996. "Evidence for Multiple AMPA Receptor Complexes in Hippocampal CA1/CA2 Neurons." *Journal of Neuroscience* 16 (6): 1982–89. https://doi.org/10.1523/jneurosci.16-06-01982.1996.

West, Katherine Stuhrman, and Aaron G Roseberry. 2017. "Neuropeptide-Y Alters VTA Dopamine Neuron Activity through Both Pre-and Postsynaptic Mechanisms." *J Neurophysiol* 118: 625–33. https://doi.org/10.1152/jn.00879.2016.-The.

Wheway, Julie, Herbert Herzog, and Fabienne Mackay. 2007. "NPY and Receptors in Immune and Inflammatory Diseases." *Current Topics in Medicinal Chemistry* 7 (17): 1743–52. https://doi.org/10.2174/156802607782341046.

Whitlock, Jonathan R., Arnold J. Heynen, Marshall G. Shuler, and Mark F. Bear. 2006. "Learning Induces Long-Term Potentiation in the Hippocampus." *Science* 313 (5790): 1093–97. https://doi.org/10.1126/science.1128134.

Windrum, P., and T. C.M. Morris. 2003. "Severe Neurotoxicity Because of Dimethyl Sulphoxide Following Peripheral Blood Stem Cell Transplantation [2]." *Bone Marrow Transplantation*. Bone Marrow Transplant. https://doi.org/10.1038/sj.bmt.1703848.

Woo, Hanwoong, Caroline Jeeyeon Hong, Seonghee Jung, Seongwon Choe, and Seong Woon Yu. 2018. "Chronic Restraint Stress Induces Hippocampal Memory Deficits by Impairing Insulin Signaling." *Molecular Brain* 11 (1): 1–13. https://doi.org/10.1186/s13041-018-0381-8.

Wu, Dick, Taulant Bacaj, Wade Morishita, Debanjan Goswami, Kristin L. Arendt, Wei Xu, Lu Chen, Robert C. Malenka, and Thomas C. Südhof. 2017. "Postsynaptic Synaptotagmins Mediate AMPA Receptor Exocytosis during LTP." *Nature* 544 (7650): 316–21. https://doi.org/10.1038/nature21720.

Bibliography

Wu, Gang, Adriana Feder, Hagit Cohen, Joanna J. Kim, Solara Calderon, Dennis S. Charney, and Aleksander A. Mathé. 2013. "Understanding Resilience." *Frontiers in Behavioral Neuroscience*. Frontiers. https://doi.org/10.3389/fnbeh.2013.00010.

Wu, Yong Fei, and Sheng Bin Li. 2005. "Neuropeptide Y Expression in Mouse Hippocampus and Its Role in Neuronal Excitotoxicity." *Acta Pharmacologica Sinica* 26 (1): 63–68. https://doi.org/10.1111/j.1745-7254.2005.00011.x.

Xapelli, S., L. Bernardino, R. Ferreira, S. Grade, A. P. Silva, J. R. Salgado, C. Cavadas, et al. 2008. "Interaction between Neuropeptide Y (NPY) and Brain-Derived Neurotrophic Factor in NPY-Mediated Neuroprotection against Excitotoxicity: A Role for Microglia." *European Journal of Neuroscience* 27 (8): 2089–2102. https://doi.org/10.1111/j.1460-9568.2008.06172.x.

Xu, Bin, Limin Lang, Shize Li, Jianbin Yuan, Jianfa Wang, Huanmin Yang, and Shuai Lian. 2019. "Corticosterone Excess-Mediated Mitochondrial Damage Induces Hippocampal Neuronal Autophagy in Mice Following Cold Exposure." *Animals* 9 (9). https://doi.org/10.3390/ani9090682.

Yamamoto, Ai, and Zhenyu Yue. 2014. "Autophagy and Its Normal and Pathogenic States in the Brain." *Annual Review of Neuroscience* 37 (1): 55–78. https://doi.org/10.1146/annurev-neuro-071013-014149.

Yan, Jingqi, Morgan W. Porch, Brenda Court-Vazquez, Michael V.L. Bennett, and R. Suzanne Zukin. 2018. "Activation of Autophagy Rescues Synaptic and Cognitive Deficits in Fragile X Mice." *Proceedings of the National Academy of Sciences of the United States of America* 115 (41): E9707–16. https://doi.org/10.1073/pnas.1808247115.

Yang, Liang, Karen A. Scott, Jayson Hyun, Kellie L. Tamashiro, Nancy Tray, Timothy H. Moran, and Sheng Bi. 2009. "Role of Dorsomedial Hypothalamic Neuropeptide Y in Modulating Food Intake and Energy Balance." *Journal of Neuroscience* 29 (1): 179–90. https://doi.org/10.1523/JNEUROSCI.4379-08.2009.

Yang, Zhifen, and Daniel J. Klionsky. 2010. "Eaten Alive: A History of Macroautophagy." *Nature Cell Biology* 12 (9): 814. https://doi.org/10.1038/NCB0910-814.

Yang, Zhifen, and Daniel J Klionsky. 2009. "An Overview of the Molecular Mechanism of Autophagy." *Current Topics in Microbiology and Immunology* 335: 1–32. https://doi.org/10.1007/978-3-642-00302-8_1.

Yorimitsu, T., and D. J. Klionsky. 2005a. "Autophagy: Molecular Machinery for Self-Eating." *Cell Death and Differentiation*. NIH Public Access. https://doi.org/10.1038/sj.cdd.4401765.

Yorimitsu, T, and D J Klionsky. 2005b. "Autophagy: Molecular Machinery for Self-Eating." *Cell Death and Differentiation* 12 Suppl 2 (Suppl 2): 1542–52. https://doi.org/10.1038/sj.cdd.4401765.

Yuen, Eunice Y., Wenhua Liu, Ilia N. Karatsoreos, Jian Feng, Bruce S. McEwen, and Zhen Yan. 2009. "Acute Stress Enhances Glutamatergic Transmission in Prefrontal Cortex and Facilitates Working Memory." *Proceedings of the National Academy of Sciences of the United States of America* 106 (33): 14075–79. https://doi.org/10.1073/pnas.0906791106.

Zaslavsky, Kirill, Wen Bo Zhang, Fraser P. McCready, Deivid C. Rodrigues, Eric Deneault, Caitlin Loo, Melody Zhao, et al. 2019. "SHANK2 Mutations Associated with Autism Spectrum Disorder Cause Hyperconnectivity of Human Neurons." *Nature Neuroscience* 22 (4): 556–64. https://doi.org/10.1038/s41593-019-0365-8.

Zhai, Baohui, Xueliang Shang, Jingxuan Fu, Fangjuan Li, and Tao Zhang. 2018. "Rapamycin Relieves Anxious Emotion and Synaptic Plasticity Deficits Induced by Hindlimb Unloading in Mice." *Neuroscience Letters* 677 (June): 44–48. https://doi.org/10.1016/j.neulet.2018.04.033.

Zhang, Yong, Robert H. Cudmore, Da Ting Lin, David J. Linden, and Richard L. Huganir. 2015. "Visualization of NMDA Receptor - Dependent AMPA Receptor Synaptic Plasticity in Vivo." *Nature Neuroscience* 18 (3): 402–9. https://doi.org/10.1038/nn.3936.

Declaration of Honour

I hereby declare that I prepared this thesis without impermissible help of third parties and that none other than the indicated tools have been used; all sources of information are clearly marked, including my own publications.

In particular I have not consciously:

• Fabricated data or rejected undesired results

• Misused statistical methods with the aim of drawing other conclusions than those warranted by the available data

• Plagiarized external data or publications

• Presented the results of other researchers in a distorted way

I am aware that violations of copyright may lead to injunction and damage claims of the author and also to prosecution by the law enforcement authorities.

I hereby agree that the thesis may be reviewed for plagiarism by mean of electronic data processing.

This work has not yet been submitted as a doctoral thesis in the same or a similar form in Germany or in any other country. It has not yet been published as a whole.

Magdeburg,

Elisa Redavide